A COMPARISON OF THE PHYSICAL RADIATION-INDUCED BYSTANDER EFFECT AND PEROXIDE-MEDIATED OXIDATIVE STRESS IN HUMAN AND MURINE EPITHELIAL CELLS

A COMPARISON OF THE PHYSICAL RADIATION-INDUCED BYSTANDER EFFECT AND PEROXIDE-MEDIATED OXIDATIVE STRESS IN HUMAN AND MURINE EPITHELIAL CELLS

by

Andrej Rusin, B.Sc.

A thesis to be submitted to the School of Graduate Studies in partial fulfillment of the requirements for the degree of

Master of Science

McMaster University

McMaster University	Hamilton, Ontario
Master of Science	Biology
Title	A comparison of the physical radiation-induced bystander effect and peroxide-mediated oxidative stress in human and murine epithelial cells
Author	Andrej Rusin
Supervisor	Dr. Carmel Mothersill
Number of Pages	ix, 185

ABSTRACT

The effects of low doses of ionizing radiation on living things is a continually evolving area of research. Importantly, low dose effects were historically overlooked and not properly accounted for the assessment of risk to human health, as is the case with the contentious linear no-threshold model. These low dose effects are now known to be relevant to human health in both accidental and intentional exposures, including doses relevant to medical diagnostics and therapeutics. Furthermore, there is a relative dearth of information on low dose effects in non-human species, which necessitates further investigation and evaluation of radiosensitivity. Radiation-induced bystander effects occur in organisms due to the receipt of signals from directly irradiated cells, which act to communicate radiation damage to surrounding cells. Recent research has identified one type of bystander signal which is carried by photons of biological origin, however the effects produced in bystander cells receiving these photons has not been extensively investigated. It was suspected, based on previous research, that reactive oxygen species participate in the manifestation of this bystander effect. Three mammalian cell lines were assessed for their ability to produce bystander photons upon direct irradiation; subsequently, radiologically unexposed cells were exposed to the resulting photons and assayed for biological effects. The human cell lines used exhibited significant photon emissions and oxidative stress, clonogenic cell death, reduced cellular metabolism, and compromised mitochondrial oxidative phosphorylation following exposure to these photons. The use of a melanocyte cell line indicated that these effects are attenuated by melanin, and this is suspected to occur through photoabsorption or antioxidant mechanisms. Additionally, the same assays were conducted following cell exposure to hydrogen peroxide at low concentrations to assess responses to oxidative stress relevant to bystander responses, indicating less overall sensitivity in the examined melanocytes. These findings are significant because they contribute to our understanding of the mechanisms behind low dose biological effects, because they further challenge the linear no-threshold model and other models based on target theory, because they provide evidence for differential responses to the physical bystander signal in non-human species, and because secondary photon emissions are likely relevant to the medical radiation sciences.

ACKNOWLEDGEMENTS

I would first like to give my thanks to Dr. Mothersill and Dr. Seymour who have shown me nothing but support, understanding, and patience during not only my graduate years, but in my undergraduate co-op and thesis projects as well. Their encouragement, positivity, and creativity made this thesis possible. This is not to mention their role in promoting the development of additional professional skills, including graphical design, programming, and writing—if they take a genuine interest in your personal development, you know you have found a truly exceptional supervisor and mentor!

I would also thank Dr. Murphy and Dr. Byun for their time, patience, and advice as my committee members. Their knowledge and insight were indispensable for this research. I greatly appreciate accommodating this project especially given the current global pandemic. I would also like to thank you both for always providing constructive feedback and experimental guidance. I would also like to thank Dr. Fernandez-Palomo for providing the mouse melanoma cell line I used in this report on such short notice and providing feedback on my methods.

Thank you to all members of the Mothersill/Seymour lab for your guidance, help, emotional support, and contributing indirectly to my work. To all those I missed from our group, I am fortunate to be part of such a unique, kind, and welcoming team! Rhea Desi, thank you for the countless drives you gave me to and from school, the long chats, and support with experiments. Nathan Vo, thank you for also offering drives, providing guidance, facilitating lab upkeep and meetings, and always being available for members of the lab when problems arose or help was needed. I must thank a few previous co-op students as well, including Sam Hancock, who assisted with radioactive contamination monitoring, and Jigar Lad, who helped in troubleshooting the electronics of the nuclear instrumentation module in my first year.

To my family, including both my parents and brother, thank you for your constant, multifaceted encouragement, advice, honesty, and love. Thank you to my parents for your immeasurable support in all aspects of my life and growth as a person—none of this would have been possible without you!

Finally, to Joe E., thank you for the support, affection, and strength you provided and continue to provide. I am forever grateful to have you by my side.

TABLE OF CONTENTS

LIST OF FIGURES

LIST OF TABLES

LIST OF EQUATIONS

Chapter 1

Introduction, review of relevant radiobiological literature, and history

Abstract: The study of radiation biology is reviewed in this chapter with an introduction to the interaction of radiation with matter, brief history of the radiation sciences, targeted and non-targeted radiobiological effects, the radiation-induced bystander and associated nontargeted effects, and non-ionizing radiation. The electromagnetic bystander signal is introduced and previous experiments elucidating its nature and role in non-targeted effects is reviewed. Finally, an overview of research questions and hypotheses is provided, which outlines the experiments performed in this thesis.

1.1. Historical introduction to radiation biology

Radiation biology is the study of the effects of radiation on living things. Radiation can be defined as wave- and subatomic particle-borne energy that moves through space or a medium[1]. In the context of radiation biology, "radiation" is typically restricted to electromagnetic and particle radiations and can broadly be classified as either ionizing or non-ionizing depending on its energy[2]. Ionizing radiation carries enough energy to eject electrons from their atomic orbits to yield ions, or break chemical bonds between atoms—hence, it is considered "ionizing"[3]. This occurs primarily with higher energy radiation that carries sufficient energy to overcome the ionization energy of electrons in an atom. Upon release of charged particle radiation, such as alpha or beta particles, energy transfer occurs along the path of the particle until its kinetic energy is depleted. Unlike particle radiations, gamma or x-photon energy transfer occurs via different mechanisms—photons pass through a uniform medium with a probability of being absorbed per unit distance, which is known as the *linear attenuation coefficient* for photons in a particular medium of a particular wavelength[1]. Electromagnetic radiation can induce ionization or excitation of electrons through several mechanisms: the photoelectric effect, where complete energy transfer to the electron causes its ejection and absorption of the photon; Compton scattering, where a high-energy photon causes electron ejection and, using the remaining photon energy, results in the formation of a novel, longer-wavelength photon with a different momentum vector; and pair production at very high photon energies, where interaction with the nuclear electric field of an atom causes conversion of the photon to an electron-positron pair, with the positron combining with an electron, which yields two photons in annihilation[1,2]. The photoelectric effect also produces characteristic x-rays which are emitted due to the electron vacancy, with photon energy equal to the electron's binding energy. The photoelectric effect has the greatest probability of occurring at lower photon energies in the ten or several hundred kiloelectron volt range, while Compton scattering is most likely to occur with higher photon energies in the megaelectron volt range—today, x-rays can have diverse energies between 0.1 keV to the megaelectron volt range (produced by linear accelerators), while gammas usually have energies higher than 100 keV[1,4]. Compton scattering is of the greatest relevance to human health due to gamma and x-ray irradiation, as it has the highest probability of occurring in the photon ranges most likely to be encountered by humans. The biological damage imparted by ionizing radiation on living matter is effected by these phenomena, among others, at the subatomic level.

The ionization of biological compounds is typically regarded as deleterious to the survival of a cell, although not invariably as discussed in further detail later in this chapter[5–10]. A second mechanism of energy transferal, which is shared between the ionizing and non-ionizing flavours of radiation, is the absorption of energy by electrons in atomic or molecular orbitals and the subsequent excitement of those electrons to a higher energy state[2]. The inevitable relaxation of this excited state is usually accompanied by the commensurate release of energy as a photon, which can be used in various applications[11–13]. Non-ionizing radiation typically does not carry enough energy to ionize electrons or break chemical bonds, but rather can perturb these bonds and thereby cause the destruction of larger molecules—for example, the UVB-induced formation of pyrimidine dimers in DNA[14–18]. This is believed to occur, much like with ionizing radiation, due to the excitation of electrons present in these molecules to a higher energy state and a consequent chemical reaction that changes the structure of the molecule[12,19]. For example, many organic photochemical reactions can be understood through the induction of these excited states[19–21]. These reactions are not only pertinent to life at the microscopic scale, but also to the techniques used for its study, as will be discussed in later chapters. This mechanism is also suspected to be responsible for emissions of ultraviolet light from cell cultures observed in our lab[22,23], which is discussed further later in this chapter.

The approximately Hegelian[24] phrase "we learn from history that we do not learn from history" is an appropriate encapsulation of the early history of non-targeted effects in radiation biology. While originally referring to statesmen or rulers of nation, this quotation draws attention to the general fact that those living in the present tend to forget history or the lessons that can be derived from it. It is therefore appropriate to briefly consider the history of the study of radiation and how this history ties into radiation-induced bystander effects, which are described later and are focal point of this report. An excellent review of the early history of the radiation sciences, including applications in medical technologies, can be found in Reed (2011)[25]. While the discovery of electromagnetic radiation is attributed to Herschel at the commencement of the nineteenth century, the history of the discovery and use of ionizing radiation for therapeutics began in the late nineteenth century. The discovery of Röntgen or x-radiation occurred in 1895, and shortly thereafter Marie and Pierre Curie observed the radioactive decay of chemical isotopes for the first time[25,26]. A few years later, radiation-induced bystander effects were first observed[27,28], however they were not widely understood nor recognized for decades afterward. Because the subject of this report, the physical bystander signal, is relevant to radiation therapy and protection of humans and natural environments—which is discussed in further detail in Chapter 11—a brief overview of study in these areas of radiation sciences is required.

The initial watershed experiments in radiation sciences facilitated the inception of a number of sub-disciplines, often incorporating other fields of study such as biochemistry, cell biology, medicine, and physics—these sub-disciplines include radiation biology. The discovery of radiation, followed shortly by a demonstration of the ablation of cutaneous lesions, prompted the first use of non-surgical therapies for cancer and other morbidities. During this period, researchers became aware that skin irritation is typically associated with prolonged x-radiation exposure[29]. Many different groups investigated and found some success using radiation to treat tumors. There were other trials on tuberculosis due to its reported bactericidal properties, with more limited success[30]. The potential dangers of ionizing radiation to human health were not widely appreciated during this time, and adverse outcomes were obnubilated by growing optimism. Becquerel himself reportedly experienced a radiation burns as a result of carrying a rod of radium in his coat pocket. The advent of radium therapy, an early predecessor to modern brachytherapy, occurred shortly thereafter and was characterized by some advantages over external Röntgen beam therapy. The utility of x-rays for diagnostic procedures was also appreciated this early as its usefulness for imaging became apparent[31,32]. Today, external beam radiotherapy or teletherapy typically involves fractionated doses of x-rays for the treatment of cancer[33]. Brachytherapy is also employed where a sealed source in close proximity to the tumor is used, which again resembles a more refined form of radium therapy[34]. Systemic or unsealed radioisotope therapy is also sometimes used, with radioisotopes that are delivered intravenously or by ingestion[34]. Today, clinicians can use radiopharmaceuticals that localize to specific parts of the body, such as the thyroid and bones, to target local malignancies[35–37]. Peptide radiopharmaceuticals, which are essentially proteins labelled with different radioisotopes, can also be implemented in diagnostic or therapeutic procedures[37–40]. Similarly, researchers can use radioactive tracers, or molecules containing one or more radioactive atoms, to "trace" reactants and products in chemical reactions[38,41–43]. Methods employing this clever use of radioactivity were and continue to be indispensable in elucidating the metabolic processes upon which all life is predicated[44–46]. Since the early days of radiographic diagnostic imaging, more sophisticated techniques were developed that complimented the traditional radiograph. Among the more broadly well-known types, computed tomography (CT) scans allow technologists to acquire cross-sectional images of a patient, in multiple planes, by using x-rays at different angles and computer-aided image compilation[47]. Descriptions of the myriad techniques used in radiotherapeutics and medical imaging are widely available in textbooks and are not a focus of this report, although bystander effects are likely relevant in these clinical settings due to the low-dose effects—these may occur in unexposed tissues where minimal exposure is required[48]. The

relevance of these effects also extends to other, now-ubiquitous applications of radiation sciences, such as nuclear energy.

The use of ionizing radiation for therapy was commonplace by the time that nuclear energy was pioneered, both in the generation of usable energy and in weapons of mass destruction. The first nuclear reactor was created in the early nineteen-forties. After further development and proliferation of nuclear energy, there have been numerous accidents in the use of nuclear energy, including Three Mile Island in the United States, Chernobyl in Ukraine, Fukushima in Japan—some of these incidents caused the uncontrolled exposure of workers and the public to ionizing radiation, resulting in morbidity and mortality in some cases. Incidents such as these have further informed health physicists on the effects of ionizing radiation on human health, and moreover provided some epidemiological data to assist in the modelling of large-scale disasters—becoming relevant after Chernobyl and the Allied bombing of Japan—and yielded lessons for the mitigation of potential future incidents. Protection of the environment against ionizing radiation is an increasing concern with the use of nuclear energy—typically, the emission of radionuclides in considerable quantities from sources of nuclear energy in the event of a catastrophe—but also from other sources such as coal-fired power plants[49,50]. The effects of radiation and heavy metal toxicity can be a concern due to uptake of different radionuclides by various species[51]. Moreover, decay products can linger in the environs of an intentional or unintentional release and have the potential to affect generations of animals and plants inhabiting the area. An understanding of radiation sensitivity across many phyla is still relatively poorly understood[52] and work is ongoing to piece together a complete picture of ecological or system-level radiation sensitivity. Species in an ecosystem could exhibit high sensitivity to radiation while other species may be less impacted due to a number of factors, such as metabolism, route of radionuclide uptake and excretion, sensitivity of target organs, trophic effects such as bioaccumulation, and differing genetic background and capacity for damage repair. Determining the radiosensitivity of flora and fauna is crucial to estimating risk and work is ongoing for many classes of organism, including amphibians[53]. It is important to remember that data derived from humans on radiation effects are not necessarily congruent with other species of animal. Therefore, there are gaps with respect to our understanding of how different types of radiation affect non-human species; this is especially the case with doses below 100 mGy, which are relevant for longer-term environmental exposures that occur with radionuclide release[54,55]. This dearth of information is extended further when considering non-targeted effects, which are known to be the predominate relevant biological processes in this dose range.

While it is known that radiation sensitivity can vary between species and that modelling risk is compounded further by the complexity of ecosystem interactions, it is useful to reconsider and investigate how these lower doses affect human and non-human species. To this end, it is crucial to obtain a broad mechanistic understanding of radiobiological effects, both targeted and non-targeted. Anthropologically, exposure to radiation today occurs mostly due to diagnostic and therapeutic procedures, however historically also occurred due to intentional and accidental exposure to or release of radioactivity, as discussed previously. Understanding the mechanisms by which radiation interacts with biological material may shed light on the inadequacy of the linear no-threshold (LNT) model in estimating the stochastic health effects of ionizing radiation—this and other details on the molecular interactions of radiation and biology must also be reviewed to fully appreciate the characteristics and function of radiation-induced bystander signals.

1.1.1. The targeted and non-targeted effects of ionizing radiation

Ionizing and non-ionizing radiations interact with biological systems with a degree of complexity that is commensurate with the complexity of the biological system in question. On a "macro" scale, ionizing radiation exposure can cause deterministic and stochastic health effects in humans and other animals. Deterministic effects can be reliably reproduced through exposure at a defined dose—for example, subcutaneous burns or acute radiation syndrome due to γ-irradiation[56]. Stochastic effects exhibit an increased probability of occurring with increasing dose—these effects include oncogenesis due to somatic cell exposure, effects in progeny upon stem cell (or other non-terminally differentiated cell) irradiation, or even hereditable diseases if germ cells are affected[57,58]. On a smaller scale and traditionally in cell radiobiology, the biological effects of ionizing radiation are grouped into targeted and non-targeted effects[2]. A targeted effect occurs due to the direct interaction of the ionizing radiation with biochemicals, such as DNA, lipids, and proteins. The energy carried by the radiation damages these compounds by breaking covalent bonds and displacing electrons from their respective orbitals. Non-targeted effects occur "out of the field" of radiation and can be conceptualized as indirect exposure. For example, the radiolysis of water produces reactive oxygen species that oxidize biochemicals, such as DNA, lipids, and proteins; the energy carried by the radiation results in the decay of a non-organic molecule, the increased concentration of highly reactive and damaging compounds, and culminates in the indirect damage of organic matter. A diagram of the various ROS that can be produced upon ionizing radiation exposure can be found in figure 7.6—reactive oxygen species (ROS) are discussed in further detail in chapter 7.

In order to determine how potential exposures could affect a population, several models have proposed a relationship between dose and stochastic effects. Deterministic effects are usually not modelled in the same way because, again, the effects typically manifest consistently above a higher dose threshold and are not as relevant to doses below that threshold. The LNT model estimates stochastic health effects, including risk of genetic mutations, cancer formation, and developmental (or "teratogenic") effects. The LNT model asserts that no lower threshold exists for health effects and ergo no safe dose exists for humans[59–62]. Moreover, sets of smaller doses are believed to cumulatively increase the risk of health effects. While it is known that high doses of ionizing radiation produce deterministic and stochastic risks to human health, the applicability of the model to lower doses is contentious[55,59–61]. Many assert that observed effects at lower doses are incongruous with the LNT model[59,61], although it is still sometimes used today to estimate rates of low-dose induction of cancer and mortality[55,62]. Two other models include the threshold model, which asserts no risk to health at doses below a threshold, and the radiation hormesis model, which claims that low doses can be beneficial to health[63,64]. Some also contend that the LNT model facilitated widespread radiophobia following the Chernobyl disaster, promulgated by physicians, leading to an increase in the number of unnecessary abortions performed in certain parts of Europe as fears of teratogenic outcomes and heritable diseases persisted[65–67]. In any case, the main subject of this report, the physical bystander signal, does not lend verisimilitude to the LNT model because it appears to be significant at lower doses, while it may be "quenched" at higher doses where the magnitude of targeted effects preponderates indirect, non-targeted effects; this is believed due to previous findings reported in the literature[68,69] and the physical signal's relationship to other radiation-induced bystander effects[70].

Many biomolecules constitute life as we know it, however these molecules are themselves constituted of a panoply of molecular bonds, functional groups, and combinations thereof. The immediate biomolecular damage due to ionizing radiation begins promptly with the breakage of bonds between sulphur, oxygen, nitrogen, hydrogen, and carbon atoms[3]. Additionally, the same radiation produces

chemical species that cause nitrosative stress in a cell less than a second following irradiation[3]; a more extensive introduction to these chemicals and oxidative stress can be found in section 7.1. The outcome of this damage is typically cell cycle arrest to repair DNA damage, protein destruction and modulation of signalling, and lysis[3,71,72].

There are theoretically many different targeted effects because there are many types of biomolecules that constitute a cell, which can vary in composition—for example, protein isoforms or gene families in the same organism[73,74], orthologous genes in different species[75], and phospholipid varieties in cell and mitochondrial membranes[76–78]—and abundance between tissues (e.g. Tau proteins in neural tissue[79]), individuals in a population, and across species. However, for many years the primary focus of radiation biologists were DNA lesions and the consequent formation of cancer. This was likely due to the idea that mutations were closely associated with oncogenic transformation and the collection of epidemiological data on new cancers in the survivors of the Hiroshima and Nagasaki bombing in 1945. It was believed for some time that, theoretically, the more exposure one has to ionizing radiation, the greater the chance that they harbour oncogenic mutations in either their germline or soma. The discovery that biological responses to radiation are not necessarily commensurate with dose—particularly at low doses below 100 mGy—prompted critical evaluation of models assessing health risk based primarily on risk of oncogenic DNA damage[80–82]. Reviewed interest in non-targeted effects followed with an increased appreciation of tumor metabolism and microenvironment, genetic background, and adaptive responses[81]. For example, dosage, oxidative stress, and a variety of other factors can influence the viability of a cell population and can even promote survival, as is the case with radioadaptive responses[83,84]. There is now considerable research indicating that cells adapt and improve outcomes if irradiated at a low dose followed by a higher challenge dose[8,85–89]. The attenuation of chromosomal aberration formation has been observed in cultured cells that have adapted to radiation exposure. Genomic instability has also been observed, along with associated transgenerational effects. Such phenomena can be expanded to include the concept of lethal mutations, which kill cells following several rounds of cell disivison[90–92]. Several groups have found that the progeny of directly irradiated cells show an increase in chromosomal defects as a result of radiation-induced genomic instability. This demonstrated that the effects of radiation can persist in cell populations derived from directly exposed cells.

Non-targeted effects come in a variety of types. However, a lot of these effects have been shown to be related. For example, genomic instability has been observed in cells that received a bystander signal[93–95]. The effects have also been termed differently in the literature over the decades. Mothersill et al. 2018[96] is an extensive review of non-targeted effects, including genomic instability, bystander effects, adaptive responses, clastogenic factors, and abscopal effects. A clastogen is usually a chemical that produces breakage or disruption of chromosomal structure; these factors have been described as plasma-borne in the literature and appear after direct irradiation. Transferral of these to tissue cultures produces these chromosomal aberrations and are evidence for a bystander signal *in vivo*. Circulating factors in the blood may also cause abscopal effects in malignant tissues. These effects result in secondary tumor shrinkage upon irradiation of a primary tumor—this is further evidence of a kind bystander effect *in vivo.* In order to understand these effects and the subject of this thesis, the physical bystander signal, a review of radiation-induced bystander effects and their relation to other phenomena is useful.

1.1.2. Radiation-induced bystander effects and related non-targeted effects

Radiation-induced bystander effects (RIBE) cover a variety of phenomena related to radiation exposure that have been known in the literature for many years. A bystander effect occurs when a cell or population of cells responds similarly to cells that have been directly irradiated, without being irradiated themselves.

It is now known that this occurs due to the release of different types of signalling factors by the directly irradiated cells (or "donor cells") and uptake by neighboring, unexposed cells (or "recipient cells" or "reporter cells"). As with the conception of "ionizing" and "non-ionizing" radiation, discussed later, both terms are also somewhat guilty of conveying conceptions of roles that lack nuance with respect to the complexity of RIBE. The terms "donor" and "reporter" seem to imply that donor cells alone produce the signal and reporter cells respond to this signal. However, evidence from our laboratory indicates that recipients of the bystander signal can themselves emit bystander signals in the form of small, extracellular vesicles known as exosomes[70]. It is due to the propagation of these signals beyond the initially irradiated cells that the terms "donor" and "recipient" are themselves not quite adequate to describe the entities in this system. Nevertheless, insofar as they represent broadly applicable experimental categories in the lab, these designators are useful. For the purposes of this report, "donor cells" refer to cells in the experiment that are hypothesized to emit bystander signals upon exposure to ionizing radiation, and "reporter cells" are cells that are hypothesized to show bystander effect after exposure to the signal. In order to appreciate the importance of the bystander effect to radiation biology, understanding the history of its study, the types of bystander signals, the various signs of a bystander effect, and related effects should be reviewed.

Interest in RIBE has waxed in recent history, although evidence for a bystander signal can be found in the literature from approximately a century ago. A comprehensive review of the history of bystander and related effects can be found in Mothersill et al. (2018)[82]. As described, a resurgence of interest in non-targeted effects and a shift in focus away from DNA-centric effects—particularly targeted DNA damage—occurred relatively recently in the field of radiation biology. Radiation-induced bystander effects were known as far back as the first decade of the twentieth century when early experiments on Röntgen radiation by Heineke in 1905[28] demonstrated their existence *in vivo*—not even a generation following the discovery of radioactivity! As early as 1941, it was demonstrably clear that the immediate area around a patch of human skin exposed to a beam will exhibit inflammation[97,98]. Much earlier than this, Heineke et al. explored the production of "lymphoid elements" upon irradiation of tumors in mice[82,99]. Further research by Murphy and Morton[100] (1915) showed that removal of tumors from mice, irradiation of the same mice, and surgical reimplantation of the tumors resulted in greater tumor shrinkage and better survival than a control group. Strangeway and Fell[101] (1927) described that radiations can "liberate into circulation, from the tissues, a substance which acts either as a toxin on certain cells, or as a stimulant to certain general organic chemical reactions"; while more fittingly describing abscopal effects or clastogens, knowledge of radiobiological effects outside of those cells directly traversed by particles is clear. McNaughton[102] (1930) reviewed the literature and described mutations that were "produced indirectly through the intermediary agency of injurious chemical substances or physical conditions that become diffused through the cell as a result of the irradiation of [a targeted cell]". Therefore, it is evident that some understanding of bystander effects has been available in the literature for over one hundred years. Another study by Pant and Kamada[103] (1977) demonstrated that plasma harvested from atomic bomb survivors can induce chromosomal breaks in cultured leukocytes more than thirty years after an exposure event. It can therefore be deduced that the propagation of the signal by descendant somatic cells can

occur following the irradiation of a progenitor cell, and that this associates bystander effects with transgenerational effects *in vivo.*

Modern research on RIBE began with a paper by Nagasawa and Little[104] (1992). The authors measured a bystander effect upon exposure of cells to low doses of alpha particles, showing sister chromatid exchanges in cells not traversed by an alpha particle beam. This paper was published among many others that questioned the existing fundamental concepts of radiation biology[80,90,105–111], including a paper that pioneered the irradiated cell-conditioned medium transfer technique (ICCMTT)[112] that is used to assess soluble-factor induced bystander effects in our lab and others to this day. As reviewed in Mothersill et al.[82], there were several key findings and observations that led to a paradigm shift toward non-targeted effects:

I. *De novo* radiobiological effects in unexposed cells, which neighbor exposed cells.
II. *De novo* radiobiological effects in unexposed cells, descended from exposed cells.
III. Cell radiation responses vary depending on several factors, not just DNA damage.

And several deductions, therefore:

i. Radiation damage is not necessarily irrevocable.
ii. Radiation damage can be communicated to unexposed cells.
iii. Irradiated and non-irradiated cells in a population do not behave independently of the population.

The significance of non-targeted effects was the subject of extensive and ardent debate during this period as the dogma of targeted, DNA-centric effects was challenged. The prevailing system of belief held that radiobiological effects occur because cells are hit by radiation directly, which results in mutations that ultimately may kill the cell, are repaired, or not influence cell viability. Much like the antecedent, exploratory phases of the radiological sciences in the late nineteenth and early twentieth centuries—which were concerned with elucidating the properties of ionizing radiation—the nuance, importance, and even utility of non-targeted effects were not fully understood nor appreciated until much later. Many resisted the shift in focus to more inclusive and holistic notions of radiobiological effects, contesting the relevance of non-targeted effects in radiation therapy, protection and dosimetry with respect to humans, and protection of the environment[113–118]. However, the juxtaposition of these two eras of history is made less appropriate by the fact that many decades of research existed before the "rediscovery" of non-targeted effects, which is in stark contrast to the dearth of literature prior to Röntgen's and the Curies' discovery of radiation and radioactivity, respectively—so we run into the paradoxically timeless Hegelian phrase for a second time.

The initial experiments that led to the elucidation of the bystander signal using cell cultures started in the late nineties (Mothersill et al. 1997). ICCMT was used to show that certain cell lines respond with apoptosis or cell cycle arrest, measured by the clonogenic survival assay, following exposure to ICCM. Mothersill and Seymour first demonstrated that cell-to-cell contact was not required for communication of the bystander signal in this paper, which uses ICCMT. In this procedure, cells are directly irradiated, the medium harvested and cell debris filtered, and then the medium is introduced to unexposed cultures. This also indicated that some signal existed in the medium in the form of soluble factors that induce bystander responses in reporters. Another group (Azzam et al.[109,119,120]) examined gap junctions and determined that the bystander signal can be propagated via these intercellular channels between connected cells. Soon

after, a series of experiments near the turn of the millennium characterized the soluble factor-borne bystander signal[69,121,122]—parameters including temperature, the presence of cells, metabolism, and mitochondrial effects were documented in subsequent experiments[123,124]. Candidates for the soluble factor(s) responsible are discussed further later in this chapter. It was noted that cells carrying a mutation in *TP53* (discussed in further detail in chapter 3) were able to produce the signal but were unable to respond to it[125,126]. Other experiments confirmed these findings, and other lab groups have investigated the role of p53 in bystander responses[127–129]. Further experiments showed that the bystander effect, like other non-targeted effects, appears to be most significant at lower doses. Additionally, it was observed that RIBE may saturate at higher doses[69]. The implications of RIBE are far-reaching and affect many facets of the radiation sciences[130].

There are several RIBE that should be discussed. Among the earliest discovered, chromosomal damage by clastogenic factors is one, which indicates that the signal can produce DNA damage much like direct exposure. Reduction in reproductive survival, including apoptosis and cell cycle arrest, have also been reported[112,131,132]. The expression of transcription factors such as AP-1 can occur following upstream activation of the classical MAPK pathway, and this has been implicated in RIBE as well[133]**.** The MAPK (or Ras-Raf-MEK-ERK pathway) communicates extracellular growth signals—typically upon binding of a mitogen, or factor that stimulates mitosis, to the EGFR transmembrane receptor—to the cell and, upon activation, promotes cell division. Calcium signalling has also been identified as an effect of receiving the bystander signal[134]. A very important characteristic of the bystander signal is that it appears to produce oxidative stress, and that these highly reactive chemical species might act to communicate cell damage intercellularly following exposure[135,136]. Mitochondrial effects have also been observed, including mutations, inner membrane depolarization, and morphological changes[124,137,138]. Moreover, various types of signals exist and are even known to coordinate in the propagation of the bystander signal[70].

Since it was demonstrated that cell-to-cell contact was not necessary for the communication of bystander signals[121], many have investigated which soluble factors may be involved. It was later determined, after extensive experimentation, that both gap-junction communication and soluble factor communication can produce a similar effect in recipient cells. Among reactive oxygen species (ROS), other factors have been demonstrated to be involved in producing bystander effects. Nitric oxide, has also been implicated in RIBE[139–142]. Cytokines such as TNF-α and interleukin-8[143–145], which are typically involved in inflammatory responses as constituents of innate immunity, have also been identified as candidates for bystander signalling molecules; this suspicion is logically sound because the indirect effects of ionizing radiation have been known for some time to produce inflammatory responses, as previously described. TGF-β was also identified as a candidate, which controls proliferation, differentiation, and different kinds of effects depending on cell type[146,147]. It has been observed that TGF-β acts in a similar manner with TNF-α in inducing transformation and may result in apoptosis if TGF-β dysregulation occurs[148,149]. Serotonin was also implicated as a putative bystander molecule by several groups along with cyclogenase-2[150]. More recently, the release of exosomes from directly irradiated cells and their uptake in cells receiving medium transfer was demonstrated by several groups to produce bystander effects[70]. Hence, it was hypothesized that whatever factors were present in these exosomes were candidates for a bystander molecule. Another group identified non-coding RNAs packaged in the exosomes as candidates[151].

The discovery of light emission from directly irradiated cells in our lab also prompted further investigation by our group. It was determined that irradiated cells can, in turn, emanate electromagnetic radiation at various wavelengths[23]. Further investigation demonstrated that this secondary photon

release can induce a reduction in survival in adjacent cells not exposed to radiation nor medium harbouring soluble factors[152]. It was soon realized that these emissions represented a novel bystander signal that may act independently or in consort with soluble factor signals *in vitro* and *in vivo*. This "electromagnetic" or "physical" or "UVA" or "biophoton" bystander signal is the primary focus of this report and experiments were performed to better characterize the signal and effects thereof. However, before describing the properties of this signal, it is crucial to understand some properties of non-ionizing radiation and the biological effects associated with exposure—because the spectra of the signal associated with biological effects is considered non-ionizing, it is imperative that the principles of these effects be understood to some degree.

1.1.3. Overview of non-ionizing radiation and effects on living systems

The demarcation between ionizing and non-ionizing electromagnetic frequencies has not been universally defined, as different atoms and molecules undergo ionization at different energies. However, generally the boundary is believed to fall somewhere in the ultraviolet (UV) range. Electromagnetic radiation can be described as "non-ionizing" in the context of radiation biology, and, as described previously, carries enough energy only to excite electrons to a higher energy state. However, this characteristic belies its potentially nocuous nature. For example, DNA damage due to gamma and x-radiation has been extensively studied; however, pyrimidine dimers may form when DNA is exposed to less-than-ionizing radiations[153].

Most of the sun's light that we are routinely exposed to is approximately 95% UVA and 5% UVB[154,155]. It is known that UVA exposure can cause sunburn and irreversible damage to skin and is also associated with some skin cancers—the mode of DNA damage occurring indirectly through the generation of ROS[153,156–158]. Light of this wavelength penetrates to more basal cells in the dermis and stimulates the release of melanin in melanocytes. UVB also causes tanning, albeit delayed, and is generally preferentially absorbed by more apical cells in human skin[159–161]. Light in this range stimulates the production of Vitamin D and melanogenesis[160]. Due to the higher energy, this type also directly produces pyrimidine dimers. Because melanin absorbs UV light, it is believed by some that this is an evolutionarily conserved mechanism for protection from harmful solar spectra in humans. Both UVA and UVB can damage proteins in the extracellular matrix—collagen and elastin, in particular—leading to the premature aging of skin[161–163].

When discussing non-ionizing radiation, the notion of thermal effects is also encountered. The deposition of energy into a system by UV radiation often culminates in the increase of the kinetic energy of the particles in that system. This can occur at wavelengths higher than those in the scope of this report and the increase of temperature depends largely on energy and intensity of the incident light. The biological effects of non-ionizing radiations are routinely dichotomized into "thermal" and "non-thermal" categories[164–166]. A thermal effect is generally limited to heating, while the production of ROS by UVA and subsequent DNA damage is considered to be a non-thermal effect[162].

1.2. An electromagnetic bystander signal

In the era of radiation biology that focused mostly on soluble factor-mediated non-targeted effects—including bystander effects, abscopal effects, "indirect effects", and clastogenic factors—another type of signal altogether was missed. As mentioned, UV-light emission from living cells following exposure to

ionizing radiation was discovered in our lab. Further investigation showed that this light could induce a reduction in survival and a host of other effects in unexposed reporter cells. We have termed this radiation-induced photon emission "biophotons", which is the main subject of this thesis.

Biophotons can be viewed as a novel radiobiological phenomenon not identified until recent times. It can be argued, however, that biophotons have been known for some time and represent a kind of invisible radioluminescence. The notion and application of radiation-induced light emission can be traced to more than a century ago when radium was used to produce self-illuminating clock dials. Essentially, a solution containing a radionuclide—which naturally emits alpha particles along with gamma rays, but whose daughter radionuclides also emit beta particles—can be mixed with a substance, or "phosphor", that emits light upon exposure to ionizing radiation[13]. The applications of radioluminescence included emergency signs, firearm sights, and wristwatches. The manifestation of the physical bystander signal is suspected share this mechanism; rather than ionizing electrons in biological molecules, the energy of the incident radiation is absorbed by these electrons. Consequently, the electrons occupy a higher energy state, and it is the relaxation of this state that produces photon emission.

Light emission due to ions has been documented by several studies, especially with polymers[23]**.** Initial experiments on this electromagnetic signal were conducted by Dr. Bilal Ahmad in our lab[23], and focused primarily on emissions in the ultraviolet range**.** Ahmad first demonstrated that bombardment of polystyrene by accelerated protons produced photon emissions. Next, he tested various materials, including oyster tissue, citrus leaves, and mylar for photon emission with the same treatment. It was concluded that, because all of these produced light emissions, that reconsideration of what constitutes a bystander signal may be warranted. Similar irradiation of HPV-G, a type of transformed epithelial cell, with a beta emitter yielded an increase in 340 nm photon measurements. Moreover, the inclusion of pigmented cell growth medium decreased counts, while inclusion of non-pigmented medium further increased counts in this range. An increase in cell density produced reduced counts and it was suggested that this could be due to light emission, absorption, and scattering by cells. The work done by Ahmad and his conceptions on follow-up research laid the groundwork for further experiments conducted by Dr. Michelle Le.

Le examined light emissions from epithelial cell cultures exposed to beta-radiation[152]. She showed that the presence of cells can increase counts sixteen-fold above cell-free controls and confirmed density as a factor in photon emission[22]. Dead cells were shown to emit higher quantities of photons than living cells, and it was suspected that this could be due to yet unknown metabolic processes modulating the photoemission. It was also determined that 340 nm appeared to be the peak emission wavelength from cells[167]. Importantly, Le demonstrated a maximum reduction in survival of approximately 23%, in reporters, and after blocking wavelengths below 390 nm observed an abolishment of this effect. Introduction of melanin into reporter cultures caused attenuation of the reduction in survival. Further experiments on p53-variant cell lines showed that those lacking wild-type p53 exhibited a reduced response to the emitted photons; significant emission from donor cells was reported irrespective of p53 status[126]. Emission in HaCaT cells was observed to be less than in HCT116 cells. Le proposed that there may be a relationship between the soluble factor and electromagnetic bystander signals and confirmed this subsequently in a paper reporting the release of exosomes from reporters exposed to biophotons[70]. These exosomes were shown to reduce survival in secondary reporters, which indicated further propagation of the bystander signal beyond initial recipient cells. Le also showed mitochondrial depolarization by cells exposed to biophotons. Finally, Le found that exposure of cells to biophotons

caused a reduction of the activities of several mitochondrial respiratory complexes[168]. Another student in our lab examined whether γ-radiation can produce the same biophotons as observed in proton and beta-irradiated cultures[85]. However, significant photon emission was not observed along with no significant reduction in survival in reporter populations.

Taking these findings together, there appeared to be justification for further characterization of RIBE in bystander cells exposed to the physical signal. It appeared that cells exposed to various types of ionizing radiation can produce secondary photon emissions that produce measurable changes in neighbouring, unexposed cells. Furthermore, mitochondria appeared to play a role in this response, with modulation of mitochondrial metabolism observed in the machinery carrying out the terminal biochemical reactions of the electron transport chain. As a result of this research, several questions emerged that required investigation.

1.3. Questions, justification, hypotheses, and approach

The primary focus of this thesis are effects in bystander reporter cells and how these effects can be modulated. A feature absent in previous research on the electromagnetic bystander signal is the examination of effects due to oxidative stress. As described previously, the soluble factor-mediated bystander effect is known to produce changes in ROS and therefore affect the redox balance in the cell. All light in the UV range has the potential to generate these chemicals upon interaction with cells. Specifically, its interactions with water can produce these radicals and cause indirect damage to DNA[162,163,169]. Measurement of oxidative stress in bystander reporter cells, specifically those receiving the electromagnetic signal was not conducted in the past, even though extensive evidence exists showing promotion of oxidative stress in bystander cells. Moreover, targeted and non-targeted DNA damage can occur which may further disrupt redox homeostasis and metabolism. Additionally, among the various effects described in previous soluble factor studies, including reduction in cell survival[112], inner mitochondrial membrane depolarization[70,170], modulation of electron transport chain enzyme activity[168,171], changes in cell signalling[133,172], chromosomal aberrations and broader DNA damage[54,173], and changes in cell metabolism[137,168], all can be induced by ROS and oxidative stress. Due to these observations, measuring oxidative stress in reporter cells was considered essential. Furthermore, modelling of oxidative stress in the absence of a bystander signal was also considered important, as this could elucidate whether similar effects appear at specific concentrations of ROS. Hence, it was suspected that ultraviolet biophotons can create ROS and oxidative stress in their interaction with reporter cells.

Another factor in previous research was the observation that these bystander effects could be somehow attenuated by the introduction of an appropriate radioprotective compound. For example, Le used melanin because certain types are known to be efficient absorbers of UV light—however, it was also suggested in the same report that melanin may possess free radical scavenging properties[22]. We also wanted to examine the role of melanin in bystander effects for these two reasons. Firstly, the aforementioned property of UV light absorption, which would theoretically diminish photon emissions from cultures. Secondly, some other groups have investigated whether melanin can act as a free-radical scavenger[174,175], while others have found that it can even promote oxidative stress depending on kind of melanin in question[176,177]. Therefore, it was believed that melanin could sequester the bystander signal before it reaches reporter cells, absorb the biophotons in reporter cells, or reduce oxidative stress altogether independently of photon absorption.

1.3.1. Hypotheses

Based on previously reviewed research and reasoning, the following primary hypotheses were tested in this report:

1. Radiation-induced biophotons and ROS cause reporter cell death upon exposure.
2. Radiation-induced biophotons and ROS cause oxidative stress in reporter cells upon exposure.
3. Radiation-induced biophotons and ROS cause mitochondrial effects.
4. Melanin protects against deleterious effects due to UV-biophotons.

1.4.1. Overview of model and approach

The present thesis is a comparative study of the biological effects of ROS and radiation-induced biophotons. One of the primary goals was to show that oxidative stress can be caused by biophoton exposure and that it may underpin responses in reporters. Three epithelial cell lines were used to this end: one keratinocyte line derived from human skin (HaCaT), one epithelial line developed from a colorectal tumor (HCT116), and one murine melanoma line (B16F10). HaCaT and HCT116 have been used extensively in RIBE research and have been shown to generate both soluble bystander factors and biophotons. They also have the capability of responding to the signal. B16F10 was chosen as a comparative epithelial cell that readily and without external stimulus produces melanin in culture. Each cell line was also chosen based on relatively similar doubling times of approximately 24 hours, ranging between 18-28 hours depending on experimental conditions[178–181].

The exogenous administration of hydrogen peroxide is appropriate in the context of modelling oxidative stress in both directly irradiated cell populations and bystander reporters. In the case of direct irradiation *in vitro*, a key effector of radiobiological damage in the low-LET exposures relevant to this thesis are ROS—these can be generated endogenously in a cell via the radiolysis of water by ionizing radiation, as discussed previously[2]. However, in a cell culture environment, the majority of water exists in the cell culture medium, which can theoretically produce ROS exogenously similar to the administration of hydrogen peroxide. While previous studies have found that cells must be present for communication of a bystander signal[182,183], this may suggest the interaction of ROS with biological tissues and other factors are required for the communication of the signal. Supplementation of hydrogen peroxide in cell culture medium generates these oxidation products, such as lipid radicals, through interaction with cell membranes and cell debris. It is now known from a variety of sources that ROS are not only generated in bystander cells but are actively involved in communicating bystander responses both *in vitro* and *in vivo,* with practical applications to tumor radiotherapy suggested[88,135,136,184,185]. Therefore, supplementation of hydrogen peroxide in cell culture medium is a practical method to achieve known concentrations of ROS extracellularly in conditions that loosely represent those under which bystander reporters grow.

In order to determine whether bystander photons were produced in β-irradiated cultures, donors were irradiated in the same fashion described in publications by Le et al.[70,126,167,168]. Tritium was used at a specific activity that was administered directly into cell culture medium for a given time to yield a specific dose. Photon emissions were first detected from directly irradiated cultures using a photomultiplier tube. Bystander reporters were then exposed in different cell culture vessels depending on the assay used. The technique involving exposure was described by the aforementioned reports in detail and necessitated the shielding of all cell cultures from ambient light both prior to and during experiments.

First, plating efficiency was experimentally determined in several culture vessels that were used in later chapters. Next, partial survival curves of each cell line in response to gamma radiation were constructed to determine general radiosensitivity. The status of p53 was then confirmed in the human

cells, as this has been shown to be a requirement for cellular responses to the bystander signal. Next, the quantity of melanin both intracellularly and released into cell culture medium was estimated in B16F10 cells using the human cells as background, since those cells do not produce melanin. Confirmation of photon emissions upon beta irradiation was performed for HCT116 and HaCaT cells and determined for B16F10 cells using the same setup as Ahmad et al.[23,186]. Next, a series of experiments using cell culture medium supplemented with hydrogen peroxide and biophotons were conducted and several parameters were measured: cell survival via clonogenic survival, oxidative stress via fluorometry, metabolic activity via colorimetry, and mitochondrial viability via fluorometry. Finally, experiments using an artificial source of UV light are described, followed by discussion and suggestions for future research. A diagram of the initial plan for the experiments in this thesis is presented in Figure 1.1.

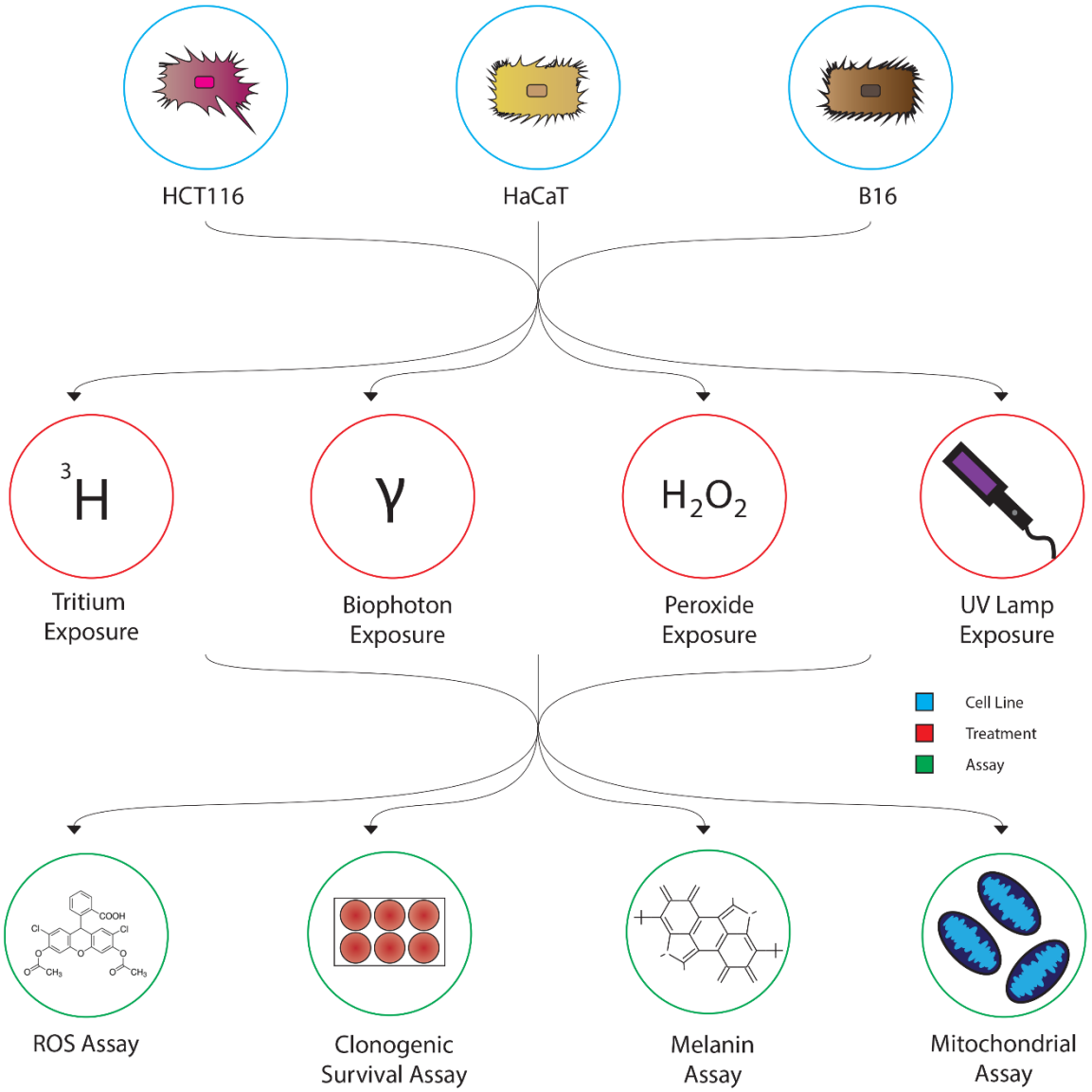

Figure 1.1: A flow diagram of the proposed experiments in this report. Three mammalian cell lines will be treated with tritium, bystander photons, hydrogen peroxide, and an artificial source of ultraviolet light. An assay for reactive oxygen species formation (DCFDA), clonogenic survival assay, melanin assay, and inner mitochondrial membrane potential assays (JC-1) were performed. This was done in addition to several other treatments and an assay for general metabolic activity (MTT) was used.

1.4. References

1. Turner JE. Interaction of ionizing radiation with matter. Health physics. 2005;88(6):520–544.

2. Hall EJ, Giaccia AJ. Radiobiology for the Radiologist. Lippincott Williams & Wilkins; 2006.

3. Reisz JA, Bansal N, Qian J, Zhao W, Furdui CM. Effects of ionizing radiation on biological molecules--mechanisms of damage and emerging methods of detection. Antioxidants & redox signaling. 2014;21(2):260–292. https://pubmed.ncbi.nlm.nih.gov/24382094. doi:10.1089/ars.2013.5489

4. Turner JE. Atoms, radiation, and radiation protection. John Wiley & Sons; 2008.

5. Mitchell SA, Marino SA, Brenner DJ, Hall EJ. Bystander effect and adaptive response in C3H 10T½ cells. International journal of radiation biology. 2004;80(7):465–472.

6. Zhou H, Randers-Pehrson G, Waldren CA, Hei TK. Radiation-induced bystander effect and adaptive response in mammalian cells. Advances in Space Research. 2004;34(6):1368–1372.

7. Bosi A, Olivieri G. Variability of the adaptive response to ionizing radiations in humans. Mutation Research/Fundamental and Molecular Mechanisms of Mutagenesis. 1989;211(1):13–17.

8. Joiner MC, Lambin P, Malaise EP, Robson T, Arrand JE, Skov KA, Marples B. Hypersensitivity to very-low single radiation doses: its relationship to the adaptive response and induced radioresistance. Mutation Research/Fundamental and Molecular Mechanisms of Mutagenesis. 1996;358(2):171–183.

9. Matsumoto H, Tomita M, Otsuka K, Hamada MH and N. Nitric Oxide is a Key Molecule Serving as a Bridge between Radiation-Induced Bystander and Adaptive Responses. Current Molecular Pharmacology. 2011;4(2):126–134. http://www.eurekaselect.com/node/94393/article. doi:http://dx.doi.org/10.2174/1874467211104020126

10. Choi VWY, Ng CYP, Kong MKY, Cheng SH, Yu KN. Adaptive response to ionising radiation induced by cadmium in zebrafish embryos. Journal of Radiological Protection. 2013;33(1):101.

11. Yanagida T. Ionizing radiation induced emission: scintillation and storage-type luminescence. Journal of Luminescence. 2016;169:544–548.

12. Kallmann H, Dresner J. Excitation of Luminescent Materials by Ionizing Radiation. Physical Review. 1959;114(1):71.

13. Robbins DJ. On predicting the maximum efficiency of phosphor systems excited by ionizing radiation. Journal of The Electrochemical Society. 1980;127(12):2694.

14. Ng K-H. Non-ionizing radiations–sources, biological effects, emissions and exposures. In: Proceedings of the international conference on non-ionizing radiation at UNITEN. 2003. p. 1–16.

15. Andley UP, Clark BA. Generation of oxidants in the near-UV photooxidation of human lens α-crystallin. Investigative Ophthalmology and Visual Science. 1989;30(4):706–713.

16. O'Reilly P, Mothersill C. Comparative effects of UV A and UV B on clonogenic survival and delayed cell death in skin cell lines from humans and fish. International journal of radiation biology. 1997;72(1):111–119.

17. Maki CG, Howley PM. Ubiquitination of p53 and p21 is differentially affected by ionizing and UV radiation. Molecular and Cellular Biology. 1997;17(1):355–363.

18. Tada-Oikawa S, Oikawa S, Kawanishi S. Determination of DNA damage, peroxide generation, mitochondrial membrane potential, and caspase-3 activity during ultraviolet A-induced apoptosis summary. Methods in Enzymology Singlet Oxygen, UV-A, and Ozone. 2000:331–342.

19. Franck J, Dymond EG. Elementary processes of photochemical reactions. Transactions of the Faraday Society. 1926;21(February):536–542.

20. Hoffmann N. Photochemical reactions as key steps in organic synthesis. Chemical Reviews. 2008;108(3):1052–1103.

21. Inoue Y. Asymmetric photochemical reactions in solution. Chemical reviews. 1992;92(5):741–770.

22. Le M, Mothersill CE, Seymour CB, Ahmad SB, Armstrong A, Rainbow AJ, McNeill FE. Factors affecting ultraviolet-A photon emission from beta-irradiated human keratinocyte cells. Physics in medicine and biology. 2015;60(16):6371–6389. doi:10.1088/0031-9155/60/16/6371

23. Ahmad SB, McNeill FE, Byun SH, Prestwich W V, Seymour C, Mothersill CE. Ion beam induced luminescence: Relevance to radiation induced bystander effects. NUCLEAR INSTRUMENTS & METHODS IN PHYSICS RESEARCH SECTION B-BEAM INTERACTIONS WITH MATERIALS AND ATOMS. 2012;288:81–88. doi:10.1016/j.nimb.2012.05.043

24. Hegel GWF. Lectures on the Philosophy of History. G. Bell and Sons; 1861.

25. Reed AB. The history of radiation use in medicine. Journal of Vascular Surgery. 2011;53(1):35–55.

26. Scatliff JH, Morris PJ. From Roentgen to magnetic resonance imaging: the history of medical imaging. North Carolina medical journal. 2014;75(2):111–113.

27. Mothersill C, Rusin A, Fernandez-Palomo C, Seymour C, Afifi OS, Shaaban OG, Abd El Razik HA, Shams El-Dine SE-DA, Ashour FA, El-Tombary AA, et al. Synthesis and biological evaluation of purine-pyrazole hybrids incorporating thiazole, thiazolidinone or rhodanine moiety as 15-LOX inhibitors endowed with anticancer and antioxidant potential. Bioorganic chemistry. 2019.

28. Heineke H. Experimental investigations on the effects of X-rays on the bone marrow, with some remarks on the radiotherapy of leukemia and pseudoleukemia and sarcoms. Deutsche Zeitschrift für Chirurgie. 1905;78:196–230.

29. Miller RW. Delayed effects of external radiation exposure: a brief history. Radiation research. 1995;144(2):160–169.

30. Lederman M. The early history of radiotherapy: 1895–1939. International Journal of Radiation Oncology* Biology* Physics. 1981;7(5):639–648.

31. Bradley WG. History of medical imaging. Proceedings of the American Philosophical Society. 2008;152(3):349–361.

32. Hendee WR. Cross sectional medical imaging: a history. Radiographics. 1989;9(6):1155–1180.

33. Agarawal JP, Swangsilpa T, Van der Linden Y, Rades D, Jeremic B, Hoskin PJ. The role of external beam radiotherapy in the management of bone metastases. Clinical Oncology. 2006;18(10):747–760.

34. Dietrich A, Koi L, Zöphel K, Sihver W, Kotzerke J, Baumann M, Krause M. Improving external beam radiotherapy by combination with internal irradiation. The British journal of radiology. 2015;88(1051):20150042.

35. Rufini V, Castaldi P, Treglia G, Perotti G, Gross MD, Al-Nahhas A, Rubello D. Nuclear medicine procedures in the diagnosis and therapy of medullary thyroid carcinoma. Biomedicine & pharmacotherapy. 2008;62(3):139–146.

36. Pandit-Taskar N, Batraki M, Divgi CR. Radiopharmaceutical therapy for palliation of bone pain from osseous metastases. Journal of Nuclear Medicine. 2004;45(8):1358–1365.

37. Signore A, Annovazzi A, Chianelli M, Corsetti F, Van De Wiele C, Watherhouse R, Scopinaro F. Peptide radiopharmaceuticals for diagnosis and therapy. European journal of nuclear medicine. 2001;28(10):1555–1565.

38. Jamous M, Haberkorn U, Mier W. Synthesis of peptide radiopharmaceuticals for the therapy and diagnosis of tumor diseases. Molecules. 2013;18(3):3379–3409.

39. Okarvi S. Recent progress in fluorine-18 labelled peptide radiopharmaceuticals. European journal of nuclear medicine. 2001;28(7):929–938.

40. Blok D, Feitsma RIJ, Vermeij P, Pauwels EJK. Peptide radiopharmaceuticals in nuclear medicine. European journal of nuclear medicine. 1999;26(11):1511–1519.

41. Mintun MA, Raichle ME, Martin WR, Herscovitch P. Brain oxygen utilization measured with O-15 radiotracers and positron emission tomography. Journal of nuclear medicine: official publication, Society of Nuclear Medicine. 1984;25(2):177–187.

42. Witney TH, Carroll L, Alam IS, Chandrashekran A, Nguyen Q-D, Sala R, Harris R, DeBerardinis RJ, Agarwal R, Aboagye EO. A novel radiotracer to image glycogen metabolism in tumors by positron emission tomography. Cancer research. 2014;74(5):1319–1328.

43. Leyton J, Smith G, Zhao Y, Perumal M, Nguyen Q-D, Robins E, Årstad E, Aboagye EO. [18F] fluoromethyl-[1, 2-2H4]-choline: a novel radiotracer for imaging choline metabolism in tumors by positron emission tomography. Cancer research. 2009;69(19):7721–7728.

44. Marsin A-S, Bouzin C, Bertrand L, Hue L. The stimulation of glycolysis by hypoxia in activated monocytes is mediated by AMP-activated protein kinase and inducible 6-phosphofructo-2-kinase. Journal of Biological Chemistry. 2002;277(34):30778–30783.

45. Minakami S, SUZUKI C, YOSHIKAWA H. Studies on Erythrocyte Glycolysis IV. Kinetics of P i 32 Incorporation into 2, 3-Diphosphoglycerate and ATP. The Journal of Biochemistry. 1966;60(6):707–712.

46. Racker E, Resnick RJ, Feldman R. Glycolysis and methylaminoisobutyrate uptake in rat-1 cells transfected with ras or myc oncogenes. Proceedings of the National Academy of Sciences. 1985;82(11):3535–3538.

47. Buzug TM. Computed tomography. In: Springer handbook of medical technology. Springer; 2011. p. 311–342.

48. Mothersill C, Rusin A, Seymour C. Relevance of Non-Targeted Effects for Radiotherapy and Diagnostic Radiology; A Historical and Conceptual Analysis of Key Players. Cancers. 2019;11(9):1236.

49. Ćujić M, Dragović S. Assessment of dose rate to terrestrial biota in the area around coal fired power plant applying ERICA tool and RESRAD BIOTA code. Journal of environmental radioactivity. 2018;188:108–114.

50. Papp Z, Dezső Z, Daroczy S. Significant radioactive contamination of soil around a coal-fired thermal

power plant. Journal of Environmental Radioactivity. 2002;59(2):191–205.

51. Hui KS, Chao CYH, Kot SC. Removal of mixed heavy metal ions in wastewater by zeolite 4A and residual products from recycled coal fly ash. Journal of Hazardous Materials. 2005;127(1–3):89–101.

52. Adam-Guillermin C, Hertal-Aas T, Oughton D, Blanchard L, Alonzo F, Armant O, Horemans N. Radiosensitivity and transgenerational effects in non-human species. Annals of the ICRP. 2018;47(3–4):327–341.

53. Vo NTK. Environmental radiobiology of amphibians–knowledge gaps to be filled using cell lines. International Journal of Radiation Biology. 2021:1–29.

54. Lad J, Rusin A, Seymour C, Mothersill C. An investigation into neutron-induced bystander effects: How low can you go? Environmental Research. 2019;175. doi:10.1016/j.envres.2019.04.033

55. Omar-Nazir L, Shi X, Moller A, Mousseau T, Byun S, Hancock S, Seymour C, Mothersill C. Long-term effects of ionizing radiation after the Chernobyl accident: Possible contribution of historic dose. Environmental research. 2018;165:55–62.

56. Harbron R, Kelly S. The sunburn effect: deterministic effects of ionising radiation. Imaging & Therapy Practice. 2011:22.

57. O'Connor MK. Risk of low-dose radiation and the BEIR VII report: A critical review of what it does and doesn't say. Physica medica : PM : an international journal devoted to the applications of physics to medicine and biology : official journal of the Italian Association of Biomedical Physics (AIFB). 2017;43:153–158. doi:10.1016/j.ejmp.2017.07.016

58. Scott BR, Walker DM, Tesfaigzi Y, Schöllnberger H, Walker V. Mechanistic basis for nonlinear dose-response relationships for low-dose radiation-induced stochastic effects. Nonlinearity in biology, toxicology, medicine. 2003;1(1):15401420390844492.

59. Averbeck D. Does scientific evidence support a change from the LNT model for low-dose radiation risk extrapolation? Health physics. 2009;97(5):493–504.

60. Mothersill C, Seymour C. Implications for human and environmental health of low doses of ionising radiation. Journal of Environmental Radioactivity. 2014;133:5–9. http://dx.doi.org/10.1016/j.jenvrad.2013.04.002. doi:10.1016/j.jenvrad.2013.04.002

61. Belyakov O V, Folkard M, Mothersill C, Prise KM, Michael BD. Non-targeted effects of radiation: Applications for radiation protection and contribution to LNT discussion. In: Proceedings of the European IRPA Congress 2002: Towards Harmonization of Radiation Protection in Europe. 2002.

62. Boice Jr JD. The Linear-NonThreshold (LNT) Model as Used in Radiation Protection: An NCRP Update. International Journal of Radiation Biology. 2017;(just-accepted):1–47.

63. Costantini D, Borremans B. The linear no-threshold model is less realistic than threshold or hormesis-based models: an evolutionary perspective. Chemico-biological interactions. 2019;301:26–33.

64. Fukushima S, Kinoshita A, Puatanachokchai R, Kushida M, Wanibuchi H, Morimura K. Hormesis and dose–response-mediated mechanisms in carcinogenesis: evidence for a threshold in carcinogenicity of non-genotoxic carcinogens. Carcinogenesis. 2005;26(11):1835–1845.

65. Hayes RB. LNT may be lethal but ALARA is inherently useful. Health physics. 2018;115(3):391–392.

66. Jaworowski Z. Observations on the Chernobyl Disaster and LNT. Dose-Response. 2010;8(2):dose-response.

67. Jaworowski Z. Observations on Chernobyl After 25 Years of Radiophobia. 21st Century Science & Technology. 2010;2010:30–46.

68. Mothersill C, Seymour C. Uncomfortable issues in radiation protection posed by low-dose radiobiology. Radiation and Environmental Biophysics. 2013;52(3):293–298. doi:10.1007/s00411-013-0472-y

69. Liu ZF, Mothersill CE, McNeill FE, Lyng FM, Byun SH, Seymour CB, Prestwich W V. A dose threshold for a medium transfer bystander effect for a human skin cell line. RADIATION RESEARCH. 2006;166(1, 1):19–23. doi:10.1667/RR3580.1

70. Le M, Fernandez-Palomo C, McNeill FE, Seymour CB, Rainbow AJ, Mothersill CE. Exosomes are released by bystander cells exposed to radiation-induced biophoton signals: Reconciling the mechanisms mediating the bystander effect. PLOS ONE. 2017;12(3):e0173685. doi:10.1371/journal.pone.0173685

71. Eriksson D, Stigbrand T. Radiation-induced cell death mechanisms. Tumor Biology. 2010;31(4):363–372.

72. Prise KM, Schettino G, Folkard M, Held KD. New insights on cell death from radiation exposure. The lancet oncology. 2005;6(7):520–528.

73. Woloschak GE, Chang-Liu C-M, Shearin-Jones P. Regulation of protein kinase C by ionizing radiation. Cancer research. 1990;50(13):3963–3967.

74. Morgan WF, Day JP, Kaplan MI, McGhee EM, Limoli CL. Genomic instability induced by ionizing radiation. Radiation research. 1996;146(3):247–258.

75. Makarova KS, Aravind L, Wolf YI, Tatusov RL, Minton KW, Koonin E V, Daly MJ. Genome of the extremely radiation-resistant bacterium Deinococcus radiodurans viewed from the perspective of comparative genomics. Microbiology and molecular biology reviews. 2001;65(1):44–79.

76. Tyurina YY, Tyurin VA, Kapralova VI, Wasserloos K, Mosher M, Epperly MW, Greenberger JS, Pitt BR, Kagan VE. Oxidative lipidomics of γ-radiation-induced lung injury: mass spectrometric characterization of cardiolipin and phosphatidylserine peroxidation. Radiation research. 2011;175(5):610–621.

77. Budhu S, Giese R, Gupta A, Fitzgerald K, Zappasodi R, Schad S, Hirschhorn D, Campesato LF, De Henau O, Gigoux M. Targeting phosphatidylserine enhances the anti-tumor response to tumor-directed radiation therapy in a preclinical model of melanoma. Cell Reports. 2021;34(2):108620.

78. Davis HW, Vallabhapurapu SD, Chu Z, Vallabhapurapu SL, Franco RS, Mierzwa M, Kassing W, Barrett WL, Qi X. Enhanced phosphatidylserine-selective cancer therapy with irradiation and SapC-DOPS nanovesicles. Oncotarget. 2019;10(8):856.

79. Avila J, Lucas JJ, Perez MAR, Hernandez F. Role of tau protein in both physiological and pathological conditions. Physiological reviews. 2004;84(2):361–384.

80. Averbeck D. Non-targeted effects as a paradigm breaking evidence. Mutation research. 2010;687(1–2):7–12. doi:10.1016/j.mrfmmm.2010.01.004

81. Mothersill C, Seymour C. Changing paradigms in radiobiology. Mutation Research - Reviews in

Mutation Research. 2012;750(2):85–95. http://dx.doi.org/10.1016/j.mrrev.2011.12.007. doi:10.1016/j.mrrev.2011.12.007

82. Mothersill CE, Rusin A, Fernandez-Palomo C, Seymour CB. History of bystander effects research 1905-present; what is in a name? International Journal of Radiation Biology. 2018;94(8):696–707. doi:10.1080/09553002.2017.1398436

83. Wolff S. Aspects of the adaptive response to very low doses of radiation and other agents. Mutation Research/Fundamental and Molecular Mechanisms of Mutagenesis. 1996;358(2):135–142.

84. Shadley JD, Wiencke JK. Induction of the adaptive response by X-rays is dependent on radiation intensity. International Journal of Radiation Biology. 1989;56(1):107–118.

85. Cohen J, Vo NTK, Seymour CB, Mothersill CE. Parallel comparison of pre-conditioning and post-conditioning effects in human cancers and keratinocytes upon acute gamma irradiation. International journal of radiation biology. 2019;95(2):170–178.

86. Calabrese EJ, Bachmann KA, Bailer AJ, Bolger PM, Borak J, Cai L, Cedergreen N, Cherian MG, Chiueh CC, Clarkson TW, et al. Biological stress response terminology: Integrating the concepts of adaptive response and preconditioning stress within a hormetic dose-response framework. TOXICOLOGY AND APPLIED PHARMACOLOGY. 2007;222(1):122–128. doi:10.1016/j.taap.2007.02.015

87. Ryan LA, Seymour CB, O'Neill-Mehlenbacher A, Mothersill CE. Radiation-induced adaptive response in fish cell lines. JOURNAL OF ENVIRONMENTAL RADIOACTIVITY. 2008;99(4):739–747. doi:10.1016/j.jenvrad.2007.10.001

88. Maguire P, Mothersill C, McClean B, Seymour C, Lyng FM. Modulation of radiation responses by pre-exposure to irradiated cell conditioned medium. RADIATION RESEARCH. 2007;167(4):485–492. doi:10.1667/RR0159.1

89. Ryan LA, Seymour CB, Joiner MC, Mothersill CE. Radiation-induced adaptive response is not seen in cell lines showing a bystander effect but is seen in lines showing HRS/IRR response. INTERNATIONAL JOURNAL OF RADIATION BIOLOGY. 2009;85(1):87–95. doi:10.1080/09553000802635062

90. ALPER T, MOTHERSILL C, SEYMOUR CB. LETHAL MUTATIONS ATTRIBUTABLE TO MISREPAIR OF Q-LESIONS. INTERNATIONAL JOURNAL OF RADIATION BIOLOGY. 1988;54(4):525–530. doi:10.1080/09553008814551961

91. SEYMOUR CB, MOTHERSILL C. LETHAL MUTATIONS, THE SURVIVAL-CURVE SHOULDER AND SPLIT-DOSE RECOVERY. INTERNATIONAL JOURNAL OF RADIATION BIOLOGY. 1989;56(6):999–1010. doi:10.1080/09553008914552451

92. MOTHERSILL C, SEYMOUR C. THE INFLUENCE OF LETHAL MUTATIONS ON THE QUANTIFICATION OF RADIATION TRANSFORMATION FREQUENCIES. INTERNATIONAL JOURNAL OF RADIATION BIOLOGY. 1987;51(4):723–729. doi:10.1080/09553008414552241

93. Lyng FM, Seymour CB, Mothersill C. Initiation of apoptosis in cells exposed to medium from the progeny of irradiated cells: A possible mechanism for bystander-induced genomic instability? RADIATION RESEARCH. 2002;157(4):365–370. doi:10.1667/0033-7587(2002)157{[}0365:IOAICE]2.0.CO;2

94. Seymour CB, Mothersill C. Delayed expression of lethal mutations and genomic instability in the progeny of human epithelial cells that survived in a bystander-killing environment. Radiation oncology investigations. 1997;5(3):106–110.

95. Morgan WF. Is there a common mechanism underlying genomic instability, bystander effects and other nontargeted effects of exposure to ionizing radiation? Oncogene. 2003;22(45):7094.

96. Mothersill C, Rusin A, Fernandez-Palomo C, Seymour C. History of bystander effects research 1905-present; what is in a name? International Journal of Radiation Biology. 2018. doi:10.1080/09553002.2017.1398436

97. Jolles B. X-ray skin reactions and the protective role of normal tissues. The British Journal of Radiology. 1941;14(159):110–112.

98. Jolles B. A diffusible substance in irradiated tissues. Nature. 1949;164(4158):63.

99. Heineke H. Über die Einwirkung der Röntgenstrahlen auf Tiere. Mènch. Med. Wochenschr. 1903;50:2090–2092.

100. Murphy JB, Morton JJ. The lymphocyte as a factor in natural and induced resistance to transplanted cancer. Proceedings of the National Academy of Sciences of the United States of America. 1915;1(7):435.

101. Strangeway TSP, Fell HB. A Study of the Direct and Indirect Action of X-Rays upon the Tissues of the Embryonic Fowl. Proceedings of the Royal Society of London. Series B, Containing Papers of a Biological Character. 1927;102(713):9–29.

102. McNaughton S. J. Radiation and Genetics. The American Naturalist. 1930;64(692):220–251.

103. Shankar Pant G, Kamada N. Chromosome aberrations in normal leukocytes induced by the plasma of exposed individuals. Hiroshima Journal of Medical Sciences. 1977;26(2–3):149–154.

104. Nagasawa H, Little JB. Induction of sister chromatid exchanges by extremely low doses of α-particles. Cancer research. 1992;52(22):6394–6396.

105. SEYMOUR CB, MOTHERSILL C, ALPER T. HIGH YIELDS OF LETHAL MUTATIONS IN SOMATIC MAMMALIAN-CELLS THAT SURVIVE IONIZING-RADIATION. BRITISH JOURNAL OF RADIOLOGY. 1986;59(707):1138.

106. SEYMOUR CB, MOTHERSILL C. LETHAL MUTATIONS AND THEIR EFFECT ON THE APPLICATION OF RADIOBIOLOGICAL RESULTS TO RADIOTHERAPY. BRITISH JOURNAL OF CANCER. 1988;58(4):531.

107. SEYMOUR CB, MOTHERSILL C, MICHAEL BD, ALPER T. FURTHER-STUDIES ON LETHAL MUTATIONS EXPRESSED BY DISTANT DESCENDANTS OF SOMATIC-CELLS THAT HAVE SURVIVED RADIATION. INTERNATIONAL JOURNAL OF RADIATION BIOLOGY. 1986;50(5):922–923.

108. Mothersill C, Seymour C. Lethal mutations and genomic instability. INTERNATIONAL JOURNAL OF RADIATION BIOLOGY. 1997;71(6):751–758.

109. Azzam EI, de Toledo SM, Spitz DR, Little JB. Oxidative metabolism modulates signal transduction and micronucleus formation in bystander cells from α-particle-irradiated normal human fibroblast cultures. Cancer research. 2002;62(19):5436–5442.

110. Azzam EI, Raaphorst GP, Mitchel REJ. Radiation-induced adaptive response for protection against micronucleus formation and neoplastic transformation in C3H 10T1/2 mouse embryo cells. Radiation research. 1994;138(1s):S28–S31.

111. Azzam EI, de Toledo SM, Little JB. Oxidative metabolism, gap junctions and the ionizing radiation-

induced bystander effect. Oncogene. 2003;22(45):7050–7057. http://dx.doi.org/10.1038/sj.onc.1206961

112. Mothersill C, Seymour C. Medium from irradiated human epithelial cells but not human fibroblasts reduces the clonogenic survival of unirradiated cells. INTERNATIONAL JOURNAL OF RADIATION BIOLOGY. 1997;71(4):421–427.

113. Mothersill C, Seymour C. Low-dose radiation effects: Experimental hematology and the changing paradigm. EXPERIMENTAL HEMATOLOGY. 2003;31(6):437–445. doi:10.1016/S0301-472X(03)00078-X

114. Mothersill C, Seymour CB. Radiation-induced bystander effects and the DNA paradigm: An ``out of field{''} perspective. MUTATION RESEARCH-FUNDAMENTAL AND MOLECULAR MECHANISMS OF MUTAGENESIS. 2006;597(1–2):5–10. doi:10.1016/j.mrfmmm.2005.10.011

115. Mothersill C, Seymour C. Changing paradigms in radiobiology. MUTATION RESEARCH-REVIEWS IN MUTATION RESEARCH. 2012;750(2):85–95. doi:10.1016/j.mrrev.2011.12.007

116. Mothersill C, Rusin A, Seymour C. Low doses and non-targeted effects in environmental radiation protection; where are we now and where should we go? Environmental Research. 2017;159:484–490.

117. Mothersill C, Seymour C. Targets, pools, shoulders, and communication - a reflection on the evolution of low-dose radiobiology. International journal of radiation biology. 2019 Mar:1–10. doi:10.1080/09553002.2019.1589016

118. Mothersill C, Abend M, Bréchignac F, Iliakis G, Impens N, Kadhim M, Møller AP, Oughton D, Powathil G, Saenen E. When a duck is not a duck; a new interdisciplinary synthesis for environmental radiation protection. Environmental research. 2018;162:318–324.

119. Azzam EI, de Toledo SM, Little JB. Direct evidence for the participation of gap junction-mediated intercellular communication in the transmission of damage signals from α-particle irradiated to nonirradiated cells. Proceedings of the National Academy of Sciences . 2001;98(2):473–478. http://www.pnas.org/content/98/2/473.abstract. doi:10.1073/pnas.98.2.473

120. de Toledo SM, Buonanno M, Harris AL, Azzam EI. Genomic instability induced in distant progeny of bystander cells depends on the connexins expressed in the irradiated cells. International journal of radiation biology. 2017;93(10):1182–1194. doi:10.1080/09553002.2017.1334980

121. Mothersill C, Seymour CB. Cell-cell contact during gamma irradiation is not required to induce a bystander effect in normal human keratinocytes: Evidence for release during irradiation of a signal controlling survival into the medium. RADIATION RESEARCH. 1998;149(3):256–262. doi:10.2307/3579958

122. Mothersill C, Stamato TD, Perez ML, Cummins R, Mooney R, Seymour CB. Involvement of energy metabolism in the production of `bystander effects' by radiation. BRITISH JOURNAL OF CANCER. 2000;82(10):1740–1746.

123. Nugent SME, Mothersill CE, Seymour C, McClean B, Lyng FM, Murphy JEJ. Increased mitochondrial mass in cells with functionally compromised mitochondria after exposure to both direct gamma radiation and bystander factors. RADIATION RESEARCH. 2007;168(1):134–142. doi:10.1667/RR0769.1

124. Murphy JEJ, Nugent S, Seymour C, Mothersill C. Mitochondrial DNA point mutations and a novel deletion induced by direct low-LET radiation and by medium from irradiated cells. MUTATION RESEARCH-GENETIC TOXICOLOGY AND ENVIRONMENTAL MUTAGENESIS. 2005;585(1–2):127–136. doi:10.1016/j.mrgentox.2005.04.011

125. Mothersill C, Bristow RG, Harding SM, Smith RW, Mersov A, Seymour CB. A role for p53 in the response of bystander cells to receipt of medium borne signals from irradiated cells. International journal of radiation biology. 2011;87(11):1120–5. http://www.ncbi.nlm.nih.gov/pubmed/21831006. doi:10.3109/09553002.2011.610866

126. Le M, Mothersill CE, Seymour CB, Rainbow AJ, McNeill FE. An Observed Effect of p53 Status on the Bystander Response to Radiation-Induced Cellular Photon Emission. Radiation Research. 2017;187(2):169–185. http://www.bioone.org/doi/10.1667/RR14342.1. doi:10.1667/RR14342.1

127. Widel M, Lalik A, Krzywon A, Poleszczuk J, Fujarewicz K, Rzeszowska-Wolny J. The different radiation response and radiation-induced bystander effects in colorectal carcinoma cells differing in p53 status. Mutation Research - Fundamental and Molecular Mechanisms of Mutagenesis. 2015;778:61–70. http://dx.doi.org/10.1016/j.mrfmmm.2015.06.003. doi:10.1016/j.mrfmmm.2015.06.003

128. Koturbash I, Loree J, Kutanzi K, Koganow C, Pogribny I, Kovalchuk O. In vivo bystander effect: cranial X-irradiation leads to elevated DNA damage, altered cellular proliferation and apoptosis, and increased p53 levels in shielded spleen. International journal of radiation oncology, biology, physics. 2008;70(2):554–562. doi:10.1016/j.ijrobp.2007.09.039

129. Lorimore SA, Rastogi S, Mukherjee D, Coates PJ, Wright EG. The influence of p53 functions on radiation-induced inflammatory bystander-type signaling in murine bone marrow. Radiation research. 2013;179(4):406–415.

130. Azzam EI, Colangelo NW, Domogauer JD, Sharma N, de Toledo SM. Is Ionizing Radiation Harmful at any Exposure? An Echo That Continues to Vibrate. Health physics. 2016;110(3):249–251. doi:10.1097/HP.0000000000000450

131. Singh H, Saroya R, Smith R, Mantha R, Guindon L, Mitchel REJ, Seymour C, Mothersill C. Radiation induced bystander effects in mice given low doses of radiation in vivo. Dose-Response. 2011;9(2):225–242. doi:10.2203/dose-response.09-062.Singh

132. Mothersill CE, Moriarty MJ, Seymour CB. Radiotherapy and the potential exploitation of bystander effects. INTERNATIONAL JOURNAL OF RADIATION ONCOLOGY BIOLOGY PHYSICS. 2004;58(2):575–579. doi:10.1016/j.ijrobp.2003.09.038

133. Lyng FM, Maguire P, McClean B, Seymour C, Mothersill C. The involvement of calcium and MAP kinase signaling pathways in the production of radiation-induced bystander effects. RADIATION RESEARCH. 2006;165(4):400–409. doi:10.1667/RR3527.1

134. Poon RCC, Agnihotri N, Seymour C, Mothersill C. Bystander effects of ionizing radiation can be modulated by signaling amines. ENVIRONMENTAL RESEARCH. 2007;105(2):200–211. doi:10.1016/j.envres.2006.12.003

135. Jiang Y, Chen X, Tian W, Yin X, Wang J, Yang H. The role of TGF-β 1–miR-21–ROS pathway in bystander responses induced by irradiated non-small-cell lung cancer cells. British journal of cancer. 2014;111(4):772–780.

136. Widel M, Przybyszewski WM, Cieslar-Pobuda A, Saenko Y V, Rzeszowska-Wolny J. Bystander normal human fibroblasts reduce damage response in radiation targeted cancer cells through intercellular ROS level modulation. Mutation Research/Fundamental and Molecular Mechanisms of Mutagenesis. 2012;731(1–2):117–124.

137. Nugent S, Mothersill CE, Seymour C, McClean B, Lyng FM, Murphy JEJ. Altered mitochondrial

function and genome frequency post exposure to gamma-radiation and bystander factors. International journal of radiation biology. 2010;86(February 2017):829–41. doi:10.3109/09553002.2010.486019

138. O'Dowd C, Mothersill CE, Cairns MT, Austin B, Lyng FM, McClean B, Talbot A, Murphy JEJ. Gene Expression and Enzyme Activity of Mitochondrial Proteins in Irradiated Rainbow Trout (Oncorhynchus Mykiss, Walbaum) Tissues In Vitro. RADIATION RESEARCH. 2009;171(4):464–473. doi:10.1667/RR1484.1

139. Matsumoto H, Takahashi A, Ohnishi T. Nitric oxide radicals choreograph a radioadaptive response. Cancer Research. 2007;67(18):8574–8579. doi:10.1158/0008-5472.CAN-07-1913

140. Matsumoto H, Hayashi S, Hatashita M, Ohnishi K, Shioura H, Ohtsubo T, Kitai R, Ohnishi T, Kano E. Induction of radioresistance by a nitric oxide-mediated bystander effect. Radiation research. 2001;155(3):387–396.

141. Shao C, Furusawa Y, Aoki M, Matsumoto H, Ando K. Nitric oxide-mediated bystander effect induced by heavy-ions in human salivary gland tumour cells. International journal of radiation biology. 2002;78(9):837–844.

142. Han W, Wu L, Chen S, Bao L, Zhang L, Jiang E, Zhao Y, Xu A, Hei TK, Yu Z. Constitutive nitric oxide acting as a possible intercellular signaling molecule in the initiation of radiation-induced DNA double strand breaks in non-irradiated bystander cells. Oncogene. 2007;26(16):2330–2339. http://www.nature.com/doifinder/10.1038/sj.onc.1210024. doi:10.1038/sj.onc.1210024

143. Zhou H, Ivanov VN, Gillespie J, Geard CR, Amundson SA, Brenner DJ, Yu Z, Lieberman HB, Hei TK. Mechanism of radiation-induced bystander effect: role of the cyclooxygenase-2 signaling pathway. Proceedings of the National Academy of Sciences of the United States of America. 2005;102(41):14641–14646.

144. Hei TK, Zhou H, Ivanov VN, Hong M, Lieberman HB, Brenner DJ, Amundson SA, Geard CR. Mechanism of radiation-induced bystander effects: a unifying model. Journal of Pharmacy and Pharmacology. 2008;60(8):943–950.

145. Shareef MM, Cui N, Burikhanov R, Gupta S, Satishkumar S, Shajahan S, Mohiuddin M, Rangnekar VM, Ahmed MM. Role of tumor necrosis factor-α and TRAIL in high-dose radiation–induced bystander signaling in lung adenocarcinoma. Cancer research. 2007;67(24):11811–11820.

146. Gow MD, Seymour CB, Ryan LA, Mothersill CE. Induction of Bystander Response in Human Glioma Cells using High-Energy Electrons: A Role for TGF-beta 1. RADIATION RESEARCH. 2010;173(6):769–778. doi:10.1667/RR1895.1

147. Yin X, Tian W, Wang L, Wang J, Zhang S, Cao J, Yang H. Radiation quality-dependence of bystander effect in unirradiated fibroblasts is associated with TGF-β1-Smad2 pathway and miR-21 in irradiated keratinocytes. Scientific reports. 2015;5:11373.

148. Ding L-H, Shingyoji M, Chen F, Hwang J-J, Burma S, Lee C, Cheng J-F, Chen DJ. Gene expression profiles of normal human fibroblasts after exposure to ionizing radiation: a comparative study of low and high doses. Radiation research. 2005;164(1):17–26.

149. Snyder AR. Review of radiation-induced bystander effects. Human & experimental toxicology. 2004;23(2):87–89.

150. Lee EG, Boone DL, Chai S, Libby SL, Chien M, Lodolce JP, Ma A. Failure to regulate TNF-induced NF-κB and cell death responses in A20-deficient mice. Science. 2000;289(5488):2350–2354.

151. Xu S, Wang J, Ding N, Hu W, Zhang X, Wang B, Hua J, Wei W, Zhu Q. Exosome-mediated microRNA transfer plays a role in radiation-induced bystander effect. RNA Biology. 2015;12(12):1355–1363. http://www.tandfonline.com/doi/full/10.1080/15476286.2015.1100795. doi:10.1080/15476286.2015.1100795

152. Le M. Investigating the Generation of Biophotons Induced by Low-Dose Beta-Irradiation and their Role in the Radiation-Induced Bystander Effect. McMaster University; 2018.

153. Premi S, Wallisch S, Mano CM, Weiner AB, Bacchiocchi A, Wakamatsu K, Bechara EJH, Halaban R, Douki T, Brash DE. Chemiexcitation of melanin derivatives induces DNA photoproducts long after UV exposure. Science. 2015. doi:10.1126/science.1256022

154. Humans IWG on the E of CR to. Solar and ultraviolet radiation. In: IARC Monographs on the Evaluation of Carcinogenic Risks to Humans. International Agency for Research on Cancer; 2012. p. 100D.

155. Diffey BL. Solar ultraviolet radiation effects on biological systems. Physics in medicine & biology. 1991;36(3):299.

156. Haywood R, Rogge F, Lee M. Protein, lipid, and DNA radicals to measure skin UVA damage and modulation by melanin. Free Radical Biology and Medicine. 2008;44(6):990–1000.

157. Greinert R, Volkmer B, Henning S, Breitbart EW, Greulich KO, Cardoso MC, Rapp A. UVA-induced DNA double-strand breaks result from the repair of clustered oxidative DNA damages. Nucleic acids research. 2012;40(20):10263–10273.

158. Armeni T, Damiani E, Battino M, Greci L, Principato G. Lack of in vitro protection by a common sunscreen ingredient on UVA-induced cytotoxicity in keratinocytes. Toxicology. 2004;203(1–3):165–178. doi:10.1016/j.tox.2004.06.008

159. Pearse AD, Gaskell SA, Marks R. Epidermal changes in human skin following irradiation with either UVB or UVA. Journal of investigative dermatology. 1987;88(1):83–87.

160. Miyamura Y, Coelho SG, Schlenz K, Batzer J, Smuda C, Choi W, Brenner M, Passeron T, Zhang G, Kolbe L. The deceptive nature of UVA tanning versus the modest protective effects of UVB tanning on human skin. Pigment cell & melanoma research. 2011;24(1):136–147.

161. Lavker RM, Gerberick GF, Veres D, Irwin CJ, Kaidbey KH. Cumulative effects from repeated exposures to suberythemal doses of UVB and UVA in human skin. Journal of the American Academy of Dermatology. 1995;32(1):53–62.

162. Cadet J, Douki T, Ravanat J. Oxidatively generated damage to cellular DNA by UVB and UVA radiation. Photochemistry and photobiology. 2015;91(1):140–155.

163. Kappes UP, Luo D, Potter M, Schulmeister K, Rünger TM. Short-and long-wave UV light (UVB and UVA) induce similar mutations in human skin cells. Journal of Investigative Dermatology. 2006;126(3):667–675.

164. Belpomme D, Hardell L, Belyaev I, Burgio E, Carpenter DO. Thermal and non-thermal health effects of low intensity non-ionizing radiation: An international perspective. Environmental pollution. 2018;242:643–658.

165. Moulder JE, Foster KR, Erdreich LS, McNamee JP. Mobile phones, mobile phone base stations and

cancer: a review. International journal of radiation biology. 2005;81(3):189–203. doi:10.1080/09553000500091097

166. Preece AW, Iwi G, Davies-Smith A, Wesnes K, Butler S, Lim E, Varey A. Effect of a 915-MHz simulated mobile phone signal on cognitive function in man. International journal of radiation biology. 1999;75(4):447–456.

167. Le M, McNeill FE, Seymour C, Rainbow AJ, Mothersill CE. An observed effect of ultraviolet radiation emitted from beta-irradiated HaCaT cells upon non-beta-irradiated bystander cells. Radiation research. 2015;183(3):279–90. http://www.bioone.org/doi/10.1667/RR13827.1%5Cnhttp://www.ncbi.nlm.nih.gov/pubmed/25710575. doi:10.1667/RR13827.1

168. Le M, McNeill FE, Seymour CB, Rusin A, Diamond K, Rainbow AJ, Murphy J, Mothersill CE. Modulation of oxidative phosphorylation (OXPHOS) by radiation- induced biophotons. Environmental Research. 2018;163:80–87. doi:10.1016/j.envres.2018.01.027

169. Widel M, Krzywon A, Gajda K, Skonieczna M, Rzeszowska-Wolny J. Induction of bystander effects by UVA, UVB, and UVC radiation in human fibroblasts and the implication of reactive oxygen species. Free Radical Biology and Medicine. 2014;68:278–287.

170. Rusin A, Le M, Seymour C, Oughton D, Team DOWC, Mothersill C. Effect of gamma radiation on the production of bystander signals from three earthworm species irradiated in vivo. Submitted. 2018.

171. Nugent S, Mothersill CE, Seymour C, McClean B, Lyng FM, Murphy JEJ. Altered mitochondrial function and genome frequency post exposure to gamma-radiation and bystander factors. INTERNATIONAL JOURNAL OF RADIATION BIOLOGY. 2010;86(10):829–841. doi:10.3109/09553002.2010.486019

172. Nugent SM, Mothersill CE, Seymour C, McClean B, Lyng FM, Murphy JEJ. Low level radiation and bystander factor(s) damage to mitochondria. BIOCHIMICA ET BIOPHYSICA ACTA-BIOENERGETICS. 2008;1777(S):S81. doi:10.1016/j.bbabio.2008.05.319

173. Havaki S, Kotsinas A, Chronopoulos E, Kletsas D, Georgakilas A, Gorgoulis VG. The role of oxidative DNA damage in radiation induced bystander effect. Cancer Letters. 2015;356(1):43–51. http://dx.doi.org/10.1016/j.canlet.2014.01.023. doi:10.1016/j.canlet.2014.01.023

174. Różanowska M, Sarna T, Land EJ, Truscott TG. Free radical scavenging properties of melanin: interaction of eu-and pheo-melanin models with reducing and oxidising radicals. Free Radical Biology and Medicine. 1999;26(5–6):518–525.

175. Herrling T, Jung K, Fuchs J. The role of melanin as protector against free radicals in skin and its role as free radical indicator in hair. Spectrochimica Acta Part A: Molecular and Biomolecular Spectroscopy. 2008;69(5):1429–1435.

176. Denat L, Kadekaro AL, Marrot L, Leachman SA, Abdel-Malek ZA. Melanocytes as instigators and victims of oxidative stress. Journal of Investigative Dermatology. 2014. doi:10.1038/jid.2014.65

177. Galván I, Erritzøe J, Wakamatsu K, Møller AP. High prevalence of cataracts in birds with pheomelanin-based colouration. Comparative Biochemistry and Physiology Part A: Molecular & Integrative Physiology. 2012;162(3):259–264.

178. Pavez Lorie E, Stricker N, Plitta-Michalak B, Chen I-P, Volkmer B, Greinert R, Jauch A, Boukamp P,

Rapp A. Characterisation of the novel spontaneously immortalized and invasively growing human skin keratinocyte line HaSKpw. Scientific reports. 2020;10(1):15196. doi:10.1038/s41598-020-71315-0

179. Danciu C, Falamas A, Dehelean C, Soica C, Radeke H, Barbu-Tudoran L, Bojin F, Pînzaru SC, Munteanu MF. A characterization of four B16 murine melanoma cell sublines molecular fingerprint and proliferation behavior. Cancer cell international. 2013;13(1):1–12.

180. Jain M, Nilsson R, Sharma S, Madhusudhan N, Kitami T, Souza AL, Kafri R, Kirschner MW, Clish CB, Mootha VK. Metabolite profiling identifies a key role for glycine in rapid cancer cell proliferation. Science. 2012;336(6084):1040–1044.

181. Petitprez A, Poindessous V, Ouaret D, Regairaz M, Bastian G, Guérin E, Escargueil AE, Larsen AK. Acquired irinotecan resistance is accompanied by stable modifications of cell cycle dynamics independent of MSI status. International journal of oncology. 2013;42(5):1644–1653.

182. Hei TK, Zhou H, Ivanov VN. Mechanism of radiation-induced bystander effects: a unifying model. Journal of Pharmacy and Pharmacology. 2008;60(8):943–950. doi:10.1211/jpp.60.8.0001.Mechanism

183. Suzuki M, Zhou H, Geard CR, Hei TK. Effect of medium on chromatin damage in bystander mammalian cells. Radiation research. 2004;162(3):264–269.

184. Hoorelbeke D, Decrock E, De Smet M, De Bock M, Descamps B, Van Haver V, Delvaeye T, Krysko D V, Vanhove C, Bultynck G. Cx43 channels and signaling via IP 3/Ca 2+, ATP, and ROS/NO propagate radiation-induced DNA damage to non-irradiated brain microvascular endothelial cells. Cell death & disease. 2020;11(3):1–17.

185. Guo S, Zhou J, Chen X, Yu Y, Ren M, Hu G, Liu Y, Zou F. Bystander effects of PC12 cells treated with Pb(2)(+) depend on ROS-mitochondria-dependent apoptotic signaling via gap-junctional intercellular communication. Toxicology letters. 2014;229(1):150–157. doi:10.1016/j.toxlet.2014.05.026

186. Ahmad SB, McNeill FE, Prestwich W V, Byun SH, Seymour C, Mothersill CE. Quantification of ultraviolet photon emission from interaction of charged particles in materials of interest in radiation biology research. NUCLEAR INSTRUMENTS & METHODS IN PHYSICS RESEARCH SECTION B-BEAM INTERACTIONS WITH MATERIALS AND ATOMS. 2014;319:48–54. doi:10.1016/j.nimb.2013.10.012

Chapter 2

Plating efficiency in experimental vessels and γ-irradiation

Abstract: This chapter covers attempts to determine the effect of cell culture vessel and seeding density on plating efficiency for three mammalian cell lines: HaCaT, HCT116, and B16F10. T25 and 6-well plates were seeded at various clonogenic densities. It was determined that variance in plating efficiency between cell lines and seeding densities were mostly within the error range expected in clonogenic survival assay experiments, and therefore that the cell culture vessels and seeding densities examined do not produce a consistent significant change in plating efficiency. The sensitivity of each cell line to gamma radiation was assessed between 0.1–3.0 Gy, and survival curves were fitted to the linear quadratic (LQ) and multitarget (MT) models. HaCaT and HCT116 exhibited similar responses to gamma radiation, although a more comprehensive dose range is required to comment on potentially different sensitivities at higher doses. Finally, an irradiated cell-conditioned medium (ICCM) transfer was conducted, with bystander donors exposed to 3 Gy of gamma radiation, to unirradiated reporter cells. The expected significant reduction in survival was not obtained; however, the emission of photons from directly irradiated cultures, which is discussed in later chapters, did produce a bystander response.

2.1. Introduction

Several types and variants of cell culture vessels were utilized in experiments, as necessitated by the different techniques performed throughout this report. Different volumes of growth medium were used in each of these vessels, and therefore there was different overall nutritional availability between vessels. Moreover, different seeding densities are typically used between vessels. Knowing plating efficiencies are considered particularly important for assays measuring clonogenicity or reproductive cell survival, there was a requirement to determine the plating efficiencies associated with these vessels. To determine the variance in plating efficiency, cells can be seeded at different densities and a clonogenic survival assay conducted. The two main cell culture vessels used in experiments were the T25 flask and 6-well plate. While others were used to culture cells, including the 96-well plate, performing a similar clonogenic survival assay was not considered a possibility because colonies visible to the naked eye are needed.

By the advent of radiotherapy, it was recognized that the cell-killing potential of radiation had medical utility. The first ever *in vitro* cloning of a human cell was performed in 1953 and the first immortalized human cell line, HeLa, was developed[1]. Soon thereafter, attempts to mathematically model cell killing were made. Puck and Marcus[2] invented a method for assaying the cell-killing potential of radiation some time ago—they called it the "clonogenic survival assay". In principle, the assay measures the ability of a treatment to reduce reproductive cell survival, or clonogenicity. While similar experiments were conducted prior to this report, this technique allowed radiation biologists to better model radiation responses *in vitro.* Moreover, the assay was and continues to be useful for modelling tumor responses to radiotherapy and drugs, and for assaying the sensitivity of different cell lines or primary cells to ionizing radiation.

It was soon appreciated, following the advent of the cell survival curve, that cells respond differently to ionizing radiation depending on a number of factors. High linear energy transfer (LET) or "densely ionizing" radiations, including those composed of heavier particles such as alphas, produce different responses than irradiation with "sparsely ionizing", low LET radiations, like betas or gammas. The mechanisms of radiation interacting with matter is described in further detail in section 1.1, wherein the processes of absorption of a photon, including the photoelectric and Compton effects, are described. Gammas and other high-energy electromagnetic radiation are usually described as "low LET" due to these mechanisms of interaction with matter. High LET radiation typically produces a survival trend against dose that is linear with a linear dose scale and logarithmic survival scale. Low LET radiations conversely display trends that show a linear shoulder followed by a curved region, if the data are plotted on a semi-log graph.

Construction of a survival curve with increasing doses of radiation plotted against surviving fraction is a common starting point in *in vitro* research in radiation biology. In order to practice and collect data using the clonogenic survival assay, as well as determine the sensitivity of my cells to γ-radiation, cells were exposed to γ-radiation at controlled doses and surviving colonies counted. Furthermore, it has been demonstrated that soluble factor-mediated bystander effects can occur following exposure to bystander photons[3]. It was thus considered important—in addition to showing the effect due to a physical signal—to demonstrate a reduction in survival following transfer of irradiated cell conditioned medium (ICCM). This may also be accomplished by exposure to γ-radiation, as demonstrated previously in the literature[4,5], by using the ICCM transfer technique (described in detail in the preceding chapter).

The use of γ-radiation was not continued after this chapter. As previously discussed, γ-radiation should act in a way that produces photon emissions theoretically due to processes such as the Compton effect. The use of the Taylor Radiation Source in experiments done previously produced significant photon emissions[6] but bystander effects due to this signal were not observed. Due to this and the known success of previous experiments using β-radiation[3,7–9], tritium was used instead using a procedure developed by

Le et al. This procedure showed promising findings using a much lower dose rate—dose rates more applicable to environmental-type exposures and other low-dose exposures—and irradiations conducted in the absence of ambient light, which would be impossible using the TRS. The use of tritium was similarly deemed to be more robust and was used in subsequent chapters. Nevertheless, characterization of survival under general low-LET radiation is still considered to be useful because general radiosensitivity can be estimated. Furthermore, low-LET radiations are relevant to direct damage as well as RIBE, as it is known that ROS contribute to the damage imparted by gammas[10].

As indicated previously, the purpose of these experiments was to measure variance in plating efficiency across a range of cell seeding densities in T25 culture flasks and 6-well plates. It was hypothesized that this variance may exist however will not affect experimental parameters significantly if properly controlled for. Additionally, these experiments will facilitate the collection of survival curve data for γ-radiation at a relatively high dose rate. The generation of a standard survival curve, likely featuring a linear shoulder followed by a quadratic reduction in survival with increasing dose, was expected. Finally, an experiment will be conducted to demonstrate ICCM-mediated bystander effect. It was predicted that, following a standard protocol for medium transfer, that a significant reduction in survival will occur in reporter cell cultures.

2.2. Methods

2.2.1. Cell culture

Three cell lines were used and cultured using standard cell culture and subculture protocols. HCT116 is an adherent colorectal carcinoma cell line that is used widely in radiobiological research. The cell line is also used in other studies on tumorigenicity and potentially ameliorative drugs of utility in cancer therapy[3,8,11–13]. These cells contain a mutation in codon 13 of the KRAS proto-oncogene and readily proliferate when provided with nutrients required growth. Such oncogenic mutations in the KRAS gene cause aberrant signalling in the downstream MAPK pathway, which in turn causes increased nuclear signalling for growth and proliferation via gene expression[14,15]. A variant of the cell line containing wild type *TP53,* which codes for functional p53 on both chromosomes, was used. This cell line was maintained using a protocol outlined in previous papers from our lab[12,16]. The cells were cultured at least weekly in Gibco Roswell Park Memorial Institute medium (RPMI) supplemented with 10% fetal bovine serum (FBS), 2 mM L-glutamine, 100 u/mL penicillin, and 100 uL streptomycin sulfate in 75 cm^2 Falcon culture flasks. Stock and experimental cell cultures were incubated in 95% humidified air and 5% CO_2 at 37°C.

HaCaT, another human cell line, was also used. These cells are immortalized, non-transformed keratinocytes and have also been used extensively in RIBE research[9,17–19]. HaCaT cells are aneuploid and harbor mutations on both copies of *TP53.* HaCaT cells were similarly cultured in Roswell Park Memorial Institute medium (RPMI) supplemented with 10% fetal bovine serum (FBS), 2 mM L-glutamine, 100 u/mL penicillin, 100 uL streptomycin sulfate, and 1% hydrocortisone solution in 75 cm^2 Falcon culture flasks. Stock and experimental cell cultures were incubated in 95% humidified air and 5% CO_2 at 37°C.

B16F16 is a mouse melanoma cell line that was also used due to its high melanin content. These cells were received in mid-2020 as a kind gift from Dr. Fernandez-Palomo of the Institute of Anatomy in the University of Bern, Switzerland. The mouse p53-coding gene, *Trp53*, is known to be wild type on both chromosomes and produce functional p53. The cells were originally grown in DMEM containing 4 mM L-glutamine, 4500 mg/L glucose, 1 mM sodium pyruvate, and 1500 mg/L sodium bicarbonate and 10% FBS (ATCC® 30-2002™). Later, high-glucose Gibco® medium was supplemented with 1 mM sodium pyruvate,

4 mM L-glutamine, and 10% FBS for use in culture. Cell cultures were maintained according to the same procedure followed for HCT116 and HaCaT.

All cell lines were subcultured every four to seven days after flasks reached 80-90% confluence. Cells were then passaged into fresh 75 cm^2 Falcon flasks. Dissociation of HCT116 cells was achieved using a 1:4 solution of 0.25% trypsin and 1 mM EDTA. HaCaT and B16F10 cells were dissociated from the flask using a 1:2 solution of 0.25% trypsin and 1 mM EDTA. Following disposal of culture medium, 5 mL of dissociation buffer was placed in the flask. The flask was then gently agitated for roughly 30 seconds and the dissociation buffer discarded. This was done to wash out residual medium, which is known to neutralize the dissociation buffer. An additional 5 mL of dissociation buffer was added to the flask. Cells were incubated under growth conditions for approximately five to seven minutes until they were observed to begin detaching. The addition of an equal or greater volume of complete culture medium to the flask to neutralize the dissociation reagent was performed. Cells were then mixed into a single cell suspension by pressing the serological pipette against the bottom of the flask while aspirating and dispensing the solution. 1 mL of this cell stock solution was then transferred into a new T75 Falcon flask. Cell lines were cultured and seeded separately in a laminar flow cabinet to prevent cross-contamination.

To ensure cell viability during periods of disuse, all three cell lines were cryopreserved in liquid nitrogen follow standard procedures in our lab. Briefly, cells were grown such that roughly $1x10^7 – 2x10^7$ were obtained in each culture flask. The cells were then detached as previously described using trypsin. The cell suspension was centrifuged in a VWR clinical centrifuge at 1500 RPM for five minutes. The supernatant was discarded, and the cell pellet thereafter resuspended in complete culture medium. 900 µL of this cell suspension was pipetted into Sarstedt Cryovials containing 100 µL culture-grade DMSO. These vials were placed in a Mr. Frosty™ Freezing container in a Styrofoam container with dry ice overnight. The next day, the vials were moved to the liquid nitrogen freezer and stored until needed.

Vials were thawed rapidly when cells were required. Upon removal from the liquid nitrogen, the vial was placed in a plastic bag. The vial was agitated in a hot water bath at 37°C until the solution therein flowed freely when inverted. The vial was promptly emptied into a T75 flask containing 20 mL of complete growth medium. After incubating at standard growth conditions overnight, the medium was changed to rid the cultures of cryopreservatives, such as DMSO, and the cells passaged as normal following the usual growth period.

2.2.2. Determination of plating efficiency via clonogenic survival assay

All cells were cultured regularly and passaged the week before an experiment. On the day of an experiment, cells were subcultured and plated in either T25 flasks or 6-well plates containing 5 mL and 3 mL complete growth medium, respectively. The cells were plated at varying densities ranging from 100-700 cells.

The cells were left to grow for the clonogenic period of nine days whereupon colonies became visible to the naked eye. A 1:3 solution of carbol fuschin and water was used to stain the cells. Briefly, fresh stain was prepared the day of staining. 5 mL stain was added to T25 flasks, while 3 mL stain was added to each well in 6-well plates. The vessels were allowed to incubate with the stain for 5 minutes, on the bench, after which the stain was discarded. The vessels were washed at least twice with water and left to rack dry. Following a drying period, colonies in each flask and well were counted manually. Colonies of 50 or more cells were discriminated and scored, while smaller colonies were not counted. Three separate trials were conducted with T25 flasks with three technical replicates (n=9) in all experiments in

this chapter, while the six-well plate trials utilized six replicate measurements with two biological replicates (n=12).

2.2.3. Taylor Radiation Source irradiation

The Taylor Radiation Source (TRS) is a source that is used for research purposes at McMaster University. The source contains a known quantity of caesium-137 and is routinely used to irradiate cell cultures by members of our lab and others at the university. The TRS contains roughly 37 tBq caesium-137 and is located at McMaster University (Hamilton, Canada). Caesium-137 first undergoes beta decay but is associated with gamma radiation as well. Irradiations were conducted such that the complete dose given to the cells were from gamma rays. About 95% of ^{137}Cs decays through beta decay to metastable isotope of barium (^{137m}Ba), the half life of which is 153 seconds. The decay of the metastable barium to its ground state produces gamma emissions, which account for the complete dose given to the cells considering beta particle attenuation in air. The cells were irradiated using a previously established procedure. The flasks were positioned 30 cm away from the opening of the source at a dose rate of 226 mGy/min. The dose given to the flasks was modified by changing the exposure time. Doses of 0.0, 0.1, 0.5, 1.0, and 3.0 Gy were given to cells seeded at clonogenic density in T25 flasks. Bystander cell donors were irradiated at 3.0 Gy.

2.2.4. Irradiated cell-conditioned medium transfer (ICCMT)

On the day of subculture, 100 000 cells were seeded in a T75 flasks and allowed to grow in 20 mL growth medium for 8 days. At eight days, the donors and reporter cells were seeded from this initial flask, each containing 5 mL growth medium. Donor cell flasks were seeded with 100 000 cells and reporter flasks with 500 cells. The flasks were then incubated for 6 hours at standard growth conditions. The donor cells were irradiated at the TRS and then incubated for an additional 1 hour. The donor medium was then collected and pooled together with medium from the same replicate flasks. This medium was filtered using a syringe filter to remove cells and cell debris. The reporter culture medium was discarded and replaced with filtered donor medium. The reporter cells were then left to incubate for a clonogenic period of 9 days, after which the cells were stained and counted as previously described.

2.2.5. Statistical analysis

The flask counts were inputted into GraphPad Prism 7. Statistical tests were performed with the aid of the Graphpad Prism 7 application. One-way ANOVA was used to determine statistical significance of the results along with Tukey's Honestly Significant Difference (HSD) test (α=0.05) and the results were plotted in the same program. Other statistical tests and curve fitting was performed using this program. Experiments for plating efficiency were performed in triplicate for three biological replicates in T25 flasks (n=9), while those in 6-well plates were performed with 6 technical replicates for 2 biological replicates (n=12). Each radiation survival curve experiment was performed in triplicate for 4 biological replicates (n=12). Finally, for the bystander experiment, 3 independent experiments were conducted in triplicate (n=9).

2.3. Results

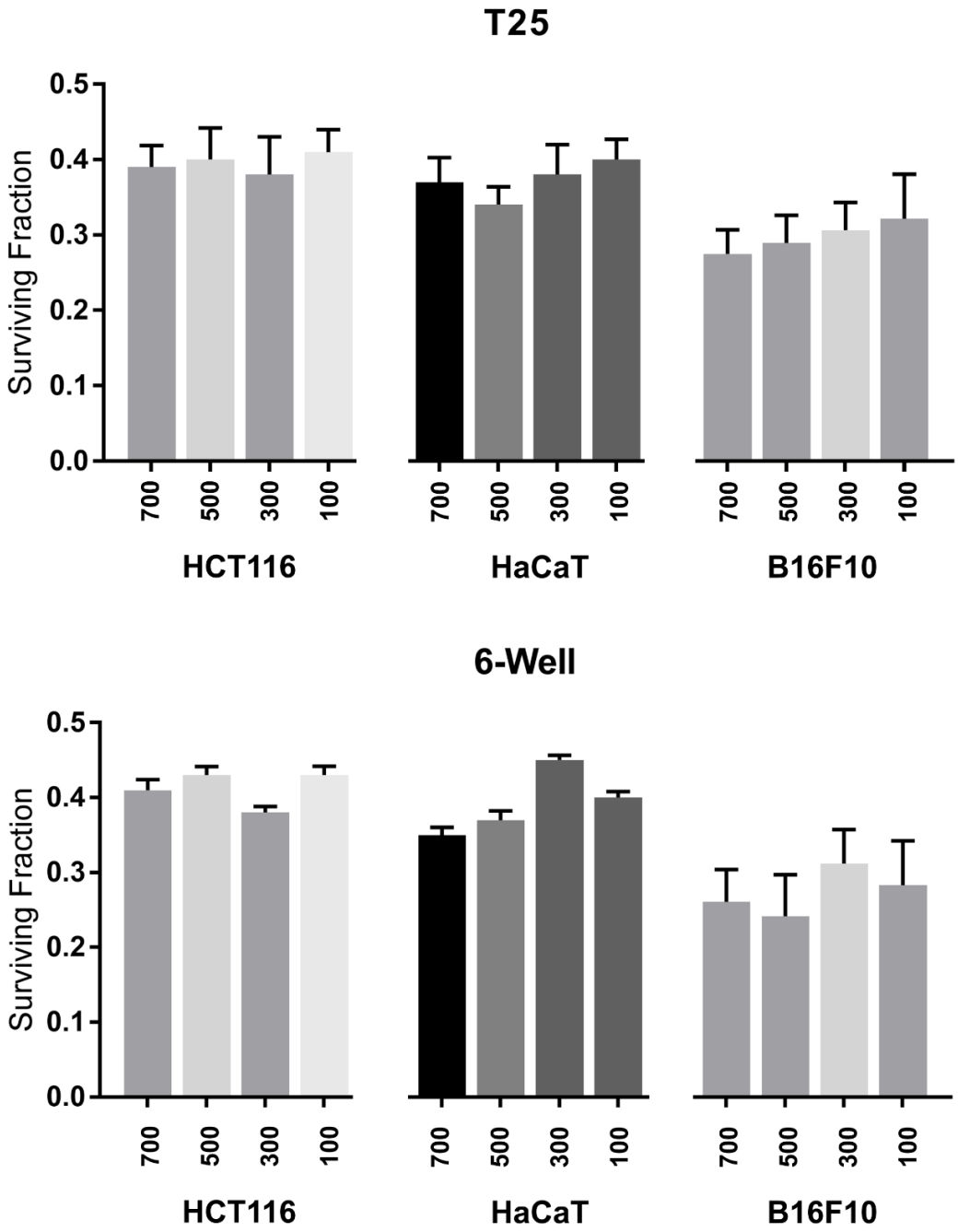

Figure 2.1: Plating efficiencies for HCT116, HaCaT, and B16F10 cells in both T25 flasks and 6-well plates. The numbers on the x-axes indicate the number of cells plated and the y-axes represent the fraction of surviving cells.

2.3.1. Plating efficiency results

The results in Figure 2.1 show plating efficiencies obtained from HCT116, HaCaT, and B16F10 plated at various densities in T25 flasks and 6-well plates. Differences in plating efficiency between the cell lines was observed. The average plating efficiency, or survival fraction, between the two culture vessels and for each respective cell line was determined to be 0.41 ± 0.069 for HCT116, 0.37 ± 0.062 for HaCaT, and 0.30 ± 0.031 for B16F10.

In the T25 group for both HCT116 and HaCaT cells, most data pairs were not significantly different from one another in each group after normalizing the data. One exception was the HaCaT 100 cells vs HaCaT 500 cells groups, which were significantly different from one another at α=0.05. This is contrasted with results in 6 well plates. These data showed more significant differences between multiple densities. These included many HCT116 and HaCaT seeding densities. This data is available in Table 2.1 below. In B16F10, only one comparison was significantly different. This comparison was between the 300 and 500 cells seeded in 6-well plates, with a difference in plating efficiency of 7%.

VESSEL	CELL LINE	COMPARISON (TUKEY)	MEAN DIFF.	95% CONFIDENCE INTERVAL	SIGNIFICANT?	ADJUSTED P
T25	HCT116	700/500	-0.01	-0.06208 to 0.04208	ns	0.9987
		700/300	0.01	-0.04208 to 0.06208	ns	0.9987
		700/100	-0.02	-0.07208 to 0.03208	ns	0.9281
		500/300	0.02	-0.03208 to 0.07208	ns	0.9281
		500/100	-0.01	-0.06208 to 0.04208	ns	0.9987
		300/100	-0.03	-0.08208 to 0.02208	ns	0.6192
	HaCaT	700/500	0.03	-0.02208 to 0.08208	ns	0.6192
		700/300	-0.01	-0.06208 to 0.04208	ns	0.9987
		700/100	-0.03	-0.08208 to 0.02208	ns	0.6192
		500/300	-0.04	-0.09208 to 0.01208	ns	0.2561
		500/100	-0.06	-0.1121 to -0.007916	*	0.0132
		300/100	-0.02	-0.07208 to 0.03208	ns	0.9281
	B16F10	700/500	-0.01	-0.06914 to 0.03968	ns	0.8829
		700/300	-0.03	-0.0861 to 0.02272	ns	0.4050
		700/100	-0.05	-0.1012 to 0.007585	ns	0.1120
		500/300	-0.02	0.07137 to 0.03745	ns	0.8327
		500/100	-0.03	-0.08651 to 0.02232	ns	0.3940
		300/100	-0.02	-0.06954 to 0.03928	ns	0.8745
6-WELL	HCT116	700/500	-0.02	-0.03345 to -0.006548	***	0.0003
		700/300	0.03	0.01655 to 0.04345	****	<0.0001
		700/100	-0.02	-0.03345 to -0.006548	***	0.0003
		500/300	0.05	0.03655 to 0.06345	****	<0.0001
		500/100	0	-0.01345 to 0.01345	ns	>0.9999
		300/100	-0.05	-0.06345 to -0.03655	****	<0.0001
	HaCaT	700/500	-0.02	-0.03345 to -0.006548	***	0.0003
		700/300	-0.1	-0.1135 to -0.08655	****	<0.0001
		700/100	-0.05	-0.06345 to -0.03655	****	<0.0001
		500/300	-0.08	-0.09345 to -0.06655	****	<0.0001
		500/100	-0.03	-0.04345 to -0.01655	****	<0.0001
		300/100	0.05	0.03655 to 0.06345	****	<0.0001
	B16F10	700/500	0.02	-0.03619 to 0.07519	ns	0.7863
		700/300	-0.05	-0.1068 to 0.004581	ns	0.0824
		700/100	-0.02	-0.07819 to 0.03319	ns	0.7042
		500/300	-0.07	-0.1263 to -0.01492	**	0.0079
		500/100	-0.04	-0.09769 to 0.01369	ns	0.1986
		300/100	-0.03	-0.02708 to 0.0843	ns	0.5234

Table 2.1. Results from Tukey's HSD test for all groups for HaCaT and HCT116 cells. Both cell lines indicate significant differences in normalized plating efficiency for multiple comparisons. Statistical significance (*) is at α=0.05.

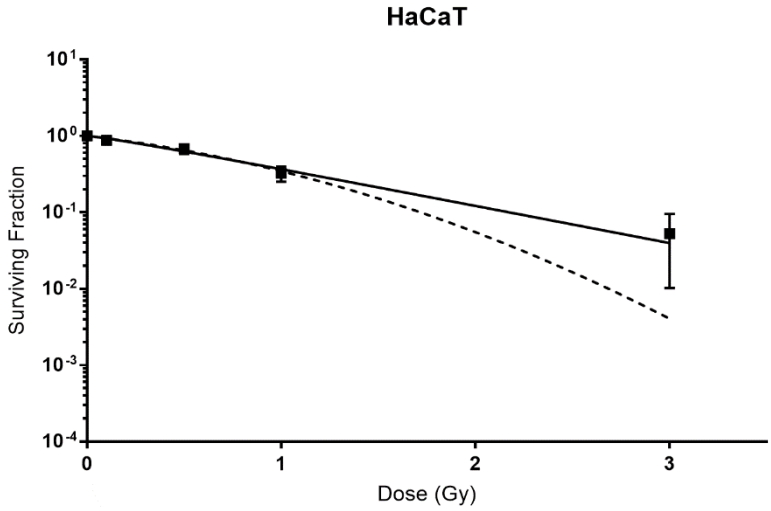
HaCaT
Surviving Fraction
10^{1}
10^{0}
10^{-1}
10^{-2}
10^{-3}
10^{-4}
0
1
2
3
Dose (Gy)

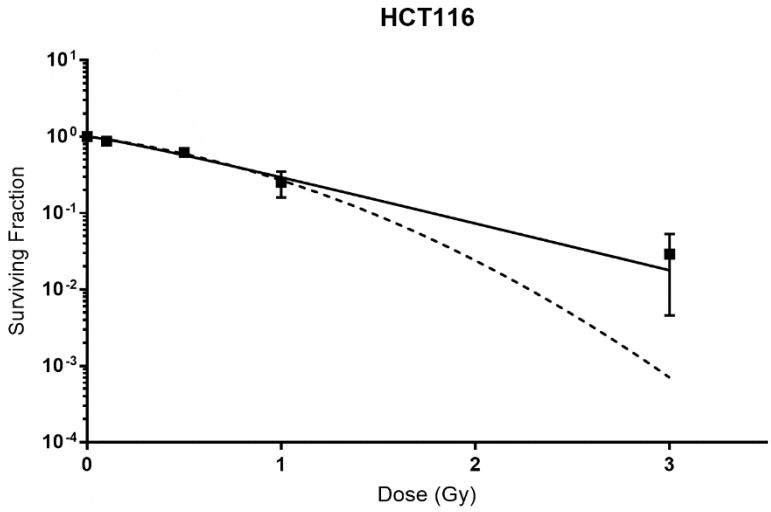
HCT116
Surviving Fraction
10^{1}
10^{0}
10^{-1}
10^{-2}
10^{-3}
10^{-4}
0
1
2
3
Dose (Gy)

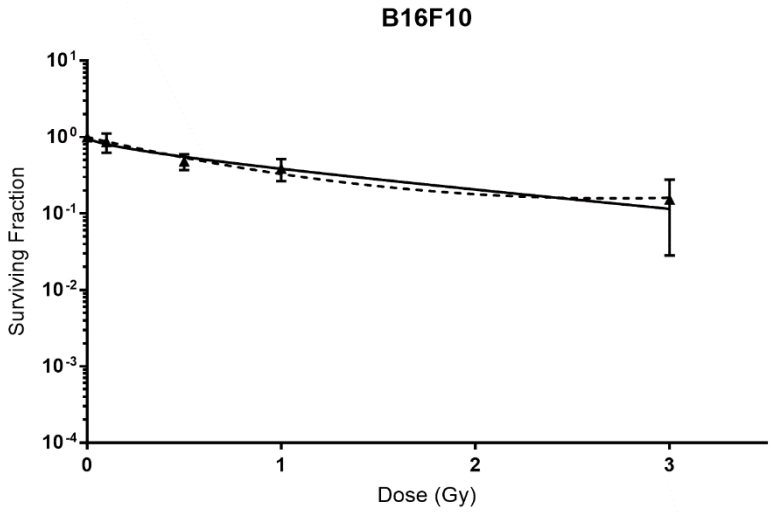
B16F10
Surviving Fraction
10^{1}
10^{0}
10^{-1}
10^{-2}
10^{-3}
10^{-4}
0
1
2
3
Dose (Gy)

Figure 2.2: Survival curves for HaCaT, HCT116, and B16F10 following exposure to gamma radiation from the TRS source. The dashed line indicates a linear-quadratic fit of the data and the solid line represents a multitarget fit of the data. Summary data for the fit of both models is available in Table 2.2. Error is shown in standard deviation of the mean.

LQ	*HaCaT*	*HCT116*	*B16F10*
α	0.6798	0.7645	1.365
β	0.3858	0.5521	-0.2521
a (S.E.)	0.1346	0.1351	0.1345
b (S.E.)	0.1695	0.181	0.05485
Degrees of Freedom	58	58	58
R square	0.9522	0.9641	0.8197
A. Sum of Squares	0.3666	0.2979	1.267
Sy.x	0.07951	0.07166	0.1478

MT	*HaCaT*	*HCT116*	*B16F10*
D_0	0.8885	0.7066	1.845
n	1.16	1.244	0.5569
D_0 *(S.E.)*	0.1102	0.07869	0.457
n (S.E.)	0.1523	0.1595	0.09692
Degrees of Freedom	58	58	58
R square	0.951	0.9606	0.8147
A. Sum of Squares	0.3759	0.3267	1.302
Sy.x	0.08051	0.07506	0.1498

Table 2.2: Summary data for the survival curve fits for each cell line, using both the linear quadratic (LQ) and multitarget (MT) models. α is the linear coefficient of the LQ curve and β is the quadtradic component conatsant. D_0 is the dose that gives, on average, one hit per target. This is governed by Poisson statistics and some cells receive more or less hits than others. At $D=D_0$, the survival fraction is 0.37, and D/D_0 is the average number of hits per cell at a given dose. The term n was originally concieved as the number of targets per cell, however is now referred to as the "extrapolation number"; at n=1, the survival curve appears close to high-LET radiation, while higher values indicate the presence of a shoulder commonly observed with gamma radiation. The use of these terms to form the model equations is shown under Equation 2.1.

$$SF = e^{-\propto D - \beta D^2} \quad (1)$$

$$SF = 1 - (1 - e^{-D/D_0})^n \quad (2)$$

Equation 2.1: Linear Quadratic (LQ; 1) and multitarget (MT; 2) equations.

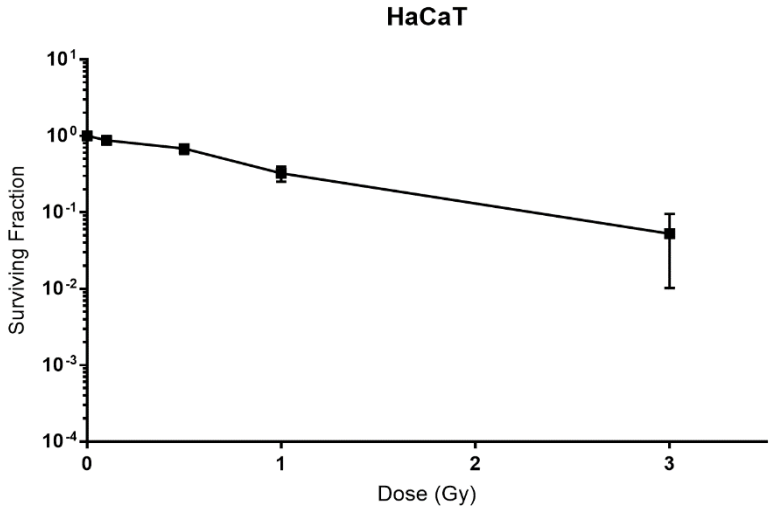
HaCaT
Surviving Fraction
10^{1}
10^{0}
10^{-1}
10^{-2}
10^{-3}
10^{-4}
0
1
2
3
Dose (Gy)

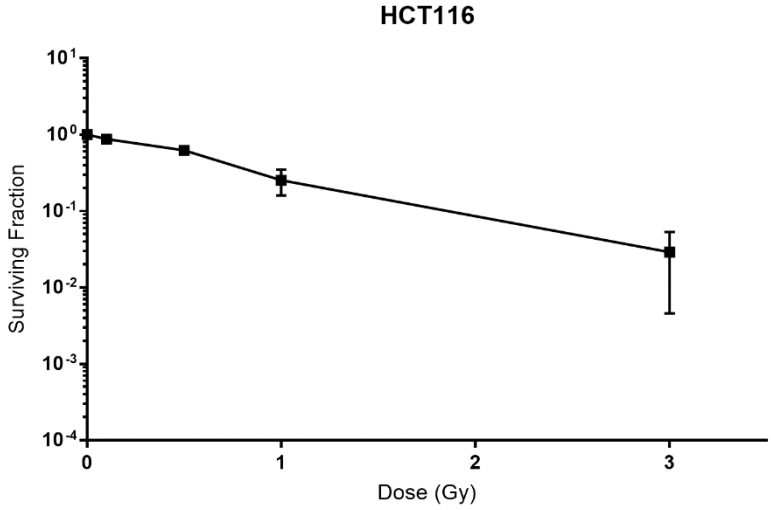
HCT116
Surviving Fraction
10^{1}
10^{0}
10^{-1}
10^{-2}
10^{-3}
10^{-4}
0
1
2
3
Dose (Gy)

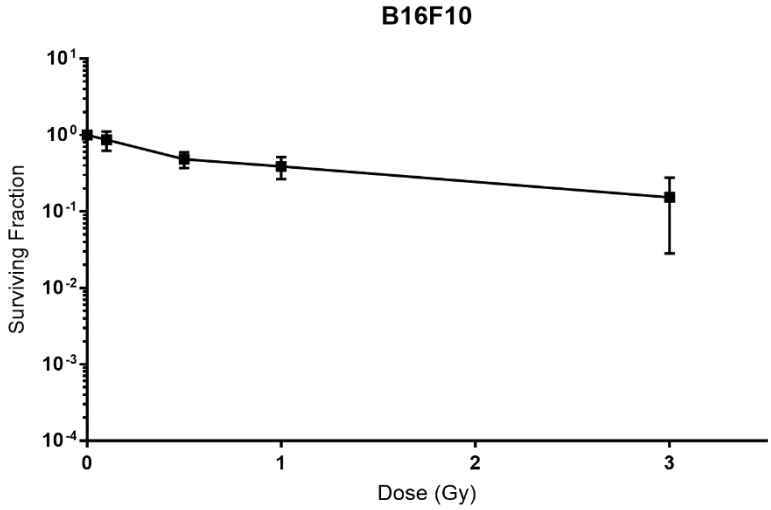
B16F10
Surviving Fraction
10^{1}
10^{0}
10^{-1}
10^{-2}
10^{-3}
10^{-4}
0
1
2
3
Dose (Gy)

Figure 2.3: The same data as plotted in Figure 2.1 but without fit lines. Error is similarly shown as standard deviation of the mean.

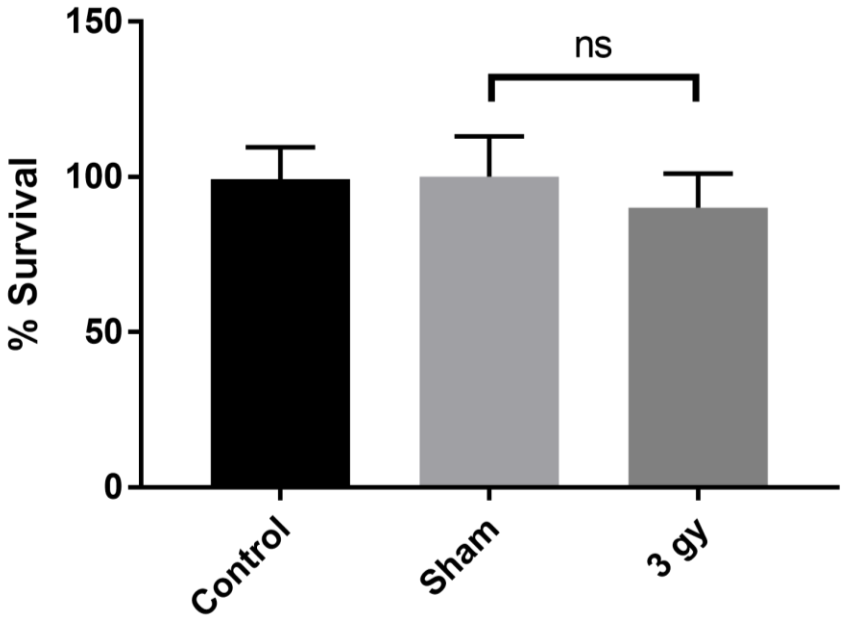

Figure 2.4: Survival fractions of bystander reporter cell populations exposed to various culture media. Medium from control flasks remained in the incubator during the course of the experiment. Medium from sham flasks was transported as if destined for irradiation, however received no dose. Medium from the 3 Gy group was harvested from flasks exposed to 3 Gy gamma radiation from the Taylor Radiation Source.

2.3.2. γ-irradiation survival curves

HCT116 cells and HaCaT cell produced relatively similar survival curves. Figure 2.2 shows survival curves for 0, 0.1, 0.5, 1.0, and 3.0 Gy for HaCaT, HCT116, and B16F10. The sham irradiated HaCaT group exhibited a slight but insignificant increase in clonogenic survival, which was not observed in the HCT116 sham irradiated group. HCT116 showed decreased survival overall compared to HaCaT with the same doses; however, this difference was not statistically significant for any dose up to 3 Gy. Linear-quadratic and multitarget fits of the data are shown in Figure 2.2.

2.3.3. Soluble factor bystander assay

An assay for bystander effects was conducted on HCT116 cells at the 3 Gy dose point. This relatively high dose was chosen because it was assumed that a greater dose may yield a stronger bystander signal before a threshold, which is based on previous research. Results from this assay are shown in Figure 2.3. While there was an observed reduction in survival in bystander reporters that received medium from donors exposed to 3 Gy, it was not statistically significant (p=0.099).

2.4. Discussion

As previously described, plating efficiency is an important concept in radiation biology. It is relevant for both direct irradiation and bystander experiments. In direct irradiation, according to target theory, the survival fraction of cell populations is related to the chance of a cell being traversed by a photon or other particle. It follows therefore that a higher density of cells present in a given field over a given time would increase probability of a cell in that population being traversed by a particle in a manner that is lethal. In bystander experiments, those involving ICCM specifically, it is believed that bystander signals present in cell culture medium may be quenched if the reporter cell population is too high[18,20] For electromagnetic bystander experiments, an ideal cell density of 2000 cells/cm^2 was determined by Le et al.[18] for photon emission, as higher densities may result in photon absorption by cells. Hence, careful ascertainment of plating efficiency was required.

By varying the cell culture vessel and medium used for culture, it was initially expected that differences in plating efficiency between the cell lines would be negligible. This was believed because it was not expected that the increased number of cells in culture would be enough to consume medium-borne nutrients or affect pH enough to influence cell proliferation and survival. The results in Figure 2.1 and Table 2.1 show data that tested this hypothesis.

The results in both types of vessels show that some observable and statistically significant change in variance in plating efficiency exists when changing cell culture vessel. It is important to note that error bars are lower in the 6-well plates most likely due to experimental design—specifically, the presence of additional replicates and not because the vessel inherently reduces plating efficiency. This is also suspected to produce the significant effects reported in Table 2.1. While indicative of significant differences, it is important to note the difference in the means between each group. Specifically, the difference be observed as being less than 5% between most comparisons in both T25 and 6-well plates for both HaCaT and HCT116. This error is expected when conducting clonogenic survival assays, as various factors including the random distribution of cells in a seeding solution, bubbles in this solution, and general pipetting error produces expectable differences in plating efficiency when conducting experiments. Some additional factors likely to affect plating efficiency include:

1. Not accounting for the displacement of medium volume due to cells in dilution calculations prior to seeding.
2. Minor time variations at several points between experiments.
3. Preciseness of volume selection on a micropipette.
4. Transport.

Furthermore, the standard deviation of the mean for nearly all groups seeded in T25 and 6-well plates were less than or equal to 0.05. Hence, while this test is indicative of a significant difference between groups, it is likely that technical error contributed to this difference.

Other factors could have affected this observed difference in plating efficiency, which also affect results within experiments wherein the plating density is not modified as an experimental variable. The data could also indicate that the effects on pH and nutrients may affect plating efficiency, as more cells in less cell culture medium may induce significant changes in the culture environs. One difficulty this explanation has with explaining the results in Figure 2.1 is that one would expect dose-dependence of this effect with respect to cell density; a negative correlation between seeding density and plating efficiency would be observed. However, the data in Figure 2.1 and Table 2.1 do not display this dose-dependence,

with the possible exception of B16F10 cells seeded in 6-well plates. Therefore, taken together with the magnitude of difference in plating efficiency between seeding densities, it is believed that these differences are due to some combination of technical errors, described previously. It is also suspected that overall status of the original cell population used for seeding—specifically, the oxidative stress, oxygenation, temperature, and other culture conditions—can influence clonogenic cell survival between experiments. As expected, HCT116, HaCaT, and B16F10 have different plating efficiencies overall—which were determined to exist at nearly every dose point with average differences higher than that expected as a result of technical error—due to intrinsic differences, such as slightly different doubling times[21–26] which affect formation of a colony of 50 cells or more. Overall, the results suggest that cell culture vessel does not produce a change in plating efficiency that would otherwise be unexpected due to technical error. However, the increased density at which cells are plated in 6-well plates overall, due to the reduced area allowed for growth, may exhibit effects on plating efficiency. Therefore, seeding density was kept consistent within experiments across chapters. This is also considered one of the confounding factors that may prevent effective comparison of results between chapters. However, overall, it is believed that plating efficiencies between culture vessels and densities was relatively consistent.

Since tritium emits low-LET radiation, it is suspected that responses may be similar to the TRS under similar doses. However, differences exist in this study that almost certainly affect cell survival—for example, disparity in dose rate, specific type of radiation used (i.e. charged versus uncharged particle), attenuation of radiation by non-living materials, internal dose of tritium as it crosses the cell membrane and differential effects to external electromagnetic radiation, et cetera), exposure time, among others. Therefore, ideally, a survival curve using tritium as a source is preferable. However, effects due to direct administration of tritium were not conducted outside of a limited number of assays. While adaptation of the assay is possible for tritium, time restrictions prevented further experiments.

Considering that the doses used in the present thesis were low, it is difficult to determine the shape of the complete survival curves at higher doses conclusively. Doses up to 3 Gy were used because it is known that the physical bystander effect begins to plateau well before this point at a 0.5 Gy donor dose[9]—it was therefore suspected that doses below 3 Gy would be most relevant to the bystander effect. Radiation cell survival curves can be made using models to fit the data, for example the linear quadratic (LQ) and multitarget (MT) models[10]. Both models are based on target theory and older experiments on exponential cell survival, which assumes that the traversal of a biological “target” by particle somehow results in cells’ reproductive inactivation (i.e. mitotic or apoptotic cell death). The LQ model assumes that reduction in survival due to “single hit” events are proportional to the dose, while a reduction due to “multiple hit” events are proportional to the square of the dose. The “single hit” events therefore occupy the linear “shoulder” of the curve, while effects due to “multiple hits” are apparent at higher doses in the curved region. Moreover, the curved region is present due to the accumulation of sublethal lesions that produce reproductive cell death, and the probability of this is directly related to the probability of getting “hit” by a particle. The MT model uses similar assumptions, with some differences. Each cell is believed to contain a number of distinct yet identical targets, and each target can be inactivated by a “hit”. Each inactivation is considered a sublethal event and all targets must be hit to produce cell death. There are many factors affecting cell survival, including mechanism of cell death (apoptosis or mitotic), LET, fractionation, oxygen availability, intrinsic radiosensitivity, and cell cycle stage of the irradiated cell[10,27]**.** These models are useful in describing the general trend of survival after radiation exposure in cultured cells, however most sources that were reviewed constructed a more comprehensive curve, including higher doses such as 10 Gy. Additionally, these models were initially conceived based on analysis of survival data at these higher doses.

Another paper from our lab published several years ago[28] described a survival curve for HaCaT cells. The results in the present thesis, specifically the LQ fit, indicate greater radiosensitivity than what is obtained in the paper, owing to the greater steepness of the LQ curve (Figure 2.2). It is suspected that this ostensible incongruence arose from differential experimental design, including higher doses in Fernandez-Palomo et al. Slightly different dose rates were used between this chapter and the paper, with the paper using a marginally higher dose rate and therefore shorter exposure. However, a lower dose rate usually produces greater survival overall, as cells are given more time to repair DNA damage. The dose rate used in this chapter was 0.226 cGy/min while the dose rate used in the paper was 289 Gy/min. The same time from seeding to clonogenic assay was used. Flasks were not placed in the incubator for approximately 30 minutes post-irradiation in this chapter, as irradiations for all doses were done in one session (respectively for biological replicates and cell lines). The time between seeding and irradiation was also different; while in the paper a period of six hour was used, the present thesis incubated cell cultures overnight. It is possible that these factors contributed to the results obtained. Most significantly, Fernandez-Palomo et al. constructed the linear quadratic curve using 11 doses, 4 of which were below 0.5 Gy. Because the LQ model is based on observations of cell survival in higher doses, the experiments in this chapter were conducted to assess cell survival following 5 doses with only 1 dose below 0.5 Gy. This difference is expected to affect the shape of the curve in two ways. Firstly, a curve including many low doses, constructed using least sum of squares, may underestimate or overestimate radiosensitivity at higher doses. Secondly, because the curve in the report uses more dose points, it is very likely that this fit is more robust than the one in the present thesis.

Better sensitivity could be obtained in future experiments by plating more than 500 cells, as this may have affected results at higher doses due to very few cells growing. This is primarily to be used at higher doses, however differences in survival curves may be observed depending on cell density due to a variety of factors. Neither target model have a firm biological basis—they cannot describe the induction of biological damage and fit cannot be used to determine which of the two better represents the data[10,29]. At high doses and on a log scale, the LQ model predicts a continually bending curve, while the MT model becomes more linear[10,30,31]. Theoretically, according to the random (Poisson) statistics governing target theory, a higher cell density would increase the likelihood of cumulative “hits” occurring in a cell population given a fixed dose. From this, it is expected that an experiment using a greater cell density may produce a lower normalized survival fraction for a given doses compared to an experiment where fewer cells were plated in exposed flasks. Additionally, more cells present in reporter flasks alters the microenvironment in which the cells are grown, which can affect the availability of nutrients and pH of the culture, which can in turn influence cell viability and reproductive cell survival.

Both the LQ and the MT model yield interesting fits to the HaCaT and HCT116 data. Some papers suggest a similar response in HaCaT cells[32], while some papers reviewed suggest lower sensitivity for HCT116 than what was obtained in this thesis[33]. However, for HCT116, some papers exhibit a similar fit to this chapter, showing a similar range for the linear shoulder[34]. This inconsistency most likely the result of the present thesis constructing the survival curve with limited doses—this is again an issue because these curve fitting models are based on higher doses. Due to results obtained in the previous section, separate control and sham flasks for plating efficiency should be ideally included when cell density is varied within an experiment. Previous research[5] has shown that HaCaT is less sensitive to radiation at the same doses as HCT116. While this was observed between the same dose groups across cell lines, statistical significance was not obtained at any dose point when comparing between HaCaT and HCT116.

The survival curve results from B16F10 cells were not expected. The LQ equation that was fitted had a negative β value, indicating an “inversion” in the quadratic trend in higher doses. It is believed that this is a product of an incomplete survival curve, as with HaCaT and HCT116. Unlike HaCaT and HCT116,

B16F10 appears to be much more radioresistant; with the interest of looking for low-dose effects, higher doses were not used and thus it is believed this curve is skewed. This can again be ameliorated by the inclusion of higher doses. It is likely that the shoulder for B16F10 when exposed to caesium-137 gamma radiation extends into 3 Gy but assumes quadratic characteristics sometime after 3 Gy. The MT model fit appears similarly nonsensical in this dose range, as the n value is less that 1 which paradoxically indicates an exponential reduction in survival (on a logarithmic scale) at low doses—it is again believed this was a product of the limited dose range used with higher doses being required for a better fit. A very interesting value in B16F10 cells is $D_{0,}$ which is approximately 1.9 in contrast to HaCaT and HCT116 (0.9 and 0.7, respectively), indicating a much higher resilience to gamma irradiation. These values would likely change however with the inclusion of higher dose points, and do not reflect their true values in all likelihood. On the other hand, the results obtained in the present report are mostly consistent for low doses for B16F10. There are some published reports that have determined survival curves for B16F10, and all suggest that 3 Gy is within the shoulder for gamma[35] and x-ray[36] radiations.

In summary, these results indicate that HaCaT and HCT116 appear sensitive to gamma radiation, which can be interpreted from the summary data in Table 2.2 for both models. However, because these results are within the dose range most relevant for non-targeted effects, the inclusion of higher doses up to 10 Gy would allow for the construction of a better curve. B16F10 appears to be much more radioresistant, a finding that is corroborated in the literature[35,36], although further experiments should be done to obtain a complete TRS survival curve. The radioresistance exhibited by B16F10 could be due, in part, to the free radical scavenging properties of melanin[37,38]—however, this is yet to be confirmed. This could be confirmed via the supplementation of melanin in cell culture medium and subsequent irradiation at the TRS. Melanin is known to act as a radioprotector, and several papers have described this effect in cell culture[39–41].

It is known that some cell lines exhibit low-dose hyper-radiosensitivity (HRS) in response to low doses of ionizing radiation, while others may exhibit increased radioresistence or adaptive responses to the challenge dose. The results in this chapter could be further expanded to interrogate whether HaCaT and HCT116 exhibit hyper-radiosensitivity—this can be done simply by the inclusion of doses under 100 mGy. The report discussed previously described HRS in HaCaT cells upon receipt of medium from irradiated T98G and HaCaT donors[28]. The report proposed that bystander effects predominate at lower doses within the HRS range. Further, the report showed that, at higher doses, T98G did not release bystander signals as it did at low doses. The authors further suggest that bystander responses need to be carefully studied and not generalized to all cells of a specific kind. While the report did not study effects in HCT116 cells, the high dose delivered to HCT116 donors could be why a significant effect was not observed in reporters.

The bystander experiments that used ICCM did not produce a significant reduction in survival. This may be the case due to number of reasons. An observed difference in cell survival was obtained, however this result was not statistically significant. Work in our lab has demonstrated that serum factors are important for the manifestation for bystander responses *in vitro*[42]. Donor dose is very important, with some previous papers showing abolishment of the bystander signal at high doses in HaCaTs[28]. Gibco FBS was used for this experiment, which was thawed in a hot water bath[5]. Preliminary results from our lab indicate that this method of thawing can cause attenuation of bystander signals through a currently unknown mechanism. However, Mothersill et al.[43] observed that the bystander effect was dependent on temperature, with high temperatures preventing communication of the signal. It could be that heating the FBS somehow prevented the bystander effect through destruction of the factors necessary for its communication. The ICCM effect is also sensitive to reporter and donor cell concentration, as too many

reporters or donors can quench the signal through excessive uptake of the soluble factors. This experiment was conducted with 500 reporters and 100 000 donor cells. More recent research has indicated that 500 could be too many cells for a significant bystander reporter response due this quenching effect. Statistical power could have also been an issue, although a standard n=9 were used for this assay. Even though a significant effect due to ICCM was not observed in this chapter, subsequent chapters discuss the generation of a physical bystander signal and its effects on reporter cells.

2.5. Conclusion

Experiments in this chapter demonstrated that all cell lines vary in plating efficiency. The difference in plating efficiency between vessels can be mostly explained by technical error. These effects can be mitigated by keeping plating efficiency consistent within an experiment. The survival curves that were constructed have limitations, as the dose range used was not comprehensive. However, results from B16F10, HaCaT, and HCT116 are similar to some papers in literature for the doses used. A bystander effect due to communication of medium-borne soluble factors was not obtained with statistical significance, however this may be explained by experimental factors. —a physical bystander effect was however observed in subsequent chapters.

2.6. References

1. Bedford JS, Hall EJ. Survival of HeLa cells cultured in vitro and exposed to protracted gamma-irradiation. International Journal of Radiation Biology and Related Studies in Physics, Chemistry and Medicine. 1963;7(4):377–383.

2. Puck TT, Marcus PI. Action of x-rays on mammalian cells. Journal of Experimental Medicine. 1956;103(5):653–666.

3. Le M, Fernandez-Palomo C, McNeill FE, Seymour CB, Rainbow AJ, Mothersill CE. Exosomes are released by bystander cells exposed to radiation-induced biophoton signals: Reconciling the mechanisms mediating the bystander effect. PLOS ONE. 2017;12(3):e0173685. doi:10.1371/journal.pone.0173685

4. Curtis JJ, Vo NTK, Seymour CB, Mothersill CE. Serotonin and 5-HT3 receptors sensitize human skin cells to direct irradiation cell death but not to soluble radiation-induced bystander signals. Environmental research. 2020;180:108807.

5. Curtis JJ, Seymour CB, Mothersill CE. Cell Line-Specific Direct Irradiation and Bystander Responses are Influenced by Fetal Bovine Serum Serotonin Concentrations. Radiation research. 2018.

6. Cohen J. INVESTIGATING THE PARAMETERS OF PRE-/POST-CONDITIONING ON HUMAN-DERIVED CANCER CELLS. McMaster University; 2019.

7. Le M, Mothersill CE, Seymour CB, Rainbow AJ, McNeill FE. An Observed Effect of p53 Status on the Bystander Response to Radiation-Induced Cellular Photon Emission. Radiation Research. 2017;187(2):169–185. http://www.bioone.org/doi/10.1667/RR14342.1. doi:10.1667/RR14342.1

8. Le M, McNeill FEFE, Seymour CBCB, Rusin A, Diamond K, Rainbow AJAJ, Murphy J, Mothersill CECE. Modulation of oxidative phosphorylation (OXPHOS) by radiation-induced biophotons. Environmental research. 2018;163:80–87. doi:10.1016/j.envres.2018.01.027

9. Le M, McNeill FE, Seymour C, Rainbow AJ, Mothersill CE. An observed effect of ultraviolet radiation emitted from beta-irradiated HaCaT cells upon non-beta-irradiated bystander cells. Radiation research. 2015;183(3):279–90. http://www.bioone.org/doi/10.1667/RR13827.1%5Cnhttp://www.ncbi.nlm.nih.gov/pubmed/25710575. doi:10.1667/RR13827.1

10. Hall EJ, Giaccia AJ. Radiobiology for the Radiologist. Lippincott Williams & Wilkins; 2006.

11. Tomita M, Maeda M. Mechanisms and biological importance of photon-induced bystander responses: Do they have an impact on low-dose radiation responses. Journal of Radiation Research. 2015;56(2):205–219. doi:10.1093/jrr/rru099

12. Mothersill C, Bristow RG, Harding SM, Smith RW, Mersov A, Seymour CB. A role for p53 in the response of bystander cells to receipt of medium borne signals from irradiated cells. International journal of radiation biology. 2011;87(11):1120–5. http://www.ncbi.nlm.nih.gov/pubmed/21831006. doi:10.3109/09553002.2011.610866

13. Ciesielska S, Bil P, Gajda K, Poterala-Hejmo A, Hudy D, Rzeszowska-Wolny J. Cell type-specific differences in redox regulation and proliferation after low UVA doses. PLoS ONE. 2019. doi:10.1371/journal.pone.0205215

14. Iordanov MS, Paranjape JM, Zhou a, Wong J, Williams BR, Meurs EF, Silverman RH, Magun BE. Activation of p38 mitogen-activated protein kinase and c-Jun NH(2)-terminal kinase by double-stranded RNA and encephalomyocarditis virus: involvement of RNase L, protein kinase R, and alternative pathways. Molecular and cellular biology. 2000;20(2):617–627. doi:10.1128/MCB.20.2.617-627.2000

15. Lyng FM, Maguire P, McClean B, Seymour C, Mothersill C. The involvement of calcium and MAP kinase signaling pathways in the production of radiation-induced bystander effects. RADIATION RESEARCH. 2006;165(4):400–409. doi:10.1667/RR3527.1

16. Le M, McNeill FE, Seymour CB, Rusin A, Diamond K, Rainbow AJ, Murphy J, Mothersill CE. Modulation of oxidative phosphorylation (OXPHOS) by radiation- induced biophotons. Environmental Research. 2018;163:80–87. doi:10.1016/j.envres.2018.01.027

17. Shi X, Mothersill C, Seymour C. No adaptive response is induced by chronic low-dose radiation from Ra-226 in the CHSE/F fish embryonic cell line and the HaCaT human epithelial cell line. ENVIRONMENTAL RESEARCH. 2016;151:537–546. doi:10.1016/j.envres.2016.08.026

18. Le M, Mothersill CE, Seymour CB, Ahmad SB, Armstrong A, Rainbow AJ, McNeill FE. Factors affecting ultraviolet-A photon emission from beta-irradiated human keratinocyte cells. Physics in medicine and biology. 2015;60(16):6371–6389. doi:10.1088/0031-9155/60/16/6371

19. Furlong H, Smith R, Wang J, Seymour C, Mothersill C, Howe O. Identification of Key Proteins in Human Epithelial Cells Responding to Bystander Signals From Irradiated Trout Skin. DOSE-RESPONSE. 2015;13(3). doi:10.1177/1559325815597669

20. Ryan LA, Smith RW, Seymour CB, Mothersill CE. Dilution of irradiated cell conditioned medium and the bystander effect. RADIATION RESEARCH. 2008;169(2):188–196. doi:10.1667/RR1141.1

21. Fidler IJ. Biological behavior of malignant melanoma cells correlated to their survival in vivo. Cancer research. 1975;35(1):218–224.

22. Cowley GS, Weir BA, Vazquez F, Tamayo P, Scott JA, Rusin S, East-Seletsky A, Ali LD, Gerath WFJ, Pantel SE. Parallel genome-scale loss of function screens in 216 cancer cell lines for the identification of context-specific genetic dependencies. Scientific data. 2014;1(1):1–12.

23. Petitprez A, Poindessous V, Ouaret D, Regairaz M, Bastian G, Guérin E, Escargueil AE, Larsen AK. Acquired irinotecan resistance is accompanied by stable modifications of cell cycle dynamics independent of MSI status. International journal of oncology. 2013;42(5):1644–1653.

24. Jain M, Nilsson R, Sharma S, Madhusudhan N, Kitami T, Souza AL, Kafri R, Kirschner MW, Clish CB, Mootha VK. Metabolite profiling identifies a key role for glycine in rapid cancer cell proliferation. Science. 2012;336(6084):1040–1044.

25. Lorie EP, Stricker N, Plitta-Michalak B, Chen I-P, Volkmer B, Greinert R, Jauch A, Boukamp P, Rapp A. characterisation of the novel spontaneously immortalized and invasively growing human skin keratinocyte line HaSKpw. Scientific reports. 2020;10(1):1–20.

26. Danciu C, Falamas A, Dehelean C, Soica C, Radeke H, Barbu-Tudoran L, Bojin F, Pînzaru SC, Munteanu MF. A characterization of four B16 murine melanoma cell sublines molecular fingerprint and proliferation behavior. Cancer cell international. 2013;13(1):1–12.

27. Astrahan M. Some implications of linear-quadratic-linear radiation dose-response with regard to hypofractionation. Medical Physics. 2008. doi:10.1118/1.2969065

28. Fernandez-Palomo C, Seymour C, Mothersill C. Inter-Relationship between Low-Dose Hyper-Radiosensitivity and Radiation-Induced Bystander Effects in the Human T98G Glioma and the Epithelial HaCaT Cell Line. RADIATION RESEARCH. 2016;185(2):124–133. doi:10.1667/RR14208.1

29. Zhao L, Mi D, Hu B, Sun Y. A generalized target theory and its applications. Scientific reports. 2015;5(1):1–11.

30. Barendsen GW. Parameters of linear-quadratic radiation dose-effect relationships: dependence on LET and mechanisms of reproductive cell death. International journal of radiation biology. 1997;71(6):649–655.

31. Hawkins RB. Survival of a mixture of cells of variable linear-quadratic sensitivity to radiation. Radiation research. 2000;153(6):840–843.

32. Jella KK, Garcia A, McClean B, Byrne HJ, Lyng FM. Cell death pathways in directly irradiated cells and cells exposed to medium from irradiated cells. International journal of radiation biology. 2013;89(3):182–190. doi:10.3109/09553002.2013.734942

33. Xu X-T, Hu W-T, Zhou J-Y, Tu Y. Celecoxib enhances the radiosensitivity of HCT116 cells in a COX-2 independent manner by up-regulating BCCIP. American journal of translational research. 2017;9(3):1088.

34. Tippayamontri T, Kotb R, Paquette B, Sanche L. Synergism in concomitant chemoradiotherapy of cisplatin and oxaliplatin and their liposomal formulation in the human colorectal cancer HCT116 model. Anticancer research. 2012;32(10):4395–4404.

35. Zapata-Benavides P, Thompson-Armendariz FG, Arellano-Rodríguez M, Franco-Molina MA, Mendoza-Gamboa E, Saavedra-Alonso S, Zacarias-Hernández JL, Trejo-Avila LM, Rodríguez-Padilla C. shRNA-WT1 potentiates anticancer effects of gemcitabine and cisplatin against B16F10 lung metastases in vitro and in vivo. in vivo. 2019;33(3):777–785.

36. Nagane M, Kanai E, Shibata Y, Shimizu T, Yoshioka C, Maruo T, Yamashita T. Sulfasalazine, an inhibitor of the cystine-glutamate antiporter, reduces DNA damage repair and enhances radiosensitivity in murine B16F10 melanoma. PLoS One. 2018;13(4):e0195151.

37. Denat L, Kadekaro AL, Marrot L, Leachman SA, Abdel-Malek ZA. Melanocytes as instigators and victims of oxidative stress. Journal of Investigative Dermatology. 2014. doi:10.1038/jid.2014.65

38. Jacobson ES, Tinnell SB. Antioxidant function of fungal melanin. Journal of Bacteriology. 1993. doi:10.1128/jb.175.21.7102-7104.1993

39. Marozik P, Mosse I, Mothersill C, Seymour C. Protection by chemicals against radiation-induced bystander effects. In: Mothersill, C and Mosse, I and Seymour, C, editor. MULTIPLE STRESSORS: A CHALLENGE FOR THE FUTURE. 2007. p. 247+. (NATO Science for Peace and Security Series C-Environmental Security). doi:10.1007/978-1-4020-6335-0_16

40. Mosse I, Marozik P, Seymour C, Mothersill C. The effect of melanin on the bystander effect in human keratinocytes. MUTATION RESEARCH-FUNDAMENTAL AND MOLECULAR MECHANISMS OF MUTAGENESIS. 2006;597(1–2):133–137. doi:10.1016/j.mrfmmm.2005.09.006

41. Marozik PM, Mosse IB, Seymour C, Mothersil C. The influence of melanin on bystander effect. 2003.

42. Pinho C, Wong R, Sur RK, Hayward JE, Farrell TJ, Seymour C, Mothersill C. The involvement of serum

serotonin levels producing radiation-induced bystander effects for an in vivo assay with fractionated high dose-rate (HDR) brachytherapy. INTERNATIONAL JOURNAL OF RADIATION BIOLOGY. 2012;88(10):791–797. doi:10.3109/09553002.2012.715794

43. Mothersill C, Seymour CB. Cell-cell contact during gamma irradiation is not required to induce a bystander effect in normal human keratinocytes: Evidence for release during irradiation of a signal controlling survival into the medium. RADIATION RESEARCH. 1998;149(3):256–262. doi:10.2307/3579958

Chapter 3

Immunocytochemical determination of p53 status in selected cell lines

Abstract: This short chapter describes the verification of p53 protein expression in HaCaT and HCT116 cells. The p53 protein has been shown to be required in reporter bystander responses in human cell lines, as null mutant reporters do not respond to any bystander signal. Both HaCaT and HCT116 show p53 expression under normal cell culture conditions, indicative of the ability of these transformed cells to respond to intracellular signalling for apoptosis and cell cycle arrest upon receipt of a bystander signal. The localization of p53 was shown to be strongest in the nuclei of both cell lines. This is further evidence of aberrant anti-proliferative signalling in these cells compared to normal, untransformed cells, as nuclear p53 is associated with expression of downstream effector genes involved in controlling the cell cycle and programmed death; it is known that this is required for the bystander effect. Overall, this is evidence that the human cell stocks used in the present thesis should be capable of bystander responses.

3.1. Introduction

It feels almost obligatory to introduce the p53 tumor suppressor protein as "the guardian of the genome" due to its known roles in the literature. This is also the case due to how extensively it has been studied. The protein and its associated gene, *TP53* in humans, is also involved intimately in the radiation response of cells and is required for cells to respond to a bystander signal. This requirement and its roles in cell cycle warrant some review and discussion of p53 in the context of radiation-induced bystander effects.[1–3].

The p53 protein can stop the cell cycle upon DNA damage or various kinds of cellular stress. After induction of stress and consequent expression of *TP53*, the associated protein is known to arrest cells in G1, S, and G2[4,5]. It is believed by a number of groups that non-targeted effects occur because of a block in the G2 phase[6–9]. It is believed that this arrest allows the repair of DNA to occur or recovery from stress before continuation of the cycle. The p53 protein can also mediate apoptotic signalling if the damage is significant[10,11]. The protein can promote this cell-sparing by its diverse activity in regulating gene expression—p53 is considered a transcription factor and has several protein domains[12]. The N-terminus carries a regulatory transcription activation domain (TAD)[13,14]. A middle region mediates DNA binding, with the adjacent region mediating tetramerization of the protein, which is necessary for transcription of target genes[13,15,16]. The C-terminal domain contains a regulatory region which can be phosphorylated by a number of kinases. The vast majority of p53 mutations occur in the domain adjacent to the N-terminal domain, which mediates DNA binding and thus recruitment of a transcriptional complex[12]. Several mutations in the p53 protein are known, including dominant negative varieties containing errors in the tetramerization domain which effectively sequesters functional p53 from DNA[17–19]. The protein is unique in that many sensory signalling pathways converge on p53 as a mediator of cell growth and survival, ranging from radiation damage to hypoxia to metabolite scarcity to viral infection[20–22]. The protein was initially believed to be an oncoprotein, but other research soon cast doubt on this idea[17,19]. Early experiments showed that the presence of a functional p53 in a cells overexpressing the oncogene Ras did not produce foci like mutant p53[23], indicating that mutant p53 is required for some transformations depending on genetic background. *TP53* is mutated in approximately 50% of cancers[1,24]. Lu-Fraumeni Syndrome, an autosomal dominant condition that predisposes carries to cancer development, is caused by mostly by mutations in the DNA binding domain of the *TP53* gene[25]. A similar syndrome can result due to mutations in enzymes regulating the activity of p53 post-translationally or due to mutations in other proteins that govern cell cycle progression, including some cyclin-dependent kinase inhibitors[26,27]. The p53 protein may also promote the generation of reactive oxygen species (ROS) directly, and this activity may mechanistically induce apoptosis through the intrinsic pathway[12].

In the context of radiation biology, p53 has been a protein of interest for some time because it signals for cell cycle arrest and DNA repair as well as apoptosis, which are crucial processes for many organisms[4]. Additionally, with respect to medical physics and the goals inherent to cancer radiation therapy, the protein obviously affects radiation-induced DNA damage responses along with tumor cell death. Two kinases, ATM and ATR, are responsible for sensing DNA damage and downstream activation of p53[28–30]. ATM is a serene/threonine kinase that acts in the sensing DNA double strand breaks, initially detected by the MRN protein complex in humans, and phosphorylates several key proteins involved in regulation of the cell cycle, including p53 and Chk2[28–30]. ATR is another serene/threonine kinase that is activated after generation of single strand breaks; ATR phosphorylates Chk1 and p53. These pathways are known to be involved in the radiation response[28–30]. With respect to radiation protection and preventative healthcare, radiation-induced mutations in *TP53* may lead to transformation and cancer formation when other oncogenic mutations are present. With respect to bystander effects, it has been observed that p53-

deficient cells can produce a signal yet are unable to respond to it; this appears to be the case both for soluble factor signalling and electromagnetic bystander signalling[31,32]. With this in mind, it was believed to be a useful exercise to validate the p53 status in the human cell lines that were used.

We wanted to determine the status of the p53 protein in the human cell lines that were used in this thesis. Additionally, we wanted to visualize the localization of p53 under normal culture conditions, as some publications have reported point mutations in HaCaT. It was hypothesized that p53 expression occurs in both cell lines, because previous research has determined expression in these cell lines. Moreover, we hypothesized that the localization and function of p53 may be affected in both cell lines compared to normal, untransformed cells.

3.2. Methods

3.2.1. Immunocytochemistry

Immunocytochemistry is a technique used for the visualization and localization of proteins in a cell or population of cells. Briefly, a primary antibody for a protein of interest—in this case a mouse antibody for human p53—is introduced into the cell. This antibody binds the antigen via its antigen binding fragment (Fab) region. A secondary antibody carrying a fluorescent tag, in this experiment a goat anti-mouse antibody covalently attached to a fluorescent Alexa Fluor tag, can bind to the primary antibody via the latter's fragment crystallizable (Fc) region. Excitation of this fluorescent tag under a specific wavelength of light allows for the visualization of the antibody-bound protein with the use of a microscope. Images captured using a microscope camera can be analyzed qualitatively or quantitatively for signal intensity and useful information can be obtained on the localization of the antigen.

100 000 HaCaT and HCT116 cells were seeded in 2 mL of complete growth medium in slide flasks following routine subculture. The human cells were grown under normal conditions for two days before the slides were prepared for imaging. Medium was removed from the slide flasks and cells were washed in 2 mL sterile DPBS at room temperature twice for two minutes. The washing solution was discarded and 1 mL cold fixative buffer (10% formalin buffered solution, Sigma *HT501128-4L*) was added to the slide flasks. The cells were incubated at 4°C for 15 minutes. The fixative was then removed and 1 mL of room temperature permeabilization buffer (0.1% Triton X-100 DPBS solution) was added. The cells were subsequently incubated at room temperature for 10 minutes. The permeabilization buffer was removed and 1 mL of blocking buffer (3% BSA, 10% goat serum, 0.1% Triton X-100 DPBS solution) and allowed to incubate with rocking at room temperature for 1 hour. The blocking buffer was removed and a solution containing the primary antibody (monoclonal p53 mouse antibody, Sigma-Aldrich P8999) diluted 1:100 with fresh blocking buffer was added to each slide well and the cells were incubated while gently rocking for 3 hours. Blank control wells were included that were treated with blocking buffer only to test for nonspecific binding of the secondary antibody. The optimum concentration of the primary antibody was determined by consulting the product specification sheet and optimization trials. The primary antibody solution was removed and the cells were washed 3 times in warm DPBS. A solution containing the secondary antibody (goat anti-mouse conjugated to Alexa Fluor 488) in a 1:3000 concentration in DPBS. The cells were then allowed to incubate for 1 hour with rocking. The secondary antibody solution was removed and each chamber was washed 3 times in fresh DPBS. 300 µL DAPI mounting solution was added to each chamber. After 10 minutes, the cells were rinsed 3 times with DPBS. Using tool included with the slide flasks, the chamber walls were broken off. The slides were then allowed to air dry for 30 minutes. 15 µL Slowfade Gold Antifade Reagent was added to the center of each chamber. Glass coverslips were then

applied. The slides were stored in aluminum foil at 4°C for 1 day prior to imaging using an EVOS Auto FL2 multichannel fluorescence microscope for DAPI and for Alexa Fluor 488 fluorescence (λ_{EX} / λ_{EM}= 495 nm / 519 nm).

Following confirmation of p53 status, cells descended from the same original population were frozen using the standard protocol described previously (in chapter 2) and kept frozen until required for future experiments.

3.3. Results

The p53 protein was detected in both cell lines assayed. Figures 3.1. and 3.2. show microscopy images with both DAPI fluorescence in blue, indicating nuclear DNA, and Alexa Fluor 488 fluorescence in green, indicating the p53 protein.

In HaCaT cells, p53 appeared to colocalize with DAPI primarily to the nucleus, although a faint signal was present in the cytoplasm in Figure 3.2. In Figure 3.1, a stronger cytoplasmic signal can be observed in some HaCaT cells.

Similarly, in HCT116 cells, p53 appears to primarily localize to the nucleus. However, in Figure 3.2, there is an obviously cytoplasmic signal from one of the cells. In Figure 3.1, there is less apparent evidence of green fluorescence in the cytoplasm.

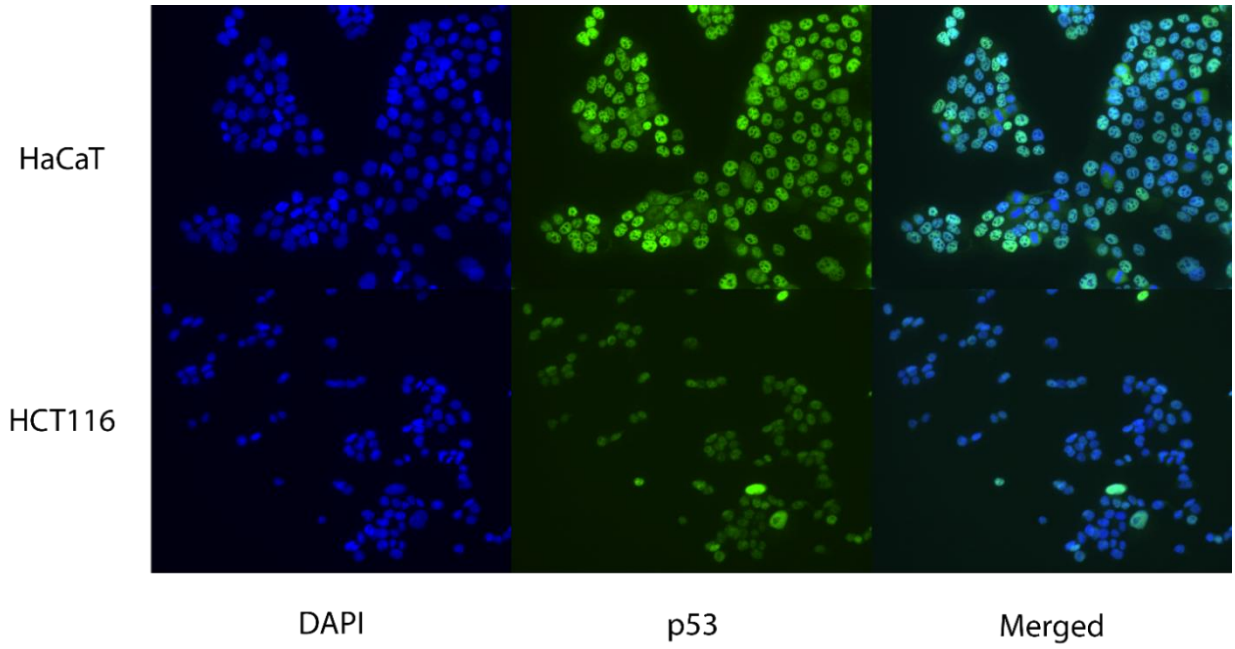

Figure 3.1: Fluorescence microscope images of fixed HaCaT and HCT116 cells. The first column shows only DAPI fluorescence. The middle column shows secondary antibody fluorescence. The rightmost column shows a merged image. fluorescence microscope for DAPI and for Alexa Fluor 488 fluorescence (λ_{EX} / λ_{EM}= 495 nm / 519 nm).

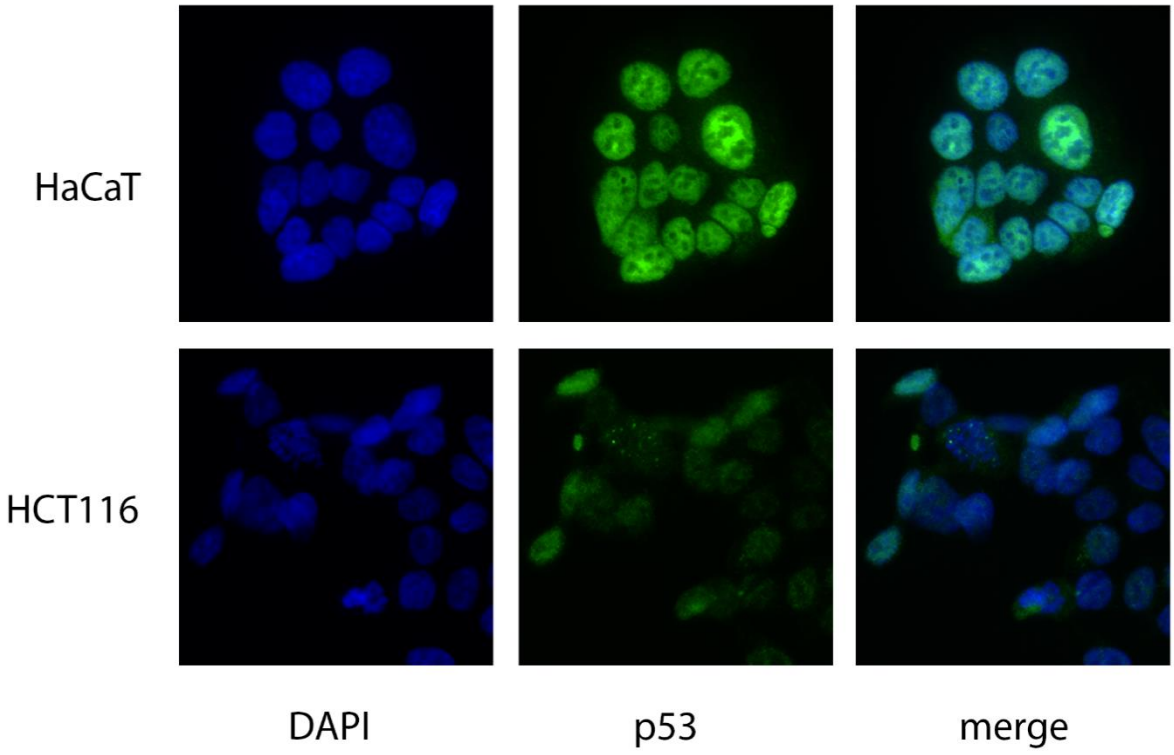

Figure 3.2: Inflated fluorescence microscope images showing localization of secondary antibody fluorescence with the same scheme as Figure 3.1.

3.4. Discussion

The p53 protein is highly dynamic and is normally shuttled between the nucleus and the cytosol in healthy, untransformed cells. In unstressed cells, p53 exists in a negative feedback system with MDM2, which is an E3 ubiquitin ligase that targets p53 for degradation; the transcription of the gene coding for MDM2 is induced by p53. In stressed cells, p53 enters the nucleus and activates the transcription of many target genes that results in either cell cycle arrest or apoptosis.

B16F10 was not used in this study for several reasons. B16F10 is a melanoma cell line of mouse origin. These cells were not obtained until later in the project and time constraints prevented further experimentation. Additionally, B16F10 would not have been assayed initially because different primary and secondary antibodies were not available—i.e., a primary not originating in mouse cells and a secondary that was not anti-mouse.

Transformed cells are characteristically deficient in their ability to regulate growth, division, and damage repair. It is not surprising therefore that transformed cells harbor nuclear p53, yet do not respond with cell cycle arrest or apoptosis. In fact, researchers noticed this disparity first in the early eighties[33]. However, some cancer cell types are known wherein p53 does not localize to the nucleus, including some colon cancers. Instead, sequestration of p53 to the cytoplasm is observed. It is suspected that this may occur due to mutations in the constituents of the biochemical machinery that permits p53 entry into the

nucleus; for example, a mutation in the nuclear localization sequence (NLS) on p53, or an associated protein that shuttles p53 to the nucleus. It is notable that other publications have reported nuclear p53 localization in HCT116 in the absence of treatment[34].

Both HaCaT and HCT116 are known to possess functional p53. However, HCT116 cells are known to carry a mutation in KRAS. The Ras family of proteins are monomeric GTPases that are involved in the first steps of growth signal transduction upon receipt of a mitogenic signal[35]. Ras targets several proteins in different pathways, including those in the MAPK pathway. Mutations in various Ras proteins, including KRAS, are common in cancers. Mutations causing persistent activation of Ras can cause malignant transformation. HaCaT cells are aneuploid and are known to harbor mutations in p53 (Cellosaurus; RRID:CVCL0038).

As described previously, p53 is known to be important for bystander responses. This makes sense intuitively, as the classical assay for RIBE measure reduction in clonogenicity, which can be induced by cell cycle arrest or apoptosis. In other words, because these cells are deficient in a key regulator of growth and proliferation, they do not behave as other bystander cells undergoing the same treatment would. It is particularly interesting that, though it has been demonstrated that HaCaTs can produce and respond to the electromagnetic signal, that their response is somewhat muted compared to HCT116[31]. The two known missense mutations of *TP53* in HaCaTs (Cellosaurus; RRID:CVCL_0038) occur in the DNA-binding region. Petra Boukamp developed the HaCaT cell line[36]; their group further characterized the cell line and *TP53* mutations it habors[37,38]. This reduced bystander response observed in previous reports could be the result of a reduction in the protein's affinity for promoters that it typically binds, and thus reduced targeted gene expression and the cellular effects thereof. However, in order to validate this claim, additional experiments must be conducted. Specifically, it would be useful to obtain a strain of HaCaT homozygous for wild type p53, which could be "knocked in" to replace the mutated copy. Following validation of this strain, bystander assays could be conducted on the regular and HaCaT$^{p53+/+}$ strains to determine if any differences in their response exists. Other explanations of the expression of p53 exist, including post-translational regulation. There have been previous studies that have shown carcinogen-induced cytoplasmic localization of p53 and associated proteins in the mitochondrial apoptotic patwhway[39]. Mutation of *TP53* was also found to be an early event in smoking-induced oral cancers[40,41]. The cytoplasmic sequestration of p53 may be indicative of stabilization of the protein. As discussed in previous reports[39], the high quantity of p53 in cultures may be indicative of negative post-translational regulation, as is the case with the MDM2 pathway[1], and therefore stable expression of inactive p53. The nuclear localization of MDM2 and p53 was found to be elevated in some cancers, such as breast cancer[42]. Further research indicated that bystander responses in normal human urothelium varied considerably between individuals[43,44].

It was noticed that HaCaT cells produced clearer fluorescence images than HCT116. It is suspected that this could be the case due to differential cell morphology**.** Cultured HCT116 cells appear to have more "depth" than HaCaT cells, which appear "flatter" under a microscope. Any object that is within the plane of focus is likely to appear clearer than those occupying multiple planes of focus, and this becomes particularly obvious at higher magnifications.

3.5. Conclusion

In conclusion, this chapter validated the expression of *TP53* in both human cell lines, HaCaT and HCT116, using immunocytochemistry. Nuclear localization of p53 in both cell lines was observed. One major limitation of these experiments is not being able to determine whether p53 remains functional in

both cell lines. However, because p53 expression is a requisite for bystander responses in reporter cells, the results in this chapter indicate that both human cell lines should be capable of bystander responses.

3.6. References

1. Efeyan A, Serrano M. p53: guardian of the genome and policeman of the oncogenes. Cell cycle. 2007;6(9):1006–1010.

2. Binayke A, Mishra S, Suman P, Das S, Chander H. Awakening the “guardian of genome”: reactivation of mutant p53. Cancer chemotherapy and pharmacology. 2019;83(1):1–15.

3. Park J, Zhuang J, Li J, Hwang PM. p53 as guardian of the mitochondrial genome. FEBS letters. 2016;590(7):924–934.

4. Kuerbitz SJ, Plunkett BS, Walsh W V, Kastan MB. Wild-type p53 is a cell cycle checkpoint determinant following irradiation. Proceedings of the National Academy of Sciences. 1992;89(16):7491–7495.

5. Stewart N, Hicks GG, Paraskevas F, Mowat M. Evidence for a second cell cycle block at G2/M by p53. Oncogene. 1995;10(1):109–115.

6. Gogineni VR, Nalla AK, Gupta R, Dinh DH, Klopfenstein JD, Rao JS. Chk2-mediated G2/M cell cycle arrest maintains radiation resistance in malignant meningioma cells. Cancer letters. 2011;313(1):64–75.

7. Jaiswal H, Lindqvist A. Bystander communication and cell cycle decisions after DNA damage. Frontiers in genetics. 2015;6:63.

8. Halloran PJ, Fenton RG. Irreversible G2-M arrest and cytoskeletal reorganization induced by cytotoxic nucleoside analogues. Cancer research. 1998;58(17):3855–3865.

9. Tu W, Dong C, Konishi T, Kobayashi A, Furusawa Y, Uchihori Y, Xie Y, Dang B, Li W, Shao C. G2-M phase-correlative bystander effects are co-mediated by DNA-PKcs and ATM after carbon ion irradiation. Mutation Research/Genetic Toxicology and Environmental Mutagenesis. 2016;795:1–6.

10. Fridman JS, Lowe SW. Control of apoptosis by p53. Oncogene. 2003;22(56):9030–9040.

11. Haupt S, Berger M, Goldberg Z, Haupt Y. Apoptosis-the p53 network. Journal of cell science. 2003;116(20):4077–4085.

12. Hainaut P, Mann K. Zinc binding and redox control of p53 structure and function. Antioxidants and Redox Signaling. 2001;3(4):611–623.

13. Bai L, Zhu W-G. p53: structure, function and therapeutic applications. J Cancer Mol. 2006;2(4):141–153.

14. Raj N, Attardi LD. The transactivation domains of the p53 protein. Cold Spring Harbor perspectives in medicine. 2017;7(1):a026047.

15. Wang P, Reed M, Wang Y, Mayr G, Stenger JE, Anderson ME, Schwedes JF, Tegtmeyer P. p53 domains: structure, oligomerization, and transformation. Molecular and cellular biology. 1994;14(8):5182–5191.

16. Pavletich NP, Chambers KA, Pabo CO. The DNA-binding domain of p53 contains the four conserved regions and the major mutation hot spots. Genes & development. 1993;7(12b):2556–2564.

17. Willis A, Jung EJ, Wakefield T, Chen X. Mutant p53 exerts a dominant negative effect by preventing wild-type p53 from binding to the promoter of its target genes. Oncogene. 2004;23(13):2330–2338.

18. Blagosklonny M V. p53 from complexity to simplicity: mutant p53 stabilization, gain-of-function, and

dominant-negative effect. The FASEB Journal. 2000;14(13):1901–1907.

19. De Vries A, Flores ER, Miranda B, Hsieh H-M, Van Oostrom CTM, Sage J, Jacks T. Targeted point mutations of p53 lead to dominant-negative inhibition of wild-type p53 function. Proceedings of the National Academy of Sciences. 2002;99(5):2948–2953.

20. Sato Y, Tsurumi T. Genome guardian p53 and viral infections. Reviews in medical virology. 2013;23(4):213–220.

21. Tasdemir E, Maiuri MC, Morselli E, Criollo A, D'Amelio M, Djavaheri-Mergny M, Cecconi F, Tavernarakis N, Kroemer G. A dual role of p53 in the control of autophagy. Autophagy. 2008;4(6):810–814.

22. Humpton TJ, Vousden KH. Regulation of cellular metabolism and hypoxia by p53. Cold Spring Harbor perspectives in medicine. 2016;6(7):a026146.

23. Parada LF, Land H, Weinberg RA, Wolf D, Rotter V. Cooperation between gene encoding p53 tumour antigen and ras in cellular transformation. Nature. 1984;312(5995):649–651.

24. Kastan MB, Canman CE, Leonard CJ. P53, cell cycle control and apoptosis: implications for cancer. Cancer and Metastasis reviews. 1995;14(1):3–15.

25. Malkin D. Li–Fraumeni syndrome. In: Adrenocortical Carcinoma. Springer; 2009. p. 173–191.

26. Evans DG, Birch JM, Narod SA. Is CHEK2 a cause of the Li–Fraumeni syndrome? Journal of Medical Genetics. 2008;45(1):63–64.

27. Ruijs MWG, Broeks A, Menko FH, Ausems MGEM, Wagner A, Oldenburg R, Meijers-Heijboer H, van't Veer LJ, Verhoef S. The contribution of CHEK2 to the TP53-negative Li-Fraumeni phenotype. Hereditary cancer in clinical practice. 2009;7(1):1–7.

28. Blackford AN, Jackson SP. ATM, ATR, and DNA-PK: the trinity at the heart of the DNA damage response. Molecular cell. 2017;66(6):801–817.

29. Stokes MP, Rush J, MacNeill J, Ren JM, Sprott K, Nardone J, Yang V, Beausoleil SA, Gygi SP, Livingstone M. Profiling of UV-induced ATM/ATR signaling pathways. Proceedings of the National Academy of Sciences. 2007;104(50):19855–19860.

30. Maréchal A, Zou L. DNA damage sensing by the ATM and ATR kinases. Cold Spring Harbor perspectives in biology. 2013;5(9):a012716.

31. Le M, Mothersill CE, Seymour CB, Rainbow AJ, McNeill FE. An Observed Effect of p53 Status on the Bystander Response to Radiation-Induced Cellular Photon Emission. Radiation Research. 2017;187(2):169–185. http://www.bioone.org/doi/10.1667/RR14342.1. doi:10.1667/RR14342.1

32. Mothersill C, Bristow RG, Harding SM, Smith RW, Mersov A, Seymour CB. A role for p53 in the response of bystander cells to receipt of medium borne signals from irradiated cells. INTERNATIONAL JOURNAL OF RADIATION BIOLOGY. 2011;87(11):1120–1125. doi:10.3109/09553002.2011.610866

33. Liang S, Clarke MF. Regulation of p53 localization. European journal of biochemistry. 2001;268(10):2779–2783.

34. Swamy M V, Herzog CR, Rao C V. Inhibition of COX-2 in colon cancer cell lines by celecoxib increases the nuclear localization of active p53. Cancer research. 2003;63(17):5239–5242.

35. Bernards A. GAPs galore! A survey of putative Ras superfamily GTPase activating proteins in man and Drosophila. Biochimica et Biophysica Acta (BBA)-Reviews on Cancer. 2003;1603(2):47–82.

36. Boukamp P, Petrussevska RT, Breitkreutz D, Hornung J, Markham A, Fusenig NE. Normal keratinization in a spontaneously immortalized aneuploid human keratinocyte cell line. The Journal of cell biology. 1988;106(3):761–771.

37. Lehman TA, Modali R, Boukamp P, Stanek J, Bennett WP, Welsh JA, Metcalf RA, Stampfer MR, Fusenig N, Rogan EM. p53 mutations in human immortalized epithelial cell lines. Carcinogenesis. 1993;14(5):833–839.

38. Härle-Bachor C, Boukamp P. Telomerase activity in the regenerative basal layer of the epidermis inhuman skin and in immortal and carcinoma-derived skin keratinocytes. Proceedings of the national academy of sciences. 1996;93(13):6476–6481.

39. HARNEY J V, SEYMOUR CB, MURPHY DM, MOTHERSILL C. VARIATION IN THE EXPRESSION OF P53, C-MYC, AND BCL-2 ONCOPROTEINS IN INDIVIDUAL PATIENT CULTURES OF NORMAL UROTHELIUM EXPOSED TO COBALT-60 GAMMA-RAYS AND N-NITROSODIETHANOLAMINE. CANCER EPIDEMIOLOGY BIOMARKERS & PREVENTION. 1995;4(6):617–625.

40. Colucci S, ElGehani R, Flint S, Mothersill C. p53 mutations and protein expression in primary cultures of normal oral mucosa in smokers and non-smokers. ORAL ONCOLOGY. 1997;33(4):240–246. doi:10.1016/S0964-1955(97)00027-4

41. MOTHERSILL C, HARNEY J, SEYMOUR CB. INDUCTION OF STABLE P53 ONCOPROTEIN AND OF C-MYC OVEREXPRESSION IN CULTURED NORMAL HUMAN UROEPITHELIUM BY RADIATION AND N-NITROSODIETHANOLAMINE. RADIATION RESEARCH. 1994;138(1):93–98. doi:10.2307/3578851

42. Park HS, Park JM, Park S, Cho J, Kim S Il, Park B-W. Subcellular localization of Mdm2 expression and prognosis of breast cancer. International journal of clinical oncology. 2014;19(5):842–851.

43. Mothersill CE, O'Malley KJ, Murphy DM, Seymour CB, Lorimore SA, Wright EG. Identification and characterization of three subtypes of radiation response in normal human urothelial cultures exposed to ionizing radiation. CARCINOGENESIS. 1999;20(12):2273–2278. doi:10.1093/carcin/20.12.2273

44. Mothersill C, Rea D, Wright EG, Lorimore SA, Murphy D, Seymour CB, O'malley K. Individual variation in the production of abystander signal'following irradiation of primary cultures of normal human urothelium. Carcinogenesis. 2001;22(9):1465–1471.

Chapter 4

Estimating the quantity of melanin produced by B16F10 cells in culture

Abstract: The concentration of melanin present in cultured B16F10 cells was estimated in this chapter using high-throughput spectrophotometry. Additionally, the concentration of secreted melanin was also estimated by the same assay. It was found that 1 million B16F10 cells contain, on average, 68.78±23.34 μM melanin intracellularly and that the same cells secreted approximately 50.775±32.33 μM melanin in the same volume of medium. These results indicate the quantity of melanin produced during routine culture and can be related to previous studies assessing the role of melanin as a radioprotector in the context of the electromagnetic bystander signal.

4.1. Introduction

Melanin refers to a set of natural pigments that occur in many organisms. In humans, natural variation in melanin production is commonly known to result in a spectrum of possible skin tones. It is produced in mammalian skin by specialized epithelial cells called melanocytes[1]. Melanin is synthesized via the oxidation and polymerization of tyrosine, which may occur following exposure to ultraviolet light. There are several subtypes of melanin. Eumelanin is the variety that is most frequently comes to mind, which can either be brown or black in colour. Other types include pheomelanin, which is responsible for red pigmentation, and neuromelanin, which is present in the central nervous system. The synthesis of melanin can be induced in human skin by exposure to UV radiation. The absorption of light, particularly UVA and UVB, is one of its more broadly appreciated properties.

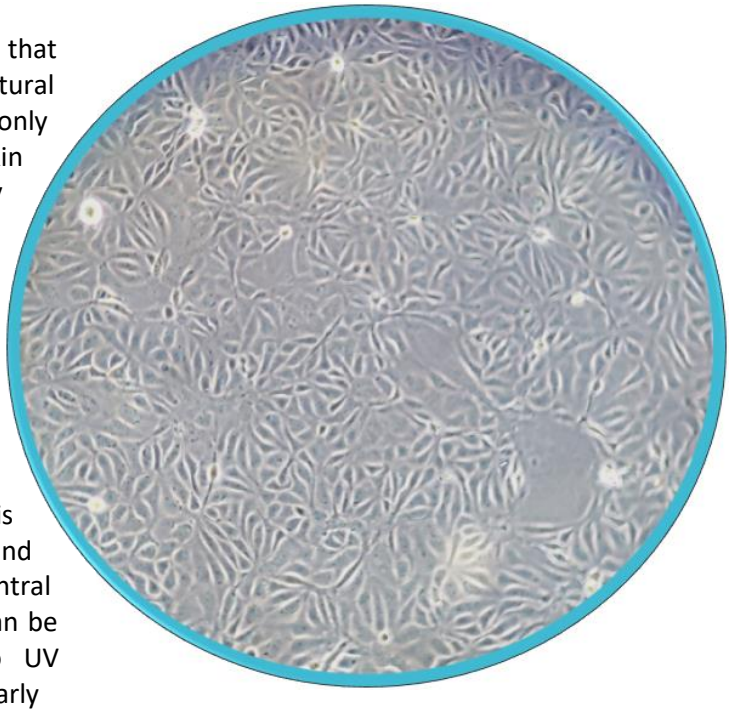

Figure 4.1: CHSE-214 (salmon embryo cells) in culture. Cultures maintained by Rhea Desai.

Melanin is considered a radioprotective compound because it can shield cells from the damaging effects of certain types of radiation, absorbing a broad range of spectra of electromagnetic radiation[2]. It is also considered of interest because of its potential properties as a free radical scavenger[1,3] There are conflicting reports in the literature on the role of melanin as a radioprotector with respect to direct free radical scavenging—some report antioxidant properties[4–6], while other groups report induction of oxidative damage, especially with varieties such as pheomelanin[7,8]**.**

The morphology of melanocytes is loosely comparable to glial cells in that they are branched, or dendritic[9]. Melanocytes secrete granules of melanin, packaged into melanosomes, which are introduced to more apical keratinocytes via endocytosis[9,10]. Melanocyte dendrites carry granules of melanin to surrounding epidermal cells. Endogenous melanosomes have been observed to accumulate near cell nuclei, suggesting a protective role for genetic material against electromagnetic radiation such as UVA[11]. It is thus appropriate that this assay can be used to measure intracellular as well as intercellular melanin concentration, which can give an estimate of how much melanin is produced and secreted by melanocytes in culture.

Melanin production can vary in B16F10 depending on various factors, with many reports focusing on the modulation of production by various plant extracts or metabolites such as citric acid[12–18]. Skin pigmentation and melanogenesis are not fully understood processes. The synthesis of melanin can be promoted by extrinsic mechanisms, including ultraviolet radiation exposure. Again, the mechanisms behind the regulation of these pathways are not completely understood[3,19].

The protective effects of melanin have been appreciated for some time. It is suspected to be relevant to the electromagnetic radiation-induced bystander effect specifically because it absorbs various spectra of UV light, with absorbance of light increasing sharply below 400 nm[20–22]. It is evident, in other chapters of this thesis, that melanin modulates signal production and responses in reporters. One prevailing question is whether melanin attenuates the effect in recipients of the signal, as it is known that irradiated donors do not produce significant biophoton emissions if they are melanocytes (see chapter 5). Le et al.[23] found that melanin attenuates reporter cell killing regardless of irradiation. Hence, it is suspected that the protective effect of melanin applies to reporters with high melanin content as well as donors.

Determination of the quantity of melanin produced by B16F10 was important for the present thesis because this quantity may vary between cultures. It was also of interest to determine the quantity of secreted melanin in cell culture medium, as phenol red-free medium turned an opaque, dark brown colour several days post routine subculture of B16F10 (see Figure 4.2.). It was also suspected that melanin present extracellularly in cultures could contribute to any attenuated effects observed in B16F10.

To determine the quantity of melanin in B16F10 cells, a concentration standard curve was created using synthetic eumelanin. A specific number of B16F10 cells were lysed, melanin extracted, and then concentration quantified by fitting absorbance points to a standard curve. Additionally, the concentration of melanin in cell culture medium was also quantified, as melanocytes readily secrete melanin and this was apparent through changes in the colour of cell culture medium (see Figure 4.2).

4.2. Methods

4.2.1. Initial determination of melanin concentration by using HaCaT and HCT116 cells

The determination of melanin concentration was possible by using existing procedure[24]. Cell cultures were grown following normal culturing procedures. On the day of subculture, cells were detached from growth flasks using a trypsin/EDTA solution. This solution was neutralized with an equal volume of complete growth medium. Determination of stock solution cell concentration was then determined for normalization purposes. The cells were then centrifuged at 2000 g in a VWR clinical centrifuge. A sample of supernatant was collected for determination of extracellular melanin concentration. Next, the supernatant was discarded and cells were resuspended in 500 µL lysis buffer (10% DMSO 1 N NaOH solution) and incubated at 80 degrees Celsius for one hour. This procedure allows for the lysing

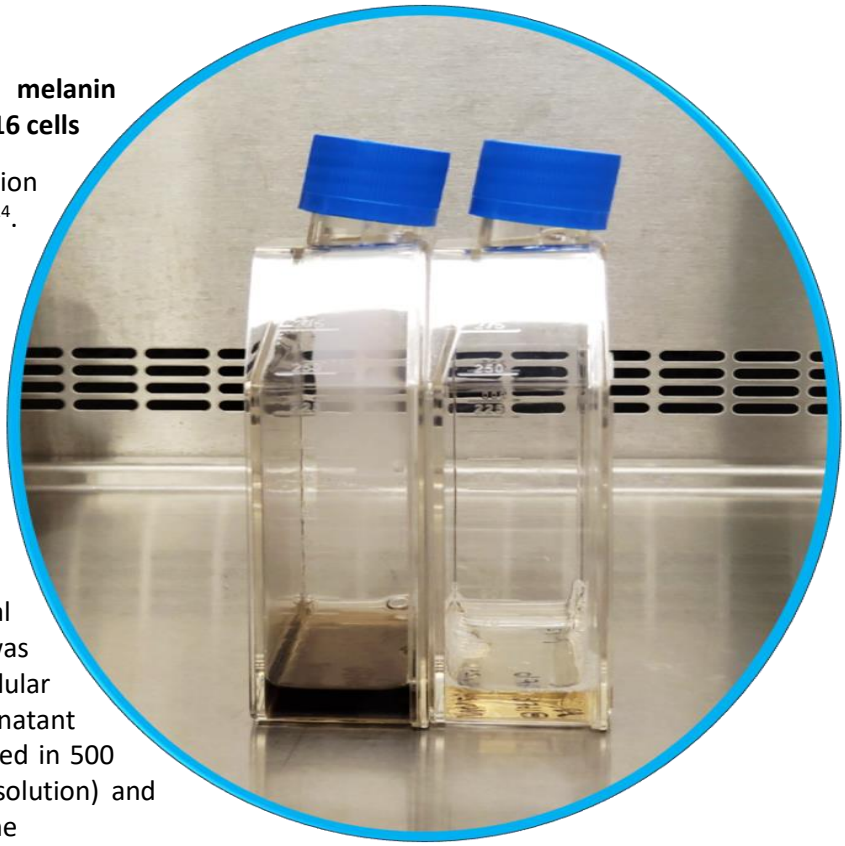

Figure 4.2: B16F10 (left) and HCT116 (right) cultures following 1 week of incubation.

of the cells and solubilization of intracellular melanin.

Synthetic eumelanin (M0418-100MG; Sigma Aldrich) was dissolved in lysis buffer at an initial concentration of 100 µM. Standards were made up using additional volumes of lysis buffer. Dilutions of the samples were also made to determine concentration more accurately. All volumes were made up to 200 µL in a black, clear-bottomed 96-well plate. The plate was read for absorbance at a Tecan 200m Pro Plate Reader 200 at 405/475 ± 3.5 nm. Using two wavelengths was appropriate for this because this can give an indication of whether melanin concentration is actually being measured by the assay; because the absorption spectrum of eumelanin is known[2,25], it can be reasonably assumed that using 405 nm light would produce results that are more sensitive because the peak absorption of this variety is between 300-400 nm.

The concentration of melanin was determined by fitting the absorbance points of sample wells to the standard curve to correlate melanin concentration. Blank wells containing complete growth medium and lysis buffer were included and the absorbance values were subtracted from each test well. This procedure was then modified to account for background absorbance due to cell debris present in the lysed samples.

4.2.2. Accounting for background absorbance

A follow-up experiment was conducted to determine the accuracy of the first measurement. Using the same lysis buffer, another standard curve was constructed. HCT116 cells were counted using the previously described procedure and assayed for melanin content. Along with normal lysates, some wells were “spiked” with melanin. This was done to determine if the presence of cell debris other than melanin can affect absorbance, and therefore if this would need to be controlled for. The quantity of HCT116 cells in each test tube was equal to subsequent attempts using B16F10, or 1 million cells. It was determined that cell debris do affect absorbance readings.

4.2.3. Revised quantification of Melanin concentration in HCT116 and B16F10 cells

Following this, a method was used to “subtract” this reading by using melanin-negative cells. HCT116 and B16F10 cells were passaged separately as normal and counted using previously described procedures. The cells were centrifuged for 5 min at 2000 g and medium harvested to assess melanin concentration and obtain background measurements. The cells were resuspended in DPBS. Stock solutions containing 4 million B16F10 cells and HCT116 cells were placed in 4 tubes, with 2 tubes per cell line, respectively. The cells were then centrifuged as previously described for a second time. The supernatant was discarded, and cells were resuspended in lysis buffer. Cells and medium were then incubated for 1 hour at 80 degrees Celsius. For extracellular melanin concentration, medium was filtered in the same fashion as described in chapter 2 for bystander experiments. Replicates from each tube were plated in a 96 well plate along with standards. This plate was then read at a Teacan 200m Pro Plate Reader 200 at 405/475 nm.

4.2.4. Statistical Analysis

Statistical tests were performed in Microsoft Excel and Graphpad Prism. A standard curve using a linear regression model was made in Graphpad Prism. Absorbance readings were used and the standard curve

equation was used to calculate melanin concentration in the samples, as originally described in Hosoi et al. (1985)[24] and adapted in subsequent studies[26].

4.3. Results

The quantity of melanin in B16F10 cells was estimated several times. Following several attempts, it was suspected that cell debris from B16F10 cells in 96-well plate could also affect melanin absorbance readings. This was confirmed and the results from this experiment are shown in Figure 4.3. A standard curve was created using melanin in buffer, while another curve was constructed with the same solution except with HCT116 cells present. The two best fit lines, calculated by linear regression, show a similar slope but have different y-intercepts, with the spiked curve appearing to have greater absorbance values overall. This result confirmed that presence of cell debris affects absorbance readings for melanin, and that a linear increase in melanin is proportional to the absorbance obtained. Furthermore, presence of cells in the assay buffer produced an expected overall increase in absorbance for each melanin concentration, relative to samples containing no cells.

The best estimate for intracellular concentration comes from measurements where background absorbance due to cell debris was accounted for by including a melanin negative cell line, HCT116, and calculation by the calculation of a standard concentration curve. This was possible because melanocytes and intestinal epithelial cells—as well as keratinocytes—are roughly equal in diameter (approximately 10–15 μM) and overall size[27,28]. Further evidence of this similar size can be found in the live-cell fluorescence microscopy images of all three cell lines, available in chapter 7. Using this method of accounting for the effects of cell debris on absorbance, it was found that 4 million B16F10 cells lysed in 4 mL buffer collectively contained 64.67-74.89 μM of melanin intracellularly (Figure 2.2). In the same graph, medium from approximately 80 million B16F10, grown for 6 days in 20 mL medium total, was found to contain between 187.2–213.5 μM of melanin.

To summarize these data as mean±SD, 1 million B16F10 cells in 1 mL were found to contain 68.78±23.34 μM melanin intracellularly, while approximately 4 million cells secreted enough melanin in 1 mL for a final extracellular concentration of 203.1±32.33 μM.

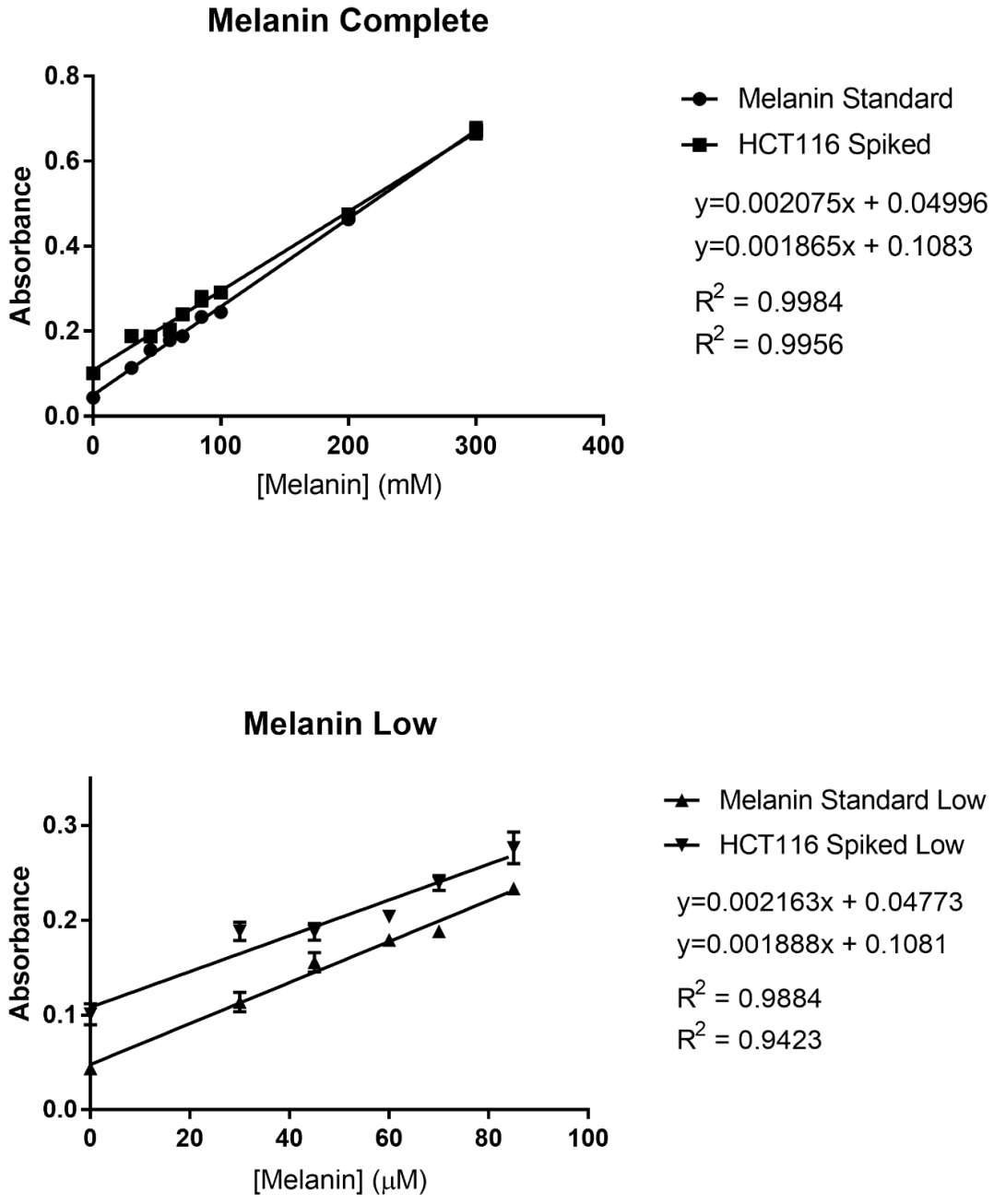

Figure 4.3: Absorbance plots for melanin standards. The top graph plots complete absorbance points from 0–300 μM melanin concentration. The bottom graph shows the same data as the graph on the top, however only the lower concentrations between 0–90 μM. Each regression line was calculated for the data in either graph. The Melanin Standard line indicates eumelanin standards dissolved in a solution of 10% DMSO in 1 N NaOH. The HCT116 Spiked line represents another test group, which is the same except for the presence of 1 million HCT116 cells in each tube in addition to varying concentrations of melanin. Error is represented as standard deviation from the mean. Note that for some data points the error was too low to display correctly on the figure.

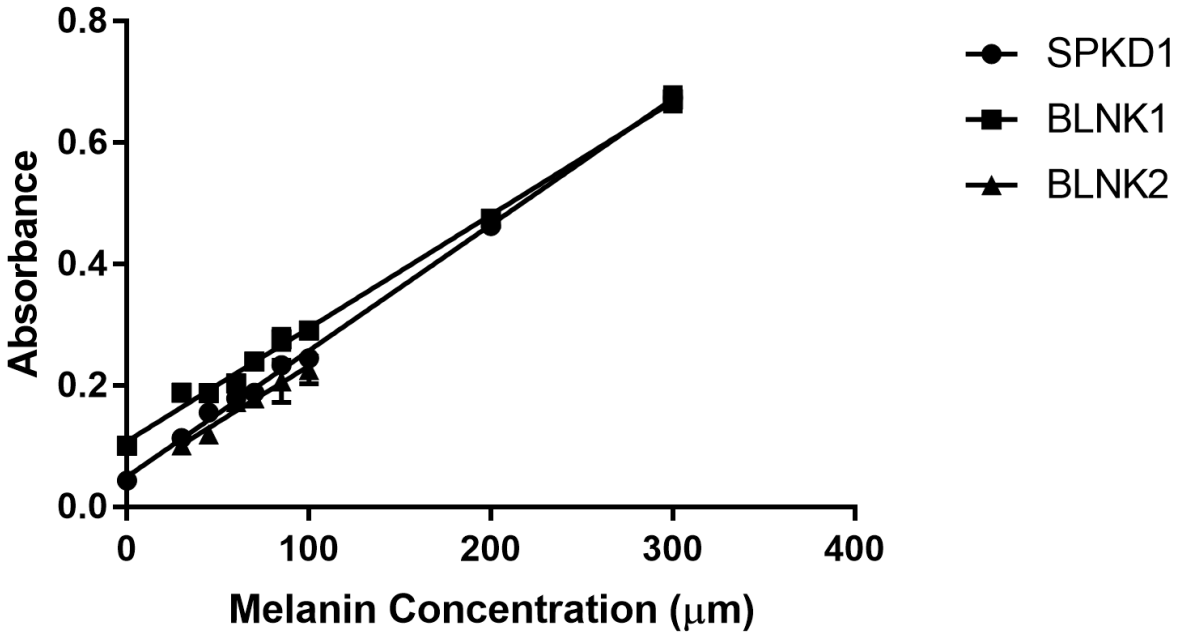

	SPKD1	BLNK1	BLNK2
Best-fit values ± SE			
Slope	0.002075 ± 3.095e-005	0.001865 ± 4.692e-005	0.001854 ± 0.0001724
Y-intercept	0.04996 ± 0.004109	0.1083 ± 0.00623	0.04697 ± 0.01191
X-intercept	-24.08	-58.07	-25.33
1/slope	481.9	536.3	539.3

Figure 4.4: This graph plots three standard regression lines, from several experiments, with data summarized below in a table. BLNK1 and BLNK2 indicate two independent replicates of pure eumelanin standards in assay buffer (10% DMSO in 1 N NaOH). BLNK2 consists of measurements of lower concentrations of melanin. SPKD1 is the same as BLNK1, however with 1 million lysed HCT116 cells to make a 1 million cells/mL solution, which represent cell debris. Error is represented as standard deviation from the mean. Note that for some data points the error is too low to display correctly on the figure. Error for some of the lower dose points can be observed in Figure 4.3.

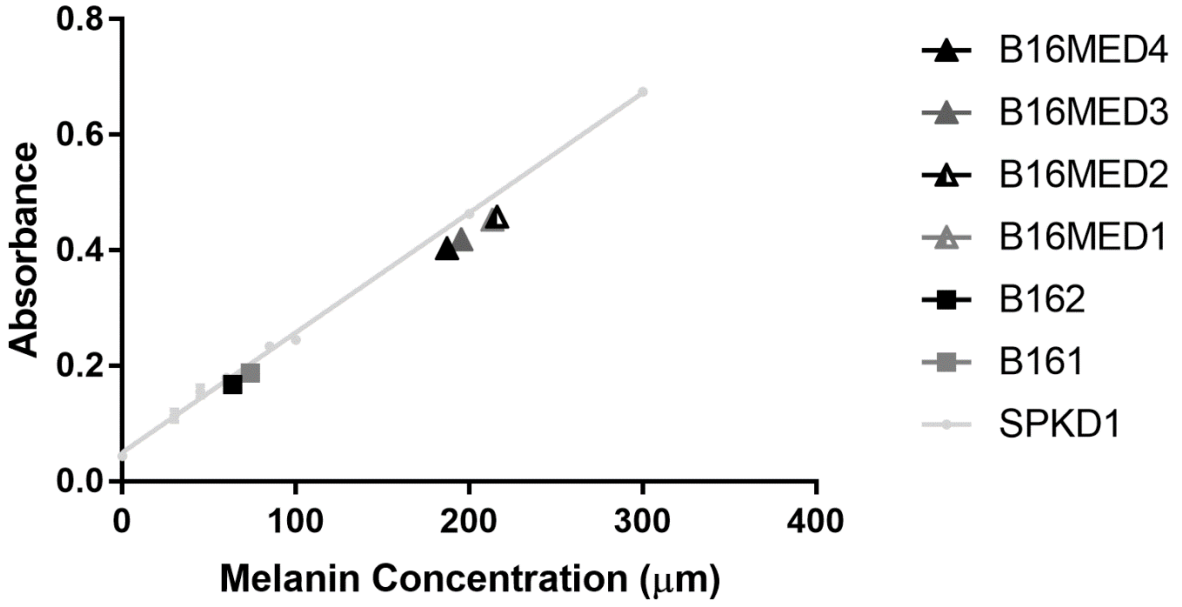

Figure 4.5: Another graph showing a standard curve from Figure 4.4, SPKD1. B16MED1-4 are samples of medium taken from cultures containing 80 million cells in 20 mL cell phenol red-free cell culture medium. These were calculated using measured absorbance values for four biological replicates and four technical replicates (n=16). The regression equation of BLNK1 (from Figure 4.4—not drawn here) was used to fit these data. B161-2 are 1 million B16F10 cells boiled in 1 N NaOH 10% DMSO lysis buffer (1 mL) in each tube. This group had two independent biological replicates and four technical replicates (n=8). These points were calculated from the linear regression of SPKD1.

4.5. Discussion

Eumelanin absorbs different spectra of UV differentially both *in vitro*[21] and *in vivo*[20]. As expected from predictions on sensitivity of the assay were it to accurately measure melanin concentration, the 475 nm results consistently showed less pronounced changes in absorbance with varying concentration across different experiments (data not shown). This is indicative that the assay was likely accurate in estimating melanin concentration, and that concentration of melanin in medium and within cells using this setup is possible.

The primary idea that can be derived from this chapter is that B16F10 cells are industrious producers of melanin! Moreover, it is apparent that these melanoma cells secrete a lot of melanin into cell culture medium under normal cell culture conditions, which is a function of normal melanocytes *in vivo.* One striking feature of these results is that essentially 4 million cells per millilitre can produce a concentration of approximately 200 μM in that volume over the course of approximately a week in culture—however, differences may exist when comparing these figures to normal melanocytes grown under the same conditions. Importantly, with respect to normal human cells *in vivo,* those with darker skin tones do not have more melanocytes but rather those that are present produce more melanin. Additionally, variance in the type of melanin produced, and size and number of

melanosomes produced—melanosome content can vary between 17.9% to 72.3%[29–31]. Further still, the variance in skin tone between individuals is known to epidemiologists to produce different skin cancer rates between individuals[29].

It was also apparent that cell debris could affect absorbance values. Although other absorbance assays such as Alamar Blue and MTT use different wavelength absorbances, this could be considered an issue in other assays that utilize absorbance. To prevent this from being a concern, a consistent cell density would be used for a particular assay across treatments was done throughout the present thesis report. Controlling for cell density within an experiment would ensure that any increase in absorbance due to presence of cell debris can be accounted for and factored into any calculations, as control wells should be affected similarly. Furthermore, the absorbance wavelengths used in these assays were not close to the one used for melanin absorbance (see chapters 8 and 10)

When a comparison between medium-borne eumelanin and intracellular eumelanin experimental groups is made, it is important to correct for the number of cells that synthesized the melanin. After correcting for this, the quantity of secreted melanin present in the medium of B16F10 cells at 7 days is roughly equivalent to the quantity of intracellular melanin in the adherent cells at the same point in time. This indicates that B16F10 cells maintain a "reserve" of melanin granules intracellularly and presumably secrete these granules packaged in extracellular vesicles during the course of normal cell culture. Melanogenesis is regulated via diverse means, and Videira et al.[32] provided an excellent review of this in the literature. Intrinsically, keratinocytes can produce factors than either promote or inhibit melanin production in melanocytes, and melanocytes produce these autocrine factors as well. The production of these factors, including nitric oxide, cytokines, and various peptides, can also be induced by ultraviolet radiation in melanocytes and keratinocytes. Ultraviolet radiation and extrinsically affect human skin pigmentation, which involves modulation of melanogenesis in persistent tanning due to UVB. Ultraviolet radiation may also increase the number of melanocyte dendrites, proliferation of melanocytes, and the provision of melanosomes to keratinocytes, ultimately occupying a nuclear position[32] to protect genetic material.

It is considered likely that melanin can attenuate the electromagnetic bystander signal, as described previously. It was confirmed in chapter 5 that photon emissions from irradiated cultures seemed to be concentrated in the UVA range (approximately 340 nm); this is the range of light that eumelanin is known to absorb most effectively[2]. Previous research has shown that exogenous inclusion of melanin in reporter cultures caused a decrease in cell killing in reporter cultures, and that melanin can produce an increase in survival regardless of treatment, possibly due to melanin's known free radical scavenging properties[23]. This effect occurred at a melanin concentration of approximately 31 µM. As was suggested in Le et al.[23] report, the effects of melanin in the present thesis was further investigated by determining the sensitivity of B16F10 cells to oxidative stress. Further, responses to the UVA bystander signal are also investigated in subsequent chapters. The first report to propose a physical component of the bystander signal was Mosse et al.[33] following ICCM transfer experiments. It had been shown before that melanin and melatonin can prevent bystander effects[34–36], and that it functions as a radioprotector in broader NTE as well[37–39]. It is suspected that melanin may attenuate the physical bystander effect in reporter cells.

4.6. Conclusion

The quantity of melanin produced by 80 million B16F10 cells in 20 mL of cell culture medium was determined. The intracellular and intercellular concentrations of melanin were determined for a fixed quantity of cells used in the assay. It is suspected that this melanin may protect against the electromagnetic radiation-induced bystander effect through two mechanisms: absorption of the light signal and scavenging of generated free radicals in bystander cells

4.7. References

1. Riley PA. Melanin. The international journal of biochemistry & cell biology. 1997;29(11):1235–1239.

2. Riesz J. The spectroscopic properties of melanin. 2007.

3. D'Mello SAN, Finlay GJ, Baguley BC, Askarian-Amiri ME. Signaling pathways in melanogenesis. International journal of molecular sciences. 2016;17(7):1144.

4. Herrling T, Jung K, Fuchs J. The role of melanin as protector against free radicals in skin and its role as free radical indicator in hair. Spectrochimica Acta Part A: Molecular and Biomolecular Spectroscopy. 2008;69(5):1429–1435.

5. Seagle B-LL, Rezai KA, Gasyna EM, Kobori Y, Rezaei KA, Norris JR. Time-resolved detection of melanin free radicals quenching reactive oxygen species. Journal of the American Chemical Society. 2005;127(32):11220–11221.

6. Cope FW, Sever RJ, Polis BD. Reversible free radical generation in the melanin granules of the eye by visible light. Archives of Biochemistry and Biophysics. 1963;100(2):171–177.

7. Duval C, Poelman MC. Scavenger effect of vitamin E and derivatives on free radicals generated by photoirradiated pheomelanin. Journal of pharmaceutical sciences. 1995;84(1):107–110.

8. Rodríguez-Martínez S, Wakamatsu K, Galván I. Increase of the benzothiazole moiety content of pheomelanin pigment after endogenous free radical inducement. Dyes and Pigments. 2020;180:108516.

9. Cichorek M, Wachulska M, Stasiewicz A, Tymińska A. Skin melanocytes: biology and development. Advances in Dermatology and Allergology/Postępy Dermatologii I Alergologii. 2013;30(1):30.

10. Shain AH, Bastian BC. From melanocytes to melanomas. nature reviews Cancer. 2016;16(6):345.

11. Boissy RE. Melanosome transfer to and translocation in the keratinocyte. Experimental dermatology. 2003;12:5–12.

12. Lee M, Yoon H, Kim J, Choi J, Byun D, Kim H. Dioxinodehydroeckol inhibits melanin synthesis through PI3K/Akt signalling pathway in α-melanocyte-stimulating hormone-treated B16F10 cells. Experimental dermatology. 2012;21(6):471–473.

13. Huang H-C, Hsieh W-Y, Niu Y-L, Chang T-M. Inhibitory effects of adlay extract on melanin production and cellular oxygen stress in B16F10 melanoma cells. International journal of molecular sciences. 2014;15(9):16665–16679.

14. Chan YY, Kim KH, Cheah SH. Inhibitory effects of Sargassum polycystum on tyrosinase activity and melanin formation in B16F10 murine melanoma cells. Journal of Ethnopharmacology. 2011;137(3):1183–1188.

15. Moleephan W, Wittayalertpanya S, Ruangrungsi N, Limpanasithikul W. Effect of xanthoxylin on melanin content and melanogenic protein expression in B16F10 melanoma. Asian Biomedicine. 2012;6(3):413–422.

16. Oh H-C, Lim K-S, Hwang C-Y, Youn I-H, Kim N-K. A study on the melanin synthesis inhibition and whitening effect of Bombysis corpus. The Journal of Korean Medicine Ophthalmology and Otolaryngology and Dermatology. 2007;20(3):1–13.

17. Park S-H, Kim D-S, Park S-H, Shin J-W, Youn S-W, Park K-C. Inhibitory effect of p-coumaric acid by Rhodiola sachalinensis on melanin synthesis in B16F10 cells. Die Pharmazie-An International Journal of Pharmaceutical Sciences. 2008;63(4):290–295.

18. Zhou S, Sakamoto K. Citric acid promoted melanin synthesis in B16F10 mouse melanoma cells, but inhibited it in human epidermal melanocytes and HMV-II melanoma cells via the GSK3β/β-catenin signaling pathway. PloS one. 2020;15(12):e0243565.

19. Park HY, Kosmadaki M, Yaar M, Gilchrest BA. Cellular mechanisms regulating human melanogenesis. Cellular and Molecular Life Sciences. 2009;66(9):1493–1506.

20. Kollias N, Baqer A. Spectroscopic characteristics of human melanin in vivo. Journal of investigative dermatology. 1985;85(1):38–42.

21. Riesz J, Gilmore J, Meredith P. Quantitative scattering of melanin solutions. Biophysical journal. 2006;90(11):4137–4144.

22. Zonios G, Dimou A, Bassukas I, Galaris D, Tsolakidis A, Kaxiras E. Melanin absorption spectroscopy: new method for noninvasive skin investigation and melanoma detection. Journal of biomedical optics. 2008;13(1):14017.

23. Le M, McNeill FE, Seymour C, Rainbow AJ, Mothersill CE. An observed effect of ultraviolet radiation emitted from beta-irradiated HaCaT cells upon non-beta-irradiated bystander cells. Radiation research. 2015;183(3):279–90. http://www.bioone.org/doi/10.1667/RR13827.1%5Cnhttp://www.ncbi.nlm.nih.gov/pubmed/25710575. doi:10.1667/RR13827.1

24. Hosoi J, Abe E, Suda T, Kuroki T. Regulation of melanin synthesis of B16 mouse melanoma cells by 1α, 25-dihydroxyvitamin D3 and retinoic acid. Cancer Research. 1985;45(4):1474–1478.

25. Ou-Yang H, Stamatas G, Kollias N. Spectral responses of melanin to ultraviolet A irradiation. Journal of investigative dermatology. 2004;122(2):492–496.

26. Peng L-H, Liu S, Xu S-Y, Chen L, Shan Y-H, Wei W, Liang W-Q, Gao J-Q. Inhibitory effects of salidroside and paeonol on tyrosinase activity and melanin synthesis in mouse B16F10 melanoma cells and ultraviolet B-induced pigmentation in guinea pig skin. Phytomedicine. 2013;20(12):1082–1087.

27. Das S, Chatterjee N, Bose D, Dey SK, Munda RN, Nandy A, Bera S, Biswas SK, Saha K Das. Anticancer potential of 3-(arylideneamino)-2-phenylquinazoline-4 (3H)-one derivatives. Cellular Physiology and Biochemistry. 2012;29(1–2):251–260.

28. Olejniczak A, Szaryńska M, Kmieć Z. In vitro characterization of spheres derived from colorectal cancer cell lines. International journal of oncology. 2018;52(2):599–612.

29. Brenner M, Hearing VJ. The protective role of melanin against UV damage in human skin. Photochemistry and Photobiology. 2008. doi:10.1111/j.1751-1097.2007.00226.x

30. Duchon J. Chemical composition of melanosomes. Dermatologische Monatschrift. 1970;156(5):371.

31. Pathak MA, Jimbow K, Fitzpatrick T. Phenotypic expression in pigment cells. Photobiology of Pigment Cell. Eds: Seiji M. University of Tokyo Press, Tokyo, Japan. 1980:655–670.

32. Videira IF dos S, Moura DFL, Magina S. Mechanisms regulating melanogenesis. Anais brasileiros de dermatologia. 2013;88(1):76–83.

33. Mosse I, Marozik P, Seymour C, Mothersill C. The effect of melanin on the bystander effect in human keratinocytes. MUTATION RESEARCH-FUNDAMENTAL AND MOLECULAR MECHANISMS OF MUTAGENESIS. 2006;597(1–2):133–137. doi:10.1016/j.mrfmmm.2005.09.006

34. Marozik P, Mothersill C, Seymour CB, Mosse I, Melnov S. Bystander effects induced by serum from survivors of the Chernobyl accident. EXPERIMENTAL HEMATOLOGY. 2007;35(4, 1):55–63. doi:10.1016/j.exphem.2007.01.029

35. Seymour CB, Mothersill C, Mooney R, Moriarty M, Tipton KF. Monoamine oxidase inhibitors l-deprenyl and clorgyline protect nonmalignant human cells from ionising radiation and chemotherapy toxicity. BRITISH JOURNAL OF CANCER. 2003;89(10):1979–1986. doi:10.1038/sj.bjc.6601361

36. Shao C, Folkard M, Michael BD, Prise KM. Bystander signaling between glioma cells and fibroblasts targeted with counted particles. International journal of cancer. 2005;116(1):45–51.

37. Marozik P, Mosse I, Mothersill C, Seymour C. Protection by chemicals against radiation-induced bystander effects. In: Mothersill, C and Mosse, I and Seymour, C, editor. MULTIPLE STRESSORS: A CHALLENGE FOR THE FUTURE. 2007. p. 247+. (NATO Science for Peace and Security Series C-Environmental Security). doi:10.1007/978-1-4020-6335-0_16

38. Marozik PM, Mosse IB, Seymour C, Mothersil C. The influence of melanin on bystander effect. 2003.

39. Mosse IB, Marozik PM. Some natural chemical antioxidants: functions and genetic effects. In: Simulation and Assessment of Chemical Processes in a Multiphase Environment. Springer; 2008. p. 409–433.

Chapter 5

Characterization of photons emitted from β-irradiated epithelial cell cultures

Abstract: According to previous reports, photons in the ultraviolet range are emitted from directly irradiated cells. Moreover, these reports indicate that photons can induce a variety of bystander effects in cells traversed by them, and therefore constitute a novel type of "physical" or "electromagnetic" bystander signal. To confirm that living cells emit these biophotons, HaCaT, HCT116, and B16F10 cells were directly irradiated with tritium for a total dose of 0.5 Gy. Following this 24-hour irradiation period, detection of photon emissions and spectral discrimination was accomplished using a photomultiplier tube, nuclear instrumentation module with a scalar component, and two optical bandpass filters. The data corroborate β-radiation-induced ultraviolet photon emissions in both HaCaT and HCT116 cells. Moreover, B16F10 cells did not exhibit increased photon emissions upon irradiation, suggesting a role for melanin in the absorption of these photons and consequent abrogation of bystander signalling. Finally, hydrogen peroxide was not found to induce photon emissions in the human cell lines. Overall, these results indicate that HCT116 and HaCaT can produce this radiation-induced bystander signal *in vitro,* thereby verifying previous findings and providing groundwork for follow-up experiments on bystander reporters receiving this signal.

5.1. Introduction

Previous reports from our lab have shown the physical bystander signal is an important component of broader bystander effects. Photon emissions from directly irradiated cultures have been demonstrated using β-radiation[1–4]. In the case of β-radiation, these photon emissions have been shown to decrease the survival of adjacent cells upon exposure[5]. These photons have also been shown to also cause the release of exosomes from these cells, which act as vehicles for the bystander signal *in vitro* and *in vivo*[3,6,7]**.** Another critical finding was the fact that these biophotons modulate the activities of several mitochondrial respiratory complexes, and hence likely have implications in the modulation of redox and metabolic homeostasis[8,9]. A more detailed description of these connections can be found in chapter 1, which also contains justifications for this research project and scope, and chapter 7. It is also important to note that these emissions are believed to be concentrated in the UVA range[2,4,5,10] and represent a relatively novel type of bystander signal, as previous research focused primarily on soluble factors and communication of the signal via gap junctions[11,12].

It was crucial therefore to consider measuring these photon emissions in cell cultures. Logically, the signal should be reproduced before its effects on reporter cells can be investigated. While biophoton production has been reported previously by our group, it has not thus far been reported in B16F10 cells; although it has been shown in HaCaT and HCT116 cells[5,8]. It was also considered pertinent to characterize the spectra of the light because previous reports have indicated that the signal appears to primarily consist of ultraviolet-range photons; moreover, effects connected to biophoton exposure were ameliorated upon blocking these UV-range photons[2]. A description of these spectra is also required because the radiobiological qualities of light differ depending on wavelength. Smaller wavelengths of light, such as those in the ultraviolet range, carry greater energy. This is noted to be very important in the UV-range because certain energies have the potential to create DNA lesions and may therefore produce indirect "targeted effects" in reporter cultures, due to the secondary radiation emitted from cultures[13–15]. Conversely, lower energies can potentially cause significant energy deposition, thermal effects, and indirect damage to cells through intermediates such as ROS, assuming adequate intensity[16–19]—further discussion of these effects can be found in chapter 1.

Finally, because hydrogen peroxide was used later to model oxidative stress, the question arose whether hydrogen peroxide treatment could somehow induce biophoton release. A small experiment was planned where one of the cell lines was treated with varying concentrations of hydrogen peroxide and monitored for photon emissions. This experiment was further justified by the deduction that, as various types of bystander signals are linked[3] and bystander responses can be ameliorated by antioxidants[20,21], that ROS may contribute to the production of bystander signals in cells.

The purpose of this chapter was to determine whether photon emission occurs in T25 flasks containing HCT116, HaCaT, and B16F10 cells after a controlled dose of β-radiation. Further, the purpose was to characterize the spectra of emissions using two optical bandpass filters, one selecting for approximately 340 nm light and the another for approximately 280 nm light—representing roughly UV-A and the UV-B/C boundary, respectively. Another goal was to determine if photon emission may occur following direct administration of hydrogen peroxide to cells in culture. These experiments were conducted to demonstrate these photon emissions and allow follow-up bioassays on reporters.

5.2. Methods

5.2.1. Experimental apparatus

The device used for counting photons was built by Dr. Bilal Ahmad in our laboratory. A schematic of the device is available in figure 5.1. The apparatus features a light-tight chamber with a small container housing a R7400 subminiature photomultiplier tube (Hamamatsu Photonics, Bridgewater, NJ, USA), a convex lens that is 25 mm in diameter, and space for optical filters. The complete specifications of this device are outlined in an existing publication[22]. The main method of collecting data from this device was the manual operation of a scalar module with buttons to start, stop, and reset the count displayed on the module, which represents photon counts. The nuclear instrumentation module (NIM) was used as described previously by Le et al.[2], Ahmad et al.[22], and Cohen[23].

In addition to measurements in the absence of filters, 340 nm (Edmund Optics, 65675) and 280 nm (Edmund Optics, 67813) hard coated, interference-type band-pass filters were used. The use of these filters allowed the discrimination of spectral bands from the initial measurement with no such filter. These filters were manufactured by Edmund Optics (Barrington, NJ USA). Both filters have a 25 mm diameter and a passband of 10 nm. The 340 nm filter has a minimum transmission of greater than 85%, while the 280 nm filter has a minimum transmission of greater than 60%. The blocking wavelengths are also slightly different between the two filters, with the 340 nm blocking 200–1200 nm, excluding 340 ±2 nm, and with the 280 blocking 200-650 nm, excluding 280 ±2 nm.

Prior to operation, the main power for the NIM was switched on, followed by the power for the high-voltage supply module. The high voltage supply was dialed to -800 V and then left for at least 20 minutes to warm up. Following this, the elastic band which seals the main chamber was removed to place flasks or petri dishes. During most experiments, the smaller container housing the PMT and associated electronics had to be moved for flask placement but was resecured in the same position. For taking readings, the lid was closed, and the band placed around the lid. The band was cursorily inspected for a proper seal and a black tarp draped over the lid to prevent background from ambient photons; a standard, extra large lab coat was also arranged superior to the tarp for the same, photon-blocking purpose.

A rough schematic of the device is depicted in figure 5.1. The distance between the cell monolayer and the lens (n) is approximately 4 cm. The length of the PMT housing (G) is 9 cm in length. Between the lens and the PMT is 7 cm, and from the lens to the optical filter is 5 cm. The PMT device is approximately 1.5 cm long and 15 mm in diameter.

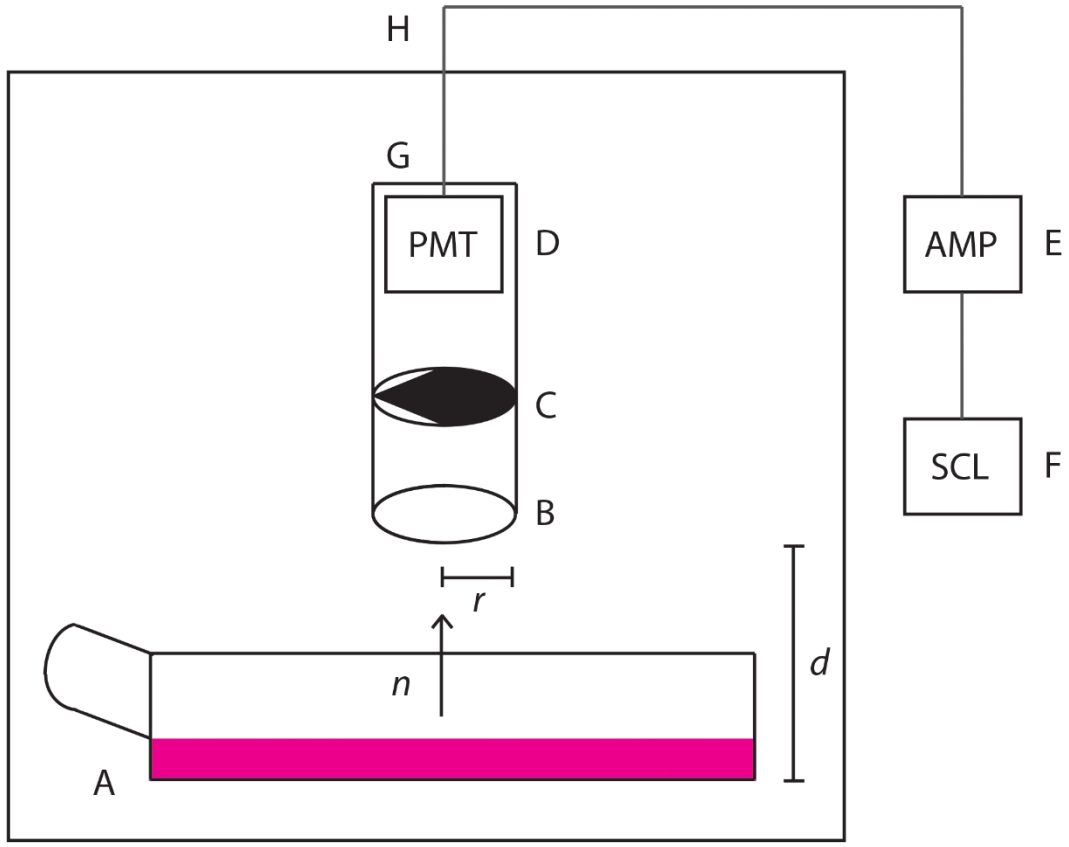

Figure 5.1: A diagram of the experimental apparatus used for photon counting. (A) flask containing medium; (B) collimating lens; (C) interference type optical bandpass filter (280 nm or 340 nm); (D) Hamamatsu Photonics r7400 photomultiplier tube (PMT); (G) PMT housing; (H) light-tight container; (E) signal amplifier module; (F) scaler module. *n* represents a single photon emission. The *r* term is the radius of the opening of the housing for the PMT (12.5 mm). The *d* represents the distance from the cell monolayer to the opening of the PMT housing (4 cm).

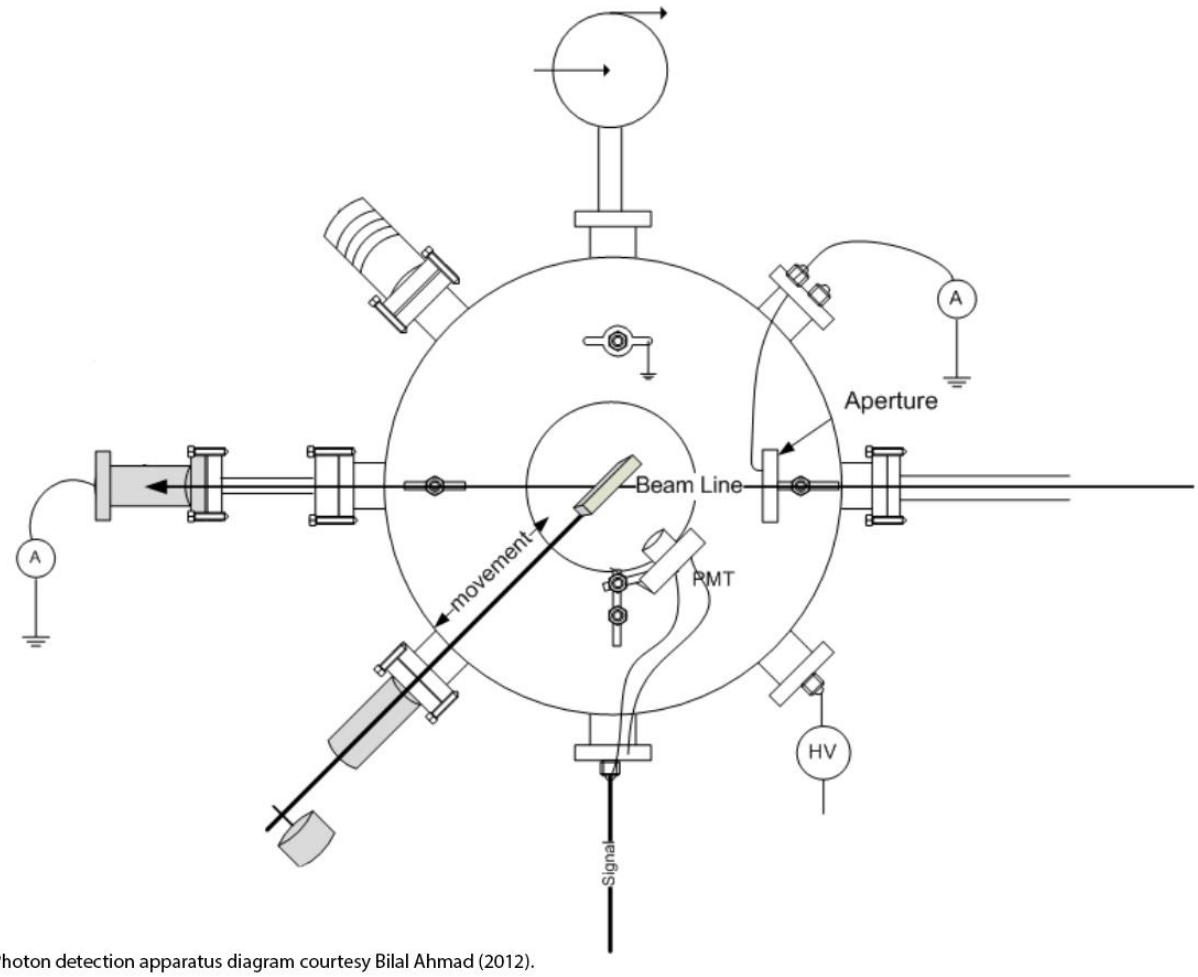

Photon detection apparatus diagram courtesy Bilal Ahmad (2012).

Figure 5.2: A bird's-eye view of the light-tight apparatus used in photon detection. Diagram by Ahmad (2012).

5.2.2. ^{3}H dose calculations and irradiation

Radiation dose is typically conceptualized as unit energy absorbed per unit mass. Dose delivered to directly irradiated cells was calculated using the same method described inn previous publications[3–5] to achieve a consistent dose with a similar experimental setup:

$$D = \frac{N_0 \lambda_R \bar{\mathrm{E}}_\beta t}{m}$$

Equation 5.1: The equation for dose of beta radiation emitted by tritium and absorbed by cell cultures, in joules per kilogram or gray. This is the same equation that appears in previous papers[3]. $N_0\lambda_R$ represents activity of tritium in decays per second, or becquerel; $\bar{\mathrm{E}}_\beta$ represents the average energy of tritium beta particles; t is the duration of irradiation in seconds; m represents the mass of the irradiated object in

kilograms. The mass of the irradiated object in this case is the mass of the cell culture medium, with an approximated to the density of normal water (~1 g/mL) under normal atmospheric conditions.

It was assumed that activity remained consistent during the irradiation time which varied across experiments and chapters between 24–72 hours. This was assumed because the half life of tritium, 12.3 years, is too long for a period of several days to cause a non-negligible reduction in activity. Experiments in this chapter were limited to a 0.5 Gy dose prior to measurement.

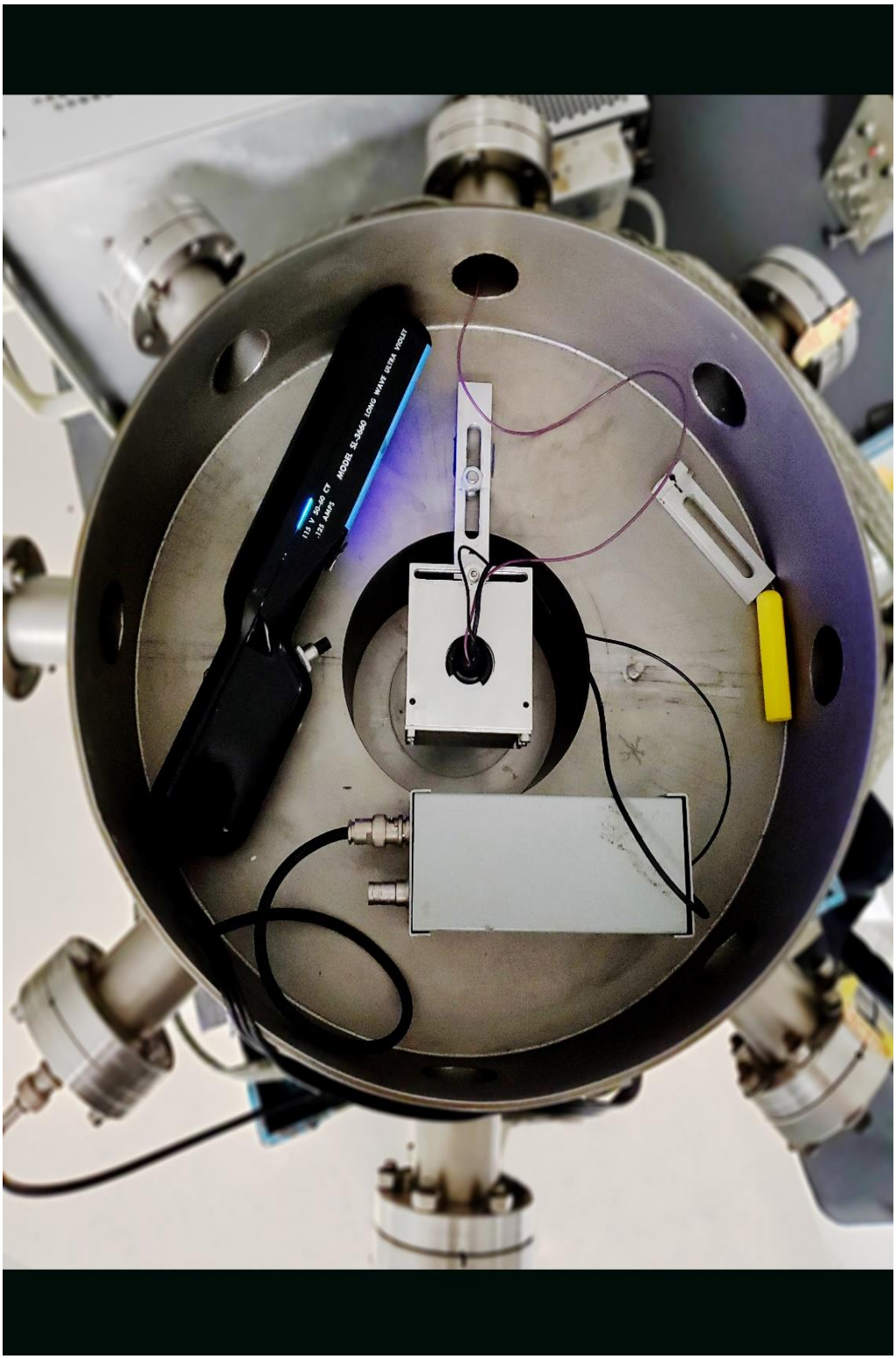

Figure 5.3: A picture that shows the position of the UV lamp inside the counting vessel. The PMT housing is in the center of the chamber, with the lens close to the bottom of the chasm. The wiring connecting it to the NIM passes through the rectangular structure at the bottom of the chamber and leads outside the chamber on the bottom left.

5.2.3. Experimental setup troubleshooting

To determine responsiveness to ultraviolet light, a Spectroline SL-3660 lamp was used. This lamp emits long wave ultraviolet light with a peak emission of 360 nm. The arrangement for this "response check" is shown in figure 5.3.

Initial attempts to obtain photon measurements were unsuccessful. 100 mm petri dishes were seeded at the optimum determined density[2] and tritium placed inside the flask with medium. Readings were immediately taken for 10 minutes, however no increase over background or cells alone was observed during this time (data not shown). The same setup was used, as described later, but 5 mL medium was placed in these dishes.

Subsequent attempts to obtain positive photon emission results were conducted in T25 flasks, primarily due to ease and safety considerations for transportation of the radioactive material—petri dishes had an observed tendency to leak, as they are not sealed like cell culture flasks. Another parameter, the dose given to the donors prior to reading, was modified to 0.5 Gy by increasing the time between tritium supplementation and photon measurement by 24 hours.

5.2.4. ^{3}H-induced photon emission detection

The final, optimized procedure involved irradiation in T25 flasks. On the day of subculture, HCT116, HaCaT, and B16F10 cells were seeded in T25 flasks with 5 mL phenol red-free complete growth medium. All cells were again seeded at the optimum density for photon production[2], 2000 cells/cm^2. These were incubated for 24 hours with the relevant treatment, protected from light. After 24 hours had elapsed and a dose of 0.5 Gy delivered to the cultures, they were transported to the photon counting apparatus.

The readout on the scalar module was observed for 10 minutes until a final photon count was obtained. This was averaged to number of counts per minute, as the variation in quantity of photons emitted between minutes in a set was determined to be negligible.

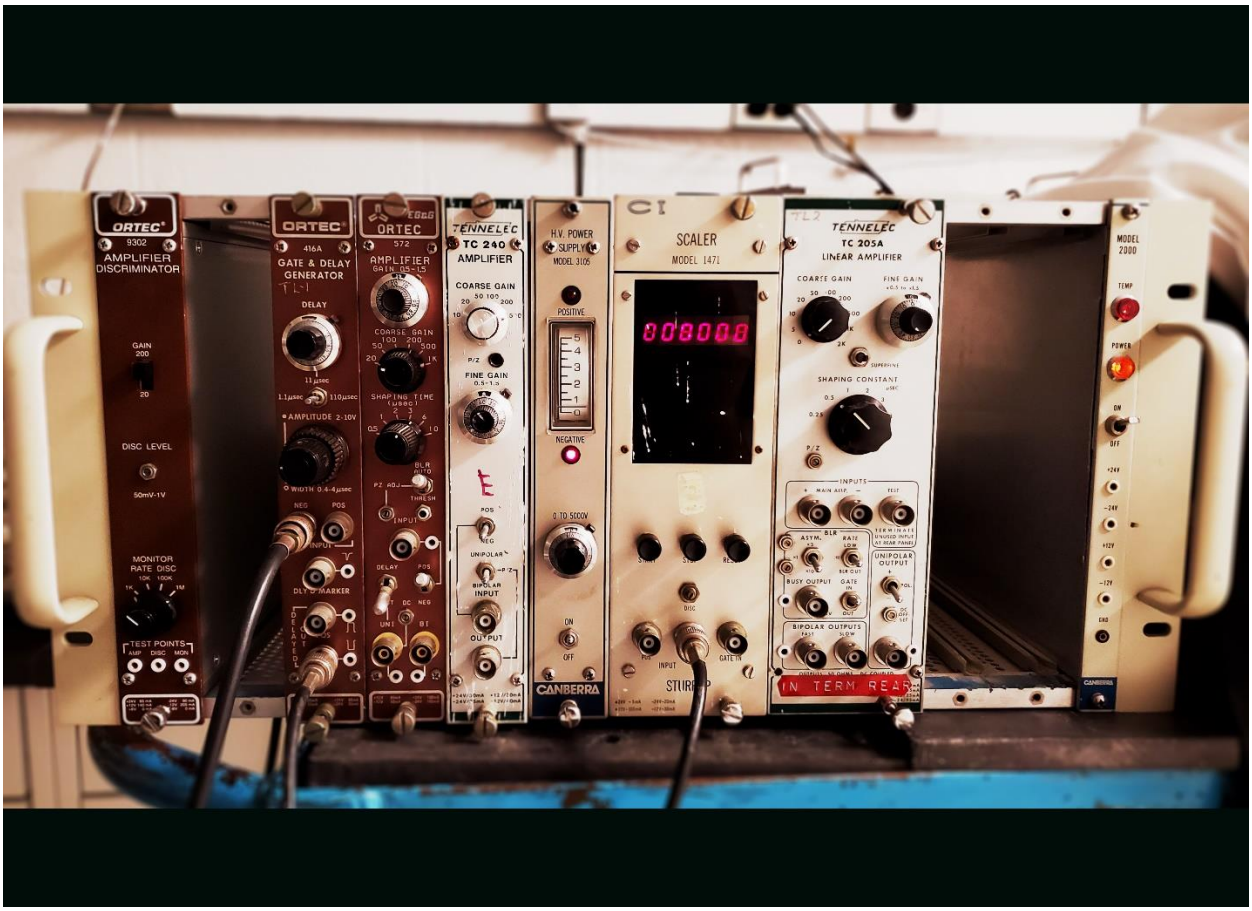

Figure 5.4: The nuclear instrumentation module (NIM) used for photon counting following power-up and warm-up period. Note the amplifier and scalar modules ("E" and "F" in Figure 5.1, respectively). These are connected on the back panel of the NIM (not shown).

5.2.5. Hydrogen peroxide-induced photon emission detection

On the day of subculture, HCT116 cells were seeded in T25 flasks at 2000 cells/cm^2. These cells were left to adhere for 24 hours. On the second day, an 880 µM solution of hydrogen peroxide was created in DPBS from an 880 mM stock solution. A specific volume was added to cell culture medium such that a final concentration of hydrogen peroxide in the medium was obtained. The cells were then left to grow for an additional 24 hours. On the third day, the flasks were read using the same photon counting procedure described previously in section 5.2.4.

5.2.6. Hydrogen peroxide supplementation

HaCaT cells were used to determine whether hydrogen peroxide supplementation could increase photon emissions. This was conducted such that potential confounding factors, such as the overall oxidative homeostasis of the cell culture, could be identified prior to further experiments, in addition to suspicions outlined in section 5.1. On the day of subculture, a set of control and test flasks were seeded at 2000 cell/cm^2 as described previously. These were incubated with varying concentrations of hydrogen peroxide, diluted in DPBS as described in sections 6.2.1 and 6.2.3, for 24 hours while protected from ambient light. The flasks were then read as previously described at the photon counting apparatus.

5.2.7. Statistical analysis

Photon counts and time elapsed were recorded during each experiment. Each group in this chapter represents three biological replicates (n=3) unless otherwise indicated. These data were inputted and analyzed in Microsoft Excel and Graphpad Prism 7. Several tests for statistical significance were conducted at α=0.05. For figure 5.6, one-way ANOVA was performed followed by Tukey's post-hoc HSD test for significance.

5.3. Results

5.3.1. Basic PMT response check

The background count varied between approximately 10–70 γ/min across all experiments. In the response check, data shown in figure 5.1, there was a slight increase in background counts overall.

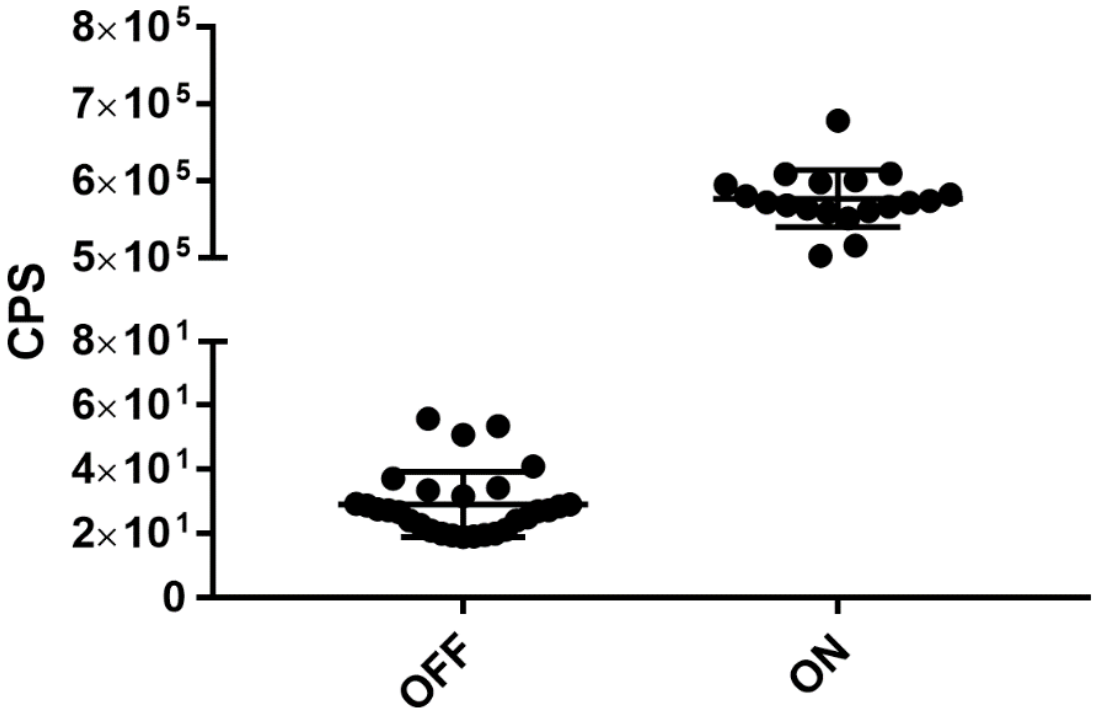

Figure 5.5: Photon counts per second (CPS) inside the light-tight apparatus before and after switching on the UVA lamp. Saturation of the scalar readout, shown in figure 5.4, occurred after approximately 1 second of engagement.

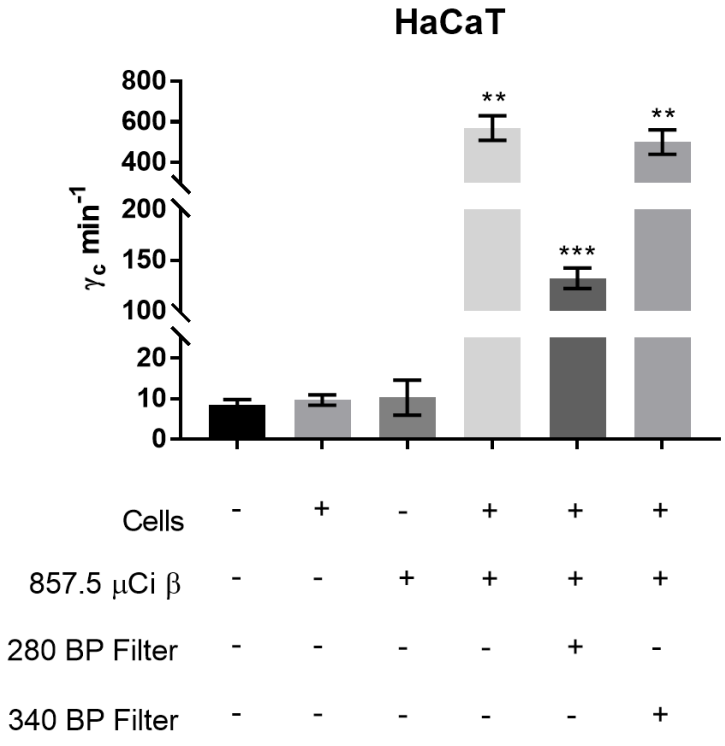
HaCaT
800
600
400
200
150
100
20
10
0
γ_c min^{-1}
**
***
**
Cells - + - + + +
857.5 μCi β - - + + + +
280 BP Filter - - - - + -
340 BP Filter - - - - - +

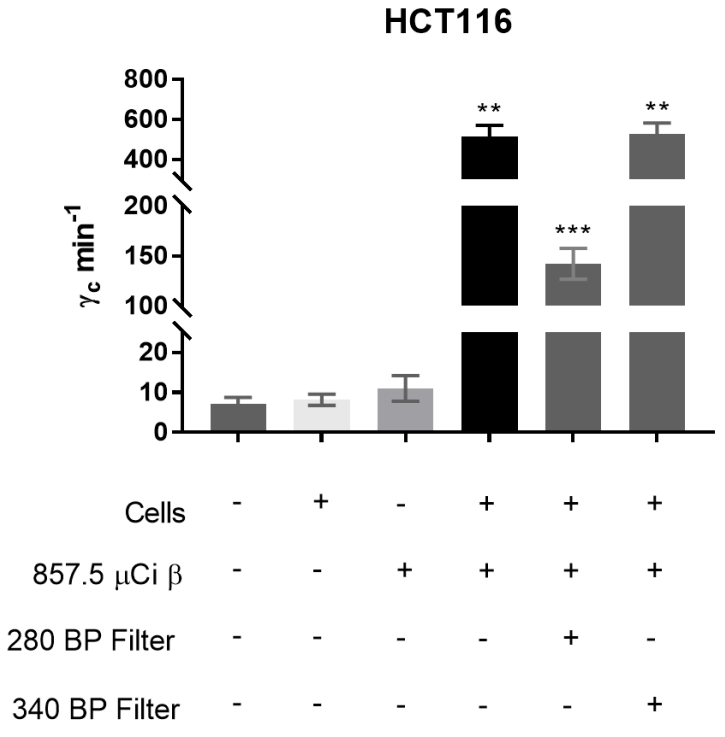
HCT116
800
600
400
200
150
100
20
10
0
γ_c min^{-1}
**
***
**
Cells - + - + + +
857.5 μCi β - - + + + +
280 BP Filter - - - - + -
340 BP Filter - - - - - +

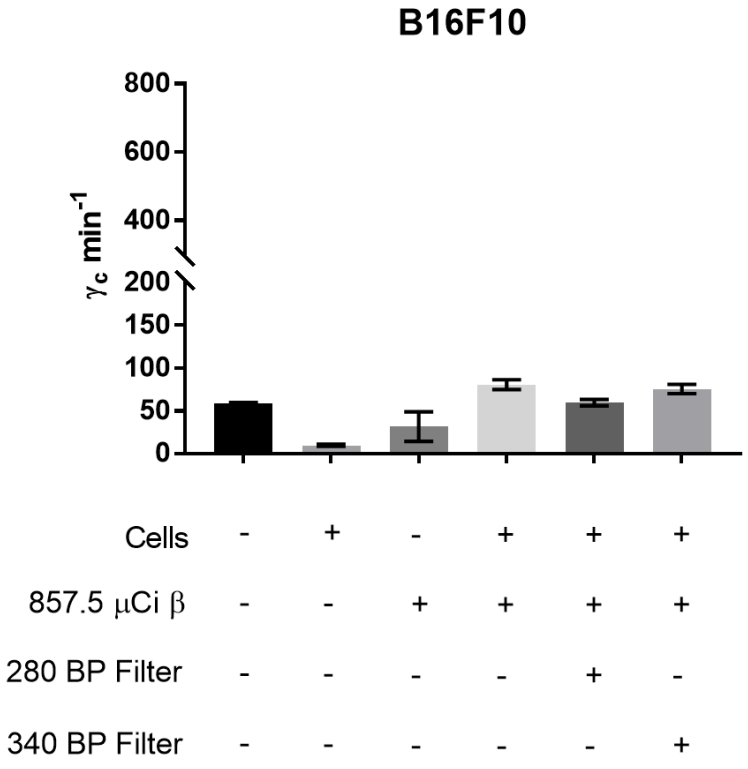

Figure 5.6: Photon counts from directly irradiated cells. The first group from the left indicates results from runs with no flask in the chamber. The second group shows results from a flask in the chamber containing cells and medium. The third shows counts from counts with a flask in the chamber containing the specified activity of tritium (857.5 μCi or 13.73 MBq). The fourth shows counts from runs with a flask in the chamber containing tritium, cells, and culture medium. The fifth set shows the same as the fourth, but with a 280 nm band pass filter situated between the lens and the PMT. The sixth and final set is the same as the first, but with a 340 nm band pass filter instead.

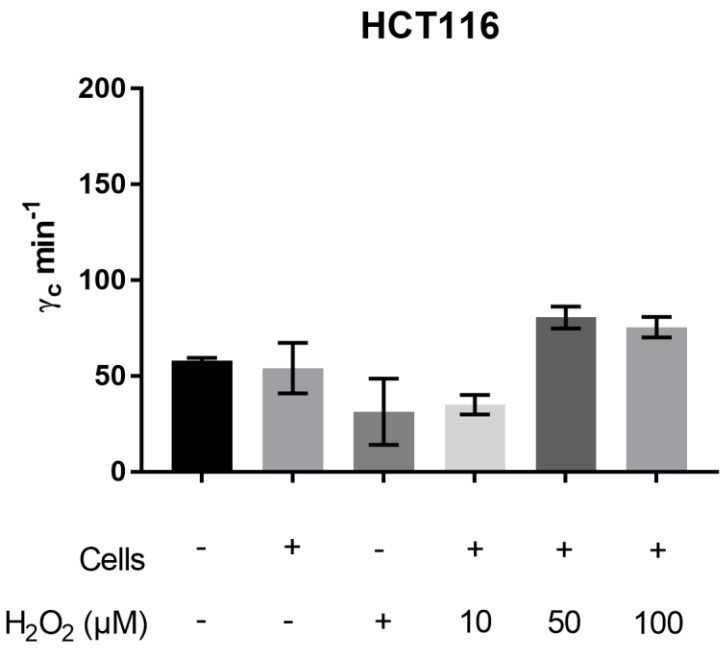

Figure 5.7: Photon counts from HCT116 cells treated with various concentrations of hydrogen peroxide.

5.3.2. ^{3}H-irradiation of epithelial cells produces photon emissions

Both HCT116 and HaCaT cells exhibited significant photon emissions following a 0.5 Gy tritium dose. Comparisons of each test mean was made to the group containing cells but no tritium. Figure 5.6 shows that inclusion of tritium and cells alone, respectively, did not produce significant photon counts above background. Inclusion of cells and tritium together induced significant photon emissions from HaCaT and HCT116 cells. B16F10 cells did not show significant photon emissions above background following the same treatment.

To summarize this data, HaCaT counts without a filter ($p<0.0001$), with the 280 filter ($p=0.0270$), and with the 340 nm filter ($p<0.00001$) were significant. HCT116 counts without a filter ($p<0.0001$), with the 280 nm filter ($p=0.0037$), and with the 340 nm filter ($p<0.0001$) were significant. The same comparisons for B16F10 were not significant ($p=0.0638$; 0.9904; 0.1696, respectively).

The photon measurements in both human cell lines were concentrated in the low-energy ultraviolet region. In figure 5.6, inclusion of a 280 nm bandpass filter significantly reduced photon counts, indicating relatively fewer photons around the generally recognized UVB/UVC boundary[24,25]. Inclusion of a 340 nm bandpass filter revealed that the majority of photons emitted appeared to be in the UVA range.

5.3.2. Hydrogen peroxide treatment of HCT116 does not induce photon emission

In figure 5.7, data is shown from HCT116 cells exposed to hydrogen peroxide. The results indicated no significant increase in photon counts above background measurements in these cells (≤100 per minute).

5.4. Discussion

Overall, these results suggest that some living cells emit bystander photons upon direct irradiation. The data confirmed that these photons are mostly in the UVA range. Moreover, while human cells emitted photons in response to irradiation, B16F10 cells did not. It is suspected that the presence of melanin in B16F10 cells effectively attenuated photon emissions, as melanin is known to readily absorb photons in the range emitted by the cells. Finally, HCT116 cells do not emit photons in response to hydrogen peroxide supplementation, which suggests that oxidative stress alone does not produce the physical bystander signal. The results imply that a physical event, such as radiation exposure, is required for production of bystander signal.

5.4.1. Limitations and comparison to results from other reports

The ascertainment of significance in treatments producing photon readings below approximately 100 γ/min was not possible because background typically readings were in this range.

The photon counts obtained do not reflect those found by two previous students, with respect to magnitude[5,10]. The counts in the present thesis were orders of magnitude lower, which may be indicative of a differential experimental setup. One possibility is that the detection apparatus was less sensitive in this report or that reduced emissions were actually being observed from cultures; it is suspected that the former is a major contributor to this disparity. Initially, the idea that older hardware could be the culprit was entertained. I believed that lossy signal transmission somewhere between the PMT and scalar card could have caused the reduction in counts. It was also suspected that perhaps the photomultiplier tube was less responsive due to age, or that settings could be different between students. However, the setup of the machine was described in detail by Ahamad, and further experiments were performed that used the same setup. Significantly, a response check was conducted in this chapter. This test indicated that the machine continues to be very sensitive to ambient or lamp light exposure. Saturation of the scalar after approximately 1 second with no bandpass filter was observed under light from a Spectroline 3660 15W UVA lamp. This data is shown in figure 5.1 and proves the contraption's extreme sensitivity to ultraviolet light. Further, troubleshooting of the PMT and associated electronics was conducted using an oscilloscope with the help of Jigar Lad, who detected no problems.

It is believed that the ostensibly reduced photon emissions resulted from a number of technical limitations that arose due to experimental design. For convenience, flasks were used for photon counting instead of petri dishes. As described previously, this was due to the tendency for dishes to leak, while flasks did not have this problem. One issue with using flasks is that they are made of virgin polystyrene. This material is known to absorb certain wavelengths of light lower than the visible range, including mid-range UVB and UVC. This means that decreased photon counts may be observed to the absorption by the top part of the T25 flask, particularly when an optical filter passing an ultraviolet band is used. Previously, Le et al.[5] used petri dishes for photon counting, allowing removal of the plastic lid, which yielded higher counts than in the present report—this was attempted twice, however significant increases in photon counts were not be obtained (data not shown). Yet, photon absorption due to polystyrene does not explain why 340 nm emissions were also affected, as polystyrene does not absorb this range as efficiently. It could also be that the scattering of photons as they interacted with the top part of the flask could have resulted in fewer reaching the detector. Furthermore, Cohen[23] found increases in photon emission that were more pronounced using gamma irradiation and flasks. Another factor could have been actual cell density in contrast to intended cell density. The time between seeding and photon measurement was 48 hours, with the assumption that the cells needed several hours to attach, with an additional 24 hours for

irradiation. This means an extra number of cells in the flask, which Le demonstrated can reduce photon measurements[2]. The "quenching" of the signal with extra cells could a result of greater numbers in the flask, which absorb more photons before they can reach the detector. It is likely that a combination of these confounding factors contributed to these different results.

5.4.3. Optical filter characteristics and attenuation of signal by polystyrene

Photon measurements in HaCaT and HCT116 cells using the 340 nm filter should have been significantly lower when compared to overall counts, as less than 15% of photons do not pass the filter due to limited transmissibility. It is unclear why counts in both HCT116 and HaCaT cells were unexpectedly high with the use of filters, as previous findings indicate significant emissions of different wavelengths including higher frequency ultraviolet[2]. The lower transmission of the 280 nm bandpass filter (>60% vs >85%) was not taken into consideration in this report, for consistency with previous studies[2,4,23,26]. Therefore, counts presented in all graphs in this range should be at least 20% higher when the differential transmission is accounted for. This effect could also have affected previous experiments prior to those in the present thesis—for example, Le et al. (2018) study on oxidative phosphorylation[8]—which leads to some interesting questions:

- How would this bystander effect differ *in vivo* without absorption due to plastics?
- What about the potential reflection of light? Refraction? Scattering and escape from the chamber?
- How could one design a bystander experiment with no polystyrene involved? This would allow the full intensity of all spectra to be represented as they would in a living organism upon radiation exposure.

With respect to #1, this could be a significant limitation of *in vitro* bystander experimental design, however it seems difficult to eliminate plastics entirely when using *in vitro* techniques such as cell culture: the use of plastics here is an inevitability. Anyway, the accuracy of the readings at 280 nm were also likely affected by the absorbance of the wavelength by the flask, which was discussed previously. Therefore, these two factors likely affected 280 nm readings.

As described in Cohen[23], not all photons emitted from the cell cultures reach the detector. The reason this occurs is because of the geometry of the apparatus and where the photons are likely to travel. Some were likely scattered by the cell culture medium. Others may be have been absorbed or scattered by the polystyrene of the culture flask. Further still, a photon may "miss" the opening to the PMT housing. The magnitude of signal the detector produces in response to light is governed by the intensity of that light, which is itself governed by the inverse square law. In other words, the distance between the cell monolayer and the PMT affects the measurement. The distance from the cell monolayer to the PMT was measured to be approximately 11 cm, and intensity weakens proportional to the square of the distance from the source. It is likely at all these factors affected photon measurements and should ideally be accounted for to produce a "true" number that represents photon emissions.

5.4.4. Significance to bystander effect propagation

One very interesting aspect of these experiments is the potential of the electromagnetic signal to lead to additional signaling in reporter cell cultures. This was demonstrated by Le et al.[3], who showed that exosomes are released from reporter cultures receiving the UVA photons. O'Reilly and Mothersill[1]

performed a series of experiments where they tested responses in several cell lines, including HaCaT, after exposure to UVA and UVB. They found that a significant decrease in survival occurred following a dose of 6000 J/cm^2 UVA and more sensitivity to UVB. Intriguingly, UVA and UVB produced delayed cell death in HaCaT cells and other cell lines, which indicates that the electromagnetic bystander signal could potentially do the same.

5.5. Conclusion

Irradiation of HCT116 and HaCaT with tritium, a pure beta emitter, produced significant photon emissions concentrated in the UVA region rather than other wavelengths of UV. Treatment of the HCT116 with hydrogen peroxide did not induce photon emissions. B16F10 did not exhibit photon emissions upon beta irradiation, suggesting a potential radioprotective role for melanin in the context of physical bystander signalling.

5.6. References

1. O'REILLY P, C. MOTHERSILL. Comparative effects of UV A and UV B on clonogenic survival and delayed cell death in skin cell lines from humans and fish. International journal of radiation biology. 1997;72(1):111–119.

2. Le M, Mothersill CE, Seymour CB, Ahmad SB, Armstrong A, Rainbow AJ, McNeill FE. Factors affecting ultraviolet-A photon emission from beta-irradiated human keratinocyte cells. Physics in medicine and biology. 2015;60(16):6371–6389. doi:10.1088/0031-9155/60/16/6371

3. Le M, Fernandez-Palomo C, McNeill FE, Seymour CB, Rainbow AJ, Mothersill CE. Exosomes are released by bystander cells exposed to radiation-induced biophoton signals: Reconciling the mechanisms mediating the bystander effect. PLOS ONE. 2017;12(3):e0173685. doi:10.1371/journal.pone.0173685

4. Le M, Mothersill CE, Seymour CB, Rainbow AJ, McNeill FE. An Observed Effect of p53 Status on the Bystander Response to Radiation-Induced Cellular Photon Emission. Radiation Research. 2017;187(2):169–185. http://www.bioone.org/doi/10.1667/RR14342.1. doi:10.1667/RR14342.1

5. Le M, McNeill FE, Seymour C, Rainbow AJ, Mothersill CE. An observed effect of ultraviolet radiation emitted from beta-irradiated HaCaT cells upon non-beta-irradiated bystander cells. Radiation research. 2015;183(3):279–90. http://www.bioone.org/doi/10.1667/RR13827.1%5Cnhttp://www.ncbi.nlm.nih.gov/pubmed/25710575. doi:10.1667/RR13827.1

6. Xu S, Wang J, Ding N, Hu W, Zhang X, Wang B, Hua J, Wei W, Zhu Q. Exosome-mediated microRNA transfer plays a role in radiation-induced bystander effect. RNA Biology. 2015;12(12):1355–1363. http://www.tandfonline.com/doi/full/10.1080/15476286.2015.1100795. doi:10.1080/15476286.2015.1100795

7. Jella KK, Rani S, O'Driscoll L, McClean B, Byrne HJ, Lyng FM. Exosomes are involved in mediating radiation induced bystander signaling in human keratinocyte cells. Radiation research. 2014;181(2):138–145. doi:10.1667/RR13337.1

8. Le M, McNeill FEFE, Seymour CBCB, Rusin A, Diamond K, Rainbow AJAJ, Murphy J, Mothersill CECE. Modulation of oxidative phosphorylation (OXPHOS) by radiation-induced biophotons. Environmental research. 2018;163:80–87. doi:10.1016/j.envres.2018.01.027

9. Mothersill C, Le M, Rusin A, Seymour C. BIOPHOTONS in RADIOBIOLOGY: INHIBITORS, COMMUNICATORS and REACTORS. Radiation Protection Dosimetry. 2019;183(1–2). doi:10.1093/rpd/ncy271

10. Ahmad SB, McNeill FE, Byun SH, Prestwich W V., Mothersill C, Seymour C, Armstrong A, Fernandez C. Ultra-violet light emission from hpv-g cells irradiated with low let radiation from 90Y; consequences for radiation induced bystander effects. Dose-Response. 2013;11(4):498–516. doi:10.2203/dose-response.12-048.ahmad

11. Maguire P, Mothersill C, Seymour C, Lyng FM. Medium from irradiated cells induces dose-dependent mitochondrial changes and BCL2 responses in unirradiated human keratinocytes. RADIATION RESEARCH. 2005;163(4):384–390. doi:10.1667/RR3325

12. Azzam EI, de Toledo SM, Little JB. Direct evidence for the participation of gap junction-mediated

intercellular communication in the transmission of damage signals from α-particle irradiated to nonirradiated cells. Proceedings of the National Academy of Sciences . 2001;98(2):473–478. http://www.pnas.org/content/98/2/473.abstract. doi:10.1073/pnas.98.2.473

13. Tada-Oikawa S, Oikawa S, Kawanishi S. Determination of DNA damage, peroxide generation, mitochondrial membrane potential, and caspase-3 activity during ultraviolet A-induced apoptosis summary. Methods in Enzymology Singlet Oxygen, UV-A, and Ozone. 2000:331–342.

14. Canman CE, Lim DS, Cimprich KA, Taya Y, Tamai K, Sakaguchi K, Appella E, Kastan MB, Siliciano JD, Lavin MF, et al. Activation of the ATM kinase by ionizing radiation and phosphorylation of p53. Science (New York, N.Y.). 1998;281(5383):1677–9. http://www.ncbi.nlm.nih.gov/pubmed/9733515. doi:10.1126/science.281.5383.1677

15. P. O'REILLY and C. MOTHERSILL J. Comparative effects of UV A and UV B on clonogenic survival and delayed cell death in skin cell lines from humans and fish. International journal of radiation biology. 1997;72(1):111–119.

16. McMillan TJ, Leatherman E, Ridley A, Shorrocks J, Tobi SE, Whiteside JR. Cellular effects of long wavelength UV light (UVA) in mammalian cells. Journal of Pharmacy and Pharmacology. 2008;60(8):969–976.

17. Sage E, Girard P-M, Francesconi S. Unravelling UVA-induced mutagenesis. Photochemical & Photobiological Sciences. 2012;11(1):74–80.

18. Belpomme D, Hardell L, Belyaev I, Burgio E, Carpenter DO. Thermal and non-thermal health effects of low intensity non-ionizing radiation: An international perspective. Environmental pollution. 2018;242:643–658.

19. Ng K-H. Non-ionizing radiations–sources, biological effects, emissions and exposures. In: Proceedings of the international conference on non-ionizing radiation at UNITEN. 2003. p. 1–16.

20. Shimura T, Kunugita N. Mitochondrial reactive oxygen species-mediated genomic instability in low-dose irradiated human cells through nuclear retention of cyclin D1. Cell cycle (Georgetown, Tex.). 2016;15(11):1410–1414. doi:10.1080/15384101.2016.1170271

21. Hei TK, Zhou H, Ivanov VN. Mechanism of radiation-induced bystander effects: a unifying model. Journal of Pharmacy and Pharmacology. 2008;60(8):943–950. doi:10.1211/jpp.60.8.0001.Mechanism

22. Ahmad SB, McNeill FE, Byun SH, Prestwich W V, Seymour C, Mothersill CE. Ion beam induced luminescence: Relevance to radiation induced bystander effects. NUCLEAR INSTRUMENTS & METHODS IN PHYSICS RESEARCH SECTION B-BEAM INTERACTIONS WITH MATERIALS AND ATOMS. 2012;288:81–88. doi:10.1016/j.nimb.2012.05.043

23. Cohen J. INVESTIGATING THE PARAMETERS OF PRE-/POST-CONDITIONING ON HUMAN-DERIVED CANCER CELLS. McMaster University; 2019.

24. Widel M, Krzywon A, Gajda K, Skonieczna M, Rzeszowska-Wolny J. Induction of bystander effects by UVA, UVB, and UVC radiation in human fibroblasts and the implication of reactive oxygen species. Free Radical Biology and Medicine. 2014;68:278–287.

25. Kappes UP, Luo D, Potter M, Schulmeister K, Rünger TM. Short-and long-wave UV light (UVB and UVA) induce similar mutations in human skin cells. Journal of Investigative Dermatology. 2006;126(3):667–675.

26. Le M, McNeill FE, Seymour CB, Rusin A, Diamond K, Rainbow AJ, Murphy J, Mothersill CE. Modulation of oxidative phosphorylation (OXPHOS) by radiation- induced biophotons. Environmental Research. 2018;163:80–87. doi:10.1016/j.envres.2018.01.027

Chapter 6

Cell survival following exposure to bystander photons and hydrogen peroxide

Abstract: The cell-killing ability of bystander photon radiation has been demonstrated previously in the literature. However, this has not been assessed in the context of oxidative stress and the ability of reactive oxygen species (ROS) to induce these effects. HaCaT, HCT116, and B16F10 were exposed to varying concentrations of hydrogen peroxide between 1–50 µM to assess the dose range that may be relevant to the induction of ROS by bystander photons. Cell survival was found to be inversely corelated to hydrogen peroxide concentration, with HCT116 exhibiting the greatest sensitivity to oxidative stress, which was similar in HaCaT but less pronounced with the same doses, and B16F10 the least. All cell survival curves followed an exponential reduction in survival with a linear increase in hydrogen peroxide concentration. Irradiation of bystander donors at 25, 50, and 75 cGy yielded significant reductions in the survival of HCT116 and HaCaT reporter cells. In B16F10, donor irradiation did not produce this reduction in survival, likely due to the signal's absorbance by melanin, the free radical scavenging properties of melanin, or a combination of the two factors—the latter also explains the reduced sensitivity to hydrogen peroxide. These results suggest a radioprotective role for melanin and provide some evidence for the induction of oxidative stress in bystander reporters, which is corroborated in later chapters.

6.1. Introduction

As previously discussed in Chapter 2, a common starting point for radiation biologists is the construction of a cell survival curve. This is important because many radiobiological effects are usually dependent on the radiation dose delivered to cells and tissues, among other factors. Other mechanisms of communicating radiation damage exist, such as soluble factor mediated bystander signalling[1]. Many studies have now observed a reduction in bystander cell survival plateaus after a certain donor dose[2–4]. Cell survival is another important endpoint of radiation-induced bystander effect (RIBE) assays. While research on the potential for the electromagnetic bystander signal to promote cell killing in reporter cultures has been documented[5,6], B16F10 has not been assessed for responses. Melanin has been investigated as a radioprotector in the context of this bystander effect[7], however never using melanocytes in particular. The relevance of oxidative stress to melanocytes and melanogenesis is discussed in further detail in the introductory section of Chapter 7. Here the mechanisms of ultraviolet-induced cellular damage is also more broadly discussed. The use of melanocytes in these experiments may provide evidence for the *in vitro* and *in vivo* role of melanin in the attenuation of bystander or oxidative stress responses.

The research that allowed the use of this technique in this thesis has a long history in the radiobiology literature. As reviewed previously, the first demonstration of a significant reduction in clonogenic survival in non-irradiated epithelial cells receiving ICCM from gamma-irradiated cells was done by Mothersill and Seymour in 1997[1]. Following this was the first indication that cell-to-cell contact was not required for the communication of the bystander signal[8]. Many additional findings were made with cell killing and an endpoint, and these are effectively summarized in Le 2018[8]. The signal was found out to be temperature-dependent, and while multiple freeze-thaw cycles did not affect the potency of the signal in medium, heating to over 70 degrees Celsius did[9]. Irradiation of cells at 0 degrees Celsius prevented the bystander effect in reporters. Presence of cells in medium was found to be required upon irradiation to establish the signal, which refuted the idea that cell culture medium itself could change chemically due to irradiation and influence cell survival. This indicated that the bystander effect involves metabolic processes in both donors and recipients of the signal. Moreover, the physical bystander signal was shown to exist due to *in vitro* work by Le et al.[5].

Hydrogen peroxide is a known participant of redox homeostasis in cells. Its role is described in more detail in Chapter 7 in this regard. Supplementation of hydrogen peroxide in cell culture medium is expected to produce a reduction in clonogenic survival. Hydrogen peroxide and related compounds produce damage to cellular components through oxidative damage. This causes lesions in membrane lipids, nucleic acids, and proteins, preventing normal function. Hydrogen peroxide is also involved in cellular signalling pathways and immune responses. Hydrogen peroxide is membrane-permeable and increasing the concentration of hydrogen peroxide in the extracellular environment produces oxidative stress within cells. This induction of damage may have different effects at extremely low doses, however generally the generation of these reactive oxygen species endogenously through metabolic processes is also believed to be similarly detrimental to cellular viability.

To acquire data on how both oxidative stress and hydrogen peroxide supplementation affect cellular viability, conducting a cell survival assay at several dose points is considered useful. The purpose of this chapter was to determine the ability of small doses of hydrogen peroxide to induce clonogenic cell death in HaCaT, HCT116, and B16F10. Further, we wanted to confirm that biophotons can reduce cell survival in the same cells.

6.2. Methods

6.2.1. Induction of cellular oxidative stress

Hydrogen peroxide was used to produce oxidative stress in cells for the present thesis following the consideration of safety, availability, practicality, and biological applicability. One negative aspect of using commercial hydrogen peroxide is the relatively rapid degradation of the hydrogen peroxide in solution over a short period of time. To prevent this from affecting results, new hydrogen peroxide was purchased prior to an experiment if more than one month had passed since the previous experiment. Hydrogen peroxide solution is a reasonably safe compound at appropriate concentration (in contrast to some alternatives like Di-tert-butyl peroxide). Moreover, a 3% solution was typically readily procurable. The use of the solution due to the aforementioned characteristics made it practical for use in the present thesis. Finally, hydrogen peroxide is an endogenously produced compound found in human and murine cells under normal physiological conditions, and therefore its exogenous administration to model oxidative stress is warranted.

Oxidative stress was induced in cells via the direct administration of hydrogen peroxide to cell culture medium at defined concentrations. An H_2O_2 solution was prepared from a 3% stock solution, with an equivalent micromolar concentration of 880 mM. Initially, a solution with a dilution factor of $1x10^3$ was created in DPBS, yielding a 880 µM solution. Complete growth media in the clonogenic flasks was supplemented with this solution at appropriate volumes to achieve a specific medium H_2O_2 concentrations for various test groups (see Equation 1). An extensive description of cellular redox homeostasis and oxidative stress is covered in Chapter 7.

$$V_R = V_M \left(\frac{880\ mM}{D_C \cdot\ 1 \times 10^3\ \mu M/mM} \right)^{-1}$$

Equation 6.1: V_M and V_R represent initial medium and required volume of H_2O_2 in µL, respectively. D_c represents desired concentration in µM. Volume added to the solution was not typically factored into the calculation, as the change in volume would insignificantly affect the final concentration in most cases. Where additional volume would affect concentration significantly, the V_M term was replaced with $V_M + V_R$.

6.2.2. Irradiation and Bystander Setup

Irradiation was accomplished by the direct addition of tritiated water to cell culture medium at a volume that carried a specific activity, as previously described. The calculation of dose is described in Section 5.2.2. Cells were seeded on the day of subculture and left to adhere overnight. Cells were kept in the dark following subculture and seeding to prevent potential interference from ambient light. Two T75 flasks containing 10 mL phenol red-free cell culture medium were seeded at 2000 cells/cm^2, the optimum density determined by Le et al. (2017)[7]. 300 cells in four wells of a 6-well plate were provided with 3 mL phenol red-free medium. The next day, tritium was added to the cell culture medium of the donors the following doses: 0.25, 0.50, and 0.75 Gy after 24, 48, and 72 hours, respectively. The donors were placed directly inferior to the donor T75 flask and incubated for the appropriate exposure time in a light-tight metal box. The donor cultures were then removed, and the cells allowed to grow for the full clonogenic period. Two sheets of aluminum foil (0.5 mm each, Alcan) were placed between the donor and reporter flasks for some doses to assess whether blocking photons emanating from the irradiated cultures could prevent the reduction in cell survival observed.

6.2.3. Clonogenic survival assay

To assess the effect of hydrogen peroxide on the survival of the cells, a clonogenic survival assay was used. This is a standard assay that is used to investigate the toxicity of drugs or other treatments to cellular growth, proliferation, and survival. 25 cm^2 T25 Falcon flasks were used for this assay. 3 mL of medium was first added to each clonogenic flask on the day of subculture. Following the creation of a single cell suspension, a Bio-Rad TC20 automated cell counter (Bio-Rad Life Science Research Division, Mississauga, Canada) was used to determine its concentration. The image was checked after this count was produced, and a gating process based on cell size was used to obtain a more accurate cell count. Furthermore, a Trypan Blue stain was performed and detected by the counter to discriminate between live and dead cells in the suspension; live cell percentages varied slightly but were >95% for this assay. When this adjusted count was obtained, the following equation was used to determine the required volume containing a specific number of cells into a clonogenic flask following a 100x dilution:

$$\mathrm{V} = 1.0\mathrm{x}10^5 \left(\frac{U}{C}\right)$$

Equation 6.2: Clonogenic survival assay volume equation.

Where V represents required volume in µL, U represents the desired number of cells to be seeded, and *C* represents stock cell concentration in cells/mL obtained from the TC20 counter. A factor of $1.0\mathrm{x}10^5$ is used to convert from mL to µL following a 100x dilution of the stock solution in complete growth medium. This volume typically ranged from 20–30 µL. The required volume to seed 300 cells was pipetted on the adherent side of each T25 flask and spread by gentle manual rocking.

The clonogenic flasks were then incubated for nine days and stained after the consequent appearance of colonies visible to the naked eye. Cell colonies were labelled using a 1:3 solution of carbolfuchsin stain in distilled water and rack dried overnight. Colonies of 50 cells or more were counted manually after the flasks fully dried and subsequently the results were tabulated in Microsoft Excel.

6.2.4. Statistical Analysis

Statistical analysis was done in Graphpad Prism 7. R^2 typically represents how well the nonlinear regression curve fits the data. A residual is the difference in the y value of a given x value between the curve and experimentally obtained value. The sy.x value is calculated by Prism and represents the standard deviation of these residuals; this is also used to represent how well the model fits the data. Each dose point in figures 6.1 and 6.2 represent three technical replicates for three independent experiments (n=9). The bystander effect experiment data represents four technical replicates and three biological replicates for each group (n=12) unless otherwise indicated.

6.3. Results

6.3.1. Clonogenic survival following hydrogen peroxide exposure

HCT116 survival reduced following an exponential decrease upon a linear [H_2O_2] increase. A one-phase decay regression curve was calculated with R^2=0.9751. HaCaT survival followed a similar exponential decrease with R^2=0.9582. The results indicate a sharper decrease in the survival of HaCaT cells in

response to increasing hydrogen peroxide supplementation. D.F. represents degrees of freedom, which shows how many independent values are present in the data set.

HCT116 cells showed a linear increase in DCF-DA fluorescence with R^2=0.9925 and a linear increase in [H_2O_2] concentration. HaCaT cells showed a similar linear increase in DCF-DA fluorescence with increasing hydrogen peroxide supplementation with R^2=0.9852.

These results indicate that growth medium containing hydrogen peroxide is sufficient to induce oxidative stress in both HCT116 and HaCaT cells. This increase in intracellar ROS also seems to lead to reduced cell survival in these cell lines.
Additional experiments must be done for the mouse melanoma cell line.

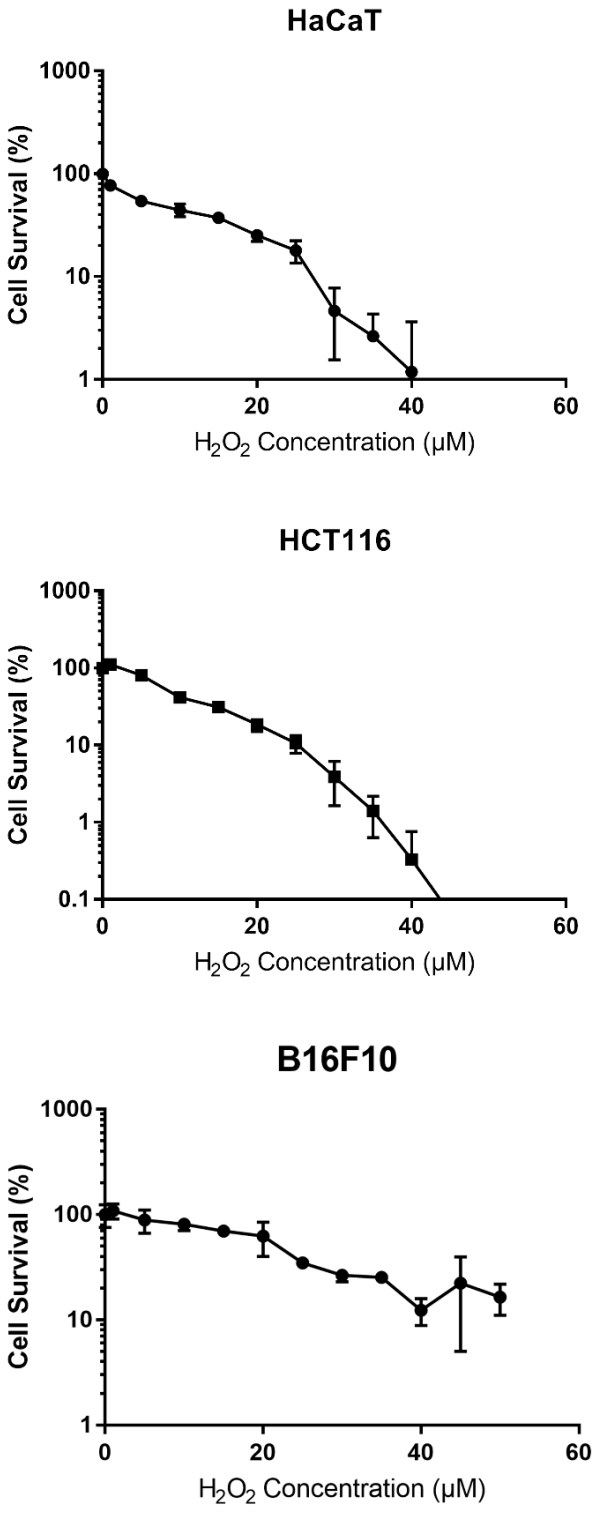

Figure 6.1: Cell survival of three cell treated with varying concentrations of hydrogen peroxide. Data represents three technical replicates for three independent experiments (n=9).

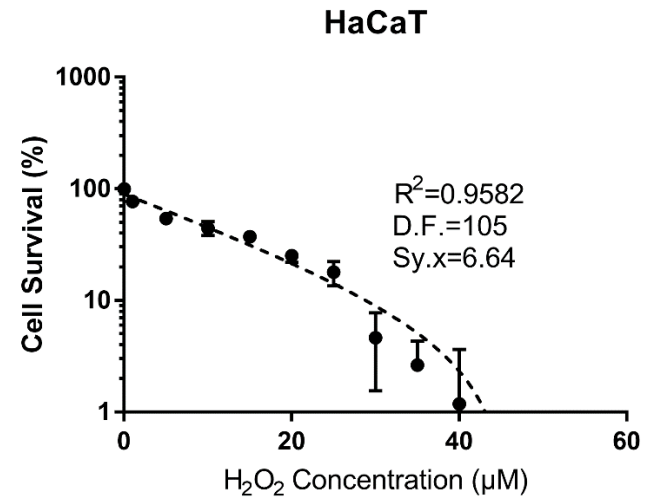

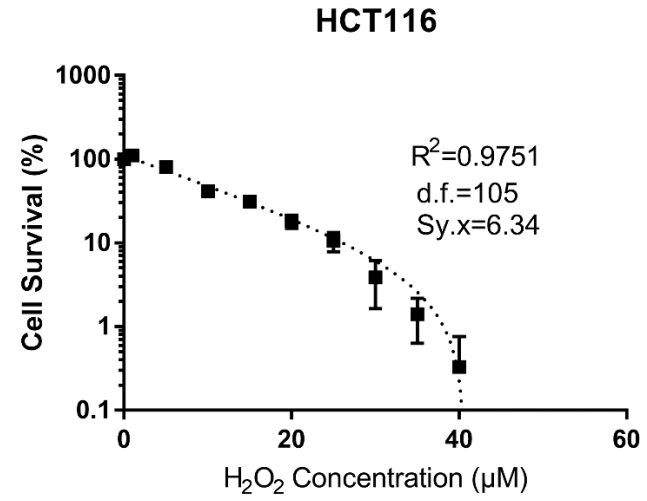

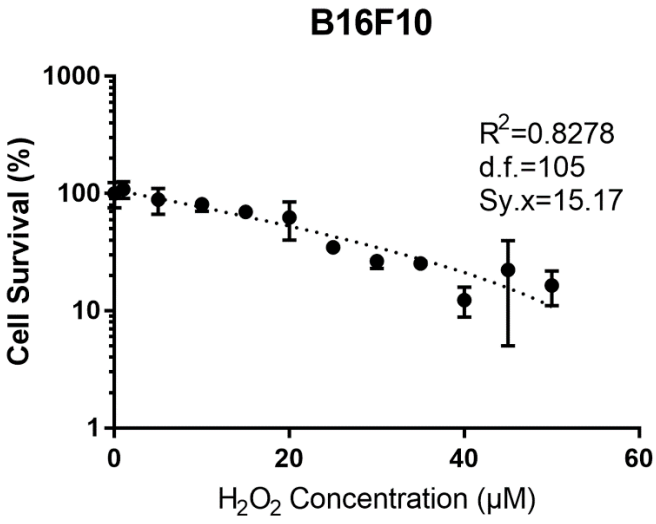

Figure 6.2: The same data in Figure 6.1. Nonlinear regression trends were calculated in GraphPad Prism using least sum of squares. Data represents three technical replicates for three independent experiments (n=9).

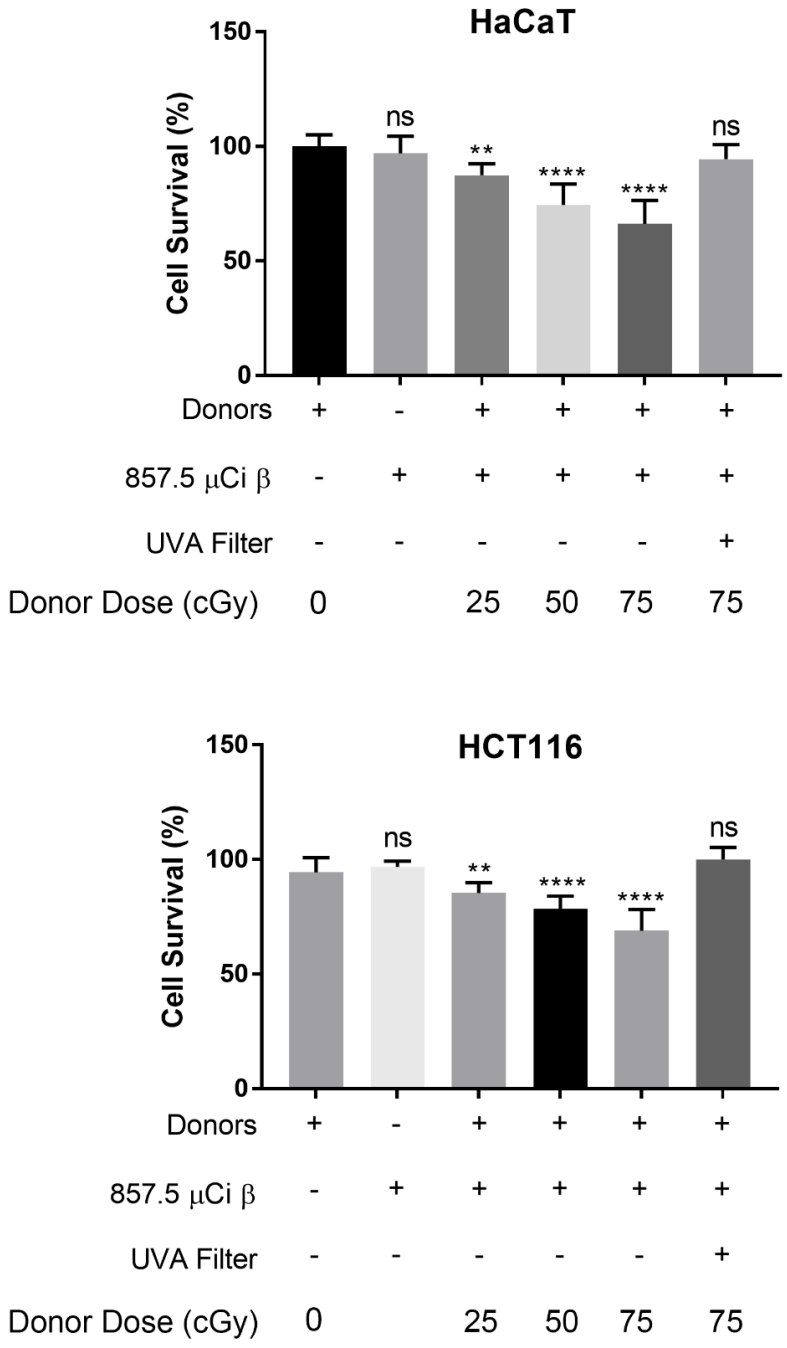

Figure 6.3: Survival of three cell line reporters following various treatments. "+" indicates the presence of a treatment, while "-" denotes absence. Presence of a donor culture, specific activity of tritiated water, and metal foil obstruction were varied. Donor doses between 0-0.75 Gy were used on donors. Statistical significance is indicated compared to the leftmost group (**p<0.01, ***p<0.001, ****p<0.0001). Summary data is available in Table 6.1.

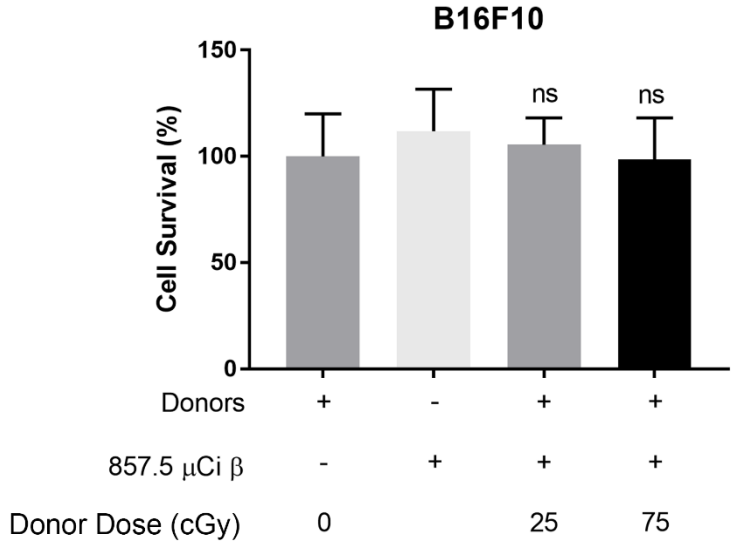

Group	*Average Colonies*	*Standard Deviation*	*n*
HaCaT Control	124.00	6.30	12
HaCaT Tritium Alone	120.20	9.35	12
HaCaT 25 cGy	108.44	6.24	12
HaCaT 50 cGy	92.32	11.30	12
HaCaT 75 cGy	82.13	12.72	12
HaCaT Obstructed	117.10	12.87	12
HCT116 Control	147.02	10.68	12
HCT116 Tritium Alone	142.40	4.90	12
HCT116 25 cGy	125.58	9.05	12
HCT116 50 cGy	115.46	11.07	12
HCT116 75 cGy	101.37	18.54	12
HCT116 Obstructed	140.16	6.99	12
B16F10 Control	80.25	16.12	12
B16F10 Tritium Alone	89.80	15.93	12
B16F10 25 cGy	84.67	10.20	12
B16F10 75 cGy	79.1	15.79	12

Table 6.1: Summary survival data displayed in Figure 6.3.

6.3.2. Cell survival upon exposure to biophotons

Figure 6.3 shows the survival of three cell line reporters following irradiation of donors. Inclusion of donor cells and tritium alone, respectively, did not induce a reduction in survival. Inclusion of both

caused a reduction in the survival of the photon recipients. This reduction was dependent on the dose received by the donor cells. Cell survival in reporters appears to decrease with increasing dose in HaCaT and HCT116. It is entirely possible that this trend does not continue, however these three doses induce an increasing reduction in clonogenicity. The obstruction of these photons from the donor flask effectively abolished this effect at the highest donor dose in HCT116 and HaCaT. Two doses were used on B16F10 donors: 25 cGy and 75 cGy; neither of these doses produced a significant reduction in survival.

6.4. Discussion

6.4.1. Cell survival, oxidative stress after hydrogen peroxide supplementation

Out of all the cell lines, it is apparent that B16F10 is the most resistant to oxidative stress using the clonogenic survival assay. It could be that B16F10 is protected against oxidative stress because of its high melanin content; melanin, specifically eumelanin, has been shown to have free-radical scavenging properties[10,11].

Similar results on cell viability were obtained from another study measuring human melanocyte viability up to 40 µM hydrogen peroxide; these cells were overall less sensitive to hydrogen peroxide than B16F10[12]. However, there is another characteristic of B16F10 that could affect sensitivity to hydrogen peroxide. Specifically, this is metabolism. Both HaCaT and HCT116 are cultured in normal RPMI that had been supplemented with several ingredients (see Section 2.2. for information on cell culture and media formulations). It should be noted well in this section that B16F10 requires completely different medium altogether, and specifically greater supplementation of pyruvate. An older report by Lee et al. (2004) demonstrated that pyruvate enhances survival in hydrogen-peroxide treated endothelial cells by inhibiting apoptotic signaling[13]. It should also be noted that this study was conducted in endothelial cells and utilized a much higher concentration of hydrogen peroxide than in the present report. However, this still could be a reason for the lower sensitivity to hydrogen peroxide. It is still suspected that melanin may play a role in the reduced response of B16F10 to hydrogen peroxide, as it is known to have free radical scavenging properties[11,14,15]. Interestingly, the effect of melanin on the bystander effect in human keratinocytes was investigated initially by Mosse et al. (2006)[16]. It was found that melanin could protect recipient cells if it was included prior to irradiation. Additionally, it was first suggested that the bystander effect could contain a physical component. In order to confirm this, an experiment could be performed in the future where melanin is supplemented in the cell culture medium of recipients before and following an electromagnetic bystander experiment. This was already performed by Le et al.[5] however, and it was determined that melanin could produce an increase in survival regardless of when it was supplemented in bystander recipient culture. Therefore, it is suspected that B16F10 may exhibit higher survival with the same doses of hydrogen peroxide due to the free radical scavenging properties of melanin—which, as demonstrated in Chapter 4, is quite a bit—metabolic consideration, and natural capacity to tolerate higher levels of oxidative stress contribute to these observable differences. Intriguingly, this may be relevant *in vivo*: one report demonstrated that keratinocytes may export ROS to melanocytes[17].

A good way to test the hypothesis that free radical scavenging may be the mechanism whereby melanin increases cell survival in peroxide- and biophoton-exposed cells is to repeat these experiments using an albino melanocyte line. These cells are available either as an immortalized cell line[18] or are obtained through primary cell culture[19,20].

6.4.2. Cell survival, potential oxidative stress after secondary photon exposure

HaCaT and HCT116 reporters show significant reductions in survival for all donor doses. Furthermore, blocking donor photons abolished this effect at the highest donor dose. This indicates that bystander photons can reduce cell survival in physically separated cultures. This was also found by Le et al.[5,6,21]; therefore, these experiments confirm previous findings. This is also compelling evidence that these bystander photons have cell-killing properties. The photons had to pass through virgin polystyrene to reach the reporter cultures, and therefore attenuation of certain wavelengths is an experimental limitation. This material tends to absorb light between 200-300 nm, which falls into the ultraviolet spectrum[22–24]; this is most of the UVB and some of the UVC range. Therefore, the effect on reporters may be somewhat muted due to this attenuation. Nevertheless, the signal appears strong enough at these donor doses to induce a statistically significant reduction in survival.

The reduction in cell survival obtained in bystander experiments can be related somewhat to cell survival following hydrogen peroxide supplementation. This is recurring theme across chapters and is intended as a comparison of two exogenous causes of oxidative stress: hydrogen peroxide and the bystander signal. This could potentially be investigated further in future studies where supplementation of hydrogen peroxide can be used to quantify the yield and concentration of various intracellular ROS.

6.4.2. Comparisons, limitations, future directions

There are some limitations to this approach, as the error, differences in experimental design, and other confounding factors may complicate these intercomparisons. For example, cells in the present chapter were exposed to hydrogen peroxide for the majority of the clonogenic period, which is approximately one week. However, cells in chapters 7, 8, and 9 were exposed for one hour due to the different incubation time between seeding and data collection. Nevertheless, it may also prove to be a useful meta-analysis of the data, so it will be attempted to some degree anyway.

B16F10 was assessed in addition to HCT116 and HaCaT, although it was expected, considering results from chapter 5 and others, that there would be no effect due to the absorption of the signal by melanin, the free radical scavenging properties of melanin, or some combination thereof. Evidence for both of these effects is described and explained in chapters 5 and 7. This was indeed the case with the experimental findings in the present chapter, which included a control group, sham-irradiated group, and various donor-recipient groups. The results did not indicate a significant reduction in survival in bystander reporters, which was expected due to the factors described above. This could be confirmed in subsequent experiments by supplementing synthetic melanin in the medium of HaCaTs to a concentration obtained in the culture of melanocytes, for example, or diluted to represent *in vivo* conditions in various human skin tones. The determination of average melanin concentration between these skin tones can be determined by sampling tissue and performing a similar assay to the one presented in chapter 4. A dose response for this radioprotective effect can be determined in the future by supplementing different quantities of melanin *in vitro* in both donors and recipients. B16F10 has been shown to be capable of producing bystander effects in the literature, although these studies are limited[25]. Interestingly, this effect is also shown to be reliant on calcium fluxes and superoxide production.

The data were normalized to the control means. The products of dividing HaCaT reporter means by the control (to obtain a normalized survival fraction) for 0.25, 0.50, and 0.75 cGy donor doses, shown in Table 6.1, are as follows: 0.87, 0.74, and 0.66; the products of dividing HCT116 reporter means by the

control for the same donor doses are as follows: 0.85, 0.79, and 0.69. Compared to data in Figure 6.1, this indicates that exogenous hydrogen peroxide doses around 1, 5, and 10 μM produce a similar reduction in survival in HCT116 and HaCaT cells. This result for the same donor dose, specifically 0.5 Gy, is somewhat different from other chapters. This may be the case due to a number of factors. Notably, different bioassays that measure different biological parameters in a system may not follow the same dose response between one another. Other sources include the aforementioned error associated with these values, which cannot be adequately estimated in this case. Furthermore, exposure to the bystander signal in this chapter was conducted using a different experimental setup; differences include distance between donors and recipients, which was necessitated by the clonogenic survival assay. Nevertheless, if this estimate is accurate, then the reduction in survival due to biophotons is relatively limited compared to hydrogen peroxide supplementation, and production of endogenous ROS may be limited to the 1-10μM in bystander cells, assuming these are primarily responsible for cell killing. Lyng et al.[26] found that membrane signaling was an early indicator of bystander responses in HaCaT cells, followed by calcium influx, specifically for irradiated cell-conditioned medium. It was proposed that calcium influxes and ROS production upon irradiation stimulate the release of factors that communicate the bystander signal to surrounding cells. In the present thesis, another interesting observation is the last two donor doses in HaCaT produced a reduction in survival in reporters that, between the 50 cGy and the 75 cGy doses, was not significantly different. However, the final HCT116 donor doses produce significantly different reductions in survival between them ($p<0.05$). This indicates that the signal in HaCaTs may plateau after 0.5 Gy, although this is not a direct demonstration of that and therefore must be investigated further before conclusions can be drawn. A great way to do this would be the inclusion of donor doses higher than 75 cGy, which would effectively demonstrate or refute saturation of these responses after a threshold dose.

Another interesting set of comparisons can be made between cell lines at the same donor doses, and this may be particularly useful with the human cell lines that show bystander responses. At the 25 cGy, reduction in survival is not significantly different between HaCaT and HCT116. At 50 cGy there is also no significant difference in cell survival. Finally, for 75 cGy, there is also no significant difference in survival. This indicates that similar doses produce similar reductions in survival in reporters for both HaCaT and HCT116 cells. This confirms findings in previous research. Le et al.[6,7] found that both HaCaT and HCT116 were responsive to the physical bystander signal and exhibited a reduction in survival with increasing exposure; the same was not observed in a HCT116 line lacking p53.

These data suggest that melanin may act as a radioprotector with respect to the physical bystander signal. This is not a novel hypothesis; in fact, it was proposed some time ago that melanin may absorb a physical component of the bystander signal[10,16], and was confirmed by Le et al.[7]. However, this is the first time that melanin from an endogenous source has been shown to modulate the physical bystander effect. It is suspected that the absorption of the photons in the ultraviolet range that act to communicate the signal to surrounding cells occurs, as well melanin acting as a free radical sink.

6.5. Conclusion

In conclusion, HCT116 cells appear most sensitive to hydrogen peroxide at the clonogenic endpoint, followed by HaCaT, and finally B16F10. The response in B16F10 indicates that melanin may act as an antioxidant and radioprotector. Three donor doses produced a significant reduction survival in HCT116 and HaCaT reporters exposed to the resulting biophotons, although B16F10 reporters did not show a significant reduction in survival. This is further evidence that melanin in B16F10 absorbs the physical bystander signal and acts as an antioxidant, ultimately preventing reporter bystander responses.

6.6. References

1. Mothersill C, Seymour C. Medium from irradiated human epithelial cells but not human fibroblasts reduces the clonogenic survival of unirradiated cells. INTERNATIONAL JOURNAL OF RADIATION BIOLOGY. 1997;71(4):421–427.

2. Choi VWY, Konishi T, Oikawa M, Cheng SH, Yu KN. The threshold number of protons to induce an adaptive response in zebrafish embryos. Journal of radiological protection : official journal of the Society for Radiological Protection. 2013;33(1):91–100. doi:10.1088/0952-4746/33/1/91

3. Liu ZF, Mothersill CE, McNeill FE, Lyng FM, Byun SH, Seymour CB, Prestwich W V. A dose threshold for a medium transfer bystander effect for a human skin cell line. RADIATION RESEARCH. 2006;166(1, 1):19–23. doi:10.1667/RR3580.1

4. Mothersill C, Seymour C. Targets, pools, shoulders, and communication - a reflection on the evolution of low-dose radiobiology. International journal of radiation biology. 2019 Mar:1–10. doi:10.1080/09553002.2019.1589016

5. Le M, McNeill FE, Seymour C, Rainbow AJ, Mothersill CE. An observed effect of ultraviolet radiation emitted from beta-irradiated HaCaT cells upon non-beta-irradiated bystander cells. Radiation research. 2015;183(3):279–90. http://www.bioone.org/doi/10.1667/RR13827.1%5Cnhttp://www.ncbi.nlm.nih.gov/pubmed/25710575. doi:10.1667/RR13827.1

6. Le M, Mothersill CE, Seymour CB, Rainbow AJ, McNeill FE. An Observed Effect of p53 Status on the Bystander Response to Radiation-Induced Cellular Photon Emission. Radiation Research. 2017;187(2):169–185. http://www.bioone.org/doi/10.1667/RR14342.1. doi:10.1667/RR14342.1

7. Le M, Mothersill CE, Seymour CB, Ahmad SB, Armstrong A, Rainbow AJ, McNeill FE. Factors affecting ultraviolet-A photon emission from beta-irradiated human keratinocyte cells. Physics in medicine and biology. 2015;60(16):6371–6389. doi:10.1088/0031-9155/60/16/6371

8. Le M. Investigating the Generation of Biophotons Induced by Low-Dose Beta-Irradiation and their Role in the Radiation-Induced Bystander Effect. McMaster University; 2018.

9. Mothersill C, Seymour CB. Cell-cell contact during gamma irradiation is not required to induce a bystander effect in normal human keratinocytes: Evidence for release during irradiation of a signal controlling survival into the medium. RADIATION RESEARCH. 1998;149(3):256–262. doi:10.2307/3579958

10. Marozik P, Mosse I, Mothersill C, Seymour C. Protection by chemicals against radiation-induced bystander effects. In: Mothersill, C and Mosse, I and Seymour, C, editor. MULTIPLE STRESSORS: A CHALLENGE FOR THE FUTURE. 2007. p. 247+. (NATO Science for Peace and Security Series C-Environmental Security). doi:10.1007/978-1-4020-6335-0_16

11. Różanowska M, Sarna T, Land EJ, Truscott TG. Free radical scavenging properties of melanin: interaction of eu-and pheo-melanin models with reducing and oxidising radicals. Free Radical Biology and Medicine. 1999;26(5–6):518–525.

12. Seo YM, Kim NS. Effect of superoxide dismutase on oxidative stress of reactive oxygen species in cultured human skin melanocyte. Journal of Korean Society of Occupational and Environmental Hygiene. 2009;19(3):261–269.

13. Lee Y-J, Kang I-J, Bunger R, Kang Y-H. Enhanced survival effect of pyruvate correlates MAPK and NF-κB activation in hydrogen peroxide-treated human endothelial cells. Journal of Applied Physiology. 2004;96(2):793–801.

14. Herrling T, Jung K, Fuchs J. The role of melanin as protector against free radicals in skin and its role as free radical indicator in hair. Spectrochimica Acta Part A: Molecular and Biomolecular Spectroscopy. 2008;69(5):1429–1435.

15. Cope FW, Sever RJ, Polis BD. Reversible free radical generation in the melanin granules of the eye by visible light. Archives of Biochemistry and Biophysics. 1963;100(2):171–177.

16. Mosse I, Marozik P, Seymour C, Mothersill C. The effect of melanin on the bystander effect in human keratinocytes. MUTATION RESEARCH-FUNDAMENTAL AND MOLECULAR MECHANISMS OF MUTAGENESIS. 2006;597(1–2):133–137. doi:10.1016/j.mrfmmm.2005.09.006

17. Pelle E, Mammone T, Maes D, Frenkel K. Keratinocytes act as a source of reactive oxygen species by transferring hydrogen peroxide to melanocytes. Journal of investigative dermatology. 2005;124(4):793–797.

18. Bennett DC, Cooper PJ, Dexter TJ, Devlin LM, Heasman J, Nester B. Cloned mouse melanocyte lines carrying the germline mutations albino and brown: complementation in culture. Development. 1989;105(2):379–385.

19. Alexeev V, Yoon K. Stable and inheritable changes in genotype and phenotype of albino melanocytes induced by an RNA-DNA oligonucleotide. Nature biotechnology. 1998;16(13):1343–1346.

20. YAMAMOTO H, Takeuchi S, KUDO T, SATO C, TAKEUCHI T. Melanin production in cultured albino melanocytes transfected with mouse tyrosinase cDNA. The Japanese Journal of Genetics. 1989;64(2):121–135.

21. Le M, Fernandez-Palomo C, McNeill FE, Seymour CB, Rainbow AJ, Mothersill CE. Exosomes are released by bystander cells exposed to radiation-induced biophoton signals: Reconciling the mechanisms mediating the bystander effect. PLOS ONE. 2017;12(3):e0173685. doi:10.1371/journal.pone.0173685

22. Li T, Zhou C, Jiang M. UV absorption spectra of polystyrene. Polymer Bulletin. 1991;25(2):211–216.

23. Partridge RH. Vacuum-ultraviolet absorption spectrum of polystyrene. The Journal of Chemical Physics. 1967;47(10):4223–4227.

24. Nurmukhametov RN, Volkova L V, Kabanov SP. Fluorescence and absorption of polystyrene exposed to UV laser radiation. Journal of Applied Spectroscopy. 2006;73(1):55–60.

25. Nardin C, Peres C, Mazzarda F, Ziraldo G, Salvatore AM, Mammano F. Photosensitizer activation drives apoptosis by interorganellar Ca2+ transfer and superoxide production in bystander cancer cells. Cells. 2019;8(10):1175.

26. Lyng FM, Howe OL, McClean B. Reactive oxygen species-induced release of signalling factors in irradiated cells triggers membrane signalling and calcium influx in bystander cells. International journal of radiation biology. 2011;87(7):683–695.

Chapter 7

Oxidative stress following exposure to bystander photons and hydrogen peroxide

Abstract: An important parameter of cell culture is redox homeostasis. Reactive oxygen species (ROS) are very reactive chemicals that act as strong oxidizing agents and are generated upon ionizing and non-ionizing radiation exposure in cells. Hydrogen peroxide supplementation in cell culture medium was used to model oxidative stress. A fluorescent probe was used to quantify ROS. It was found that HaCaT was the most susceptible to induction of oxidative stress by hydrogen peroxide, HCT116 intermediately so, and B16F10 the least. It is suspected that this may be due in part to the free radical scavenging properties of melanin. Exposure of all cell lines to bystander donors irradiated with 0.5 Gy by tritium supplementation found significant oxidative stress in HaCaT and HCT116, but not B16F10. It is suspected that this may be due to absorbance of the bystander signal in donor cultures by melanin, as deduced in previous chapters. These results elucidate the effects of hydrogen peroxide supplementation on oxidative stress in three cell lines and confirm ROS generation in recipients of the electromagnetic bystander signal.

7.1. Introduction

Oxidative stress refers to the persistence of type of highly reactive chemical species in a biological system. These chemical species are made especially reactive due to the presence of one or several unpaired valence electrons, and they react with biomolecules integral the normal functioning of the cell in unexpected ways. Specifically, oxidative stress is usually conceptualized to result primarily from the formation of reactive oxygen species (ROS)—however, reactive nitrogen species (RNS) also cause nitrosative stress via analogous reactions, and therefore contribute to redox homeostasis in the cell as well. Because reactive nitrogen species typically contain nitrogen as well as oxygen and for brevity, "ROS" and "oxidative stress" will be used herein to describe chemicals containing either radical oxygen and nitrogen.

ROS can cause extensive damage to a wide variety of cellular structures—including DNA, cell membrane lipids, and proteins such as those with iron-sulphur clusters—if efficient antioxidant processes are not mounted by the cell. Signalling is another important role of ROS—for example, higher concentrations of ROS can induce apoptosis in a variety of cell types directly through oxidation of mitochondrial membrane lipids in the intrinsic programmed cell death pathway[1–4]. The presence of ROS in a biological system is not necessarily deleterious to homeostasis. In fact, ROS are required in a variety of cellular processes and are constantly generated under normal physiological conditions by the metabolism of oxygen. ROS are generated as a by-product of the reduction of oxygen in the electron transport chain–at Complex I and III, the typical reduction of oxygen to water has been documented to be sometimes incomplete, yielding ROS. Electron transfer by mitochondrial cytochrome P450 in certain tissues causes generation of ROS as well. Following tissue injury and inflammation, the NOX (NAD(P)H oxidase) pathway in immune cells catalyses the production of superoxide by partially reducing diatomic oxygen extracellularly. This is termed the "respiratory burst" and results in the rapid release of ROS from cells during an immune response, usually from macrophages and neutrophils[5–7]. A major source NAD(P)H is the pentose phosphate pathway, however additional routes to generation exist[8–12]. These include the use of TCA cycle enzymes and other mitochondrial proteins[13–15]. Hence, oxidative stress is interconnected with metabolism and the metabolic requirements of a cell. To understand oxidative homeostasis in the cell, some key pathways of ROS generation must be reviewed.

In mitochondria, formation of ROS can occur through the partial reduction of diatomic oxygen—usually using an electron donor such as ubiquinone or cytochrome c—into superoxide ($^{\bullet}O_2^-$). Ubiquinone and cytochrome c are electron carriers that shuttle electrons between complexes in the electron transport chain—these are described in further detail in chapter 9. The synthesis of ROS occurs in cellular mitochondria as a by-product of oxidative phosphorylation. Superoxide dismutase—present in mammalian cells as either cytoplasmic SOD1 or mitochondrial SOD2—mediates the dismutation of superoxide to two superoxide molecules, along with two protons, into one molecule of hydrogen peroxide (H_2O_2) and one molecule of diatomic oxygen[16,17]. Another mechanism of sequestering hydrogen peroxide is through the activity of glutathione peroxidases, which nullify its reactivity by converting it to water; a similar role is observed in the electron-donating thioredoxin present in the cytoplasm and mitochondria[18,19]. Another enzyme present in the cellular peroxisome, catalase, catalyses the similar decomposition of two hydrogen peroxide molecules into two water molecules and one molecule of diatomic oxygen[20–22]. Other ROS include the hydroxyl radical ($^{\bullet}OH^-$) in this system. Hydrogen peroxide has a relatively short biological half-life and is highly toxic to cells; the oxidation of proteins, lipids, and DNA occurs upon exposure in consort with other reactants. These damaging effects are compounded by the fact that hydrogen peroxide is membrane-permeable, unlike some other species. On the other hand, on its own, hydrogen peroxide is considered less chemically reactive than other reactive oxygen species, particularly in its damaging action on lipids and other cellular structures. But in the presence of metal ions

such as iron, hydrogen peroxide can produce the hydroxyl radical through the Fenton reaction which is more likely to produce lesions such as lipid peroxides. A great diagram that shows how various ROS are related in a cell is shown in Figure 7.6.The array enzymes and compounds with free radical scavenging activity present in a cell at a given time, which include those with dual electron capacity such as ubiquinone or Coenzyme Q10, contribute to the "fine tuning" of oxidative stress responses in living cells[23–26].

To summarize, hydrogen peroxide in a biological context exists at the interface between *de novo* reactions, attempted amelioration through antioxidants like glutathione, catalase, and ubiquinone, and deleterious biological consequences such as lipid peroxidation. Moreover, hydrogen peroxide is available ubiquitously in low concentrations as a topical antiseptic, so its procurement was never an issue. Further, it is understood that one aspect of low-LET biological damage is the intracellular formation of ROS through the radiolysis of water. Because of these properties, extracellular hydrogen peroxide concentration was used to model intracellular oxidative stress in the present thesis.

Oxidative stress is known to occur following radiation exposure, and ROS are considered important effectors of radiation damage, particularly in low-LET radiations. ROS is important in radiation responses because it can be generated in both targeted and non-targeted processes as a result of radiation exposure. As described previously, the targeted effects of ionizing radiation involve damage to cellular structures through direct interaction with the radiation beam—for example, DNA lesions formed through the ionization or excitation of associated molecular electrons. In a directly exposed cells, indirect radiolytic events, including the radiolysis of water, can generate ROS and cause the communication of damage to neighbouring, untargeted cells.. Radiolysis occurs when water—the ubiquitous constituent of cells and the extracellular milieu—ultimately decomposes to H^+ and $^{\bullet}OH^-$ due to interaction with ionizing radiation. This decomposition leads to the formation of related radical species, including H_2O_2, $^{\bullet}O_2^-$, and others through subsequent reactions. Radiation damage can also cause ROS formation via non-targeted mechanisms. Moreover, indirect effects can occur in neighboring cells not exposed to radiation. Several ROS, including H_2O_2 and NO, can diffuse between cell membranes. *In vivo* and *in vitro,* inflammatory processes that typically underpin the innate immune response can act as a vehicle for the propagation of intercellular signals of radiation damage. Cytokines and calcium ions released from directly irradiated cells can cause bystander responses in adjacent cells and even longer-distance phenomena such as abscopal effects. Radiation effects and ROS are therefore linked in a biological context. ROS are implicated in non-targeted and bystander effects mechanistically and are pertinent in a wider range of radiobiological processes, such as inflammation, metabolism, and damage repair. Hydrogen peroxide has been shown to be involved in UVA-induced DNA damage in HaCaT Cells[27,28].Administration of hydrogen peroxide has been shown to produce radioadaptive responses in some cells, suggesting that the formation of oxidative stress acts as a "priming dose" that prepares cells for radiation-induced damage through oxidative mechanisms. Up-regulation of superoxide dismutase and catalase in bystander cells reduces the activity of cell cycle inhibitor p21 and prevents micronucleus formation[29]. It was thus a priority to measure ROS in bystander cells and, in so doing, to estimate oxidative stress. Furthermore, it was a common theme in the present thesis to model oxidative stress via administration of exogenous hydrogen peroxide.

Oxidative stress and hydrogen peroxide are also linked to melanogenesis. Hydrogen peroxide can trigger melanin production in B16F10, and presumably in other melanocytes too[30], which could promote further, long-term adaptive responses to the physical bystander signal as well as direct irradiation. Conversely, there are many papers that report oxidative stress *in vivo* either causing or being related to vitiligo[31–33]. Some studies even suggest that lower levels of serum glutathione are associated with vitiligo. Though melanogenesis due to oxidative stress is not a subject of research in this report, this interplay

provides further justification for the measurement and modelling of oxidative stress in epithelial cells exposed to ultraviolet light.

7.2. Methods

7.2.1. Reactive oxygen species assay

2',7' –dichlorofluorescin diacetate (DCFDA) is a membrane-permeable chemical commonly used to detect the induction of oxidative stress in cultured cells. Following diffusion into the cell, DCF-DA is deacetylated by cellular esterases into a non-fluorescent compound, yielding 2',7' –dichlorofluorescin. This compound is then oxidized by reactive oxygen species into 2', 7' –dichlorofluorescein (DCF). DCF is a fluorescent compound that can be detected using fluorometric spectroscopy with λ_{EX} / λ_{EM}= 490 nm / 535 nm, respectively.

For both fluorescence microscopy and microplate reading, a protocol was optimized and adapted from an Abcam DCFDA kit (ab113851; Abcam, UK). 50 mg DCF-DA powder (Sigma Aldrich, Canada; D6883) was dissolved in 2.565 mL dimethyl sulfoxide (DMSO) (Thermofisher, Canada; 85190) to create a 40 mM stock dye solution. This solution was aliquoted and frozen at -20°C until needed for an experiment up to three months. The solid form of DCF-DA was also stored under the same conditions. The stock solution was diluted to a final DCF-DA concentration of 25 µM in sterile DPBS.

7.2.1.1. Fluorescence Microscope

To measure induction of ROS in the reporter cells, medium was removed from each T25 flask seeded one day prior with 200 000 cells. The cells were then washed once in 5 mL DPBS and then incubated with 5 mL loading buffer for one hour. The loading buffer was discarded, and each flask was washed three times using 3 mL DPBS. 5 mL DPBS was added to each flask and then cells were taken to be imaged at an Olympus inverted IX51 microscope fitted with a FITCI filter (λ_{EX} / λ_{EM} = 495 nm/519 nm). Certain settings on the microscope were important to facilitate a controlled experiment with comparable data. To be able to compare the intensity of fluorescence between flasks, the control flask was first used to establish a defined exposure time and optimum gain to acquire images with an informative signal. These two parameters were then locked in the software for each experimental group to allow comparison of fluorescence intensity. On some occasions, a 100 mm petri dish was used in the T25 flask's stead. Imaging quality was observed to not be altered significantly between vessel types over the course of experimentation. 4 mL of medium was used for these petri dishes rather than 5 mL.

As fluorescent molecules are exposed to light, photobleaching typically occurs where the fluorescence intensity of the molecule decreases. Intracellular DCF appeared to increase in fluorescence with longer and more intense exposures, presumably as a result of photooxidation of the compound rather than strictly chemical oxidation due to ROS. Great care was taken in the handling of cells to ensure experimental validity, including the prevention of unnecessary light exposure and controlling for this exposure.

7.2.1.2. Microplate Reader

One day prior to reading and upon subculture, 25 000 cells were plated into each well in a clear-bottomed black 96-well plate. Each well contained 200 µL complete growth medium. These cells were incubated for 24 hours prior to treatment to allow for adherence. After 24 hours, medium was removed from each well using a multichannel Epindorf micropipette. Cells were then washed with 200 µL DPBS once. A 25 µM

DCF-DA loading buffer, made up in DPBS, was then added to each well at a volume of 200 µL. The plate was left in the incubator for 45–60 minutes to allow the dye to enter the cells.

The loading buffer was then removed from each well. Cells were washed with 200 µL DPBS. 200 µL of varying concentrations of H_2O_2 in DPBS was then added into each well. The cells were then incubated for an additional hour. Following this incubation step, the plate was removed from the incubator and fluorescence read at at λ_{EX} / λ_{EM}= 490 nm / 535 nm in a Tecan Infinite® 200 PRO microplate reader. The script and parameters thereof—including signal gain, well selection, controls, temperature, et cetera—were informed by the Abcam procedure, optimized, and kept consistent for data collection.

7.2.2. Image Analysis and Statistics

After stained colonies were counted in each flask, the data was inputted into Graphpad Prism 7. Means were calculated along with standard deviation. Graphs were plotted and a one-phase exponential regression trend was calculated for both cell lines based on best fit.

High-quality fluorescence microscope images were analyzed using the ImageJ software. Samples of groups of twelve cells were computationally interrogated to determine mean intensity. Regions of background without cells were used to determine mean background intensity, which is shown alongside regions containing cells. A student's t-test was used to determine the difference between the control and two concentrations of hydrogen peroxide. This analysis and the graphs generated were generated in Graphpad Prism 6.

The Tecan Infinite® 200 PRO plate reader provided raw fluorescence readings in a Microsoft Excel file. Through the use of several controls—specifically, a blank control for background fluorescence containing cells not loaded with DCFDA, and a control for baseline cell fluorescence consisting of cells loaded with dye without hydrogen peroxide treatment—a relative fluorescence intensity could be calculated. First, the mean value of the former control was subtracted from all the data. Then the mean value of the second control was used to normalize the remaining data, which is represented as fluorescence fold change.

7.3. Results

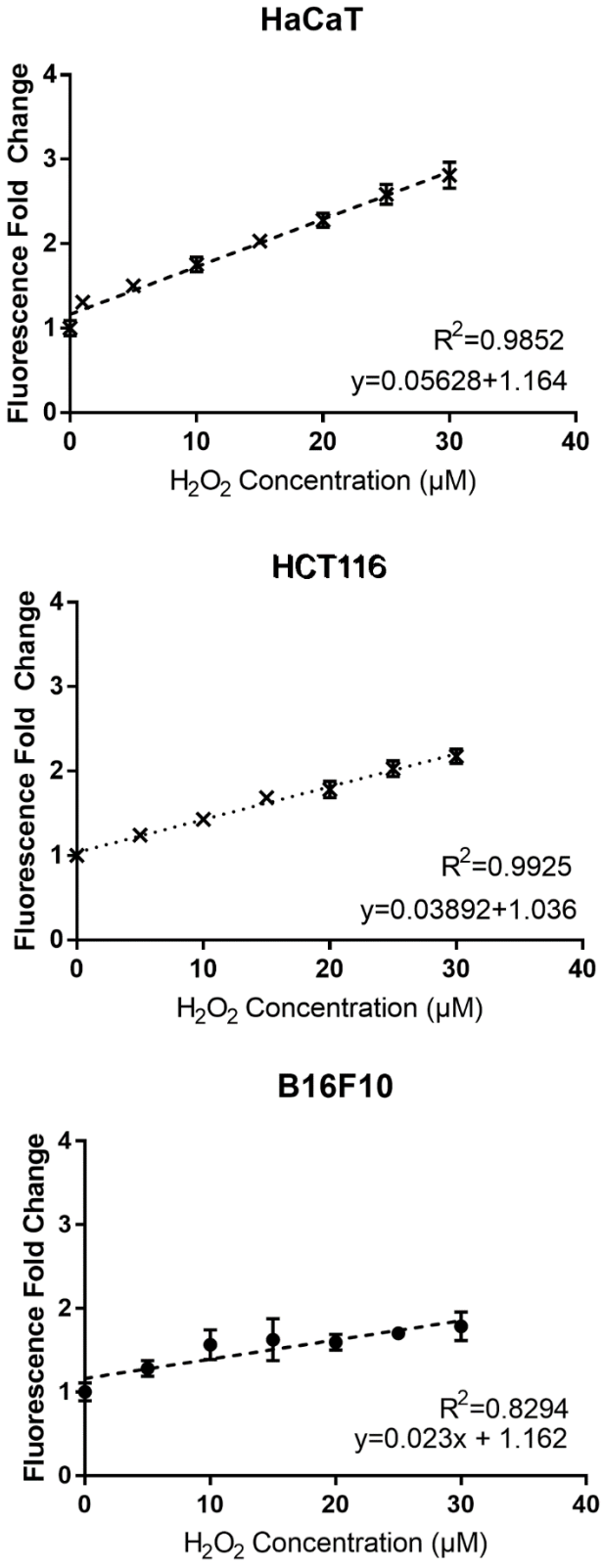

Figure 7.1: Relative DCF fluorescence following hydrogen peroxide treatment. Trends were calculated in

Graphpad Prism 7. HaCaT (Sy.x = 0.0.0831; p<0.0001), HCT116 Sy.x = 0.04012; p<0.0001) and B16F10 (Sy.x = 0.1234; p=0.0044) show a linear increase in fluorescence fold change with a linear increase in hydrogen peroxide concentration.

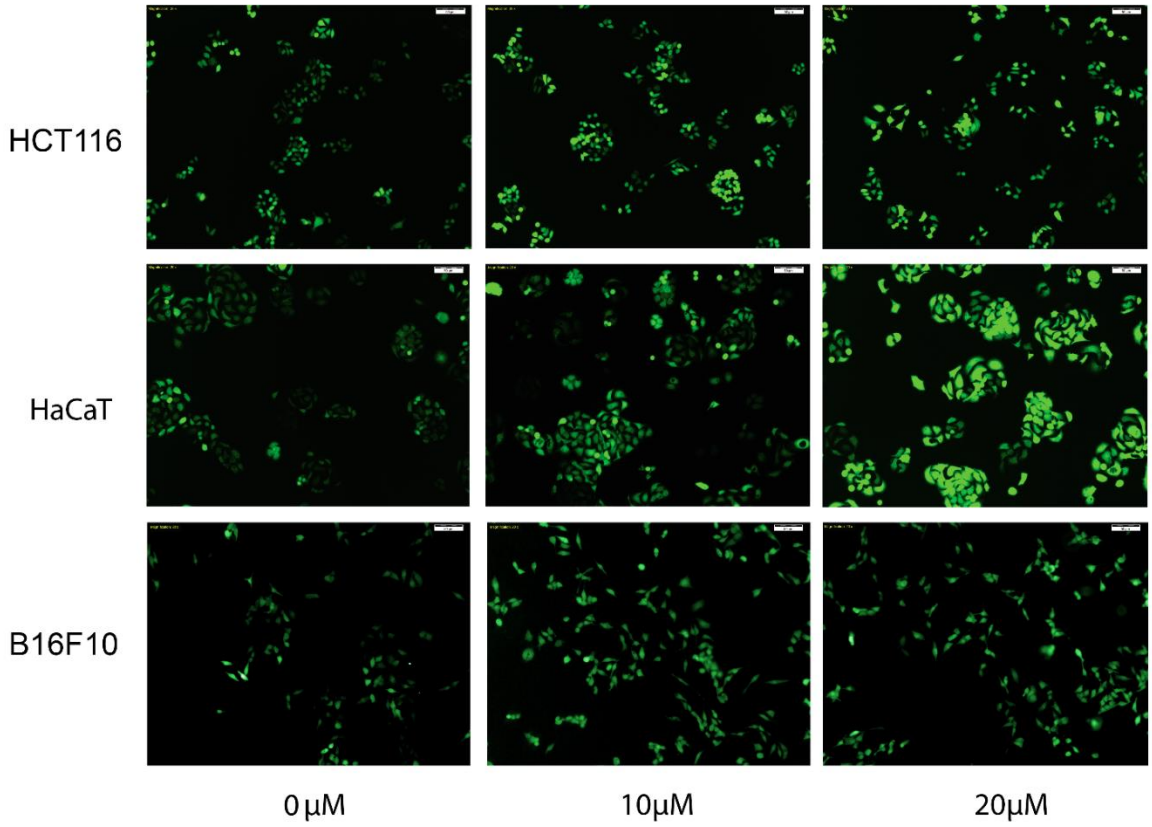

Figure 7.2: HCT116, HaCaT, and B16F10 cells loaded with DCFDA and treated with hydrogen peroxide at various concentrations. The original images were grayscale and falsely colourized to imitate DCF fluorescence.

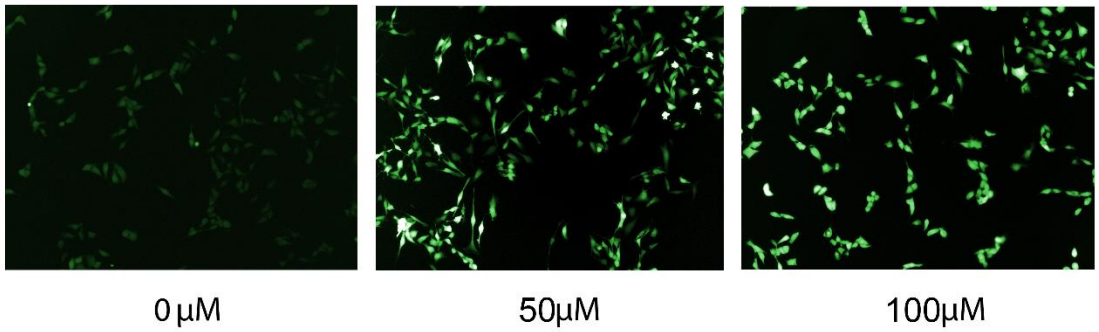

Figure 7.3: B16F10 cells loaded with DCFDA and treated with higher doses of hydrogen peroxide. The original images were grayscale and falsely colorized to imitate DCF fluorescence.

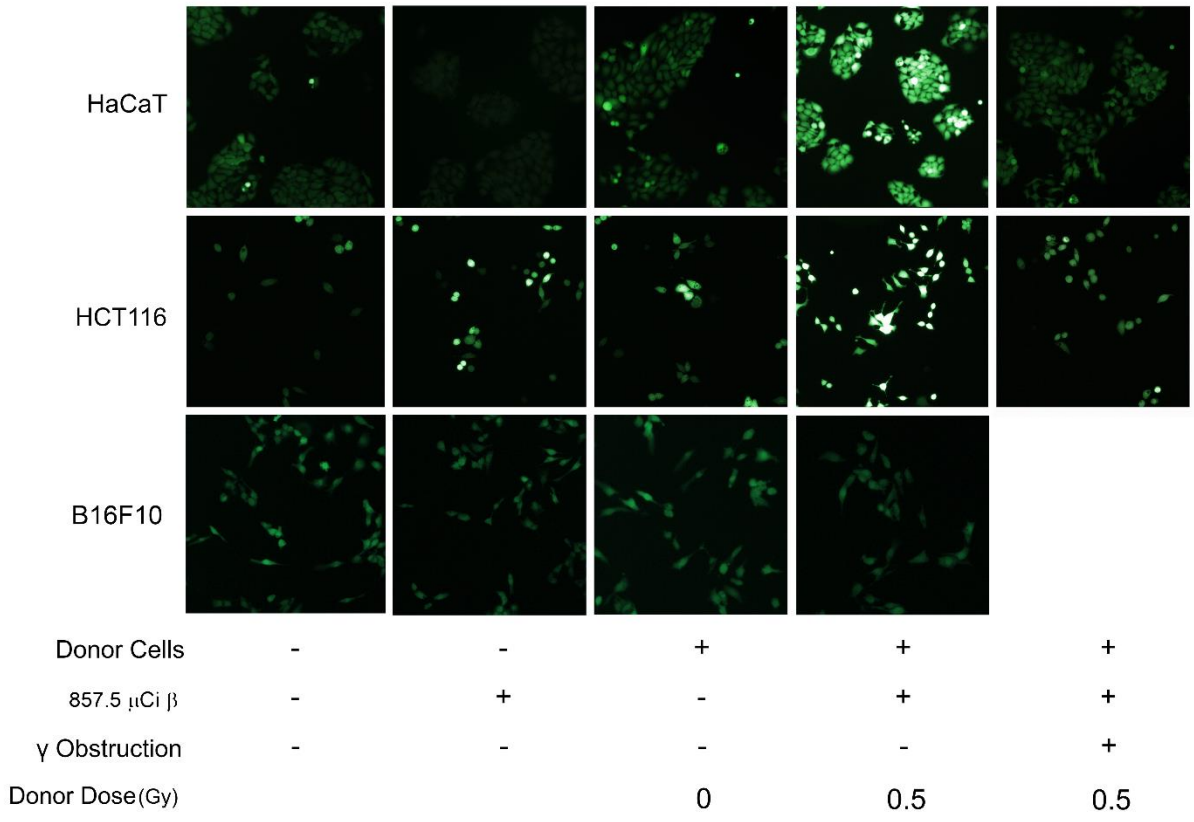

Figure 7.4: Bystander reporters and controls following exposure to various treatments under the fluorescence microscope. "+" indicates the presence of a treatment, while "-" indicates its absence. These images are similarly falsely colorized as in Figure 7.2.

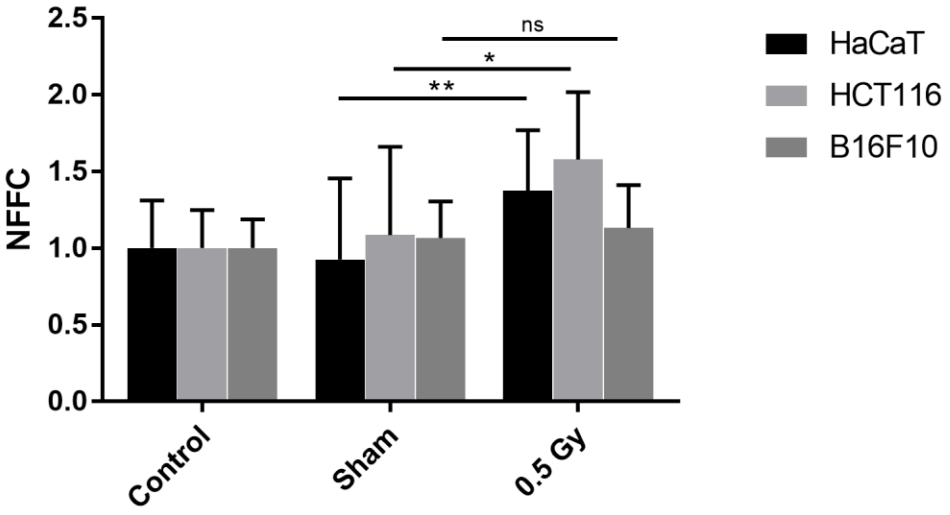

Figure 7.5: Normalized fluorescence fold change of bystander reporters exposed to various treatments. Error is shown as standard deviation of the mean and statistical significance is similarly denoted in previous chapters.

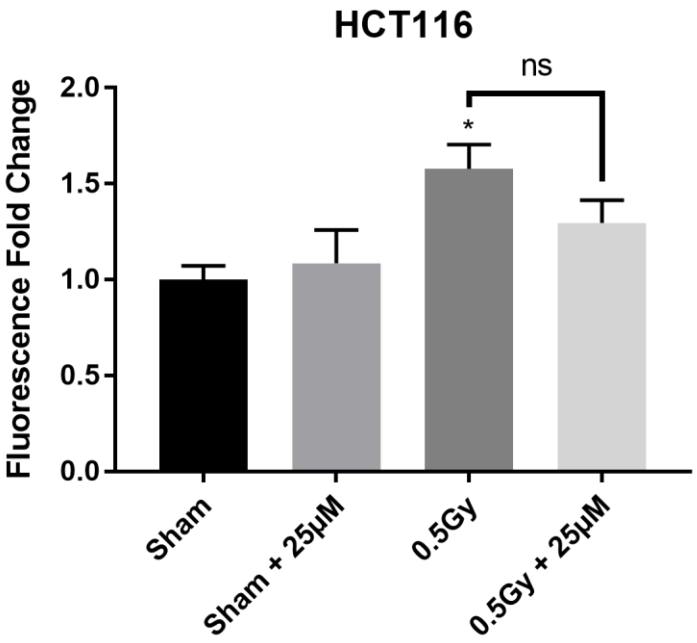

Figure 7.6: HCT116 reporters exposed to donors treated with tritium, 25 μM synthetic eumelanin (described in Chapter 4), and both. The 0.5 Gy group shows a significant increase in fluorescence fold change of DCF, however is not significantly different from the donor group treated with tritium and melanin.

7.3.1. Epithelial cells exhibit oxidative stress with increasing hydrogen peroxide supplementation

Figure 7.1 shows data collected from the exposure of all three cell lines to hydrogen peroxide. All cell lines exhibited a linear increase in DCF fluorescence with a linear increase in hydrogen peroxide micromolarity, suggesting the induction of oxidative stress with the administration of exogenous ROS. HaCaT was observed to fluoresce most relative to other cell lines. HCT116 exhibited intermediate fluorescence while B16F10 appeared least affected by hydrogen peroxide exposure. This can be interpreted from the trends calculated in Figure 7.1 as well as live fluorescence microscopy images in Figures 7.2 and 7.3. It was noted that an increased fluorescence signal was observed with longer exposure to the polarized light source or ambient light.

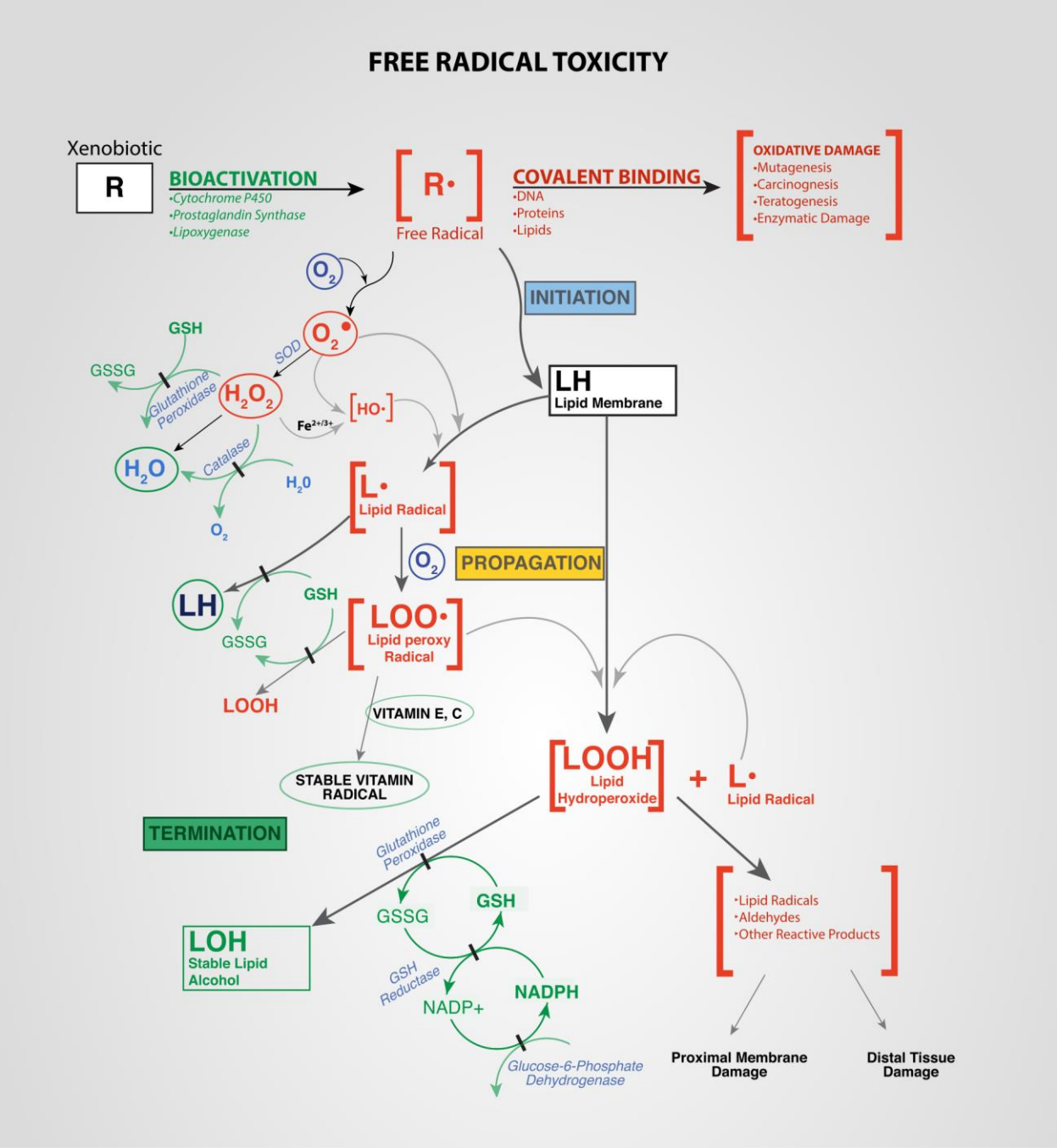

Figure 7.7: A diagram of the various types of free radicals that may form in a cells, including broader categories like lipid radicals and by-products such as aldehydes. Diagram courtesy Dan Cojocari, Princess Margaret Cancer Centre, University of Toronto (CC BY-SA 4.0).

7.3.2. Human epithelial cells, but not murine melanocytes, exhibit oxidative stress upon exposure to bystander photons and melanin abrogates electromagnetic bystander signalling

The results in Figures 7.4 and 7.5 represent bystander reporters exposed to various treatments. In Figure 7.4, HaCaT reporters were demonstrated to fluoresce in the presence of bystander donors and tritium together, while separate inclusion did not induce significant DCF fluorescence. Obstruction of bystander photons from donor cultures by the inclusion of two sheets of metal foil between the donor and recipient vessels. In HCT116 cells, a similar pattern of fluorescence was observed as in HaCaT cells. B16F10 cells did not exhibit a noticeable increase in fluorescence following the same treatments.

These results are corroborated by microplate assay in Figure 7.5. Here, HaCaT reporters showed a significant increase in DCF fluorescence following a donor dose of 0.5 Gy ($p=0.0348$). HCT116 reporters similarly showed a significant increase in fluorescence ($p=0.0289$). B16F10 reporters however did not exhibit a significant increase in fluorescence ($p=0.7844$).

The results shown in Figure 5.6 indicate that melanin supplementation in donors may reduce oxidative stress in reporters, however a significant reduction in DCF fluorescence was not obtained.

7.4. Discussion

These results indicate several things about the three mammalian cell lines exposed to hydrogen peroxide and biophotons. In terms of susceptibility to oxidative stress following exposure to hydrogen peroxide, HaCaT appears to be most sensitive, followed by HCT116. This can be interpreted from Figure 7.1, as the slope of the best fit line for HaCaT cell data is steepest. This is followed in magnitude by HCT116. B16F10 appears to be the least sensitive to oxidative stress at the same doses. These comparisons are possible because the models fitting the data appear to sufficiently robust. Finally, B16F10 is the least susceptible to oxidative stress, which can be observed in Figure 7.1 as well as the microscopy images in Figures 7.2 and 7.3.

Confirmation of these findings can be found in Figure 7.2. Microscopy images suggest a noticeable increase in fluorescence in both HCT116 and HaCaT cells. B16F10 cells appear more resilient to the increase in oxidative stress. Higher doses of hydrogen peroxide produced a major increase in fluorescence (in B16F10), however the effect at higher doses does not seem to increase greatly between 50-100 uM. However, the B16F10 microplate results show a more steady trend than is apparent in microscopy images. This could be due to B16F10 fluorescing more strongly following 10 or 20 µM, however this not being obvious in the microscopy images because it is a relatively minor increase. Though precautions were taken to prevent DCF photobleaching, this could also be a possibility in these ranges for B16F10. Sufficient photooxidation could completely “overwhelm” the signal that occurs due to hydrogen peroxide exposure.

Doses between 0–30 µM were chosen because it was believed that these low doses would be relevant to biophoton exposure—this suspicion was correct. In Figure 7.3, it is evident that the increase in DCFDA fluorescence in HaCaT and HCT116, though statistically significant, is relatively small compared to hydrogen peroxide exposures. The fluorescence fold increase in HaCaT bystanders was 1.38 ±0.39 and in HCT116 was 1.58 ±0.44, with error shown as standard deviation of the mean. An interesting exercise would be to use these values to estimate the equivalent quantity of hydrogen peroxide required to induce the same amount of oxidative stress in this system. For HaCaT, this value is about 21 µM and for HCT116 this value is about 14 µM. These values are merely an estimate, however these comparisons are also possible because the experimental setup was similar in bystander and peroxide trials.

The bystander reporter results suggest that both HaCaT and HCT116 are capable of responding to the physical bystander signal, with the HCT116 oxidative stress response being greater than the HaCaT

response. B16F10 did not show this increase in fluorescence, which suggests that melanin could play a protective role in reporters, acting as a free-radical sink. Evidence for abrogation of the bystander signal by melanin was described in Chapter 5, wherein B16F10 cells were shown to not emit bystander photons. Previous studies have suggested that melanin could act as both an absorber of bystander photons and a free radical scavenger, and thereby could exert its radioprotective effect in both donors and recipients via different mechanisms[34,35]. A synthetic melanin supplementation experiment was performed on HCT116 cells, where reporters were provided with 25 µM eumelanin and exposed to biophotons. It was found that this concentration of melanin was insufficient to produce a significant change in DCF fluorescence over the control. With additional data collected in Chapter 4, it is suspected that this could be the case due to an inadequate quantity of solubilized melanin given to reporters, as 25 µM is much lower than the amount synthesized and secreted by B16F10 cells under normal culture conditions. Future experiments should focus on the supplementation of melanin at various concentrations to determine if a dose-dependent radioprotective effect in the context of this bystander effect Problems associated with the DCFDA assay have been discussed in the literature, specifically with respect to ultraviolet irradiations[36]. This concern was noted, and the phenomenon was observed upon exposure in the present thesis. This is obvious evidence for the photooxidation of the DCF dye. Intuitively, DCF is used to measure the quantity of ROS in a cell population because oxidation of DCF by ROS yields a fluorescent product. Therefore, increased fluorescence upon light exposure may indicate an oxidative interaction, which is known as photooxidation. This feature of the dye is also widely recognized in the literature[36–40]. Despite this susceptibility, the experimental design of this chapter effectively ameliorates some of these issues. Firstly, cells loaded with DCFDA—whether destined for microscopic examination or readout in a microplate—were protected from light. Moreover, bystander assays were conducted in a manner that precluded photooxidation of DCFDA by UV; cells were loaded post irradiation and not preceding it. Additionally, great care was taken to prevent unnecessary exposure of cells to high-intensity polarized light in microscopy experiments. Therefore, inadvertent oxidation of DCF by light was effectively addressed in these experiments.

7.5. Conclusion

HaCaT appears to be the most susceptible to hydrogen peroxide-induced oxidative stress, with HCT116 following as a close second. B16F10 is least susceptible to this effect, which could be indicative of the antioxidant properties of melanin. HCT116 and HaCaT bystander reporters exhibited increased oxidative stress, while B16F10 reporters did not, indicating that melanin in donors absorbs the signal in donors, prevents oxidative stress in reporters, or a combination of both. It is suspected that melanin is responsible for radioprotection in the context of the physical bystander signal—although a significant rection in oxidative stress was not observed in reporters where donors were provided melanin, it is believed this could be due to insufficient melanin concentration in donor cultures. These results suggest that electromagnetic bystander mechanisms are underpinned by processes involving oxidative stress.

7.6. References

1. Guo S, Zhou J, Chen X, Yu Y, Ren M, Hu G, Liu Y, Zou F. Bystander effects of PC12 cells treated with Pb(2)(+) depend on ROS-mitochondria-dependent apoptotic signaling via gap-junctional intercellular communication. Toxicology letters. 2014;229(1):150–157. doi:10.1016/j.toxlet.2014.05.026

2. Kotsinas A, Aggarwal V, Tan E-J, Levy B, Gorgoulis VG. PIG3: A novel link between oxidative stress and DNA damage response in cancer. Cancer Letters. 2012;327(1–2):97–102. http://dx.doi.org/10.1016/j.canlet.2011.12.009. doi:10.1016/j.canlet.2011.12.009

3. Tang FR, Loke WK. Molecular mechanisms of low dose ionizing radiation-induced hormesis, adaptive responses, radioresistance, bystander effects, and genomic instability. International journal of radiation biology. 2015;91(1):13–27. doi:10.3109/09553002.2014.937510

4. Shimura T, Kunugita N. Mitochondrial reactive oxygen species-mediated genomic instability in low-dose irradiated human cells through nuclear retention of cyclin D1. Cell cycle (Georgetown, Tex.). 2016;15(11):1410–1414. doi:10.1080/15384101.2016.1170271

5. Rada B, Leto T. Oxidative innate immune defenses by Nox/Duox Family NADPH oxidases. Contributions to Microbiology. 2008. doi:10.1159/000136357

6. Sharma P, Chakraborty R, Wang L, Min B, Tremblay ML, Kawahara T, Lambeth JD, Haque SJ. Redox Regulation of Interleukin-4 Signaling. Immunity. 2008. doi:10.1016/j.immuni.2008.07.019

7. Roy K, Wu Y, Meitzler JL, Juhasz A, Liu H, Jiang G, Lu J, Antony S, Doroshow JH. NADPH oxidases and cancer. Clinical Science. 2015. doi:10.1042/CS20140542

8. Sellés Vidal L, Kelly CL, Mordaka PM, Heap JT. Review of NAD(P)H-dependent oxidoreductases: Properties, engineering and application. Biochimica et Biophysica Acta - Proteins and Proteomics. 2018. doi:10.1016/j.bbapap.2017.11.005

9. Patra KC, Hay N. The pentose phosphate pathway and cancer. Trends in biochemical sciences. 2014;39(8):347–354.

10. Stincone A, Prigione A, Cramer T, Wamelink MMC, Campbell K, Cheung E, Olin-Sandoval V, Grüning NM, Krüger A, Tauqeer Alam M, et al. The return of metabolism: Biochemistry and physiology of the pentose phosphate pathway. Biological Reviews. 2015. doi:10.1111/brv.12140

11. Kruger NJ, Von Schaewen A. The oxidative pentose phosphate pathway: Structure and organisation. Current Opinion in Plant Biology. 2003. doi:10.1016/S1369-5266(03)00039-6

12. Jiang P, Du W, Wu M. Regulation of the pentose phosphate pathway in cancer. Protein and Cell. 2014. doi:10.1007/s13238-014-0082-8

13. Gansemer ER, McCommis KS, Martino M, King-McAlpin AQ, Potthoff MJ, Finck BN, Taylor EB, Rutkowski DT. NADPH and glutathione redox link TCA cycle activity to endoplasmic reticulum homeostasis. Iscience. 2020;23(5):101116.

14. Behrends V, Giskeødegård GF, Bravo-Santano N, Letek M, Keun HC. Acetaminophen cytotoxicity in HepG2 cells is associated with a decoupling of glycolysis from the TCA cycle, loss of NADPH production, and suppression of anabolism. Archives of toxicology. 2019;93(2):341–353.

15. Sauer U, Canonaco F, Heri S, Perrenoud A, Fischer E. The soluble and membrane-bound transhydrogenases UdhA and PntAB have divergent functions in NADPH metabolism of Escherichia coli.

Journal of Biological Chemistry. 2004;279(8):6613–6619.

16. Culotta VC, Yang M, O'Halloran T V. Activation of superoxide dismutases: Putting the metal to the pedal. Biochimica et Biophysica Acta - Molecular Cell Research. 2006. doi:10.1016/j.bbamcr.2006.05.003

17. Papa L, Hahn M, Marsh EL, Evans BS, Germain D. SOD2 to SOD1 switch in breast cancer. Journal of Biological Chemistry. 2014. doi:10.1074/jbc.C113.526475

18. Arnér ESJ, Holmgren A. Physiological functions of thioredoxin and thioredoxin reductase. European Journal of Biochemistry. 2000. doi:10.1046/j.1432-1327.2000.01701.x

19. Lu J, Holmgren A. The thioredoxin antioxidant system. Free Radical Biology and Medicine. 2014. doi:10.1016/j.freeradbiomed.2013.07.036

20. Sepasi Tehrani H, Moosavi-Movahedi AA. Catalase and its mysteries. Progress in Biophysics and Molecular Biology. 2018. doi:10.1016/j.pbiomolbio.2018.03.001

21. Kono Y, Fridovich I. Superoxide radical inhibits catalase. Journal of Biological Chemistry. 1982. doi:10.1016/s0021-9258(19)83842-5

22. Day BJ. Catalase and glutathione peroxidase mimics. Biochemical Pharmacology. 2009. doi:10.1016/j.bcp.2008.09.029

23. Liu Y, Fiskum G, Schubert D. Generation of reactive oxygen species by the mitochondrial electron transport chain. Journal of Neurochemistry. 2002. doi:10.1046/j.0022-3042.2002.00744.x

24. Quinlan CL, Orr AL, Perevoshchikova I V., Treberg JR, Ackrell BA, Brand MD. Mitochondrial complex II can generate reactive oxygen species at high rates in both the forward and reverse reactions. Journal of Biological Chemistry. 2012. doi:10.1074/jbc.M112.374629

25. Wang Y, Hekimi S. Understanding Ubiquinone. Trends in Cell Biology. 2016. doi:10.1016/j.tcb.2015.12.007

26. McLennan HR, Esposti MD. The contribution of mitochondrial respiratory complexes to the production of reactive oxygen species. Journal of Bioenergetics and Biomembranes. 2000. doi:10.1023/A:1005507913372

27. Petersen AB, Gniadecki R, Vicanova J, Thorn T, Wulf HC. Hydrogen peroxide is responsible for UVA-induced DNA damage measured by alkaline comet assay in HaCaT keratinocytes. Journal of Photochemistry and Photobiology B: Biology. 2000;59(1–3):123–131.

28. Bae S, Lee E-J, Lee JH, Park I-C, Lee S-J, Hahn HJ, Ahn KJ, An S, An I-S, Cha HJ. Oridonin protects HaCaT keratinocytes against hydrogen peroxide-induced oxidative stress by altering microRNA expression. International Journal of Molecular Medicine. 2014;33(1):185–193.

29. Azzam EI, de Toledo SM, Spitz DR, Little JB. Oxidative metabolism modulates signal transduction and micronucleus formation in bystander cells from α-particle-irradiated normal human fibroblast cultures. Cancer research. 2002;62(19):5436–5442.

30. Cho H, Kim O, Lee Y, Kang L-J, Nguyen CN, Ishihara A, Kim H-E. Feruloylserotonin inhibits hydrogen peroxide-induced melanogenesis and apoptosis in B16F10 and SK-Mel-2 melanoma cells. Biochemical and biophysical research communications. 2017;491(4):973–979.

31. Dell'Anna ML, Ottaviani M, Albanesi V, Vidolin AP, Leone G, Ferraro C, Cossarizza A, Rossi L, Picardo

M. Membrane lipid alterations as a possible basis for melanocyte degeneration in vitiligo. Journal of Investigative Dermatology. 2007;127(5):1226–1233.

32. Al-Hussainy ADO, Al-Gazally ME, Ewadh W. Oxidative stress, Anti-melanocyte and anti tyrosinase antibody in vitiligo and response to treatment. Annals of Tropical Medicine and Health. 2020;23:202–209.

33. Arican O, Kurutas EB. Oxidative stress in the blood of patients with active localized vitiligo. ACTA DERMATOVENEROLOGICA ALPINA PANONICA ET ADRIATICA. 2008;17(1):12.

34. Le M, Mothersill CE, Seymour CB, Ahmad SB, Armstrong A, Rainbow AJ, McNeill FE. Factors affecting ultraviolet-A photon emission from beta-irradiated human keratinocyte cells. Physics in medicine and biology. 2015;60(16):6371–6389. doi:10.1088/0031-9155/60/16/6371

35. Le M. Investigating the Generation of Biophotons Induced by Low-Dose Beta-Irradiation and their Role in the Radiation-Induced Bystander Effect. McMaster University; 2018.

36. Tetz LM, Kamau PW, Cheng AA, Meeker JD, Loch-Caruso R. Troubleshooting the dichlorofluorescein assay to avoid artifacts in measurement of toxicant-stimulated cellular production of reactive oxidant species. Journal of pharmacological and toxicological methods. 2013;67(2):56–60.

37. Chang W, Li J, Haung H, Liu H, Han M, Ramachandran S, Li C, Sharp WW, Hamann KJ, Yuan C. Baicalein protects against doxorubicin-induced cardiotoxicity by attenuation of mitochondrial oxidant injury and JNK activation. Journal of cellular biochemistry. 2011;112(10):2873–2881.

38. Souza C, Mônico DA, Tedesco AC. Implications of dichlorofluorescein photoinstability for detection of UVA-induced oxidative stress in fibroblasts and keratinocyte cells. Photochemical & Photobiological Sciences. 2020;19(1):40–48.

39. Denamur S, Tyteca D, Marchand-Brynaert J, Van Bambeke F, Tulkens PM, Courtoy PJ, Mingeot-Leclercq M-P. Role of oxidative stress in lysosomal membrane permeabilization and apoptosis induced by gentamicin, an aminoglycoside antibiotic. Free Radical Biology and Medicine. 2011;51(9):1656–1665.

40. Kristiansen KA, Jensen PE, Møller IM, Schulz A. Monitoring reactive oxygen species formation and localisation in living cells by use of the fluorescent probe CM-H2DCFDA and confocal laser microscopy. Physiologia plantarum. 2009;136(4):369–383.

Chapter 8

Cell metabolic viability following exposure to biophotons and hydrogen peroxide

Abstract: An indicator of overall cell health in a population can be determined by the assay of metabolic activity. MTT is a compound that turns into a purple formazan through the activity of mitochondrial and cytosolic NAD(P)H oxidoreductases and can therefore be used to assess the viability of a cell population through optical absorbance. Modulation of metabolic activity with increasing dose was observed in HCT116 cells, with apparent low dose hypersensitivity. In HaCaT, the trend was also a linear decrease in absorbance with a linear increase in hydrogen peroxide concentration, which can be explained by different treatment times between this chapter and chapter 6, as the MTT assay usually follows a similar trend to the clonogenic survival assay. The trend in B16F10 was also somewhat dose-dependent, although the relationship was less clear and the fit not as robust as with HaCaT and HCT116. Human biophoton reporters exhibited a reduction in absorbance with a donor dose of 0.5 Gy, however B16F10 did not show this effect. The results overall demonstrate broad modulation of metabolism in human cells due to hydrogen peroxide in all cell lines, likely due in part to cell killing, and the same in bystander reporters. The results furthermore suggest a role for melanin in attenuating these effects.

8.1. Introduction

Cellular metabolism is undoubtedly a hallmark of life; the term "metabolism" collectively refers to the set of chemical reactions in an organism that are required to sustain life. Metabolism can be broadly classified as catabolic metabolism, referring to reactions that serve to break down larger molecules such as those required to derive energy from food; and anabolic metabolism, referring to reactions that build larger molecules such as those that construct complex molecules like nucleic acids.

The observation of metabolic effects is inevitable in radiation biology. Cancer cells "reprogram" their metabolism to meet the energetic and synthetic requirements for maintenance of the cancerous state and its progression—these are known classically as "the hallmarks of cancer"[1]. The first studies on energy metabolism in tumors were carried out in by Warburg. He characterized the shift from aerobic respiration to fermentation in tumors[2,3]. Today, an understanding of the underlying genetic and molecular mechanisms that persist in nearly all cancers is required, however the importance of metabolic changes is widely appreciated as well. Importantly, these concepts are vital to radiation therapy, as oxygenation and metabolic states are key players in direct cell killing[4–6]. Radiation responses in general are known to be dependent on cell metabolic state, irrespective of transformation. Seymour et al. (1985) found that treatment of cells with two glucose analogues sensitizes cells to gamma radiation[7], and another report by the same group confirmed these effects using glycolysis inhibitors[8]. The same group discovered earlier that prolonged exposure to lactate also sensitizes cells to ionizing radiation in a series of papers[9,10]. Thus, metabolic status is a very useful indicator of how a cell may respond to ionizing radiation, even *in vitro*. A shift in metabolism is also crucial for tumorigenesis *in vivo* and these aspects may be exploited in cancer therapy.

In terms of the physical bystander signal, previous results in the present thesis, notably from chapters 5-7, indicate that this signal produces various effects in reporter cell cultures. First, a primarily UVA signal is emitted from directly irradiated cells, in absence of radioprotective compounds such as melanin, and is received by bystander cells. These cells ultimately experience a reduction in reproductive cell death—which is suspected to be due to apoptosis, mitotic death, necrosis, or a combination thereof—upon receipt of this signal in a dose-dependent manner. Lastly, these cells experience an increase in oxidative stress upon receipt of the signal. After reviewing considerations from previous research[11–16], it was hypothesized that changes in metabolic activity could also be observed in these bystander cells. Therefore, we sought to determine an appropriate test for overall metabolic activity that could be used to measure potential effects in bystander cells. We also wanted to ensure that the same test could be used in cells treated with hydrogen peroxide to model oxidative stress. It is also known that redox homeostasis is important in multiple metabolic processes—for example, radical species are naturally generated in the mitochondrial electron transport chain via the partial reduction of oxygen; the activation of superoxide-producing NADPH oxidases or xanathine oxidase in certain tissues; and the activation of certain cytochrome P450 enzymes with the partial reduction of water[17,18]. Therefore, we also wanted to assess the same effects when oxidative stress is induced in these cells.

The MTT assay has been used in radiobiological studies for some time. In principle, this assay measures overall cell metabolic activity through the conversion of the chemical compound MTT, described in further detail in Section 8.2, to a purple compound. The spectrophotometric determination of absorbance at a particular wavelength relative to a control group is then used as an estimate of relative cell viability. Some work using MTT has been conducted in the past. For example, a donor dose-dependent bystander response was observed in human fibroblasts (MRC5) and lung tumor (QU-DB) cell lines, which was measured in part by the MTT assay[19]. Another bystander study using MTT found that Rosmarinic Acid does not act as a radioprotector in RIBE as it does with direct irradiation[20]. The conversion of MTT requires

NAD(P)H, which is a cofactor used primarily in anabolic reactions as a reducing agent. In eukaryotes, mitochondria can produce NAD(P)H using several pathways involving enzymes in the citric acid cycle, and eukaryotes can also produce NAD(P)H in the pentose phosphate pathway. Limitations of the assay exist when primary tumor cells are not in the exponential growth phase[21], and both mitochondrial and cytosolic enzymes reduce the dye[22] in transformed hepatocytes. Therefore, MTT does not measure mitochondrial effects independently from the activity of other oxidoreductases, at least in some cell types. In another hepatoma study found that most formazan aggregates were local to nonmitochondrial cellular fractions, but that MTT could "displace" mitochondrial specific probes like JC1 from mitochondria[23]. Conversely, another group found that reduction occurs mainly in neurons[24]. In the cell lines used for the present thesis, the literature typically prescribes the MTT assay for the measurement of "anti-proliferative effects" or treatments that influence "cell viability"[25–27].

The purpose of this chapter was to measure metabolic activity in cells receiving hydrogen peroxide or biophoton signals. It was predicted that these results would confirm the results obtained in Chapter 6, where cell survival was measured. This is believed because a reduction in reproductive cell survival under both treatments should produce an equivalent (or at least related) effect on overall metabolic activity. Additionally, it is believed that these effects can be related to the MTT assay on a "lower-level" as well through the ubiquity of NAD(P)H. NAD(P)H, which is required for the activity that this assay measures, is also involved in reactions that protect the cell against oxidative stress such as the regeneration of antioxidant glutathione[28,29]. Moreover, NAD(P)H is involved in the respiratory burst required for the rapid generation of superoxide extracellularly by leukocytes[30,31].

8.2. Methods

8.2.1. MTT assay overview

The MTT assay is used to determine metabolic activity in a cell population. NAD(P)H-dependent oxidoreductases reduce membrane-permeable MTT—3-(4,5-dimethylthiazol-2-yl)-2,5-diphenyltetrazolium bromide—to an insoluble, purple formazan compound. Because more formazan is produced more metabolically active cell populations, typically including those with greater numbers of live cells, the quantity of formazan produced can be used as an informative measure of the quantity of viable cells. The production of NADPH occurs primarily in the pentose phosphate pathway Following a period to allow for the passage of MTT into the cells and production of the formazan, the formazan can be solubilized in DMSO. A spectrophotometer or microplate reader can then use absorbance to measure the quantity of formazan in solution, which again indicates overall metabolic state in the cell population. Medium free from phenol red was used for the MTT assay in all steps following subculture.

8.2.2. Peroxide treatment protocol

The protocol for using MTT was adapted and optimized from the Vybrant® MTT Cell Proliferation Assay Kit (V013154) document, available on the ThermoFisher Scientific website. One day prior to the assay, cells were subcultured and passaged as normal. The concentration of live cells in the cell suspension was determined using Trypan Blue and a BioRad TC20 automated cell counter, as described previously. 50 000 cells were seeded in each well of a 96-well plate, excluding relevant controls. The required volume was dispensed into multiple wells of a 96-well plate using a multichannel micropipette. A volume of complete

growth medium was then placed such that the final volume in each well was 200 µL. The plate was left to incubate overnight to allow for cell attachment.

The following day, an 880 µM solution of H_2O_2 was made in DPBS from 3% stock and serially diluted further in DPBS where needed. The calculations used to determine appropriate dilutions and volumes is described in further detail in Chapter 2. Medium from each well was discarded and cells washed once with 150 µL DPBS. Appropriate volumes were added to each well to produce each tested molarity, and the plate was left to incubate for 1 hour. 5 g MTT (Sigma-Aldrich, M2128) was dissolved in 1 mL sterile DPBS to make a 12 mM solution. This was mixed with 2 mL complete growth medium to create a loading solution. After 1 hour, the medium was removed from each well and 110 µL loading solution was added to each well.

After 4 hours, all but 25 µL of medium was removed from each well. Cell colonies at this point had turned a purple hue. Then 50 µL of pure DMSO was added to each well and mixed thoroughly to solubilize the formazan. The plate was incubated for 10 minutes and each well mixed again. The plate was then read for absorbance in a Tecan 200m Pro plate reader at 540 nm.

8.2.3. Biophoton treatment protocol

A similar protocol was followed for experiments on bystander reporter cells. Both donor and reporter cells were kept in the dark as much as possible to avoid saturation of the potential bystander signal with ambient light. On the first day and after subculture, 2000 cells/cm^2 were plated in two T25 flasks containing 5 mL medium; these cells were designated as bystander donors. 25 000 cells were plated in each well destined for exposure to bystander photons with 200 mL medium. On the final day this initial population was expected to double to the desired 50 000 cells per well. Both flasks and the plate were left to incubate overnight. The following day, 857.5 µCi tritiated water was added to one donor flask with the other serving as the control. Next, these flasks were placed directly superior to the reporter cells in the 96-well plate. This arrangement was kept in a light-tight container and incubated for 24 hours to achieve a donor dose of 0.5 Gy. On the final day, the donor flasks were discarded and the plate prepared for absorbance measurement as described previously; readings were collected in the same manner as described in this chapter's hydrogen peroxide section.

8.2.4. Statistics

Data was obtained in relative absorption units for 540 nm light. Background absorbance measurements were obtained from wells containing no cells but both loading buffer and DMSO; the average of these values was subtracted from measurements for each well. These measurements were then normalized to negative control wells, or those containing loaded cells but not exposed to hydrogen peroxide or biophotons, and the data were presented as normalized absorbance in arbitrary units.

The data were graphed in Graphpad Prism 7, and statistical tests were conducted in this software as well. The data are presented as average values for data points and error is presented as standard deviation in all figures—4 technical replicates for 2 biological replicates (n=8) in hydrogen peroxide-treated groups were used, while at least 10 technical replicates for 3 biological replicates (n=30) were used for cells receiving biophoton treatment. This is the same setup as in Chapters 7 and 9 for consistency. Linear regression was calculated for an absorbance trend against dose—the best fit line equation is shown on each graph, followed by the R^2 value and Sy.x, which both represent goodness-of-fit, and degrees of freedom (DF). Sy.x is a term used in Graphpad Prism 7 that represents the standard deviation of the residuals, and therefore a smaller value suggests a better fit, while a larger value suggests a comparatively

worse or “more varied” fit. One-way ANOVA followed by Tukey’s Honestly Standard Difference (HSD) test α=0.05 was performed for all biophoton treatment groups.

8.3. Results

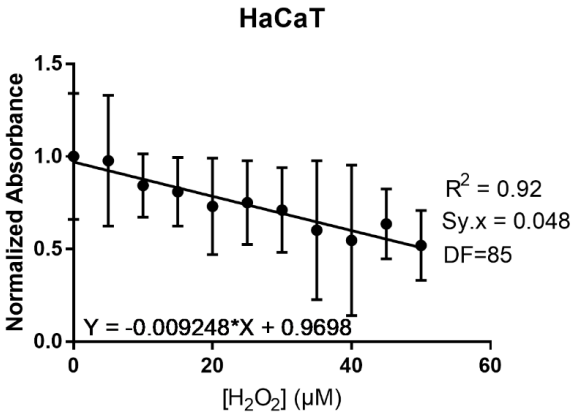

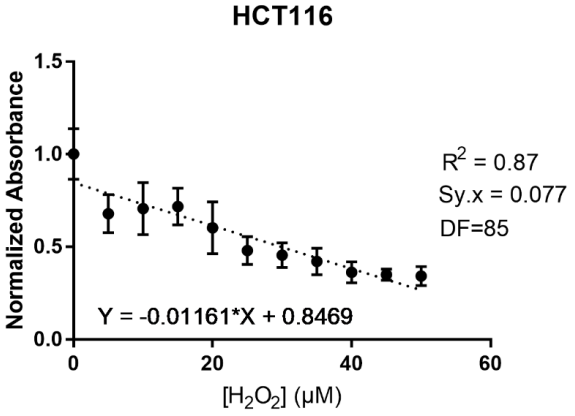

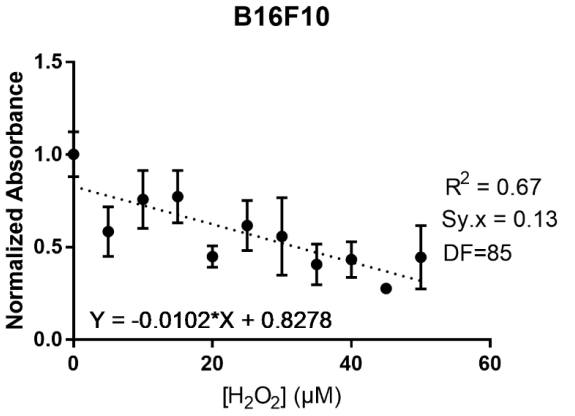

Figure 8.1: This graph shows linear fits of the data for relative formazan absorbance over hydrogen peroxide concentration in three cell lines. The trend was significant for HCT116 ($p<0.0001$), HaCaT ($p<0.0001$) and B16F10 ($p=0.0021$). The same data without a fitted trends is presented in Figure 8.2.

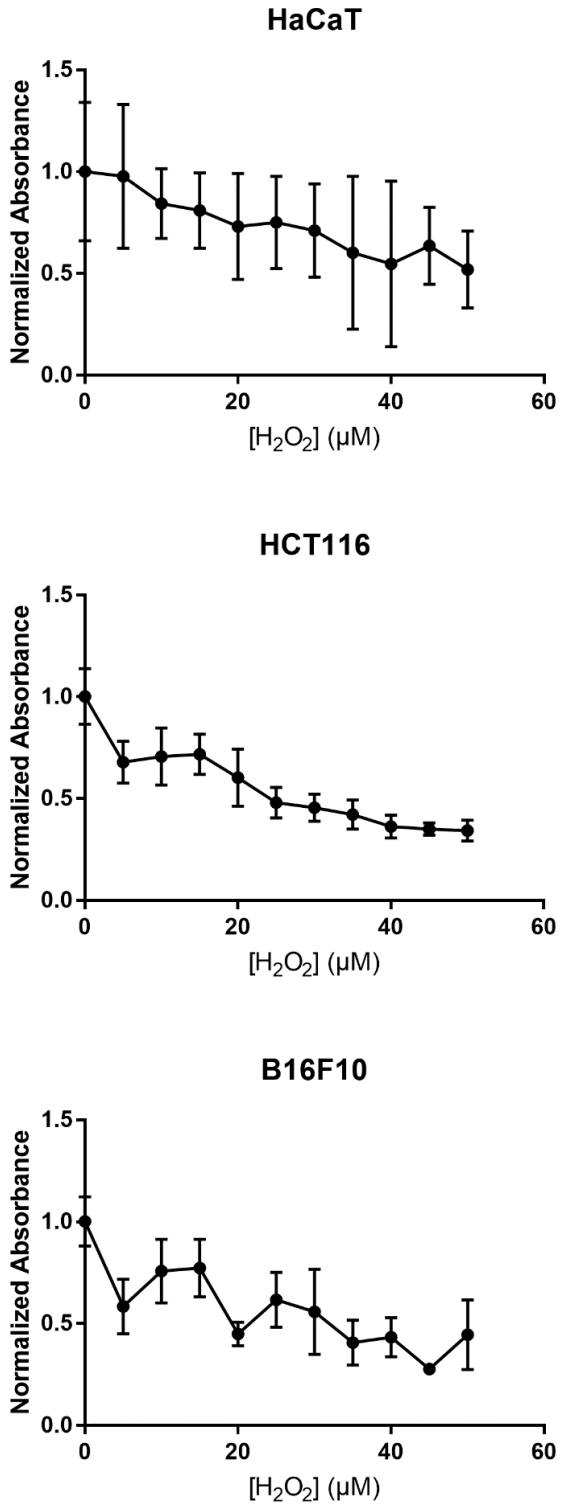

Figure 8.2: This graph shows relative formazan absorbance over hydrogen peroxide concentration in three cell lines.

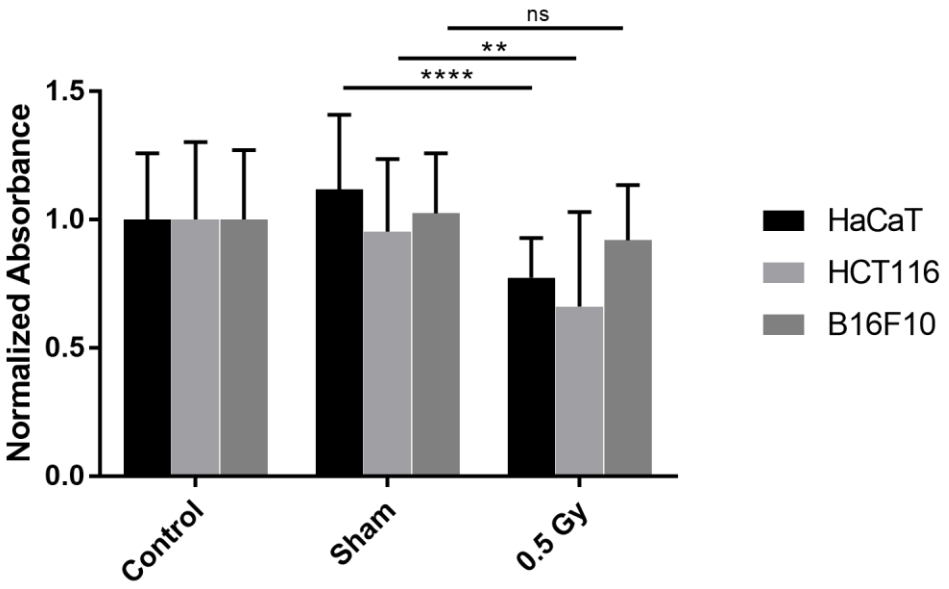

Figure 8.3: Formazan absorbance in three cell lines following exposure to bystander photons. The dose given to donor cells is shown on the x-axis. Statistically significant reductions in absorbance were observed in HaCaT ($p<0.0001$) and HCT116 ($p=0.0011$), but not in B16F10 ($p=0.0771$). Error is shown as standard deviation of the mean.

8.3.1. H_2O_2 treatment reduces metabolism overall in all cell lines

Figure 8.1 shows relative formazan absorbance following hydrogen peroxide treatment. All cell lines indicate a linear reduction in absorbance with a linear increase in hydrogen peroxide concentration. In terms of sensitivity to hydrogen peroxide, HaCaT and HCT116 appear to modulate their metabolism similarly, however HaCaT appears overall more resistant to this modulation according to its trendline. This is also apparent due to the variance observed in HaCaT as opposed to HCT116 cells. An interesting quality observed in HCT116 but not in HaCaT was apparent low dose hypersensitivity, as 5 µM produced a significant and large reduction in survival compared to HaCaT.

The overall trend of B16F10 is less clear, as a similarly robust dose-dependent curve was not obtained as in human cell lines. While the fit of the B16F10 data is not as robust, Figure 8.2 suggests a similarly inverse relationship between hydrogen peroxide concentration and metabolic activity.

8.3.2. Bystander photons reduce metabolism in human cell lines

Figure 8.3 shows absorbance of formazan in bystander reporters following several treatments. The metabolic activity was significantly reduced in HaCaT and HCT116 reporters for donors exposed to 0.5 Gy compared to the sham dose. The same reduction was not observed in

8.4. Discussion

Some troubleshooting was required prior to a successful MTT assay. This occurred because a change in colour upon inclusion of DMSO was not observed in several attempts, which indicated some issue with experimental design. It was determined that more cells had to be seeded the day prior to an experiment for a successful assay. The optimal number of cells seeded per well was 50,000.

It is interesting that the MTT peroxide curves are not the same as peroxide survival curves. This is likely due to a number of factors. It is noted that the clonogenic survival assay results showed an exponential decrease in survival with a linear increase in hydrogen peroxide concentration, while the MTT assay shows a linear decrease in absorbance with a linear increase in peroxide concentration. The most obvious explanation for this is that the clonogenic survival assay measures reproductive death, while MTT is distinct in that it is a metabolic assay. Additionally, these results were likely affected due to the time that the cells were incubated with hydrogen peroxide; for the DCFDA assay, this time was approximately one hour, and for the MTT assay it was approximately one hour as well. In the clonogenic survival assay curves, the peroxide incubation time was approximately 8 days. Therefore, it is believed that the linear pattern observed in both assays could be a result of this difference in experimental design compared to the clonogenic survival assay. This is also likely a confounding factor that would not permit a robust comparison of these data to the clonogenic survival assay data. It makes sense that longer exposure produces greater effects, especially at concentrations where catalase and repair pathways cannot keep up with oxidative damage. Additionally, perhaps metabolic status is not linearly related to cell survival in the context of hydrogen peroxide exposure—another report has shown that a linear decrease in absorbance can be observed in HaCaT cells with linear increase in hydrogen peroxide supplementation[32]. It should be noted that the results in this paper for HaCaT were similar, albeit HaCaT in my system appear to be more sensitive to hydrogen peroxide. HCT116 also follows a similar MTT trend with hydrogen peroxide treatment as in the literature under the same treatment[33]. Unfortunately, there is a dearth in the literature on the same effects in B16F10, so the trend observed cannot be compared to existing data.

Comparing the survival assay and MTT assay peroxide exposure results is helpful because it provides an indication of how exogenous oxidative stress may produce cellular effects and different exposure times. While hydrogen peroxide should be decomposed by catalase, which is extremely efficient in this task, this enzyme is present primarily in peroxisomes and sometimes mitochondria[34]. Therefore, formation of lipid peroxides and the oxidation products of proteins and nucleic acids may still occur upon the interaction of hydrogen peroxide with cells from the extracellular environment. Furthermore, especially at higher concentrations, toxic ROS may persist in the cell growth environment from

The peroxide trend observed in B16F10 could be the result of varying concentrations of melanin in the cultures producing a commensurately varied protection against exogenous oxidative stress, assuming eumelanin has antioxidant properties[35–37]. The amount of melanin produced by cells and secreted into medium likewise varied in the present thesis, which is discussed in chapter 4. However, this cannot be confirmed, and it could be that other factors protect B16F10 against oxidative damage and thus a compromised metabolism. In all, the results suggest hypersensitivity to low doses of hydrogen peroxide in HCT116 cells, moderate sensitivity in HaCaT, and unclear sensitivity in B16F10 cells.

The results in Figure 8.3 corroborate the idea that electromagnetic bystander signalling induces reduced metabolism in bystander reporters[13,38]. The reduction observed in HaCaT and HCT116 reporters indicates reduced mitochondrial and cytosolic NAD(P)H-dependent oxidoreductase activity, which is indicative of overall reduced metabolism in the reporter culture. This could be due to one of two effects, or a combination of both. First, the signal can downregulate enzymes such as mitochondrial respiratory Complex I and IV[13]; secondly, the signal can induce reproductive cell death in reporters, an effect observed

in this report in chapter 6 and in the literature[14,39], which would reduce the gross conversion of MTT to the purple formazan in each well. The lack of response in B16F10 further justifies the notion that melanin protects B16F10 cells from bystander responses, either through attenuation of the signal in donors or photoprotective effects in the reporters, or a combination of both.

The rationale for providing a dose of 0.5 Gy to donors was based on results from an experiment using a clonogenic endpoint. Le at al.[14] found that clonogenic survival in reporter cells decreased most dramatically using doses between 0 and 20 cGy; the reduction began to plateau afterward. This is further corroborated by the difference in survival in Chapter 6 between the 50 and 75 cGy doses, which was lower in HCT116 and HaCaT compared to the difference between 25 and 50 cGy. Therefore, bystander cells may experience low-dose hyper-radiosensitivity in response to a dose given to donor cells.

8.5. Conclusion

The radiation-induced bystander effect is known to modulate metabolism in cells exposed to bystander signals[13]. This may also occur due to the effects of oxidative stress. Supplementation of hydrogen peroxide in the medium of three mammalian cells induced varying responses: HCT116 were hypersensitive, HaCaT moderately so, and B16F10 exhibited an unclear relationship, possibly due to the free radical scavenging properties of melanin. HaCaT and HCT116 bystander reporters responded with a significant reduction in metabolism upon receipt of the bystander signal, while the same was not observed in B16F10 donor-reporter pairs. These results also indicate that melanin could protect against the physical bystander effect and may contribute to B16F10's relatively low sensitivity to ionizing radiation.

8.6. References

1. DeBerardinis RJ, Chandel NS. Fundamentals of cancer metabolism. Science advances. 2016;2(5):e1600200.

2. Warburg O. The metabolism of carcinoma cells. The Journal of Cancer Research. 1925;9(1):148–163.

3. Warburg O. The chemical constitution of respiration ferment. Science. 1928;68(1767):437–443.

4. Vander Heiden MG. Targeting cancer metabolism: a therapeutic window opens. Nature reviews Drug discovery. 2011;10(9):671–684.

5. Nordsmark M, Overgaard M, Overgaard J. Pretreatment oxygenation predicts radiation response in advanced squamous cell carcinoma of the head and neck. Radiotherapy and oncology. 1996;41(1):31–39.

6. Fyles AW, Milosevic M, Wong R, Kavanagh M-C, Pintilie M, Sun A, Chapman W, Levin W, Manchul L, Keane TJ. Oxygenation predicts radiation response and survival in patients with cervix cancer. Radiotherapy and Oncology. 1998;48(2):149–156.

7. Seymour CB, Mothersill C, Moriarty MJ. Glucose analogues alter the response of CHO-KI cells to gamma irradiation. Acta Radiologica: Oncology. 1985;24(4):351–356.

8. SEYMOUR CB, MOTHERSILL C. THE EFFECT OF GLYCOLYSIS INHIBITORS ON THE RADIATION RESPONSE OF CHO-K1 CELLS. RADIATION AND ENVIRONMENTAL BIOPHYSICS. 1988;27(1):49–57. doi:10.1007/BF01211109

9. SEYMOUR CB, MOTHERSILL C. THE EFFECT OF LACTATE ON THE RADIATION RESPONSE OF CHO-K1 CELLS IN CULTURE. INTERNATIONAL JOURNAL OF RADIATION BIOLOGY. 1981;40(3):283–291. doi:10.1080/09553008114551201

10. MOTHERSILL C, SEYMOUR CB. EFFECT OF LACTATE ON THE RECOVERY OF CHO-KI CELLS FROM GAMMA-RADIATION DAMAGE. ACTA RADIOLOGICA ONCOLOGY. 1986;25(1):71–76.

11. Ahmad SB, McNeill FE, Byun SH, Prestwich W V., Mothersill C, Seymour C, Armstrong A, Fernandez C. Ultra-violet light emission from hpv-g cells irradiated with low let radiation from 90Y; consequences for radiation induced bystander effects. Dose-Response. 2013;11(4):498–516. doi:10.2203/dose-response.12-048.ahmad

12. Le M, Fernandez-Palomo C, McNeill FE, Seymour CB, Rainbow AJ, Mothersill CE. Exosomes are released by bystander cells exposed to radiation-induced biophoton signals: Reconciling the mechanisms mediating the bystander effect. PLOS ONE. 2017;12(3):e0173685. doi:10.1371/journal.pone.0173685

13. Le M, McNeill FE, Seymour CB, Rusin A, Diamond K, Rainbow AJ, Murphy J, Mothersill CE. Modulation of oxidative phosphorylation (OXPHOS) by radiation- induced biophotons. Environmental Research. 2018;163:80–87. doi:10.1016/j.envres.2018.01.027

14. Le M, McNeill FE, Seymour C, Rainbow AJ, Mothersill CE. An observed effect of ultraviolet radiation emitted from beta-irradiated HaCaT cells upon non-beta-irradiated bystander cells. Radiation research. 2015;183(3):279–90. http://www.bioone.org/doi/10.1667/RR13827.1%5Cnhttp://www.ncbi.nlm.nih.gov/pubmed/25710575. doi:10.1667/RR13827.1

15. Le M, McNeill FEFE, Seymour CBCB, Rusin A, Diamond K, Rainbow AJAJ, Murphy J, Mothersill CECE. Modulation of oxidative phosphorylation (OXPHOS) by radiation-induced biophotons. Environmental research. 2018;163:80–87. doi:10.1016/j.envres.2018.01.027

16. Le M, Mothersill CE, Seymour CB, Ahmad SB, Armstrong A, Rainbow AJ, McNeill FE. Factors affecting ultraviolet-A photon emission from beta-irradiated human keratinocyte cells. Physics in medicine and biology. 2015;60(16):6371–6389. doi:10.1088/0031-9155/60/16/6371

17. Eghbal MA, Pennefather PS, O'Brien PJ. H2S cytotoxicity mechanism involves reactive oxygen species formation and mitochondrial depolarisation. Toxicology. 2004. doi:10.1016/j.tox.2004.05.020

18. Letelier ME, López-Valladares M, Peredo-Silva L, Rojas-Sepúlveda D, Aracena P. Microsomal oxidative damage promoted by acetaminophen metabolism. Toxicology in Vitro. 2011. doi:10.1016/j.tiv.2011.04.022

19. Toossi MTB, Khademi S, Azimian H, Mohebbi S, Soleymanifard S. Assessment of the dose-response relationship of radiation-induced bystander effect in two cell lines exposed to high doses of ionizing radiation (6 and 8 Gy). Cell Journal (Yakhteh). 2017;19(3):434.

20. Olivares A, Alcaraz-Saura M, Achel DG, Berná-Mestre J de D, Alcaraz M. Radiation-Induced Bystander Effect: Loss of Radioprotective Capacity of Rosmarinic Acid In Vivo and In Vitro. Antioxidants. 2021;10(2):231.

21. Price P, McMillan TJ. Use of the tetrazolium assay in measuring the response of human tumor cells to ionizing radiation. Cancer research. 1990;50(5):1392–1396.

22. Gonzalez RJ, Tarloff JB. Evaluation of hepatic subcellular fractions for Alamar blue and MTT reductase activity. Toxicology in vitro. 2001;15(3):257–259.

23. Bernas T, Dobrucki J. Mitochondrial and nonmitochondrial reduction of MTT: Interaction of MTT with TMRE, JC-1, and NAO mitochondrial fluorescent probes. Cytometry: The Journal of the International Society for Analytical Cytology. 2002;47(4):236–242.

24. Surin AM, Sharipov RR, Krasil'nikova IA, Boyarkin DP, Lisina OY, Gorbacheva LR, Avetisyan A V, Pinelis VG. Disruption of functional activity of mitochondria during MTT assay of viability of cultured neurons. Biochemistry (Moscow). 2017;82(6):737–749.

25. Tse W-P, Che C-T, Liu K, Lin Z-X. Evaluation of the anti-proliferative properties of selected psoriasis-treating Chinese medicines on cultured HaCaT cells. Journal of ethnopharmacology. 2006;108(1):133–141.

26. Yu J, Kim AK. Effect of taurine on antioxidant enzyme system in B16F10 melanoma cells. In: Taurine 7. Springer; 2009. p. 491–499.

27. Zhang L, Zheng Y, Deng H, Liang L, Peng J. Aloperine induces G2/M phase cell cycle arrest and apoptosis in HCT116 human colon cancer cells. International journal of molecular medicine. 2014;33(6):1613–1620.

28. Margis R, Dunand C, Teixeira FK, Margis-Pinheiro M. Glutathione peroxidase family - An evolutionary overview. FEBS Journal. 2008. doi:10.1111/j.1742-4658.2008.06542.x

29. Wendel A. Glutathione Peroxidase. Methods in Enzymology. 1981. doi:10.1016/S0076-6879(81)77046-0

30. Pendyala S, Natarajan V. Redox regulation of Nox proteins. Respiratory Physiology and Neurobiology. 2010. doi:10.1016/j.resp.2010.09.016

31. Lambeth JD, Kawahara T, Diebold B. Regulation of Nox and Duox enzymatic activity and expression. Free Radical Biology and Medicine. 2007. doi:10.1016/j.freeradbiomed.2007.03.028

32. Liu L, Xie H, Chen X, Shi W, Xiao X, Lei D, Li J. Differential response of normal human epidermal keratinocytes and HaCaT cells to hydrogen peroxide-induced oxidative stress. Clinical and Experimental Dermatology: Experimental dermatology. 2012;37(7):772–780.

33. Salem I Ben, Boussabbeh M, Bacha H, Abid S. Dichlorvos-induced toxicity in HCT116 cells: involvement of oxidative stress and apoptosis. Pesticide biochemistry and physiology. 2015;119:62–66.

34. Kryston TB, Georgiev AB, Pissis P, Georgakilas AG. Role of oxidative stress and DNA damage in human carcinogenesis. Mutation Research - Fundamental and Molecular Mechanisms of Mutagenesis. 2011;711(1–2):193–201. http://dx.doi.org/10.1016/j.mrfmmm.2010.12.016. doi:10.1016/j.mrfmmm.2010.12.016

35. Denat L, Kadekaro AL, Marrot L, Leachman SA, Abdel-Malek ZA. Melanocytes as instigators and victims of oxidative stress. Journal of Investigative Dermatology. 2014. doi:10.1038/jid.2014.65

36. Brenner M, Hearing VJ. The protective role of melanin against UV damage in human skin. Photochemistry and Photobiology. 2008. doi:10.1111/j.1751-1097.2007.00226.x

37. Jacobson ES, Tinnell SB. Antioxidant function of fungal melanin. Journal of Bacteriology. 1993. doi:10.1128/jb.175.21.7102-7104.1993

38. Mothersill C, Le M, Rusin A, Seymour C. BIOPHOTONS in RADIOBIOLOGY: INHIBITORS, COMMUNICATORS and REACTORS. Radiation Protection Dosimetry. 2019;183(1–2). doi:10.1093/rpd/ncy271

39. Le M, Mothersill CE, Seymour CB, Rainbow AJ, McNeill FE. An Observed Effect of p53 Status on the Bystander Response to Radiation-Induced Cellular Photon Emission. Radiation Research. 2017;187(2):169–185. http://www.bioone.org/doi/10.1667/RR14342.1. doi:10.1667/RR14342.1

Chapter 9

Inner mitochondrial membrane polarization following exposure to biophotons and hydrogen peroxide

Abstract: Mitochondria are multifaceted organelles that fulfill a range of functions in the eukaryotic cell. Their relevance to cell signalling, metabolism, and place in radiation responses is reviewed. The JC-1 assay was used to assess inner mitochondrial membrane polarization in both bystander reporters receiving biophotons from directly irradiated cultures and cells exposed to hydrogen peroxide. An obvious threshold dose for effects in HCT116 is apparent around 35 µM of hydrogen peroxide. HaCaT cells did not exhibit mitochondrial depolarization at any dose between 0-50 µM, while B16F10 cells did but inconsistently across doses. Both HaCaT and HCT116 bystander reporters exhibit a decrease in mitochondrial membrane polarization, while B16F10 cells do not. This indicates again that melanin may protect cells from the electromagnetic bystander signal, and that the mechanism involved in attenuating damage upon generation of ROS may be complex.

9.1. Introduction

The mitochondrion is an oft-referenced subcellular "powerhouse" or "factory" wherein eukaryotic cells generate much of their adenosine triphosphate (ATP) reserve. ATP effectively shuttles usable energy for work around the cell and is recognized in the literature as a major "energy currency" in the cell. However, this description also tends oversimplify the incredibly diverse role that mitochondria play in the cell, which includes catabolism, anabolism, anaplerosis, and signaling. The mitochondrion is a double membrane-bound organelle with a small circular genome and a wide array of associated mitochondrial proteins—both of nuclear and native origins—that function to carry out assorted tasks, from constituting membrane transporters to dismutation of ROS to electron shuttling to oxidative phosphorylation. A good overview of the mitochondrion, as well as its sensitivities to various types of radiation, is outlined in Kam et al. (2013)[1].

As discussed in Rusin & Murphy (*in preparation*) and other publications[2], mitochondria exist at a signaling "terminus" of sorts. Mitochondria influence the fate of a cell through several mechanisms. The most obvious form of control exists in the generation of usable energy for biochemical reactions around the cell. Progression to the mitochondrial electron transport chain can be influenced at several points in the classical catabolism of glucose; notably, the activity of mitochondrial enzymes is crucial in the processing of metabolites generated from glucose. Pyruvate dehydrogenase, for example, converts pyruvate, NAD+, and coenzyme A into acetyl-CoA and NADH. Acetyl-CoA can enter the citric acid cycle to generate citrate in a reaction with oxaloacetate; acetyl-CoA can also be generated through the β-oxidation of fatty acids, which occurs within the mitochondrion. NADH, which is generated in greatest quantities in the citric acid cycle, enters the electron transport chain by donating two electrons to respiratory Complex I, which eventually passes the electrons to ubiquinone (creating ubiquinol). Complex I moves four protons across the membrane to create a proton gradient. Notably, electron leakage to oxygen is known to occur at Complex I, which leads to the formation of superoxide. At Complex II, succinate is dehydrogenated (generating fumarate) and additional electrons are donated to the ubiquinone, with no additional protons transported to the intermembrane space. Complex III removes two electrons from ubiquinol and then transfers those to cytochrome c, a second electron carrier. Two additional protons are translocated by complex III to the intermembrane space. Complex IV, or cytochrome c oxidase, removes electrons from cytochrome c and reduces diatomic oxygen to water. An additional four protons are moved into the intermembrane space by Complex IV. Finally, chemiosmotic coupling occurs where Complex V allows passage of protons back to the matrix. This efflux from the intermembrane space releases free energy and allows the synthesis of ATP from ADP and Pi. Through these processes, mitochondria essentially control the bulk of energy generated in a cell.

Mitochondria also influence apoptotic signaling. While extrinsic induction of apoptosis may occur upon ligand binding to cell membrane receptors, the intrinsic apoptotic pathway in mammalian cells is governed by mitochondria. The BCL2 pathway describes the interaction of a set of mitochondrial-associated proteins that either promotes or reduces apoptotic signaling. Typically, cytochrome c binds to cardiolipin in the inner mitochondrial membrane, which prevents its accidental release out of mitochondria. Upon generation of mitochondrial ROS that typically occurs prior to apoptosis, oxidative changes to mitochondrial membrane lipids, such as cardiolipin, weaken the interaction between cytochrome c and the membrane causing cytosolic release. Pro-apoptotic members of the BCL2 family, including Bax and Bak, promote apoptosis by inducing outer mitochondrial membrane permeabilization, allowing the release of ROS and cytochrome c. Cytochrome c binds to Apaf-1, which initiates the programmed cell death pathways with various caspases as effectors. Therefore, mitochondria are very important in the regulation of bioenergetics, general metabolism, cell fate determination, and broader cell signaling.

In terms of pertinence to radiobiology, mitochondria are a key consideration for both targeted and non-targeted effects. As discussed in chapter 2, attempts to justify the various cell survival models under target theory typically describe nuclear DNA damage, the quantity of lesions generated, and sometimes repair mechanisms that affect reproductive cell survival. However, most classical models eschew the mitochondrion and its genome as biologically relevant sources of targets—which is perplexing given its importance and centrality in many functions in eukaryotic cells. However, unlike nuclear DNA—of which two copies exist in diploid organisms—mitochondrial DNA and inheritance cannot be adequately described in the language of Mendelian genetics. Indeed, there are many issues in incorporating mitochondria in target theory, which chiefly stem from the fact that mitochondrial stasis, distribution, and dynamics are complicated. To start, the number of genome copies within a mitochondrion can vary. For a given cell type, the quantity of mitochondria in each cell varies; moreover, between cell types, mitochondrial numbers can be vastly different. Although target theory does not usually consider transgenerational effects, mitochondrial inheritance proceeds in a matrilinear fashion almost exclusively in humans and is therefore distinct from nuclear DNA, which can recombine. However, there is some evidence that mitochondria may "exchange" copies of their genomes between one another. Additionally, because so many copies of the genome exist in a cell, dosage effects are typically important. Finally, mitochondria also coordinate division and even fusion independently of the cell. These organelles can be found dispersed throughout the cytoplasm, or sometimes in more ordered networks. Therefore, it is very difficult to account for targeted mitochondrial effects. Be this as it may, because of their ubiquity, the mitochondrion is a substantial target or set of targets upon direct radiation exposure. The matter is complicated further by non-targeted effects.

As previously described, mitochondrial bystander effects are well known in the literature. Nugent et al.[3] found that bystander factors present in medium produced a significant increase in mitochondrial mass and reduced oxygen consumption rates in both human (HPV-G) and Chinese hamster (CHO-K1) cells. Maguire et al.[4] demonstrated dose-dependent effects in HPV-G reporters, finding an increase in BCL2 expression at low donor doses and significantly increased expression at high doses. Olwell et al. found a change in mitochondrial morphology and production of ROS in primary cultures of rainbow trout skin follow exposure to both direct gamma radiation and bystander factors[5,6]. It was also shown that a novel deletion in mitochondrial genome occurred following exposure to ICCM from donors irradiated at 0.5 Gy[7]. Both ICCM[3,8] and biophotons[9] have been shown to induce loss of oxidative phosphorylation. Recovery from ICCM treatment occurs inconsistently between 12–96 hours following treatment[8]. Additional work has shown that the signaling pathways modulated in bystander cells occur upstream of potential mitochondrial signaling[10–12], which include the MAPK pathway and p53. Medium from irradiated cells is known to induce apoptotic signaling in unirradiated cells, with increases in ROS occurring approximately 6 hours after medium transfer[13]. Due to these findings and others, it was considered important to assess the effects that exogenous administration of ROS and biophotons have on cells in the present thesis.

The JC-1 probe has been used extensively to investigate mitochondrial effects, and this is no exception in the context of bystander effect research. This probe provides an indication of the status of oxidative phosphorylation, or generally mitochondrial carbohydrate and/or fatty acid catabolism, after a treatment. Although it is recognized that the status of oxidative phosphorylation is only one limited aspect of mitochondrial activity in bystander effects, it was nonetheless important to determine whether biophotons and hydrogen peroxide could induce the loss of oxidative phosphorylation. Additionally, when used together with the MTT assay, the JC-1 assay provides a better picture of the overall metabolic processes occurring in the cell population and how this changes with the addition of hydrogen peroxide or with biophoton exposure.

9.2. Methods

9.2.1. JC-1 assay

The JC-1 assay has been used extensively previously to measure inner mitochondrial membrane potential. 5,5,6,6'-tetrachloro-1,1',3,3'-tetraethylbenzimi-dazoylcarbocyanine iodide (JC-1) is a membrane-permeable, dual emission, fluorescent dye that localizes to and accumulates in cellular mitochondria. In its unbound monomeric form, JC-1 fluoresces green upon excitation (λ_{EX} / λ_{EM} = 488 nm/ 527 nm). The dye accumulates in viable, respiring mitochondria and forms aggregates that fluoresce red upon excitation (λ_{EX} / λ_{EM} = 488 nm/ 590 nm). Under stressful conditions where inner membrane potential is lost—including situations involving apoptotic signaling and mitochondrial membrane permeability, reduced oxidative phosphorylation, and so on—the aggregates dissociate, and JC-1 fluoresces green in its monomeric form. Following fluorometric measurement, the ratio of red to green fluorescence, typically provided in relative fluorescence units, can be used as an indicator of cell health and status of oxidative phosphorylation; differential JC-1 measurements are associated with apoptotic signaling, the generation of mitochondrial ROS, and compromised oxidative phosphorylation.

Initially, the procedure for the JC-1 assay was optimized and adapted from the MitoPT® JC-1 Assay Kit Manual enclosed a kit by ImmunoChemistry Technologies (document: #F18-911-1-E). This procedure was used for HCT116 cells treated with hydrogen peroxide, however a significant trend was not observed with increasing dose (see supplementary figure 9.1). A similar procedure was adapted for adherent cells in Rusin et al. (2019)[14] and was used for the remainder of this chapter following these considerations. This was also done in the hope of observing a dose-dependent relationship.

On the day of subculture, 100 000 cells were seeded in each well of a 96 well plate for those cells destined to receive hydrogen peroxide. Those destined for biophoton exposure were seeded at a density of 50 000 cells two days prior to the assay. The cell loading procedure followed was similar between the two treatments, and the entire assay was conducted under minimal lighting conditions. A 400x JC-1 solution, which had been suspended in DMSO and stored in a -20 degrees Celsius freezer protected from light, was diluted in an appropriate volume of DPBS to create a loading buffer solution. Medium was removed from the cells and each well was washed once with 150 µL fresh DPBS at ambient temperature. 200 µL of loading buffer was placed in each well containing cells in addition to those containing the appropriate controls. The plate was incubated protected from light at standard culture conditions for 25 minutes. The loading buffer was then removed, and cells were washed a second time with 150 µL fresh DPBS. 200 µL new DPBS was then added to each well. 2 µL of carbonyl cyanide m-chlorophenyl hydrazone (CCCP), included in the kit as a positive control for inner mitochondrial membrane depolarization, was added to appropriate wells at this stage. The plate was then incubated for an additional 10 minutes before fluorescence was promptly quantified at a Tecan 200m Pro plate reader using the incident and emission wavelengths described above.

9.2.2. Peroxide treatment

Cells were treated with hydrogen peroxide exactly as in Chapter 8. On the day of an experiment, cultures were treated with hydrogen peroxide prior to staining with JC-1. Section 6.2.1 describes the dilution of a 3% hydrogen peroxide stock to yield a working solution that was similarly included in this chapter in each well of a 96-well plate. Briefly, medium was removed from each well and cells were washed once in 150 µM DPBS. 200 µM fresh cell culture medium was then included in each well. An appropriate volume of hydrogen peroxide working solution was then added in each well for a final concentration of interest. Cells were then incubated for 1 hour at standard culture conditions. Following this period, the peroxide-infused medium from each well was discarded and cells loaded with JC-1 as described previously.

9.2.3. Biophoton exposure

Cell reporters were treated similarly in this chapter to Chapters 7 and 8—this procedure is almost identical to the one found in Chapter 8. Cells were initially seeded on the day of subculture as previously described. The cells seeded in the 96-well plate were destined to receive biophoton signals from biophoton donors. On the same day, T25 flasks were seeded at 2000 cells/cm^2 and provided with 10 mL complete growth medium; these acted as biophoton donors. The next day, 857.5 µCi of tritium was added to donor cultures. Control flasks were included where donors were supplemented with the same volume of DPBS. The T25 flasks were placed directly superior to wells in the 96-well plate intended to receive biophoton signals in an arrangement that included 2 T25 flasks on 1 96-well plate. Together, these vessels were placed in a light-tight metal container. This container was incubated at standard culture conditions for 24 hours to yield a donor dose of 0.5 Gy; the method for tritium dose calculations is available in Chapter 2. Following this time period, donor cultures were discarded, and cells immediately loaded with JC-1 dye as described above.

9.2.4. Statistical analysis

Data was obtained in relative fluorescence units initially for both the red and green signal. Background fluorescence measurements were gathered from wells containing no cells; the average of these values was subtracted from measurements for each well, for red and green fluorescence, respectively. These measurements were then normalized to negative control wells, or those containing loaded cells but not exposed to hydrogen peroxide or biophotons, and the data were presented as relative mitochondrial membrane potential ($\Delta\Psi_{mn}$) in arbitrary units.

The data were graphed in Graphpad Prism 7, and statistical tests were conducted in this software as well. The data are presented as average values for data points and error is presented as standard deviation in all figures—4 technical replicates for 2 biological replicates (n=8) in hydrogen peroxide-treated groups were used, while at least 10 technical replicates for 3 biological replicates (n=30) were used for cells receiving biophoton treatment. One-way ANOVA followed by Tukey's Honestly Standard Difference (HSD) test at α=0.05 was performed for each set of data. These data were presented both as average values on a bar graph and box-and-whisker plots to better visualize data distribution.

9.3. Results

9.3.1. Peroxide results

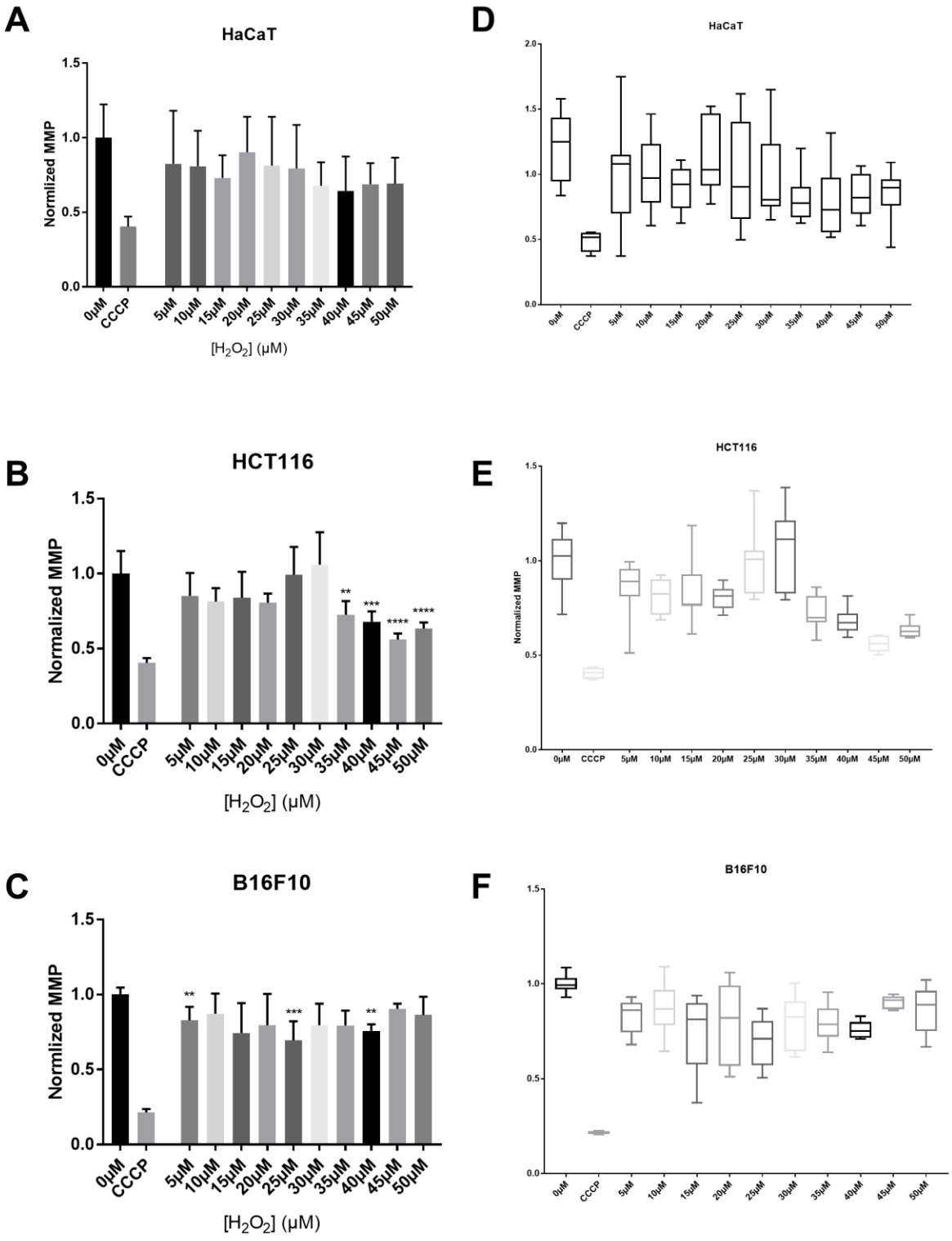

Figure 9.1: The normalized mitochondrial membrane potential ($\Delta\Psi_{mn}$ or MMP) of three cell lines plotted along with hydrogen peroxide concentration, with a positive control for depolarization (CCCP). The bar

and box-and-whisker plots represent the same data. Significance is denoted by asterisks at α=0.05 (*p<0.05; **p<0.01; ***p<0.001; ****p<0.0001).

Figure 9.1 shows the data obtained from hydrogen peroxide-treated cells. The positive control (CCCP) indicates mitochodnrial membrane depolarization, while the negative control (0 µM) shows no hydrogen peroxide treatment. No trend was calculated for these data, as a true dose response in this dose range could not be ascertained.

In HaCaT cells, doses between 0–50 µM did not induce a significant change in mitochodnrial membrane polarization. In HCT116 cells, a threshold for the effect appeared to be 35 µM, as all dose points greater than this produced a significant reduction in mitochondrial membrane polarization. In B16F10, membrane depolarization can be observed even at the 5 µM dose, however this trend does not continue obviously with increasing dose.

The distribution of the data was broadest in HaCaT, however the majority of the data points indicate that membrane polarization is not peturbed by doses between 0–50 µM. In HCT116, a tighter distribution after 30 µM shows a more uniform response to higher doses across cultures. In B16F10, the data are similar in their distribution to HCT116, however significant results are apparent only at some doses and hence the effect is not invariably comensurate with dose.

In every cell line, treatment with the positive control produced a significant reduction membrane polarization—the magnitude of this reduction was not ontained through hydrogen peroxide supplmentation at any dose for any of the cell lines used in this study. Moreover, significant results in both HCT116 and B16F10 are related to the degree of distribition observed in the control and each test group, with those data sets exhibiting lower varience tending towards statistical significance.

9.3.2. Biophoton results

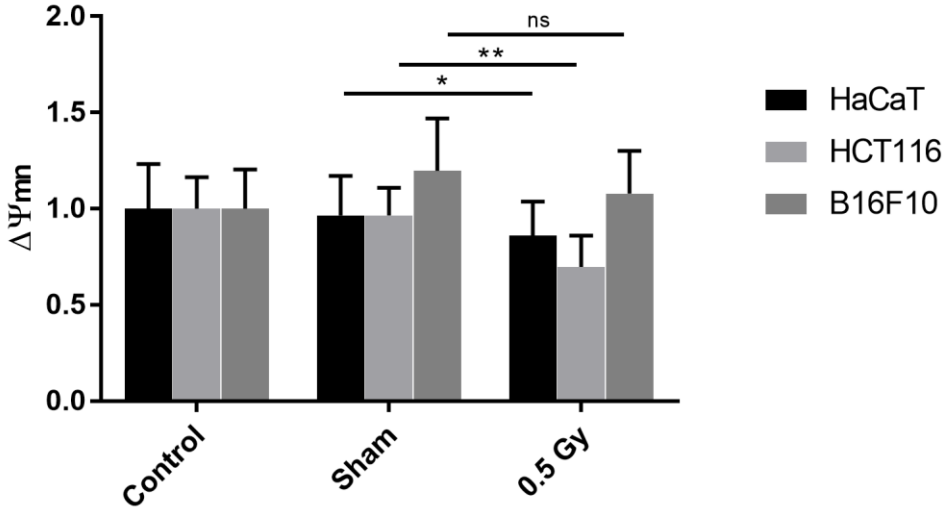

Figure 9.2: The normalized mitochondrial membrane potential in bystander reporters incubated with biophoton donors. The x axis indicates donor treatments similarly to previous chapters.

Figure 9.2 shows mitochondrial membrane polarization following biophoton exposure in HaCaT, HCT116, and B16F10 cells. At the 0.5 Gy donor dose point, HaCaT and HCT116 reporters show a significant ($p<0.0001$; $=0.035$) reduction in mitochondrial membrane polarization compared to the sham dose. B16F10 control and sham doses were insignificantly different from the 0.5 donor dose ($p=0.152$; 0.071).

9.4. Discussion

Variation is an important parameter to describe when using the JC-1 assay for a number of reasons[15]. Mitochondrial membrane potential can vary between cells in a population, and even mitochondria in the same cell may exhibit different electrochemical potentials across their membranes. It follows that a reduction in variance may indicate a conserved or more uniform response to a treatment. Reduced cell number due to death in these groups may have skewed the overall distribution of the data, although it is believed that this is unlikely because the deviation was observed to generally be lower than control groups.

These results indicate that hydrogen peroxide can affect mitochondrial metabolism in some cells at higher doses. Mitochondrial DNA is also susceptible to ROS[16]. HaCaT does not appear to exhibit significant mitochondrial effects at the doses used. This does not mean that mitochondrial membrane depolarization does not occur at higher doses beyond those used in this chapter, only that their mitochondria do not respond to the same doses as HCT116. HCT116 mitochondria show a consistent reduction in inner membrane potential from 35 µM and up. This indicates that hydrogen peroxide at these concentrations can significantly affect mitochondrial metabolic viability. In B16F10, mitochondria appear to depolarize inconsistently depending on dose with no obvious trend.

Based on these results, one would predict that cell death due to oxidative stress may occur with mitochondrial signaling as an effector in HCT116 cells. This directly demonstrates that oxidative stress can induce mitochondrial phenomena, likely related to the reduction in activity of respiratory Complex I, as described in previous research in HCT116 bystander cells[9]. In HaCaT cells, oxidative stress does not appear to produce a response in mitochondria that may affect cell survival, at least in doses up to 50 µM. Instead, in these cells, cell killing due to receipt of the bystander response may be dependent on other mechanisms, such as ROS interacting with “biological machinery” including membrane lipids, enzymes, and DNA. In B16F10 cells, mitochondrial depolarization appears to occur in response to oxidative stress in some doses, however this effect cannot be easily related to dose in the range used.

The data also show that biophotons can induce a reduction in mitochondrial membrane polarization in bystander reporters. This occurred in HaCaT cells and HCT116 significantly. This corroborates previous research by Le et al.[9], and further supports the idea that bystander effects are reliant on mitochondrial responses observed in previous reports from our lab[17] and others[18]. Mitochondrial depolarization is directly indicative of reduced oxidative phosphorylation, as polarization is required for this process. Therefore, the observation of complex I and V modulation[9] likely occurs at the same time. This is also a potential sign of an early apoptotic cascade in bystander cells, especially considering results from chapter 7 that indicate the upregulation of ROS in bystander cells. In B16F10, there was no induction of membrane depolarization, indicative of the ability for melanin to inhibit bystander signaling. When taken together with hydrogen peroxide results, this indicates that melanin may sequester ROS through direct antioxidant activity. Moreover, considering that membrane depolarization is not induced in HaCaT by hydrogen peroxide, yet is by biophotons, that the early events in the bystander cascade involve processes outside of generation of ROS. Furthermore, results from chapter 5 and previous findings[19] indicate that melanin absorbs biophotons as well.

9.6. Conclusion

The treatment of cells with hydrogen peroxide was assessed by a fluorescence assay for inner mitochondrial membrane polarization. HaCaT was not found to exhibit membrane depolarization at any ROS dose. HCT116 showed a threshold peroxide dose that induced membrane depolarization, while B16F10 showed inconsistent depolarization between doses. Both HCT116 and HaCaT bystanders exhibited mitochondrial membrane depolarization, however B16F10 did not. This confirms previous findings and further demonstrates that melanin acts as a radioprotector in the context of the physical bystander signal.

9.7. References

1. Kam WW-Y, Banati RB. Effects of ionizing radiation on mitochondria. Free Radical Biology and Medicine. 2013;65:607–619.

2. Vakifahmetoglu-Norberg H, Ouchida AT, Norberg E. The role of mitochondria in metabolism and cell death. Biochemical and biophysical research communications. 2017;482(3):426–431.

3. Nugent SME, Mothersill CE, Seymour C, McClean B, Lyng FM, Murphy JEJ. Increased mitochondrial mass in cells with functionally compromised mitochondria after exposure to both direct gamma radiation and bystander factors. RADIATION RESEARCH. 2007;168(1):134–142. doi:10.1667/RR0769.1

4. Maguire P, Mothersill C, Seymour C, Lyng FM. Medium from irradiated cells induces dose-dependent mitochondrial changes and BCL2 responses in unirradiated human keratinocytes. RADIATION RESEARCH. 2005;163(4):384–390. doi:10.1667/RR3325

5. O'Dowd C, Mothersill CE, T Cairns M, Austin B, McClean B, Lyng FM, Murphy JEJ. The release of bystander factor(s) from tissue explant cultures of rainbow trout (Onchorhynchus mykiss) after exposure to gamma radiation. RADIATION RESEARCH. 2006;166(4):611–617. doi:10.1667/RR0606.1

6. Olwell PM, Lyng FM, Seymour CB, Mothersill C, Cottell CD. Ultrastructural effects of ionising radiation on primary cultures of rainbow trout skin. 2003.

7. Murphy JEJ, Nugent S, Seymour C, Mothersill C. Mitochondrial DNA point mutations and a novel deletion induced by direct low-LET radiation and by medium from irradiated cells. MUTATION RESEARCH-GENETIC TOXICOLOGY AND ENVIRONMENTAL MUTAGENESIS. 2005;585(1–2):127–136. doi:10.1016/j.mrgentox.2005.04.011

8. Nugent S, Mothersill CE, Seymour C, McClean B, Lyng FM, Murphy JEJ. Altered mitochondrial function and genome frequency post exposure to gamma-radiation and bystander factors. International journal of radiation biology. 2010;86(February 2017):829–41. doi:10.3109/09553002.2010.486019

9. Le M, McNeill FE, Seymour CB, Rusin A, Diamond K, Rainbow AJ, Murphy J, Mothersill CE. Modulation of oxidative phosphorylation (OXPHOS) by radiation- induced biophotons. Environmental Research. 2018;163:80–87. doi:10.1016/j.envres.2018.01.027

10. Mothersill C, Rusin A, Seymour C. Relevance of non-targeted effects for radiotherapy and diagnostic radiology; A historical and conceptual analysis of key players. Cancers. 2019. doi:10.3390/cancers11091236

11. Lyng FM, Maguire P, McClean B, Seymour C, Mothersill C. The involvement of calcium and MAP kinase signaling pathways in the production of radiation-induced bystander effects. RADIATION RESEARCH. 2006;165(4):400–409. doi:10.1667/RR3527.1

12. Le M, Mothersill CE, Seymour CB, Rainbow AJ, McNeill FE. An Observed Effect of p53 Status on the Bystander Response to Radiation-Induced Cellular Photon Emission. Radiation Research. 2017;187(2):169–185. http://www.bioone.org/doi/10.1667/RR14342.1. doi:10.1667/RR14342.1

13. Lyng FM, Seymour CB, Mothersill C. Oxidative stress in cells exposed to low levels of ionizing radiation. BIOCHEMICAL SOCIETY TRANSACTIONS. 2001;29(2):350–353.

14. Rusin A, Lapied E, Le M, Seymour C, Oughton D, Haanes H, Mothersill C. Effect of gamma radiation on the production of bystander signals from three earthworm species irradiated in vivo. Environmental

Research. 2019;168. doi:10.1016/j.envres.2018.09.023

15. Reers M, Smiley ST, Mottola-Hartshorn C, Chen A, Lin M, Chen LB. Mitochondrial membrane potential monitored by JC-1 dye. Methods in Enzymology. 1995;260:406–417.

16. Park J, Zhuang J, Li J, Hwang PM. p53 as guardian of the mitochondrial genome. FEBS letters. 2016;590(7):924–934.

17. Nugent S, Mothersill CE, Seymour C, McClean B, Lyng FM, Murphy JEJ. Altered mitochondrial function and genome frequency post exposure to gamma-radiation and bystander factors. INTERNATIONAL JOURNAL OF RADIATION BIOLOGY. 2010;86(10):829–841. doi:10.3109/09553002.2010.486019

18. Ariyoshi K, Miura T, Kasai K, Fujishima Y, Nakata A, Yoshida M. Radiation-Induced Bystander Effect is Mediated by Mitochondrial DNA in Exosome-Like Vesicles. Scientific reports. 2019;9(1):9103. doi:10.1038/s41598-019-45669-z

19. Le M, McNeill FE, Seymour C, Rainbow AJ, Mothersill CE. An observed effect of ultraviolet radiation emitted from beta-irradiated HaCaT cells upon non-beta-irradiated bystander cells. Radiation research. 2015;183(3):279–90. http://www.bioone.org/doi/10.1667/RR13827.1%5Cnhttp://www.ncbi.nlm.nih.gov/pubmed/25710575. doi:10.1667/RR13827.1

Chapter 10

Attempts to model bystander photon exposure responses in reporters using an artificial source

Abstract: The contribution of ultraviolet-A light (UVA) to biological effects in recipients of the physical bystander signal can be assessed and modelled via the exposure of cells to light from an artificial source. This has some advantages to biophoton exposure, mostly in the control of experimental variables. Both HaCaT and HCT116 were exposed to UVA from a lamp, and formation of ROS and metabolic activity was determined. Both cell lines did not exhibit oxidative stress following 30 minutes of exposure to UVA, however a significant reduction in aerobic metabolic activity was found. This implies that mitochondrial effects are important in cellular responses to long-wave ultraviolet light and that generation of ROS may be a delayed effect in exposure to both biophotons and UVA from abiotic sources. Biophotons could also potentially be caused due to stress induced by ROS, although we did not find evidence of this in the present thesis. Future directions are suggested for research, with an emphasis on UV dosimetry and follow-up experiments in bystander reporters.

10.1. Introduction

As described in previous chapters, we are routinely exposed to photons in the ultraviolet range. It is known that both UVA and UVB light can induce a variety of effects in human skin, including tanning[1], indirect and direct DNA damage[2–4], and heating. These effects are demonstrably linked to the generation of oxidative stress and free radicals such as hydrogen peroxide[2,5], which impart biological damage by virtue of their reactivity. Further and similarly, it was shown in chapter 7 that biophotons can induce oxidative stress in reporter cells, characteristic of ultraviolet exposure. Currently, it is suspected that photons in the ultraviolet range promote bystander responses through mechanisms similar to general UV exposure.

Ultraviolet light is not only implicated in physical bystander responses. Lethal mutations occur in HaCaT cells exposed to UVA and UVB light and both induce reproductive cell death at appropriate doses (3000-9000 J/m^2)[6]. Further work by Whiteside and McMillan[7] found a bystander effect that was induced by UVA but not UVB in HaCaT cells. UVA and UVB, after donor exposure, were found to produce more pronounced bystander responses in reporters than UVC[8]. Moreover, ROS was found to be elevated in these bystander cells. Zanchetta et al.[9] found that simulated sunlight irradiation of keratinocytes causes elevated ROS, and that this effect was dependent on cell density. Moreover, they found an increase in mitochondrial mass with low doses, while higher doses caused a decrease in mitochondrial mass.

Since previous reports showed that cells emit photons upon exposure to radiation, the question arose whether photons from an artificial source can induce similar bystander responses in cells. It is known that many spectra of light can be emitted from directly irradiated cells[10–12]. It is also suspected, based on findings in the literature[13], that most of the biological effect can be abrogated by blocking ultraviolet photons. Because of these observations, we sought to determine whether photons from an artificial source can produce similar effects.

There are several advantages in performing these experiments together with bystander experiments, where the source of the photons is biological. Probably most significantly, many experimental parameters can be known and modified to suit what is being modelled. Key factors such as intensity of light, energy, and consistency of emission can be controlled for using an ultraviolet lamp, or several ultraviolet lamps. Dose can be effectively modified both as a result of a decreased dose rate—related to the intensity of the light emitted or distance to the sample—or kept consistent within an experiment. It would also be easier to discriminate between effects that may be due to different wavelengths of light, or determine if synergistic or antagonistic effects occur depending on different wavelength combinations.

As discussed in chapter 1, ultraviolet-A light is not considered ionizing, however there is no exact demarcation because different molecules have different ionization energies. A major phenomenon of ultraviolet and other traditionally “less-than-ionizing” frequencies are thermal effects, where the energy of the photons is converted to the kinetic energy of particles in biological matter. However, other, non-thermal effects have been reported in much lower-energy frequencies by some sources[14,15]. Temperature was therefore important to monitor in exposed cell cultures to ensure that cell death was not induced by excessive heating.

The purpose of experiments in this chapter were to model ultraviolet light exposure in human epithelial cells using an artificial source. An ultraviolet lamp was used and an assay for induction of oxidative stress was performed. Temperature following exposure was then assessed over 1 hour. Finally, cells exposed to

ultraviolet light from the lamp were assessed using Alamar Blue for metabolic activity as an indirect measure of cell viability and proliferative potential.

10.2. Methods

10.2.1. UVA Irradiation and DCF-DA Assay

To determine the induction of potential bystander-like effects, ROS was used as an endpoint in this chapter initially. This was done with the hope of expanding experiments to other assays, such as the clonogenic survival and MTT assays. Cells were exposed in complete growth medium without phenol red to prevent absorption of the UVA rays.

Prior to irradiating cells and exposing reporter cells to biophotons, UVA radiation from a lamp was used to simulate this secondary exposure. The lamp that was used is a Spectroline SL-3660. The lamp has an emission maximum of 366 nM, which corresponds to mostly UVA. Direct dosimetry was not performed for this chapter—exposure times and lamp distance to the culture remained consistent between exposures for a "proof of concept" prior to rigorous experimentation. The dose delivered to the cells can be estimated two ways, which give similar results.

Blacklight bulbs usually have a power efficiency between 5-15%. The bulb uses 4W of power, so therefore it can be assumed that the bulb emits between 0.2-0.6W across its surface area. The whole surface area of the lamp that emits UV light is approximately 3.2 cm x 8.5 cm (27.2 cm^2 or 2.72x10^{-3} m^2). If this output of "useful" energy as UV is assumed, then approximately 360-1080 J of energy was emitted by the lamp in 30 minutes total. This means that, assuming the entire area of the lamp window was used in the cell exposure, the cells experienced between 13.2-39.7 J/cm^2 of UVA dose over the 30 minute exposure. According to the dimensions provided by Corning, the area of the wells is actually 7.58 cm^2 (Corning LSR00005 Technical Data Sheet), while the remainder of the area on the plate is not occupied by wells. Therefore, the actual dose given to the cells was between 3.68-11.04 J/cm^2.

There is a report that describes exposures using the same Spectroline SL-3660 lamp at a distance of 30 cm for 30 minutes; this exposure yielded a dose of 3550 erg/mm^2, or 355 J/m^2 [16]. The distance used in the present study was different, however. Assuming the inverse square law, the distance is reduced by a factor of 30, so ideally the energy that the cells were exposed to was 31.95 J/cm^2. However, this assumes that all of the light from the lamp was used in the exposure, while the dimensions provided by Corning show the growth area in the wells is approximately 7.58 cm^2. Therefore, the actual dose given to the cells can be estimated to be around 8.9 J/cm^2.

Using these two estimates, it is believed that the cells were exposed to approximately 9 J/cm^2 of UVA light after 30 minutes. Further validation of these estimates can be done by using a light meter, which measures irradiance, to determine the actual dose delivered to the cells.

Cells were plated at a density of 25 000 per well in 200 uL medium in a 96 well plate. Cells were exposed to UVA for 60 minutes at approximately 1 cm from the lamp, with the lamp placed inferior to the 96-well plate. Following exposure, the cells were immediately washed using DPBS twice and incubated with 25 uM loading buffer for 45 minutes. Cells were then washed three times in DPBS and taken to be read at a Tecan Infinite® 200 PRO plate reader. Other than exposure to artificial UVA, the DCFDA protocol used was identical to the one in chapter 7. The results from three independent experiments containing 8

replicates were plotted in Graphpad Prism. A Student's t-test was conducted at α=0.05 to determine significance.

10.2.2. Monitoring temperature during UVA exposure

To account for the change in temperature in the wells, a Mastercraft Digital Temperature Reader was used; temperature monitoring of the lab bench was also performed as a background measurement. Heat was monitored for a period of 30 minutes while cells were exposed to UVA. Measurements were taken from the bottom of each well, containing complete cell culture medium, following an overnight incubation period at 37°C in a cell culture incubator. Temperature measurements were also taken in a control well at room temperature on the bench. Finally, several "background" measurements were taken of the lab bench. Two independent experiments were performed with eight replicates each (n=16).

10.2.3. Alamar Blue Assay

To determine the metabolic activity of cells following UV exposure, the Alamar Blue assay was used along with measurement by a plate reader. Resazurin, a non-toxic and non-fluorescent membrane-permeable chemical, is the active ingredient in the Alamar Blue assay solution. Upon entering cells, resazurin is reduced to resorufin, which is fluorescent when excited with chartreuse light. The dye essentially measures metabolic activity in cells and is a versatile tool for determining the proliferative potential of a population of cells. The protocol was adapted from the protocol from Thermofisher Scientific for the product (cat no. DAL1025). 25 000 cells were seeded in a 96-well plate and left to grow overnight. 24 hours after cells were plated in 96 well plates containing 90 uL phenol red-free medium, cells were exposed to UVA radiation for 30 minutes as described previously. 10 uL of Alamar Blue solution was added into each well (Thermofisher Scientific, cat no. DAL1025). The cells were then incubated for one hour. Appropriate controls were included in-well, including blank wells containing 90 uL medium without cells and sham-irradiated cells stained with Alamar Blue. Following the incubation step, the plate was taken to be read at a Tecan Infinite® 200 PRO plate reader at Ex/Em = 560nm/590nm. Results from two independent experiments containing four replicates each (n=8) were plotted in GraphPad prism. A Student's t-test was conducted at α=0.05 to determine significance.

10.3. Results

The initial results from the DCFDA assay showed that no significant induction of ROS in UVA cells exposed to the lamp for 30 minutes. Figure 10.1 shows this lack of effect.

The results in figure 10.2 suggest that UVA from the lamp can raise the temperature of an exposed 96-well plate significantly. These measurements were taken in the presence of cell culture medium, however no cells. The results show a significant increase in temperature after one hour; however, after 30 minutes, the plate did not reach a temperature higher than incubation conditions (28.6 ± 0.35 °C).

In figure 10.3, Alamar blue results are shown following exposure to the UVA lamp. The results indicate that a significant reduction in metabolic activity occurs in both HCT116 and HaCaT cells following exposure to ultraviolet light.

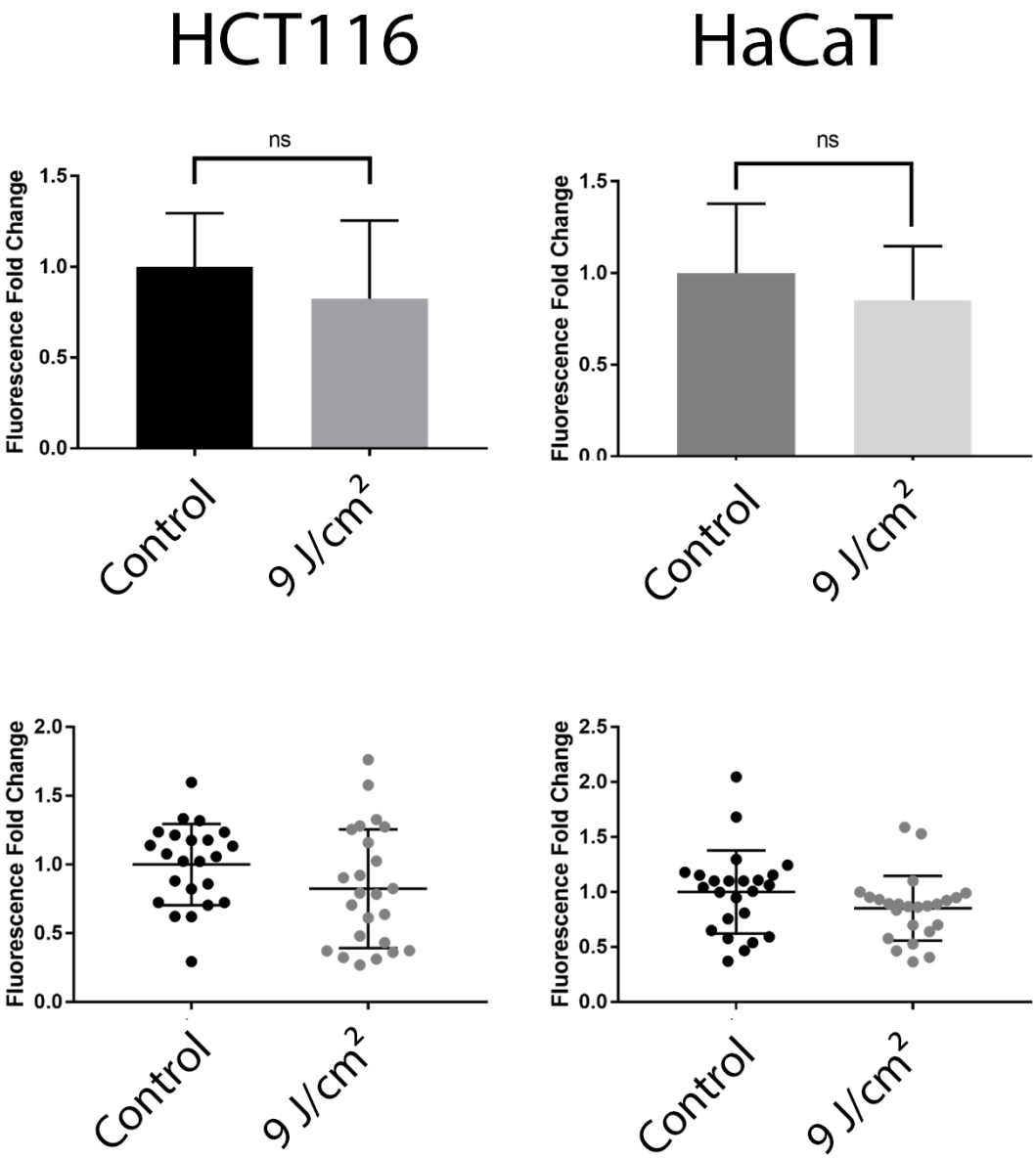

Figure 10.1: The fluorescence fold change of DCF following exposure to 30 minutes of ultraviolet light from the UVA lamp. The top graphs show means for both HCT116 and HaCaT, left and right, respectively. The bottom graphs plot individual measurements from each well and represent the same data as in the above plots. Error is shown as standard deviation of the mean in all figures.

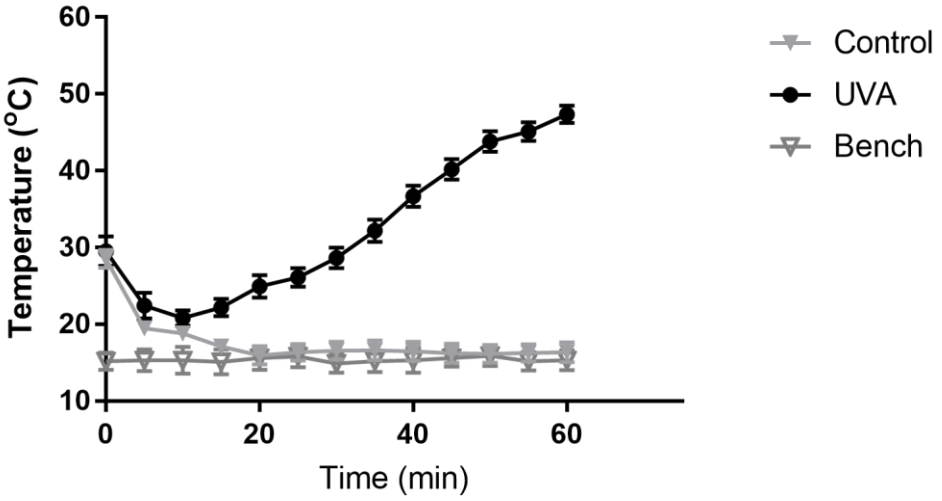

Figure 10.2: The temperature of a 96-well plate immediately following removal from a cell culture incubator. The control was a 96-well plate at room temperature. The bench measurements were taken beside the control plate. Each point indicates two independent experiments with eight replicates each, representing each exposed well (n=16). Error is standard deviation of the mean.

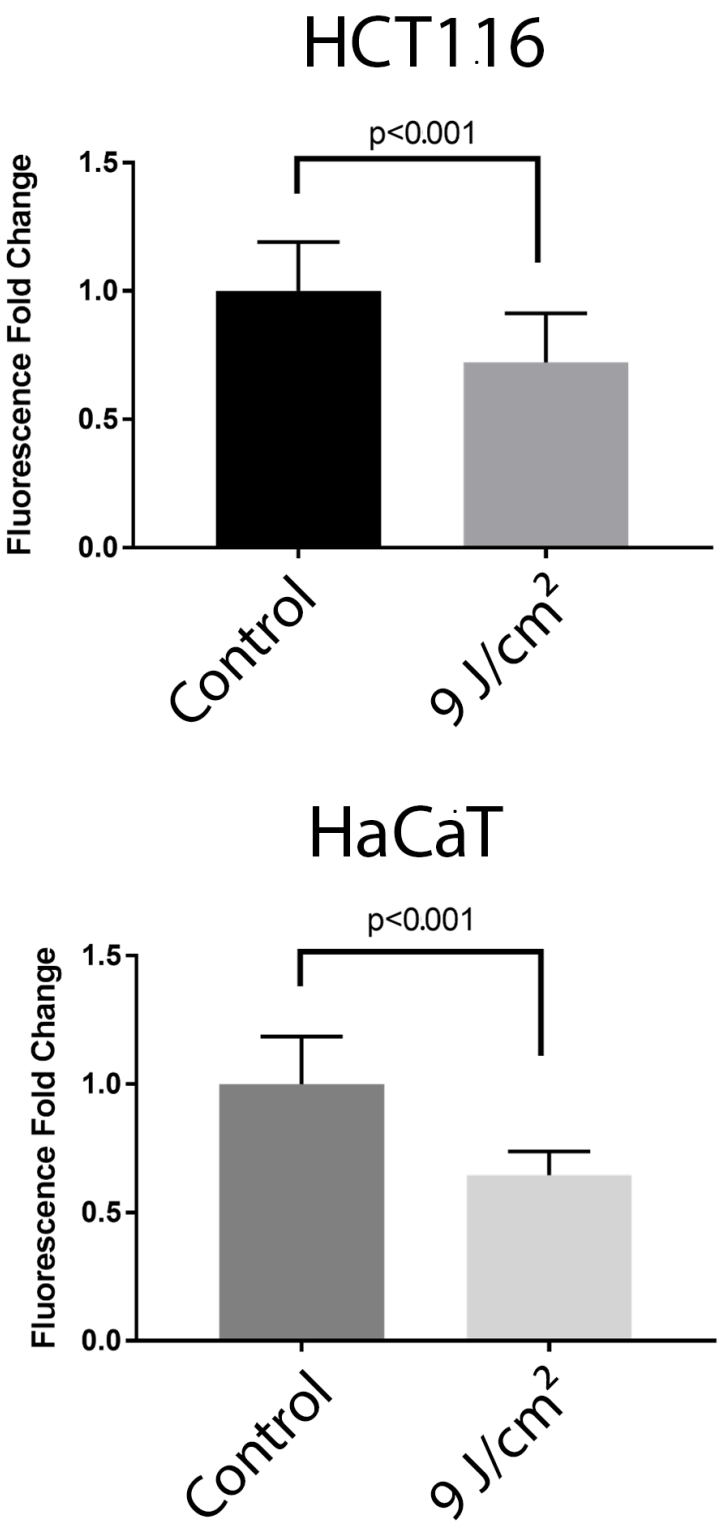

Figure 10.3: Alamar blue fluorescence following exposure to 30 minutes of UVA light exposure. Error is standard deviation of the mean. These results are from two independent experiments with 4 replicates each (n=8).

10.4. Discussion

Initially, it was expected that ultraviolet light from an artificial source would induce significant generation of ROS in both HaCaTs and HCT116 within the exposure time used in this chapter. This was based partly on results from chapter 7—where cells were exposed to photons of biological origin showed this response after 24 hours—and therefore the results shown in figure 10.1 were perplexing at first. It could be that the formation of ROS in cells exposed to ultraviolet light is delayed in some circumstances. In chapter 7, cells were exposed to biophoton signals for 24 hours, which is different from this chapter where the total time from the beginning of exposure to data collection was approximately 1 hour. Therefore, in future experiments, timeframe and dose rate may affect results. Moreover, it is recognized that dosimetry for this chapter could allow for a more informative description of the dose delivered to the cells and is thus a future direction of research. At this point, it is difficult quantify photon emissions from the ultraviolet lamp, as the photon counter described in chapter 5 experienced saturation of the scalar after approximately one second of exposure. Hence, other methods of measuring dose should be used. Moreover, to effectively model exposure to any source of radiation, it is important to properly dose cells particularly if dose responses are predicted. There are commercial devices that can measure irradiance and wavelength of light, and these may be used for dosimetry.

UVA is known to cause delayed formation of DNA lesions and ROS[17–20]. Additionally, Delayed effects were also reported by our lab after both UVA and UVB exposure, specifically lethal mutations[21]. It is therefore not unexpected that some delayed effects were suggested in this chapter.

It was also initially suspected that temperature could have killed cells exposed to ultraviolet light from the lamp, which could explain the result in figure 10.1. There are several problems with this explanation. The data in figure 10.2 do not suggest the warming of the plate such that heat shock would be induced in the cells used[22,23]. It is suspected the generation of ROS, as described above, may simply be a delayed process that requires further exposure for a significant effect to be measured. The results are also different because the assays used in this chapter differ in what is being measured. Alamar blue measures oxidation-reduction, is an indicator of mitochondrial metabolic activity, and is linked to the generation of NADH or NADPH. However, DCFDA is an indicator of the concentration of intracellular ROS in a cell. The two assays measure different endpoints, and therefore the results would be expected not to be the same.

The results in Figure 10.3 are interesting for several reasons. UVA appears to inhibit metabolism in HaCaT and HCT116, which was also found in biophoton exposures in Chapter 9; however, it also does not appear to induce reactive oxygen species at this time point. Most notably, the data indicate that UVA exposure, within the range known to be emitted by bystander cells[24], can reduce the overall metabolic activity of cell cultures rapidly. UVA and UVB are known to modulate the metabolic activity of various kinds of cells *in vitro* and *in vivo,* with differing responses depending on the cell[25–27]. It is very interesting that these effects may be based in mitochondria, as Alamar Blue measures mitochondrial metabolic activity indirectly, which may be a conserved response to ultraviolet light exposure between biophotons[28] and “conventional” exposures. This is also further evidence that metabolic effects may precede the generation of ROS in the early events following ultraviolet exposure. One potentially informative follow-up experiment could be to measure Alamar Blue fluorescence after a more chronic exposure to ultraviolet light, together with DCF fluorescence. It is expected that one would observe a significant increase in oxidative stress, as this is known to occur in other ultraviolet-exposed cells as discussed above. The Alamar Blue assay was not conducted on bystander cells in the present thesis—however, this could be useful in the future to obtain further information on bystander responses in cells receiving the electromagnetic bystander signal.

ROS was found to be an early signal in the bystander effect—several papers showed that formation of ROS causes calcium influxes and membrane signalling[29,30]. The results in the present thesis indicate that ROS are induced by exposure to bystander photons and suggest that their formation is downstream of this initial signaling event. It would be interesting to perform a follow-up study where calcium fluxes are examined in the context of physical bystander signaling.

10.5. Conclusion

The biological responses to ultraviolet-A light exposure in HaCaTs and HCT116, with photons generated using an artificial source, was assessed using an assay for oxidative stress and an assay for aerobic metabolism. Further, temperature was monitored during a simulated exposure to ultraviolet light. The results suggested no induction of ROS after 30 minutes of exposure and a significant reduction in oxidative metabolism in the cell populations. This suggests that mitochondrial and associated metabolic pathways may be affected early when cells are exposed to ultraviolet biophotons, which confirms results obtained previously in our lab[28]. In the future, would be useful to perform dosimetry for the experimental setup, perform additional assays with different endpoints, and perform the Alamar Blue metabolic assay on recipients of the electromagnetic bystander signal.

10.7. References

1. Miyamura Y, Coelho SG, Schlenz K, Batzer J, Smuda C, Choi W, Brenner M, Passeron T, Zhang G, Kolbe L. The deceptive nature of UVA tanning versus the modest protective effects of UVB tanning on human skin. Pigment cell & melanoma research. 2011;24(1):136–147.

2. Petersen AB, Gniadecki R, Vicanova J, Thorn T, Wulf HC. Hydrogen peroxide is responsible for UVA-induced DNA damage measured by alkaline comet assay in HaCaT keratinocytes. Journal of Photochemistry and Photobiology B: Biology. 2000;59(1–3):123–131.

3. Cadet J, Douki T, Ravanat J. Oxidatively generated damage to cellular DNA by UVB and UVA radiation. Photochemistry and photobiology. 2015;91(1):140–155.

4. Greinert R, Volkmer B, Henning S, Breitbart EW, Greulich KO, Cardoso MC, Rapp A. UVA-induced DNA double-strand breaks result from the repair of clustered oxidative DNA damages. Nucleic acids research. 2012;40(20):10263–10273.

5. Ciesielska S, Bil P, Gajda K, Poterala-Hejmo A, Hudy D, Rzeszowska-Wolny J. Cell type-specific differences in redox regulation and proliferation after low UVA doses. PLoS ONE. 2019. doi:10.1371/journal.pone.0205215

6. O'REILLY P, C. MOTHERSILL. Comparative effects of UV A and UV B on clonogenic survival and delayed cell death in skin cell lines from humans and fish. International journal of radiation biology. 1997;72(1):111–119.

7. Whiteside JR, McMillan TJ. A bystander effect is induced in human cells treated with UVA radiation but not UVB radiation. Radiation research. 2009;171(2):204–211.

8. Widel M, Krzywon A, Gajda K, Skonieczna M, Rzeszowska-Wolny J. Induction of bystander effects by UVA, UVB, and UVC radiation in human fibroblasts and the implication of reactive oxygen species. Free Radical Biology and Medicine. 2014;68:278–287.

9. Zanchetta LM, Kirk D, Lyng F, Walsh J, Murphy JEJ. Cell-density-dependent changes in mitochondrial membrane potential and reactive oxygen species production in human skin cells post sunlight exposure. Photodermatology, photoimmunology & photomedicine. 2010;26(6):311–317.

10. Le M. Investigating the Generation of Biophotons Induced by Low-Dose Beta-Irradiation and their Role in the Radiation-Induced Bystander Effect. McMaster University; 2018.

11. Ahmad SB, McNeill FE, Byun SH, Prestwich W V., Mothersill C, Seymour C, Armstrong A, Fernandez C. Ultra-violet light emission from hpv-g cells irradiated with low let radiation from 90Y; consequences for radiation induced bystander effects. Dose-Response. 2013;11(4):498–516. doi:10.2203/dose-response.12-048.ahmad

12. Ahmad SB, McNeill FE, Prestwich W V, Byun SH, Seymour C, Mothersill CE. Quantification of ultraviolet photon emission from interaction of charged particles in materials of interest in radiation biology research. NUCLEAR INSTRUMENTS & METHODS IN PHYSICS RESEARCH SECTION B-BEAM INTERACTIONS WITH MATERIALS AND ATOMS. 2014;319:48–54. doi:10.1016/j.nimb.2013.10.012

13. Le M, McNeill FE, Seymour C, Rainbow AJ, Mothersill CE. An observed effect of ultraviolet radiation emitted from beta-irradiated HaCaT cells upon non-beta-irradiated bystander cells. Radiation research. 2015;183(3):279–90. http://www.bioone.org/doi/10.1667/RR13827.1%5Cnhttp://www.ncbi.nlm.nih.gov/pubmed/25710575.

doi:10.1667/RR13827.1

14. Belpomme D, Hardell L, Belyaev I, Burgio E, Carpenter DO. Thermal and non-thermal health effects of low intensity non-ionizing radiation: An international perspective. Environmental pollution. 2018;242:643–658.

15. Lai H, Singh NP. Single- and double-strand DNA breaks in rat brain cells after acute exposure to radiofrequency electromagnetic radiation. International journal of radiation biology. 1996;69(4):513–521.

16. Yang CY. Effects of ultraviolet irradiation on production of aflatoxins by Aspergillus flavus Link ex. Fries. Radiation Botany. 1972;12(2):105–111.

17. Dahle J, Kvam E, Stokke T. Bystander effects in UV-induced genomic instability: antioxidants inhibit delayed mutagenesis induced by ultraviolet A and B radiation. Journal of carcinogenesis. 2005;4:11.

18. Han W, Wu L, Chen S, Bao L, Zhang L, Jiang E, Zhao Y, Xu A, Hei TK, Yu Z. Constitutive nitric oxide acting as a possible intercellular signaling molecule in the initiation of radiation-induced DNA double strand breaks in non-irradiated bystander cells. Oncogene. 2007;26(16):2330–2339. http://www.nature.com/doifinder/10.1038/sj.onc.1210024. doi:10.1038/sj.onc.1210024

19. Reisz JA, Bansal N, Qian J, Zhao W, Furdui CM. Effects of Ionizing Radiation on Biological Molecules—Mechanisms of Damage and Emerging Methods of Detection. Antioxidants & Redox Signaling. 2014;21(2):260–292. http://online.liebertpub.com/doi/abs/10.1089/ars.2013.5489. doi:10.1089/ars.2013.5489

20. Armeni T, Damiani E, Battino M, Greci L, Principato G. Lack of in vitro protection by a common sunscreen ingredient on UVA-induced cytotoxicity in keratinocytes. Toxicology. 2004;203(1–3):165–178. doi:10.1016/j.tox.2004.06.008

21. O'Reilly JP, Mothersill C. Comparative effects of UV A and UV B on clonogenic survival and delayed cell death in skin cell lines from humans and fish. International journal of radiation biology. 1997;72(1):111–119.

22. Zhang Y, Bai X, Wang Y, Li N, Li X, Han F, Su L, Hu D. Role for heat shock protein 90α in the proliferation and migration of HaCaT cells and in the deep second-degree burn wound healing in mice. PloS one. 2014;9(8):e103723.

23. Özören N, El-Deiry W. Heat shock protects HCT116 and H460 cells from TRAIL-induced apoptosis. Experimental cell research. 2002;281(2):175–181.

24. Le M, Mothersill CE, Seymour CB, Ahmad SB, Armstrong A, Rainbow AJ, McNeill FE. Factors affecting ultraviolet-A photon emission from beta-irradiated human keratinocyte cells. Physics in medicine and biology. 2015;60(16):6371–6389. doi:10.1088/0031-9155/60/16/6371

25. Kamenisch Y, Ivanova I, Drexler K, Berneburg M. UVA, metabolism and melanoma: UVA makes melanoma hungry for metastasis. Experimental dermatology. 2018;27(9):941–949.

26. Gęgotek A, Rybałtowska-Kawałko P, Skrzydlewska E. Rutin as a mediator of lipid metabolism and cellular signaling pathways interactions in fibroblasts altered by UVA and UVB radiation. Oxidative Medicine and Cellular Longevity. 2017;2017.

27. RAPP LM, GHALAYINI AJ. Influence of UVA light stress on photoreceptor cell metabolism: decreased

rates of rhodopsin regeneration and opsin synthesis. Experimental eye research. 1999;68(6):757–764.

28. Le M, McNeill FE, Seymour CB, Rusin A, Diamond K, Rainbow AJ, Murphy J, Mothersill CE. Modulation of oxidative phosphorylation (OXPHOS) by radiation- induced biophotons. Environmental Research. 2018;163:80–87. doi:10.1016/j.envres.2018.01.027

29. Lyng FM, Howe OL, McClean B. Reactive oxygen species-induced release of signalling factors in irradiated cells triggers membrane signalling and calcium influx in bystander cells. International journal of radiation biology. 2011;87(7):683–695.

30. Jella KK, Moriarty R, McClean B, Byrne HJ, Lyng FM. Reactive oxygen species and nitric oxide signaling in bystander cells. PloS one. 2018;13(4):e0195371.

Chapter 11

Further discussions and future directions

Abstract: This concluding chapter reviews the results collected in chapters 2-10 and summarizes key findings. Further deductions are made based on qualitative comparisons between these chapters. The induction of oxidative stress by administration of hydrogen peroxide was found to be most pronounced in HaCaT, yet cell survival and metabolism was more affected in HCT116 at the same doses, indicating a greater resilience to baseline oxidative stress in HaCaT cells. B16F10 cells do not show oxidative stress in the same dose range nor the associated effects of oxidative stress, indicating a role for melanin as a free-radical scavenger. Both HCT116 and HaCaT cells were found to emit bystander photons and reporters showed decreased cell survival, increased oxidative stress, decreased cellular metabolism, and decreased mitochondrial membrane polarization, indicating that these were bystander effects. B16F10 did not show biophoton emission nor its associated effects on cells, which suggests that melanin acts to absorb the photons that elicit the effect in bystander reporters. The significance of this thesis to several aspects of radiation biology is then discussed and some future directions to research are proposed.

11.1. Summary of key findings

Bystander photons from beta-irradiated cells induce a variety of effects in reporter cells. A review of the literature in chapter 1 noted that photon emissions from directly irradiated cells are known to produce a multitude of effects in human cells[1–7], but also expounded the relative lack of information on oxidative stress in these bystander cells. Additionally, chapter 1 questioned whether melanin could act as a radioprotector in the context of the physical bystander effect. Low-LET irradiations were conducted in chapter 2 along with plating efficiency experiments. In chapter 3, HCT116 and HaCaT were found to express the p53 protein and thus expected to be able to respond to a bystander signal. The measurement of melanin production in B16F10 cells was done in chapter 4. Chapter 5 verified the emission of photons upon beta irradiation in all cultures but B16F10, indicating a role for melanin in the absorption of these photons of biological origin. In chapter 6, reproductive cell death was found to be reduced in HaCaT and HCT116 bystanders. The induction of oxidative stress was found in chapter 7 in the same cells. Modulation of overall metabolic activity was observed in HaCaT and HCT116, measured by an MTT assay, in chapter 8. JC1 was used in Chapter 9 to show inner mitochondrial membrane depolarization in both HaCaT and HCT116 bystander cells. The results in chapters 6 and 7 also imply that melanin may act as a free radical scavenger, as B16F10 was observed to be much less sensitive to hydrogen peroxide than both HCT116 and HaCaT. Finally, chapter 10 reviews attempts to model exposure to UVA photons using a lamp.

The effects listed above that occur in bystander cells are also noted to occur upon exposure to exogenous ROS, with the exception of mitochondrial membrane depolarization in HaCaT. A summary of results from each cell line are available below. The induction of oxidative stress in these bystander cells may be generated as due to cell signalling[8–11]. Alternatively, ROS may act as signalling molecules to effect bystander responses directly, acting upstream of other known phenomena associated with bystander effects[10,12,13]; these roles appear to not be mutually exclusive. The results in chapter 10 suggest that the formation of ROS is an early event in responses to UVA, which may be similar in bystander cells. It is difficult to make a conclusive judgement on whether the timeframe of the effect is the same in bystander cells receiving biophotons for two reasons. Firstly, it is known that different types of photons are emitted from bystander cells and it has been suggested that photons of different wavelengths, emitted from cells, work together to induce bystander responses[5,7,14]. Secondly, the intensity of light was different in the exposure to artificial UVA and biophotons, which is also apparent in chapter 5; the light from the lamp promptly saturated the photon counter, while exposed cells achieved a count of approximately 1000 photons after 10 minutes of exposure. This means that responses in cells receiving this light would be different, theoretically, as it was reviewed in chapter 1 that radiation responses are influenced by the characteristics of the radiation used.

Another major finding of this report is that melanin appears to block a wide variety of responses to biophotons. As noted in chapter 5, melanin appears to reduce emission of photons from cells to approximately background. A good follow-up experiment would be to expose B16F10 reporters to donor cells known to produce biophotons, such as HaCaT, for further evidence that melanin prevents bystander responses in reporters and not only donors; it is suspected that melanin—present in cell culture medium and in the melanocytes as described in chapter 4—would absorb the photons that typically elicit effects in a reporter cell Further, it is believed that the free radical scavenging properties of melanin would also prevent bystander responses in these reporter cells. A good control to include could be an albino melanocyte cell line to account for potentially differential responses compared to other cell types; albino melanocyte cells are available[15–17]. As discussed in previous chapters, exosomes are released by cells exposed to ionizing radiation and biophotons[4,18,19] and “transmit” or communicate radiation damage to

unexposed cells by carrying various factors, such as non-coding RNAs (ncRNA)[18,20–22], to these cells. It would be very interesting to expose B16F10 to these exosomes. It is expected that B16F10 could respond to these signals, as melanin is believed to exert its radioprotective effects by absorption of bystander photons, sequestration of free radicals, or some combination thereof depending on the cell in question.

To summarize, these results suggest that HaCaT and HCT116 emit photons, primarily in the UVA range, upon irradiation with tritium. These cells, although unirradiated directly by tritium, also exhibit reduced cell survival, oxidative stress, reduced metabolism, and inner mitochondrial membrane depolarization upon receipt of these bystander photons. B16F10, on the other hand, did not exhibit these effects, likely due to the dual radioprotective properties of melanin. HCT116 was found to be overall more sensitive to oxidative stress than HaCaT, while hydrogen peroxide supplementation most readily increased oxidative stress in HaCaT over HCT116. B16F10 was the most resistant to the induction of and cellular effects of oxidative stress by hydrogen peroxide supplementation, which further confirms the role for melanin in protection from bystander effects. A detailed overview of key results is available below.

11.2. Qualitative comparisons and discussion

A qualitative compilation of results obtained in this report is shown below. These tables attempt to characterize the magnitude of effect observed between different experiments through qualitative analysis. It is difficult to directly relate findings—through a qualitative procedure or "meta-analysis" of chapters—between experiments because there are a number of confounding variables that render the process inappropriate. For example, plating efficiency was shown to vary between different culture vessels. Although 96-well plates were not assessed in this way, it is likely that plating efficiency in these is significantly different from plating efficiency in a T75 or T25 flask, owing to the considerably reduced area for growth. Therefore, the quantitative comparison of experimental results, where factors such as plating efficiency are not consistent, would be difficult. Rather, a qualitative comparison can be made, based on statistical significance and difference between experimental groups, between different experiments.

OXIDATIVE STRESS RESPONSES

	HaCaT	HCT116	B16F10
Baseline (DCFDA)	✓✓✓ , ✓✓✓✓	✓✓✓ , ✓✓✓ ††	✓
Biophoton Emission	x	x	x
PER Death	✓✓	✓✓✓	✓
PER Metabolism (MTT)	✓✓	✓✓✓	✓
PER Mitochondria (JC-1)	x	✓✓✓	✓

RADIATION RESPONSES

	HaCaT	HCT116	B16F10
Baseline (Low LET, Low Dose)	✓✓ , ✓✓	✓✓✓ , ✓✓ †††	✓
Biophoton (BP) emission	✓	✓	x
BP Oxidative Stress (DCFDA)	✓✓✓ , ✓✓✓	✓✓,✓✓ ††	X
BP Death	✓✓	✓✓ †	x
BP Metabolism (MTT)	✓✓	✓✓✓	x
BP Mitochondria (JC-1)	✓	✓✓	x

Table 11.1: Summary data obtained across this report for both oxidative stress responses due to hydrogen peroxide supplementation and secondary UVA photon exposure through physical bystander conditions. "PER" represents treatment of cells with hydrogen peroxide; "BP" indicates the treatment of reporter cells by biophotons, and associated assays in the same cells. A "baseline" for oxidative stress was obtained by treating cells with varying concentrations of hydrogen peroxide, administered directly in cell culture medium. A "baseline" for responsiveness to direct low-LET radiation was initially obtained through a clonogenic survival assay following gamma exposure. Note that checkmarks abstractly and qualitatively represent the magnitude of effect observed—derived from statistical significance and difference between means—within each row relative to the three columns in that row, but irrespective of other rows. An "x" represents failure to demonstrate an effect.

[†]HCT and HaCaT more/less sensitive at a clonogenic endpoint depending on the dose delivered to donors, but insignificantly so.

[††]Microplate/Microscope result. Note that microscope results were qualitatively assessed.

[†††]According to the linear quadratic/multitarget model fits, respectively. Please see chapter 2 for a discussion on the limitations of these fits in the context of the dose range used.

In hydrogen peroxide exposures, the main goal was to model oxidative stress. Considering that DCFDA is a common indicator of intracellular oxidative stress[23] and the results in chapter 7, this can be considered successful. In nearly all assays besides DCFDA, hydrogen peroxide appeared to produce somewhat more pronounced effects in HCT116 than HaCaT. The endpoints of these assays included clonogenic cell survival and cell and mitochondrial metabolic activity. For HaCaT cells, induction of oxidative stress by hydrogen peroxide—measured by DCFDA fluorescence—occurred readily at the doses used and the cells appeared to be more sensitive to hydrogen peroxide supplementation than other cell types using the same assay. Taken together with other data, these results show that HaCaT cells can endure a greater baseline state of oxidative stress than HCT116 in the same peroxide dose range, however they do not experience the same magnitude of effects that HCT116 experience at these doses. This may be evidence that HaCaT cells are somehow more resistant to baseline oxidative stress than HCT116. This trend is similar to the magnitude of effects observed in biophoton exposures, where HCT116 reporters typically showed a greater effect. This trend and the result that both HaCaT and HCT116 exhibit oxidative stress upon exposure to biophotons is evidence for the notion that effects due to the physical bystander signal manifest in cells because of the formation of ROS, at least partly. Therefore, it is believed that inclusion of other free radical scavengers in future experiments, including glutathione[24], could potentially annul or attenuate effects in reporters. HaCaT also appears to be slightly less radiosensitive to low-LET radiation than HCT116, which may be a result of this natural resistance to oxidative damage; it is known that a major contributor to damage in low-LET exposures is the formation of free radicals and subsequent damage[25].

B16F10 appears to be best protected from the induction of oxidative stress and its associated effects, which is evidence for the protective role of melanin as a free radical scavenger. Furthermore, it was discussed previously that B16F10 appears to be very radioresistant to gamma radiation as well compared to HCT116 and HaCaT, which is also corroborated by other survival curves the literature[26]. Cell death occurs upon exposure to low-LET, such as gamma and beta radiation, partly due to the generation of ROS by the ionizing radiation, which leads to non-targeted damage. B16F10 cells also did not enter a state of oxidative stress until provided with greater concentrations of hydrogen peroxide than HaCaT and HCT116. In this system, it is suspected that melanin present in the B16F10 donors or recipients will effectively abrogate the communication of the signal at some stage. While B16F10 can exhibit obvious oxidative stress between 0–100 μM hydrogen peroxide, they do not appear capable of generating nor receiving this bystander signal from the findings in this report.

In HaCaT cells, hydrogen peroxide induced a reduction in general metabolic activity, measured using MTT in Chapter 8. However, the effect was slightly more pronounced in HCT116 treated with the same doses of hydrogen peroxide. Conversely, HaCaT showed a slightly greater reduction in cell survival than HCT116 when exposed to biophotons. This indicates that, while the generation of oxidative stress by biophotons was demonstrated to occur in both HaCaT and HCT116 cells and is involved in this effect, the mechanisms behind the cell killing action of this bystander signal may be multifaceted. In other words, oxidative stress may account for one aspect of this bystander effect, however the existence of other related or unrelated mechanisms is likely. For example, Le et al. demonstrated a reduction in mitochondrial metabolism in HCT116 cells[1], determined through the reduced activity of Complex I, which is itself related to the generation of ROS as Complex I is a site of premature electron escape[27]. Related effects were observed in the present thesis as well using different methods—inner mitochondrial membrane depolarization, which indicated a response in primarily HCT116 but to a lesser degree in HaCaT; NAD(P)H-dependent oxidoreductase activity, which indicated overall great responses in HCT116 than HaCaT; and ROS concentration, which indicated more efficient induction of oxidative stress in HaCaT overall. It is apparent that, upon examination of mitochondria alone, it is obvious why Le et al. also found greater sensitivity to the signal in HCT116[5]; it is suspected that a reduced apoptotic signal from mitochondria in HaCaT, perhaps due to mutations in p53 and other apoptotic proteins[5,28], could account for this discrepancy; this is also stated in the same report. Clonogenic survival in biophoton reporters in the present thesis indicates that HCT116 is slightly more sensitive to the signal at some donor doses, although not significantly compared to HaCaT. In this report[1], the authors found that Complex I activity in HCT116 was significantly impaired. Follow-up studies could be conducted on other cell lines that have been shown to exhibit the bystander effect upon receipt of biophotons, such as HaCaT. This would be helpful because different mitochondrial responses between cell lines could indicate diverse means of responding to the signal, while similar results would imply a more conserved response that utilizes the same pathways between cell types. Moreover, extension of these experiments to non-human cell lines could be planned, like on an albino murine melanocyte cell line, to investigate whether responses to radiation-induced biophotons are evolutionarily conserved or different across phyla.

To summarize this comparative analysis, these results indicate a role for ROS in bystander cells responding to the physical bystander signal. HaCaT cells respond to hydrogen peroxide supplementation most efficiently yet exhibit muted effects on cells compared to HCT116, owing to a difference in sensitivity to oxidative stress—this can be traced to no response of HaCaT mitochondria to peroxide, which effectively increases cell viability overall, as well as reduced effects in other assays. Both human cell lines emit similar amounts of biophotons and reduction in reproductive cell survival was observed to be similar between the two cell lines. Comparable generation of oxidative stress also occurs in HaCaT and HCT116 reporters exposed to donor biophotons. Greater reduction in NAD(P)H-dependent enzyme activity was observed in HCT116 and a more significant reduction in inner mitochondrial membrane potential was observed in HCT116. These results from biophoton exposures and differences in sensitivity to oxidative stress suggests several things. Firstly, induction of ROS is crucial for a response to the physical bystander signal. Secondly, there are multiple roles for the electromagnetic bystander signal in modulating responses in reporter cells, which are local to mitochondria and more broadly in other parts of the cell, and these likely involve mechanisms independent of the generation of ROS. However, these pathways may be connected in some way to oxidative stress and the “final status” of the cell in terms of death or survival. Induction of oxidative stress in B16F10 indicates a comparatively high natural resistance to hydrogen peroxide. Hydrogen peroxide can induce cell death and mitochondrial membrane depolarization in B16F10, albeit less so than in HCT116 as higher doses are required. Effects on overall cell metabolism were not as clear as with B16F10 and HaCaT. B16F10 did not produce significant bystander photons, which was likely a result of absorption due to melanin. B16F10 reporters also did not exhibit any

of the effects observed in HCT116 and HaCaT cells. Finally, hydrogen peroxide supplementation does not produce biophoton emission, which suggests that generation of ROS is necessary but not sufficient for biophoton emission.

11.3. Significance

The significance of this research lies in elucidating the mechanisms behind the communication of radiation damage to cells in a population exposed to low dose radiation (LDR). Cells, both *in vivo* and in cell culture contexts, do not exist in isolation from other cells and signalling molecules. It can be argued that these results show that reactive oxygen species generated within bystander cells could represent some mechanism of "receiving" and communicating the signal, a process analogous to signal transduction by a membrane receptor. It has been known for some time now that reactive oxygen species and associated molecules are involved in bystander effects[10,29,30], however their role in the context of the physical bystander signal was not extensively investigated before this thesis. This comparative report offers evidence that ROS, delivered exogenously, may induce the same or similar effects in cells as bystander photons.

The data and interpretation in this thesis do not support the linear no-threshold (LNT) model. Further, the physical bystander signal and the effects demonstrated in this report provide evidence that the risk assessment for radiation exposure is complicated beyond any prospect of reconciliation to this model. The very existence of non-targeted effects creates a major problem for the LNT model because these effects are not always dependent to or easily predicted by dose[31–36], and moreover appear to be the dominant effects at low doses rather than high ones[33–36]. The persistence of signalling factors in a biological system, both as soluble molecules and electromagnetic emissions from cells, has the potential to promote the effects described in this thesis, among others: cell death, modulation of cellular and mitochondrial metabolism, and oxidative stress. This is particularly of relevance *in vivo* because previous research has shown that the signal mediated by soluble factors and ultraviolet light are connected[4], and this may allow for the propagation and persistence of signalling in a biological system. These effects do not arise directly as a result of the deposition of energy into living matter, but rather serve to communicate radiation damage to unexposed cells, which is not accounted for in the LNT model. Therefore, due to the existence of the effect described in this report and others such as abscopal effects and genomic instability, the LNT model will never be able to fit experimental data adequately nor accurately predict the stochastic health effects of lower doses—including the cumulative effects of multiple, repeated exposures. To further complicate the modelling of risk, it is now known that non-targeted effects vary depending on the cell type and radiation used, and may be completely absent in certain cell types[37–41]. Moreover, non-targeted effects may vary considerably between different species[42–47].

Radiation-induced bystander effects do not only occur in human cells, but also *in vivo* and in different species of animal, including fish and mice[42–47]. To my knowledge, this report is the first that investigates potential physical bystander mechanisms in non-human cells. As described in chapter 1, radiation sensitivity varies across the kingdoms and domains of life, and there is a dearth of information on the radiosensitivity of some phyla. It is equally important to investigate radiation response mechanisms in non-human biota because constituents of an ecosystem would benefit from an informed assessment of risk following an environmentally relevant exposure, which in turn may benefit humans or spare vulnerable species from deleterious effects. It is now known, especially in cases of the accidental release

of relatively long-lived radionuclides and their decay products, that historic dose and transgenerational effects persist which affect population health many years after an exposure event[36,48–50].

Finally, the electromagnetic bystander signal may be relevant for human health, specifically with respect to radiotherapy and diagnostic radiology. In radiotherapy, the goal is to expose tumor cells to high doses of ionizing radiation. This is done in the hope that cell death occurs in the tumor and non-malignant tissue is spared[25]. The primary mode of cellular damage in these contexts involves targeted effects and specifically DNA damage. Bystander and associated non-targeted effects have been shown to reduce the clonogenic survival of cells[39,51], and further studies from primary cultures and *in vivo* indicate that it may be relevant as a mechanism of cell killing or resistance to cell killing in some tumors[52–56]. It is suspected that a better understanding of these mechanisms behind communicating radiation damage to unexposed cells may be exploited in the future to remove tumorigenic cells using radiotherapy. Moreover, differing responses upon irradiation with some tumors can be expected, which could affect radiotherapy efficacy. Alternatively, irradiation of tumor cells could produce factors, such as bystander photons, that could conceivably cause destruction of surrounding, healthy tissue. Therefore, understanding and accounting for these effects would be conducive to more effective radiotherapy, even though these exposures typically involve higher doses. These effects are clearly also relevant for broader therapeutics, such as brachytherapy or systemic radiotherapy.

These findings may also be relevant to the branch of nuclear medicine and radiology concerned with diagnostics. Radiation-induced bystander effects may be relevant for diagnostic radiology, such as x-ray imaging. These methods can employ the use of high energy x-rays (hard x-rays) for internal imaging[57,58]. Typically, dose to the patient and the operator is routinely minimized as best practice[59,60]. Other imaging methods involve the use of radioisotopes for PET scans, which involve positron emission. Again, especially in these diagnostic settings, keeping doses as low as reasonably achievable (ALARA) is considered best practice for both patient and clinician. In settings relevant to human exposure wherein doses kept low, non-targeted effects may cause health effects. Moreover, it has been suggested in the literature that these low doses may contribute to the underlying etiology of diseases such as chronic fatigue and immune dysfunction syndrome (CFIDS)[61,62]. Thus, an appreciation of the physical bystander signal both *in vitro* and *in vivo* would be helpful for determining potential effects in humans where low doses are employed.

11.4. Future directions

There are several follow-up experiments that may be conducted to further elucidate the role of melanin in the *in vitro* protection of cells against bystander effects. As mentioned previously, a study with mixed donors and reporters could help determine whether melanin present in reporters alone prevents the effects discussed in this thesis. Further, inclusion of an albino melanoma cell line and similar supplementation of melanin in cell culture medium could be performed to determine if a dose response for the radioprotective effect exists.

For oxidative stress studies, future experiments may benefit from examining a variety of cellular ROS in addition to hydrogen peroxide. Similarly, some probes are available that only measure one variety of ROS, such as superoxide. A good method to confirm the induction of oxidative stress in recipients of the physical bystander signal is through the activity of superoxide dismutase and catalase, which has been done extensively in the literature[63–65]. Furthermore, the inclusion of antioxidants, such as glutathione, in reporter cell cultures would determine if suppression of ROS alone can prevent the bystander effect.

As discussed in chapter 2, a more complete curve for all cell lines can be obtained by including more dose points, particularly higher doses. Moreover, inclusion of higher doses would likely change the characteristics of both fits and give different n and D_0 values. B16F10 could also be probed for mouse p53 expression, even though it has been shown in the literature that it expresses wild type p53[66,67]. All the assays conducted in this thesis could benefit from the inclusion of mix-match studies for donors and recipients. Better dosimetry in chapter 10 and the inclusion of more doses could allow for a more comprehensive understanding of how the cells used respond to artificial UVA. The inclusion of more doses in all chapters other than 0.5 Gy, and potentially using other sources of radiation, would further assist in our understanding of the physical bystander signal and its effects.

11.5. Conclusions

A physical radiation-induced bystander effect, communicated chiefly by UVA-photon emitted from directly irradiated cells, was demonstrated in two human epithelial cell lines: HaCaT and HCT116. Bystander reporters in both cell lines exhibited reproductive cell death, oxidative stress, reduction in cellular metabolism, and reduction in mitochondrial metabolism upon exposure to the signal. B16F10, a mouse melanoma cell line, did not exhibit these effects, which is suspected to be due to the radioprotective role of melanin. B16F10 exhibited the least oxidative stress upon administration of hydrogen peroxide, which is indicative of melanin's free radical scavenging properties. ROS was most readily induced in HaCaTs upon peroxide supplementation, however cell death, oxidative stress, reduction in cellular metabolism, and reduction in mitochondrial metabolism were less pronounced than in HCT116. It is therefore suspected that HaCaT cells are accustomed to higher baseline oxidative stress than HCT116. The results strongly indicate that ROS is involved producing the bystander effect in recipients of the electromagnetic bystander signal, and that other mechanisms are likely involved in promoting this effect. The significance of these findings is broad and includes elucidating how cells communicate radiation damage in a population, challenging the linear no-threshold (LNT) model, determining bystander effects in non-human species, and its potential relevance to radiotherapeutics and diagnostic medicine.

11.6. References

1. Le M, McNeill FEFE, Seymour CBCB, Rusin A, Diamond K, Rainbow AJAJ, Murphy J, Mothersill CECE. Modulation of oxidative phosphorylation (OXPHOS) by radiation-induced biophotons. Environmental research. 2018;163:80–87. doi:10.1016/j.envres.2018.01.027

2. Le M, McNeill FE, Seymour C, Rainbow AJ, Mothersill CE. An observed effect of ultraviolet radiation emitted from beta-irradiated HaCaT cells upon non-beta-irradiated bystander cells. Radiation research. 2015;183(3):279–90. http://www.bioone.org/doi/10.1667/RR13827.1%5Cnhttp://www.ncbi.nlm.nih.gov/pubmed/25710575. doi:10.1667/RR13827.1

3. Le M, Mothersill CE, Seymour CB, Ahmad SB, Armstrong A, Rainbow AJ, McNeill FE. Factors affecting ultraviolet-A photon emission from beta-irradiated human keratinocyte cells. Physics in medicine and biology. 2015;60(16):6371–6389. doi:10.1088/0031-9155/60/16/6371

4. Le M, Fernandez-Palomo C, McNeill FE, Seymour CB, Rainbow AJ, Mothersill CE. Exosomes are released by bystander cells exposed to radiation-induced biophoton signals: Reconciling the mechanisms mediating the bystander effect. PLOS ONE. 2017;12(3):e0173685. doi:10.1371/journal.pone.0173685

5. Le M, Mothersill CE, Seymour CB, Rainbow AJ, McNeill FE. An Observed Effect of p53 Status on the Bystander Response to Radiation-Induced Cellular Photon Emission. Radiation Research. 2017;187(2):169–185. http://www.bioone.org/doi/10.1667/RR14342.1. doi:10.1667/RR14342.1

6. Ahmad SB, McNeill FE, Byun SH, Prestwich W V., Mothersill C, Seymour C, Armstrong A, Fernandez C. Ultra-violet light emission from hpv-g cells irradiated with low let radiation from 90Y; consequences for radiation induced bystander effects. Dose-Response. 2013;11(4):498–516. doi:10.2203/dose-response.12-048.ahmad

7. Ahmad SB, McNeill FE, Prestwich W V, Byun SH, Seymour C, Mothersill CE. Quantification of ultraviolet photon emission from interaction of charged particles in materials of interest in radiation biology research. NUCLEAR INSTRUMENTS & METHODS IN PHYSICS RESEARCH SECTION B-BEAM INTERACTIONS WITH MATERIALS AND ATOMS. 2014;319:48–54. doi:10.1016/j.nimb.2013.10.012

8. Marchi S, Giorgi C, Suski JM, Agnoletto C, Bononi A, Bonora M, De Marchi E, Missiroli S, Patergnani S, Poletti F, et al. Mitochondria-Ros Crosstalk in the Control of Cell Death and Aging. Journal of Signal Transduction. 2012;2012:1–17. doi:10.1155/2012/329635

9. Giorgio M, Migliaccio E, Orsini F, Paolucci D, Moroni M, Contursi C, Pelliccia G, Luzi L, Minucci S, Marcaccio M, et al. Electron transfer between cytochrome c and p66Shc generates reactive oxygen species that trigger mitochondrial apoptosis. Cell. 2005;122(2):221–233. doi:10.1016/j.cell.2005.05.011

10. Lyng FM, Howe OL, McClean B. Reactive oxygen species-induced release of signalling factors in irradiated cells triggers membrane signalling and calcium influx in bystander cells. International journal of radiation biology. 2011;87(7):683–695.

11. Lyng FM, Maguire P, Kilmurray N, Mothersill C, Shao C, Folkard M, Prise KM. Apoptosis is initiated in human keratinocytes exposed to signalling factors from microbeam irradiated cells. INTERNATIONAL JOURNAL OF RADIATION BIOLOGY. 2006;82(6):393–399. doi:10.1080/09553000600803904

12. Guo S, Zhou J, Chen X, Yu Y, Ren M, Hu G, Liu Y, Zou F. Bystander effects of PC12 cells treated with

Pb(2)(+) depend on ROS-mitochondria-dependent apoptotic signaling via gap-junctional intercellular communication. Toxicology letters. 2014;229(1):150–157. doi:10.1016/j.toxlet.2014.05.026

13. Hamada N, Maeda M, Otsuka K, Tomita M. Signaling pathways underpinning the manifestations of ionizing radiation-induced bystander effects. Current molecular pharmacology. 2011;4(2):79–95.

14. Le M, McNeill FE, Seymour CB, Rusin A, Diamond K, Rainbow AJ, Murphy J, Mothersill CE. Modulation of oxidative phosphorylation (OXPHOS) by radiation- induced biophotons. Environmental Research. 2018;163:80–87. doi:10.1016/j.envres.2018.01.027

15. Bennett DC, Cooper PJ, Dexter TJ, Devlin LM, Heasman J, Nester B. Cloned mouse melanocyte lines carrying the germline mutations albino and brown: complementation in culture. Development. 1989;105(2):379–385.

16. YAMAMOTO H, Takeuchi S, KUDO T, SATO C, TAKEUCHI T. Melanin production in cultured albino melanocytes transfected with mouse tyrosinase cDNA. The Japanese Journal of Genetics. 1989;64(2):121–135.

17. Alexeev V, Yoon K. Stable and inheritable changes in genotype and phenotype of albino melanocytes induced by an RNA-DNA oligonucleotide. Nature biotechnology. 1998;16(13):1343–1346.

18. Al-Mayah AHJ, Irons SL, Pink RC, Carter DRF, Kadhim MA. Possible role of exosomes containing RNA in mediating nontargeted effect of ionizing radiation. Radiation research. 2012;177(5):539–545.

19. Jelonek K, Widlak P, Pietrowska M. The Influence of Ionizing Radiation on Exosome Composition, Secretion and Intercellular Communication. Protein and peptide letters. 2016;23(7):656–663. doi:10.2174/0929866523666160427105138

20. Xu S, Wang J, Ding N, Hu W, Zhang X, Wang B, Hua J, Wei W, Zhu Q. Exosome-mediated microRNA transfer plays a role in radiation-induced bystander effect. RNA biology. 2015;12(12):1355–1363.

21. Yentrapalli R, Merl-Pham J, Azimzadeh O, Mutschelknaus L, Peters C, Hauck SM, Atkinson MJ, Tapio S, Moertl S. Quantitative changes in the protein and miRNA cargo of plasma exosome-like vesicles after exposure to ionizing radiation. International journal of radiation biology. 2017;93(6):569–580. doi:10.1080/09553002.2017.1294772

22. Jella KK, Rani S, O'Driscoll L, McClean B, Byrne HJ, Lyng FM. Exosomes are involved in mediating radiation induced bystander signaling in human keratinocyte cells. Radiation research. 2014;181(2):138–145. doi:10.1667/RR13337.1

23. Eruslanov E, Kusmartsev S. Identification of ROS using oxidized DCFDA and flow-cytometry. In: Advanced protocols in oxidative stress II. Springer; 2010. p. 57–72.

24. Fulle S, Mecocci P, Fanó G, Vecchiet I, Vecchini A, Racciotti D, Cherubini A, Pizzigallo E, Vecchiet L, Senin U, et al. Specific oxidative alterations in vastus lateralis muscle of patients with the diagnosis of chronic fatigue syndrome. Free Radical Biology and Medicine. 2000;29(12):1252–1259. doi:10.1016/S0891-5849(00)00419-6

25. Hall EJ, Giaccia AJ. Radiobiology for the Radiologist. Lippincott Williams & Wilkins; 2006.

26. Nagane M, Kanai E, Shibata Y, Shimizu T, Yoshioka C, Maruo T, Yamashita T. Sulfasalazine, an inhibitor of the cystine-glutamate antiporter, reduces DNA damage repair and enhances radiosensitivity in murine B16F10 melanoma. PLoS One. 2018;13(4):e0195151.

27. Liu Y, Fiskum G, Schubert D. Generation of reactive oxygen species by the mitochondrial electron transport chain. Journal of Neurochemistry. 2002. doi:10.1046/j.0022-3042.2002.00744.x

28. Furlong H, Smith R, Wang J, Seymour C, Mothersill C, Howe O. Identification of Key Proteins in Human Epithelial Cells Responding to Bystander Signals From Irradiated Trout Skin. DOSE-RESPONSE. 2015;13(3). doi:10.1177/1559325815597669

29. O'Dowd C, Mothersill CE, T Cairns M, Austin B, McClean B, Lyng FM, Murphy JEJ. The release of bystander factor(s) from tissue explant cultures of rainbow trout (Onchorhynchus mykiss) after exposure to gamma radiation. RADIATION RESEARCH. 2006;166(4):611–617. doi:10.1667/RR0606.1

30. Maguire P, Mothersill C, McClean B, Seymour C, Lyng FM. Modulation of radiation responses by pre-exposure to irradiated cell conditioned medium. RADIATION RESEARCH. 2007;167(4):485–492. doi:10.1667/RR0159.1

31. Liu ZF, Mothersill CE, McNeill FE, Lyng FM, Byun SH, Seymour CB, Prestwich W V. A dose threshold for a medium transfer bystander effect for a human skin cell line. RADIATION RESEARCH. 2006;166(1, 1):19–23. doi:10.1667/RR3580.1

32. Kilemade M, Mothersill C. Expression of delayed cell death (DCD) in the progeny of fish cells surviving 2,4-dichloro aniline (2,4-DCA) exposure. AQUATIC TOXICOLOGY. 2003;63(3):207–219. doi:10.1016/S0166-445X(02)00180-7

33. Mothersill C, Seymour C. Implications for human and environmental health of low doses of ionising radiation. Journal of Environmental Radioactivity. 2014;133:5–9. http://dx.doi.org/10.1016/j.jenvrad.2013.04.002. doi:10.1016/j.jenvrad.2013.04.002

34. Mothersill C, Rusin A, Seymour C. Low doses and non-targeted effects in environmental radiation protection; where are we now and where should we go? Environmental Research. 2017. doi:10.1016/j.envres.2017.08.029

35. Belyakov O V, Folkard M, Mothersill C, Prise KM, Michael BD. Non-targeted effects of radiation: Applications for radiation protection and contribution to LNT discussion. In: Proceedings of the European IRPA Congress 2002: Towards Harmonization of Radiation Protection in Europe. 2002.

36. Hancock S, Vo NTK, Goncharova RI, Seymour CB, Byun SH, Mothersill CE. One-Decade-Spanning transgenerational effects of historic radiation dose in wild populations of bank voles exposed to radioactive contamination following the chernobyl nuclear disaster. Environmental research. 2020;180:108816. doi:10.1016/j.envres.2019.108816

37. Fernandez-Palomo C, Seymour C, Mothersill C. Inter-Relationship between Low-Dose Hyper-Radiosensitivity and Radiation-Induced Bystander Effects in the Human T98G Glioma and the Epithelial HaCaT Cell Line. Radiation research. 2016;185(2):124–33. http://www.bioone.org/doi/10.1667/RR14208.1%5Cnhttp://www.ncbi.nlm.nih.gov/pubmed/26849405. doi:10.1667/RR14208.1

38. Shi X, Mothersill C, Seymour C. No adaptive response is induced by chronic low-dose radiation from Ra-226 in the CHSE/F fish embryonic cell line and the HaCaT human epithelial cell line. ENVIRONMENTAL RESEARCH. 2016;151:537–546. doi:10.1016/j.envres.2016.08.026

39. Mothersill C, Seymour C. Medium from irradiated human epithelial cells but not human fibroblasts reduces the clonogenic survival of unirradiated cells. INTERNATIONAL JOURNAL OF RADIATION BIOLOGY. 1997;71(4):421–427.

40. Hanu C, Wong R, Sur RK, Hayward JE, Seymour C, Mothersill C. Low-dose non-targeted radiation effects in human esophageal adenocarcinoma cell lines. 2017;93(2):165–173. doi:10.1080/09553002.2017.1237057

41. Mothersill C, Bristow RG, Harding SM, Smith RW, Mersov A, Seymour CB. A role for p53 in the response of bystander cells to receipt of medium borne signals from irradiated cells. INTERNATIONAL JOURNAL OF RADIATION BIOLOGY. 2011;87(11):1120–1125. doi:10.3109/09553002.2011.610866

42. Smith RW, Seymour CB, Moccia RD, Hinton TG, Mothersill CE. The induction of a radiation-induced bystander effect in fish transcends taxonomic group and trophic level. INTERNATIONAL JOURNAL OF RADIATION BIOLOGY. 2013;89(4):225–233. doi:10.3109/09553002.2013.754558

43. Rusin A, Lapied E, Le M, Seymour C, Oughton D, Haanes H, Mothersill C. Effect of gamma radiation on the production of bystander signals from three earthworm species irradiated in vivo. Environmental Research. 2019;168. doi:10.1016/j.envres.2018.09.023

44. Mothersill C, Lyng F, Seymour C, Maguire P, Lorimore S, Wright E. Genetic factors influencing bystander signaling in murine bladder epithelium after low-dose irradiation in vivo. RADIATION RESEARCH. 2005;163(4):391–399. doi:10.1667/RR3320

45. Mothersill C, Smith RW, Agnihotri N, Seymour CB. Characterization of a radiation-induced stress response communicated in vivo between zebrafish. ENVIRONMENTAL SCIENCE & TECHNOLOGY. 2007;41(9):3382–3387. doi:10.1021/es062978n

46. Vo NTK, Sokeechand BSH, Seymour CB, Mothersill CE. Characterizing responses to gamma radiation by a highly clonogenic fish brain endothelial cell line. Environmental research. 2017;156:297–305. doi:10.1016/j.envres.2017.03.039

47. Smith RW, Seymour CB, Moccia RD, Mothersill CE. Irradiation of rainbow trout at early life stages results in trans-generational effects including the induction of a bystander effect in non-irradiated fish. Environmental Research. 2016;145:26–38. http://dx.doi.org/10.1016/j.envres.2015.11.019. doi:10.1016/j.envres.2015.11.019

48. Hancock S, Vo NTK, Byun SH, Zainullin VG, Seymour CB, Mothersill C. Effects of historic radiation dose on the frequency of sex-linked recessive lethals in Drosophila populations following the Chernobyl nuclear accident. Environmental research. 2019;172:333–337. doi:10.1016/j.envres.2019.02.014

49. Hancock S, Vo NTK, Omar-Nazir L, Batlle JVI, Otaki JM, Hiyama A, Byun SH, Seymour CB, Mothersill C. Transgenerational effects of historic radiation dose in pale grass blue butterflies around Fukushima following the Fukushima Dai-ichi Nuclear Power Plant meltdown accident. Environmental research. 2019;168:230–240. doi:10.1016/j.envres.2018.09.039

50. Omar-Nazir L, Shi X, Moller A, Mousseau T, Byun S, Hancock S, Seymour C, Mothersill C. Long-term effects of ionizing radiation after the Chernobyl accident: Possible contribution of historic dose. Environmental research. 2018;165:55–62.

51. Mothersill C, Seymour CB. Cell-cell contact during gamma irradiation is not required to induce a bystander effect in normal human keratinocytes: Evidence for release during irradiation of a signal controlling survival into the medium. RADIATION RESEARCH. 1998;149(3):256–262. doi:10.2307/3579958

52. Belyakov O V, Folkard M, Mothersill C, Prise KM, Michael BD. A proliferation-dependent bystander effect in primary porcine and human urothelial explants in response to targeted irradiation. BRITISH

JOURNAL OF CANCER. 2003;88(5):767–774. doi:10.1038/sj.bjc.6600804

53. Fernandez-Palomo C, Schültke E, Smith R, Bräuer-Krisch E, Laissue J, Schroll C, Fazzari J, Seymour C, Mothersill C. Bystander effects in tumor-free and tumor-bearing rat brains following irradiation by synchrotron X-rays. International journal of radiation biology. 2013;89(6):445–53. http://www.ncbi.nlm.nih.gov/pubmed/23363251. doi:10.3109/09553002.2013.766770

54. Fernandez-Palomo C, Schültke E, Bräuer-Krisch E, Laissue JA, Blattmann H, Seymour C, Mothersill C. Investigation of Abscopal and Bystander Effects in Immunocompromised Mice After Exposure to Pencilbeam and Microbeam Synchrotron Radiation. Health physics. 2016;111(2):149–59. http://content.wkhealth.com/linkback/openurl?sid=WKPTLP:landingpage&an=00004032-201608000-00012%5Cnhttp://www.ncbi.nlm.nih.gov/pubmed/27356059. doi:10.1097/HP.0000000000000525

55. Fernandez-Palomo C, Bräuer-Krisch E, Laissue J, Vukmirovic D, Blattmann H, Seymour C, Schültke E, Mothersill C. Use of synchrotron medical microbeam irradiation to investigate radiation-induced bystander and abscopal effects in vivo. Physica Medica. 2015;31(6):584–595. doi:10.1016/j.ejmp.2015.03.004

56. Hanu C, Timotin E, Wong R, Sur RK, Hayward JE, Seymour CB, Mothersill CE. The influence of smoking on radiation-induced bystander signal production in esophageal cancer patients. Environmental Research. 2016;147:565–571. http://dx.doi.org/10.1016/j.envres.2015.12.030. doi:10.1016/j.envres.2015.12.030

57. Chodick G, Kim KP, Shwarz M, Horev G, Shalev V, Ron E. Radiation risks from pediatric computed tomography scanning. Pediatric endocrinology reviews: PER. 2009;7(2):29–36.

58. Tatum JL, Kelloff GJ, Gillies RJ, Arbeit JM, Brown JM, Chao KSC, Chapman JD, Eckelman WC, Fyles AW, Giaccia AJ, et al. Hypoxia: importance in tumor biology, noninvasive measurement by imaging, and value of its measurement in the management of cancer therapy. International journal of radiation biology. 2006;82(10):699–757. doi:10.1080/09553000601002324

59. Sodhi KS, Krishna S, Saxena AK, Sinha A, Khandelwal N, Lee EY. Clinical application of “Justification” and “Optimization” principle of ALARA in pediatric CT imaging: ‘How many children can be protected from unnecessary radiation?’. European journal of radiology. 2015;84(9):1752–1757. doi:10.1016/j.ejrad.2015.05.030

60. Hayes RB. LNT may be lethal but ALARA is inherently useful. Health physics. 2018;115(3):391–392.

61. Loganovsky KN. Chronic fatigue syndrome in the Chernobyl accident consequences liquidators. International Journal of Radiation Medicine. 2001;3(1–2):76.

62. Rusin A, Seymour C, Mothersill C. Chronic fatigue and immune deficiency syndrome (CFIDS), cellular metabolism, and ionizing radiation: a review of contemporary scientific literature and suggested directions for future research. International Journal of Radiation Biology. 2018;94(3). doi:10.1080/09553002.2018.1422871

63. Weydert CJ, Cullen JJ. Measurement of superoxide dismutase, catalase and glutathione peroxidase in cultured cells and tissue. Nature Protocols. 2010. doi:10.1038/nprot.2009.197

64. Wheeler CR, Salzman JA, Elsayed NM, Omaye ST, Korte DW. Automated assays for superoxide dismutase, catalase, glutathione peroxidase, and glutathione reductase activity. Analytical Biochemistry. 1990. doi:10.1016/0003-2697(90)90668-Y

65. Paoletti F, Aldinucci D, Mocali A, Caparrini A. A sensitive spectrophotometric method for the determination of superoxide dismutase activity in tissue extracts. Analytical Biochemistry. 1986. doi:10.1016/0003-2697(86)90026-6

66. Yerlikaya A, Okur E, Ulukaya E. The p53-independent induction of apoptosis in breast cancer cells in response to proteasome inhibitor bortezomib. Tumor Biology. 2012;33(5):1385–1392.

67. Yerlikaya A, Erin N. Differential sensitivity of breast cancer and melanoma cells to proteasome inhibitor Velcade. International journal of molecular medicine. 2008;22(6):817–823.

12 Appendix

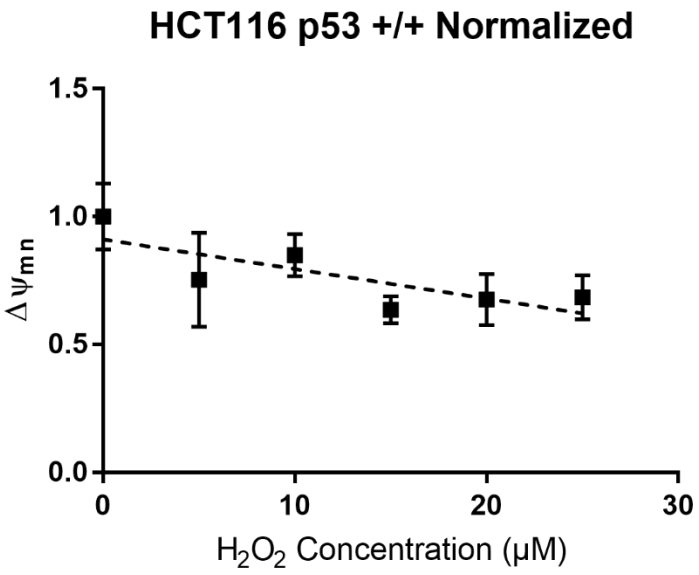

Supplementary Figure 9.1: A dose-response curve for HCT116 cells treated with hydrogen peroxide. $\Delta\Psi_{mn}$ represents normalized inner mitochondrial membrane polarization. While the trend appears negative, it is not significantly different from zero (p=0.062). Error is shown as standard deviation of the mean.